
THE UNIVERSITY
*of* EDINBURGH

# Susceptibility and Resistance to Nematode Infection: Role of Recruited vs. Resident Macrophages


Sharon Campbell

Submitted for the Degree of Doctor of Philosophy

The University of Edinburgh

2016

# Table of Figures

## Chapter 1



## Chapter 2



## Chapter 3

## Chapter 4



## Chapter 5

# Declaration

I declare that this thesis has been composed by myself, contains my research and has not been submitted in any other application for a higher degree.

Technical assistance from Alison Fulton and Nicola Logan was received for all *Litomosoides sigmodontis* experiments outlined in this thesis. In particular Alison Fulton generated the parasitological data pertaining to worm recovery, length and width. Sheelagh Duncan assisted in many of the *Salmonella* Typhimurium experiments. Experiments carried out in Chapter 3 where part of collaboration with Dr. Johanna Knipper, as such she has generated the information regarding the T cell immune response. Louise O'Grady assisted the graphical design of Figure 1-3.

Sharon Campbell

January 2017

# Acknowledgements

Firstly, I would like to thank my supervisor, Prof. Judith Allen whose constant support has made this thesis possible. Judi, thank you for always making time to discuss my data, both good and bad, for encouragement when needed and insight for experimental design.

I'd like to thank the members of the Allen lab, past and present, for making these three years a great experience. Dominik thank you for your time, mentorship and providing me with the skills necessary to explore my project. Tara, thank you for your cheery presence and scientific contributions at lab meeting. Sheelagh, for being an excellent and patient teacher in the lab. To Nicola and Alison thank you for always being willing to help with the early harvests and long days. Without your assistance I never would have managed the mammoth number of experiments in the third year. I want to extend my gratitude to Dr. Matthew Taylor and Dr. Johanna Knipper with whom I have collaborated with to generate much of the data presented in Chapter 3. Johanna, thank you for making a long day in the lab that little shorter and a lot happier. Further thanks goes to Dr. Steve Jenkins for his intellectual input in the analysis of the bone marrow chimeric experiments presented in Chapter 2.

Thanks to all the staff at the Ann Walker animal unit and the University and Home Office veterinarians for their diligence and care of my animals, who tended to be long term residents.

I am grateful to all my friends for the fun and laughter which they have provided over the past three years. To name a few: Emma Ringqvist, Carlos Minutti, Johanna Knipper, Wiebke Nahrendorf, Sarah Roche, Lukas Fisher, Mel Clerc, Kim Prior, Charlotte Regan, Alex Sparks, Amy Munro-Faure, Kara Dicks, Lisa Cooper, Josh Moatt, Divya Malik and anyone that I've managed to miss.

To my family – Mum, Dad, Emma and Peter. Thank you for always taking my calls and being the voice I needed to hear. Your love, support, and unwavering belief in my capabilities have made this journey possible.

Finally, I would like to thank Ian for all the flights and late night Canto Skypes.

# Abbreviations

| | |
|---|---|
| ~ | Approximately |
| AAMΦ | Alternatively activated macrophage |
| AGM | Aorta, gonad and mesonephros |
| AMΦ | Alveolar macrophages |
| APC | Antigen presenting cell |
| Arg-1 | Arginase 1 |
| BAT | Brown adipose tissue |
| BMD | Bone marrow derived |
| C3 | Complement component 3 |
| CAMΦ | Classically activated macrophage |
| CD | Cluster of differentiation |
| CFU | Colony forming units |
| CLR | C-type lectin receptor |
| CR | Complement receptor |
| CSF-1 | Colony Stimulating Factor 1 |
| CSF-1R | Colony stimulating factor-1 receptor |
| CTL | Cytotoxic lymphocyte |
| DCs | Dendritic cell |
| dLN | Draining lymph nodes |

| | |
|---|---|
| E7-9 | Embryonic day 7-9 |
| ELISA | Enzyme-linked immunosorbent assay |
| eYFP | Enhanced yellow fluorescent protein |
| FACS | Fluorescent activated cell sorting |
| FL | Foetal liver |
| GFP | Green fluorescent protein |
| GI | Gastrointestinal |
| GM-CSF | Granulocyte macrophage colony stimulating factor |
| HSC | Hematopoietic stem cells |
| i.v. | Intravenous |
| ICAM2 | Intracellular adhesion molecule 2 |
| i.p. | Intraperitoneal |
| i.pl. | Intrapleural |
| IFNγ | Interferon γ |
| Ig | Immunoglobulin |
| IL-4 | Interleukin 4 |
| ILCs | Innate lymphoid cells |
| iNOS | Inducible nitric oxide synthase |
| iTregs | Inducible T regulatory cells |
| LFA-1 | Lymphocyte function associated antigen 1 |
| LG | L-Glutamine |

| | |
|---|---|
| LPM | Large peritoneal macrophage |
| LPS | Lipopolysaccharide |
| Ly6C | Lymphocyte antigen 6 complex |
| MAb | Monoclonal antibody |
| MDR | Macrophage disappearance reaction |
| mf | Microfilaria |
| MHC | Major histocompatibility complex |
| MOI | Multiplicity of infection |
| MoMΦ | Bone marrow derived macrophages – $F4/80^{lo}$, MHC $II^{hi}$, $Ly6C^{-}$ |
| MPS | Mononuclear phagocyte system |
| MΦ | Macrophage |
| NeMΦ | Nematode elicited macrophage |
| NFκβ | Nuclear factor κβ |
| NK cells | Natural killer cell |
| NLRs | NOD-like receptors |
| PAMPs | Pathogen associated molecular patterns |
| PAP | Pulmonary alveolar proteinosis |
| PBS | Phosphate buffered saline |
| PD-1 | Programmed death-1 |
| PD-L1 | Programmed death ligand 1 |
| PD-L2 | Programmed death ligand 2 |

| | |
|---|---|
| PEC | Peritoneal exudate cells |
| pi | post infection |
| PLEC | Pleural exudate cells |
| PRR | Pathogen Recognition Receptors |
| PS | Penicillin streptomycin |
| RA | Retinoic acid |
| Raldh2 | Aldehyde dehydrogenase 2 |
| RELMα | Resistin-like molecule α |
| ResMΦ | Resident macrophage |
| RLRs | RIG-I-like receptors |
| RNS | Reactive nitrogen species |
| ROS | Reactive oxygen species |
| RPM | Rotations per minute |
| RPMI | Roswell Park Memorial Institute |
| s.c. | Subcutaneous |
| SCV | Salmonella containing vacuole |
| SEA | Soluble egg antigen |
| SEM | Standard error of mean |
| SPI-2 | *Salmonella* Pathogenicity Island-2 |
| SPM | Small peritoneal macrophage |
| STAT | Signal transducer and activator of transcription |

| | |
|---|---|
| TCR | T cell receptor |
| TGF-β | Transforming growth factor β |
| $T_H$ | T helper cell |
| TIR | Toll-interleukin |
| TLR | Toll-like receptor |
| TNF-α | Tumour necrosis factor α |
| UCP-1 | Uncoupling protein-1 |
| WAT | White adipose tissue |
| WT | Wild type |

# Abstract

Macrophages are phagocytic cells of the innate immune system, which have a central role in immune surveillance, tissue homeostasis and the immune response to bacterial, viral, protozoan and helminth parasites. It is now appreciated that many tissue resident macrophage (resMΦ) populations, including those in the peritoneal and pleural cavity, are derived prenatally prior to the establishment of definitive haematopoiesis in the bone marrow.

Once seeded, these resMΦ populations are long-lived and capable of self-renewal via *in situ* proliferation driven by CSF-1. An inflammatory insult, such as bacterial infection, results in the recruitment of bone marrow derived macrophages (BMDMΦ) and the disappearance of the resMΦ population. BMDMΦ recruited to the site of infection become classically activated upon engagement of pathogen recognition receptors and subsequent STAT1 induction. Classically activated macrophages (CAMΦ) are highly bactericidal through the production of inflammatory cytokines, which direct the $T_H1$ immune response, and upregulation of iNOS to generate high concentrations of intracellular nitric oxide. During resolution of acute inflammation resMΦ undergo a CSF-1 driven proliferative burst to repopulate the tissue. In contrast to bacterial infection, helminth parasites drive a $T_H2$ immune response characterised by $CD4^+$ T cell production of IL-4, which induces proliferation and alternative activation of the resMΦ population, thereby overcoming the need for an inflammatory influx of BMDMΦ. Alternatively activated macrophages (AAMΦ) are generated through signalling from the IL-4Rα subunit and subsequent expression of the molecules RELMα, YM1 and arginase-1. While both BMDMΦ and resMΦ upregulate RELMα, YM1 and Arg-1 in response to IL-4Rα stimulation, microarray analysis revealed an otherwise diverse transcriptional and cell surface phenotype between these populations. It was hypothesised that the diverse modes of macrophage accumulation enlisted by bacterial and helminth parasites, combined with the distinct alternative activation phenotypes employed by BMDMΦ and resMΦ populations would translate into important functional differences as regards anti-parasitic immunity.

Chapter 1 and 2 of this thesis addresses the importance of macrophage origin during infection with the filarial nematode *Litomosoides sigmodontis*, taking advantage of the naturally occurring resistant C57BL/6 and susceptible BALB/c strains. A large disparity in MΦ accumulation was observed throughout the infection time course, with significantly larger numbers present within the pleural cavity of resistant C57BL/6 mice. This difference in MΦ number was a reflection of enhanced F4/80$^{hi}$ resMΦ accumulation. Through Ki67$^{hi}$ staining and the use of CCR2$^{-/-}$ and partial bone marrow chimeric mice, the expanded F4/80$^{hi}$ population in resistant C57BL/6 mice was shown to be a result of proliferation of the local F4/80$^{hi}$GATA6$^{+}$CD102$^{+}$ resMΦ population. A high degree of BMDMΦ incorporation into the resMΦ pool through assumption of an F4/80$^{hi}$GATA6$^{+}$CD102$^{+}$ phenotype was observed in both naïve and infected bone marrow chimeric animals, supporting a recent publication showing gradual incorporation of these cells into the resMΦ niche with age. Importantly, the degree of BMDMΦ incorporation into the F4/80$^{hi}$ population was equivalent between naïve and infected animals, despite a 27-fold difference in cell number, illustrating that expansion is a result of proliferation of local resMΦ, independent of origin.

Susceptibility was marked by reduced resMΦ proliferation and enhanced recruitment of bone marrow derived F4/80$^{lo}$ MΦ and monocytes. These recruited BMDMΦ displaced the resMΦ population, failed to integrate the resMΦ niche and were highly positive for PD-L2, a marker specific to BMD AAMΦ. Prevention of monocyte influx and subsequent resMΦ displacement resulted in increased worm killing and a stronger $T_H2$ immune response in susceptible BALB/c mice, thereby confirming a detrimental role for BMD AAMΦ in worm killing. Conversely, in order to confirm a protective role for the expanded resMΦ in resistant C57BL/6 mice we attempted to deplete the resMΦ population through intrapleural delivery of clodronate-loaded liposomes. Due to technical issues we were unable generate statistically significant results when depleting the resMΦ population, however a trend toward decreased worm killing in the absence of resMΦ is evident.

Previously generated microarrays in the lab identified the complement cascade as being highly upregulated by AAMΦ induced in response to *Brugia malayi* infection

compared to BMDMΦ (thioglycollate elicited). To investigate the role of complement in resistance to *L. sigmodontis,* Chapter 3 briefly phenotypes the macrophage compartment of $C3^{-/-}$ C57BL/6 mice during infection. No differences in worm burden or macrophage phenotype could be detected in $C3^{-/-}$ mice compared to WT controls, however this may be explained through differences in strain or MΦ origin. This chapter provides an important foundation for future studies on complement and its role in worm killing during *L. sigmodontis* infection.

The final chapter of the thesis focuses on examining the bactericidal capabilities of BMD and resMΦ populations. An *in vitro* system was utilised to assess the interaction of bone marrow derived macrophages (thioglycollate elicited) and ResMΦ (from naïve mice) with *Salmonella enterica* serovar Typhimurium SL3261. I found that *in vitro* BMDMΦ are infected by/ingest SL3261 to a much greater degree than resMΦ. The resMΦ population is less efficient at both controlling the spread and killing intracellular SL3261 overtime, compared to the BMDMΦ population. *In vivo* however, there appears to be no difference in the ability of the monocyte derived $F4/80^{lo}$ MΦ and the $F4/80^{hi}$ resident MΦ to be infected by/ ingest SL3261, nor was a difference in bactericidal ability detected.

Ultimately my work highlights that the anti-parasitic functions of MΦ populations are not dictated by origin but rather the activation phenotype upon infection and ability to respond to local stimuli.

# Chapter 1 Introduction

The immune system has evolved to protect the host from invasion by a wide variety of pathogenic organisms; viruses, bacteria, fungi and parasites. In order to mount an effective response against such a diverse range of pathogens distinct immunological responses are elicited.

The immune system is activated once the physical barriers of the skin and mucosal surfaces have been breached. The mucosal surfaces, such as the eye, respiratory, gastrointestinal tract (GI) and genitals tracts are most exposed to the environment and thus to pathogenic infection. The mucosal layer overlying the intestinal epithelial barrier contains antibacterial proteins such as defensins and cathlicidins, secretory IgA antibodies and complement proteins, which collectively aim to destroy the pathogen before it interacts with the underlying epithelial barrier.

However, when these mechanisms fail and the epithelial layer is breached the immune system is activated. Classically the immune system has been described as consisting of innate and adaptive arms. Traditionally the innate immune arm was viewed as non-specific. However as predicted by Janeway, the innate arm is highly sophisticated, possessing an array of pathogen recognition receptors (PRRs) which enable discrimination between self and non-self (Janeway, 1989). Additionally it has been realised that the innate immune response plays an essential role in activating the adaptive arm and in determining the nature of the response e.g. type 1 vs. type 2 (Edwards et al., 2002).

Macrophages and dendritic cells are innate phagocytic cells capable of presenting antigenic peptides on their surface via MHC I/ MHC II and activating naïve T cells of the adaptive immune arm. Dendritic cells are professional antigen presenting cells (APC), capable of ingesting apoptotic/virally infected cells and presenting peptide via MHC I molecules in addition to presenting processed antigenic peptides on MHC II molecules. Antigen loaded MHC I molecules on activated DCs recognise cognate T cell receptor (TCR) on $CD8^+$ cytotoxic lymphocytes (CTL). Activated $CD8^+$ CTL migrate to the periphery and kill virally infected cells presenting target antigen on MHC I. Similarly, antigen loaded MHC II molecules bind cognate $CD4^+$ TCR, in

local lymph nodes. To become activated naïve $CD4^+$ T cells must recognise the MHC II loaded antigen, bind co-stimulatory molecules on the APC and receive a cytokine stimulus. The activation status of the innate immune APC in combination with the cytokine environment, determine the differentiation path of the naïve T cell, which can clonally expand into one of four $CD4^+$ T helper ($T_H$) cell subtypes; $T_H1$, $T_H17$, $T_H2$ and Treg. Thus innate APCs play a central role in determining the outcome of an adaptive immune response.

$T_H1$ and $T_H17$ cells are induced in immune responses against viral, bacterial and fungal pathogens. These cells secrete pro-inflammatory cytokines that further activate innate immune cells, promote the development of $CD8^+$ CTL and enhance the generation of antigen specific antibodies. $T_H2$ cells in contrast are activated in response to helminth parasites or allergens and promote the activation of alternatively activated macrophages (AAMΦ), eosinophils, mast cells and B cell switching to produce IgE antibodies.

Regulatory T cells (Treg) act to suppress T cell mediated immune responses, limiting damage caused by an overzealous immune response, preventing the development of autoimmunity and ultimately maintaining tolerance.

## 1.1 Macrophage Origins

### 1.1.1 Mononuclear Phagocyte System

From the mid-19$^{th}$ century there were several accounts of the ability of leukocytes to ingest foreign material. However it was not until 1897 that Elie Metchnikoff coined the term phagocytosis and hypothesised this to be a host-protective mechanism (Buryachkovskaya et al., 2013, Yona and Gordon, 2015). Since this seminal work, the classification of MΦ found in the tissues, their precursors and origins have been in continual flux and debate. In 1969 Cohn, Van Furth and Hirsch proposed the mononuclear phagocyte system (MPS), as way in which to classify macrophages and their precursors. The MPS was based on experiments illustrating the replacement of resident macrophages (resMΦ) by monocytes derived from the bone marrow after X-ray irradiation and chronic inflammation (van Furth and Cohn, 1968, Volkman, 1970, Ryan and Spector, 1970). The MPS stated that tissue resident macrophages

were a terminally differentiated 'end cell', derived from blood monocytes, which in turn arose from promonocytes in the bone marrow.

Since the initial discovery of the promonocytes, much research has focused on delineating the development of macrophages from haematopoietic stem cells (HSC), which derive from definitive haematopoiesis in the bone marrow. In 2006, the macrophage-dendritic cell precursor (MDP) was identified as a myeloid progenitor which gives rise to both macrophages and dendritic cells (DCs) (Fogg et al., 2006). The MDP is negative for lineage markers and positive for c-kit (CD117, the receptor for stem cell factor), CX3CR1 (the fractalkine receptor, a chemokine receptor expressed by monocytes, DCs, subsets of NK cells and T cells but not by most differentiated macrophage populations), FLT-3 (the receptor for Fms-like tyrosine kinase 3 ligand, which is required for the development of most DCs but not MΦ) and CSF1R (CD115, the receptor for the colony stimulating factor 1, upon which monocyte development is dependent). Subsequently, the MDP can differentiate into a common DC precursor (CDP) (Naik et al., 2007, Onai et al., 2007, Hettinger et al., 2013) or a common monocyte progenitor (cMoP)(Hettinger et al., 2013), to give rise to blood circulating pre-DCs which seed tissues with conventional DCs ($CD8\alpha^-$ /$CD103^+$ or $CD11b^+$) (Liu et al., 2009, Ginhoux et al., 2009) and blood circulating monocytes (both $Ly6C^{hi}$ and $Ly6C^{lo}$) respectively (see Figure 1-1).

$Ly6C^{hi}$ (classical monocytes) and $Ly6C^{lo}$ (non-classical/patrolling) monocytes can be found constitutively within the blood and are the murine counterparts to human $CD14^{low}CD16^+$ and $CD14^+$ peripheral blood monocytes. The relationship between $Ly6C^{hi}$ and $Ly6C^{lo}$ monocyte subsets is currently still debated. It is appreciated that both arise from the cMoP, but whether $Ly6C^{hi}$ monocytes are a precursor to $Ly6C^{lo}$ monocytes remains unclear. Under homeostatic conditions, $Ly6C^{lo}$ monocytes derive from $Ly6C^{hi}$ monocytes in the blood (Yona et al., 2013) and function in patrolling the endothelium and recruiting neutrophils to damaged tissue (Auffray et al., 2007, Carlin et al., 2013) (Figure 1-1). However, under inflammatory conditions $Ly6C^{hi}$ monocytes are recruited in a CCR2-dependent manner directly to the site of inflammation where they differentiate into monocyte derived macrophages or monocyte derived dendritic cells (Tsou et al., 2007, Ziegler-Heitbrock and Hofer,

2013). The infiltration of these monocytes derived/bone marrow derived macrophages into tissues (BMDMΦ) under inflammatory conditions typically results in the disappearance of the resMΦ population (Barth et al., 1995). The macrophage disappearance reaction is characterised as the inability to retrieve the resMΦ population from a tissue, whether this reflects the migration of the population to another tissue/site, increased adherence within a cavity or cellular death remains a topic of debate.

Specialised populations of ResMΦ are found in the brain, spleen, lungs, liver, skin, intestines, peritoneal and pleural spaces. Each resident macrophage population can be identified by a distinct cell surface and transcription factor phenotype (Table 1). Furthermore, in many tissues the resMΦ population exists alongside a smaller population of recently recruited BMDMΦ, which were suggested to be an intermediate cell between monocyte and fully differentiated resMΦ. For example within the peritoneal cavity, the resMΦ population which is often referred to as large peritoneal MΦ (LPM) exist alongside a more recently bone marrow derived, small peritoneal MΦ population (SPM)(Ghosn et al., 2010). The rapid influx of BMDMΦ into the pleural space, the disappearance of the resMΦ population and the replacement of resMΦ by BMDMΦ upon lethal irradiation collectively supported the MPS framework. However the MPS was inconsistent with reports of tissue macrophages being long-lived and capable of local proliferation and with the detection of macrophages in multiple tissues prior to the establishment of definitive haematopoiesis in the bone marrow (Melnicoff et al., 1988, Naito et al., 1996).

## Table 1 Tissue Macrophage phenotype and function

References: Microglia - (Butovsky et al., 2014). Red pulp MΦ -(Kohyama et al., 2009, Haldar et al., 2014). Skin -(Tamoutounour et al., 2013, Merad et al., 2008). Kupffer cells- (Scott et al., 2016). Intestines- (Bain et al., 2014). Peritoneal and pleural MΦ -(Okabe and Medzhitov, 2014, Rosas et al., 2014, Wang and Kubes, 2016).

| Tissue | Cell surface phenotype | Transcription factors | Functional specialization |
|---|---|---|---|
| Brain -Microglia | $CD117^{+}$, $Iba1^{+}$,$CX3CR1^{+}$, $CD11c^{lo}$,$CD86^{lo}$, MHC $II^{lo}$ | $SMAD1/2^{+}$ | Immune surveillance |
| Spleen – red pulp MΦ | $F4/80^{hi}$, $CD11b^{lo}$, $VCAM1^{hi}$, $TREML4^{hi}$ | $SPI\text{-}C^{+}$ | Iron recycling |
| Lung – alveolar MΦ | $CD11b^{lo/-}$, $F4/80^{+}$. $CD11c^{hi/+}$, $SigF^{+}$ | | Immune surveillance and surfactant clearance |
| Skin – Langerhans cells-dermal DCs | $CD11b^{+}$,$CD24^{lo}$,$Ly6C^{-}$, $CD64^{-}$, MHC $II^{lo}$, $CD207^{+}$, $CD11c^{+}$, $F4/80^{+}$ | | Immune surveillance/ antigen presentation |
| Liver – Kupffer cells | $CLEC4F^{+}$, $F4/80^{+}$, $CD11b^{int}$ | | Iron recycling |
| Intestines | $Lin^{-}$,$CD11c^{+}$,$F4/80^{lo}$, $CD11b^{hi}$, $CD64^{int}$, $CX3CR1^{int}$ | | Immune surveillance and tolerance |
| Peritoneal and pleural resMΦ | $Lin^{-}$,$CD11c^{-}$,$CSF\text{-}1R^{+}$, $CD11b^{+}$, $F4/80^{hi}$, $CD102^{+}$ | $GATA6^{+}$ | Wound repair |

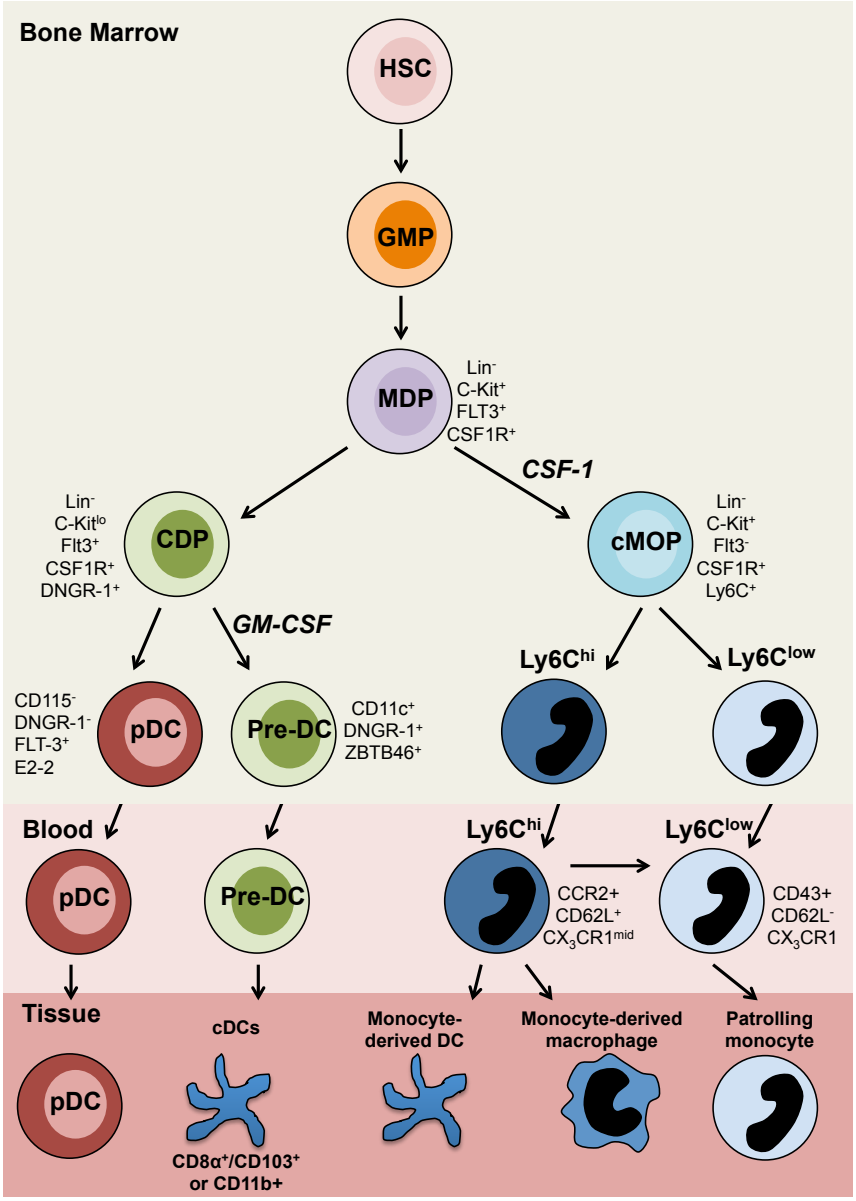


**Figure 1-1 Monocyte and dendritic cell development in the murine bone marrow**

Adapted from (Schraml and Reis e Sousa, 2015, Ginhoux and Jung, 2014). In the bone marrow, hematopoietic stem cells (HSC) give rise to granulocyte macrophage progenitors (GMP), which in turn give rise to the macrophage dendritic cell precursor (MDP). The MDP is negative for lineage markers: CD11b, CD3, CD19, NK1.1.Ia$^{b}$, CD11c, B220, Ter-119 and Gr1.Common DC precursors (CDP) and common myeloid progenitors (cMOP) arise from the MDP. Within the bone marrow, CDP differentiate into plasmacytoid DCs, which are integral to antiviral immunity and Pre-DCs which subsequently enter circulation and seed tissues with conventional dendritic cells (cDCs). pDCs terminally differentiate in the BM and migrate through the circulation to the tissues. The cMOP gives rise to Ly6C$^{hi}$ and Ly6C$^{low}$ monocytes. In the steady state Ly6C$^{lo}$ monocytes patrol the endothelium and recruit neutrophils upon detection of damage. Ly6C$^{hi}$ monocytes are rapidly recruited to the site of inflammation in a CCR2-dependent manner, these cells subsequently differentiate into monocyte derived macrophages/ bone marrow derived macrophages (BMDMΦ) or monocyte derived DCs.

### 1.1.2 Prenatal origin of resident macrophages

Definitive haematopoiesis is the second wave of haematopoiesis that is initiated in the aorta, gonad and mesonephros (AGM) region of the embryo from embryonic day 10.5 (E10.5). From the AGM HSCs migrate to the foetal liver, which is the primary haematopoietic organ from E11.5 (Lichanska and Hume, 2000, Orkin and Zon, 2008). It is these HSCs, which originate from the AGM region that seed the foetal bone marrow, giving rise to foetal monocytes and eventually the adult bone marrow. Primitive haematopoiesis is the 1$^{st}$ haematopoietic wave, which arises from the extra-embryonic yolk sac between embryonic day 7 - 9 (E7-9) (Lichanska and Hume, 2000, Orkin and Zon, 2008). This occurs prior to the establishment of definitive haematopoiesis and the two waves are independent of one another. Investigation into the contributions of primitive vs. definitive haematopoiesis to the seeding of resMΦ populations was hindered until recent years by the lack of fate mapping models. However, since 2010 there has been an explosion of research into this area resulting in a paradigm shift in how we view macrophage origin.

Expression of runt-related transcription factor 1 (runx1) is first detected at E6.5 and is restricted to the YS until E8.0. Through crossing of tamoxifen inducible Runx1MER-Cre-MER mice to *Roasa26*$^{R26R\text{-}eYFP/R26\text{-}eYFP}$ mice Ginhoux et al. generated mice in which a single injection of 4-hydroxytamoxifen (4'OHT) into pregnant females results in irreversible expression of eYFP by Runx1$^{+}$ cells and subsequent progeny within a 24-hour window. Consequently, injection of 4'OHT at E7.25-7.5, during primitive haematopoiesis, resulted in detection of eYFP$^{+}$ macrophages throughout the embryo including the microglia at E10.5. However only microglia remained eYFP$^{+}$ in adult mice, highlighting that the brain resMΦ population can be seeded prenatally independent of HSC and can be maintained until adulthood, whereas most other tissues would appear to be dependent on HSC development (Ginhoux et al., 2010). At this time point our lab was actively investigating the role of MΦ, which accumulate within the pleural space, during infection with the filarial nematode *Litomosoides sigmodontis*. Through intravenous injection of clodronate loaded liposomes and infection of partial bone marrow chimeric mice, it was discovered that the large accumulation of MΦ within the pleural space was a occurring independently of blood monocyte recruitment and was

the result of local resMΦ proliferation, driven by the $T_H2$-derived cytokine IL-4 (Jenkins et al., 2011). Furthermore the resMΦ population was shown to proliferate, under the control of CSF-1, in the resolution of zymosan-induced inflammation to reconstitute the resMΦ compartment (Davies et al., 2011). This data highlighted that in the face of mild inflammation, the resMΦ population recovers rather than be replaced by infiltrating BMDMΦ (Davies et al., 2013). Consequently, through analysis of the macrophage compartment of mice deficient for the transcription factor *Myb (myb$^{-/-}$)*, which is necessary for the development of HSC, Schultz et al. showed that CD45$^{+}$F4/80$^{hi}$CD11b$^{+}$ macrophages of the skin (Langerhans cells), spleen (Kupffer cells), pancreases, kidney and lung (Alveolar MΦ) develop normally in Myb$^{-/-}$ mice, illustrating the independence of these resMΦ populations from hematopoietic bone marrow precursors (Schulz et al., 2012). Further studies carried out using *Cx3cr1$^{eGFP}$* and *Cx3Cr1$^{cre}$:R26-yfp* mice, in which cells constitutively expressing CX3CR1 are positive for GFP and YFP whereas those which originated from a CX3CR1 positive precursor but no longer express CX3CR1 are GFP negative, reiterated the prenatal origin of microglia, splenic MΦ, Kupffer cells, Langerhans cells, alveolar MΦ and extended these finding to resMΦ of the peritoneal cavity (Yona et al., 2013). Tissues resident macrophages in the lung, spleen, peritoneum and BM were subsequently shown to be long-lived and capable of self-renewal following irradiation, through *in situ* proliferation driven by the cytokine Colony Stimulating Factor 1 (CSF-1)(Hashimoto et al., 2013).

Thus, by early 2013 the view of MΦ origin had changed substantially with it becoming increasingly clear that the majority of tissue resMΦ populations are seeded prenatally independent of definitive haematopoiesis. These prenatally seeded resMΦ are long-lived, capable of local expansion during $T_H2$ driven inflammation, disappear during classical inflammation, yet return to repopulate their niche through local proliferation. Amidst the realisation that resMΦ are prenatally derived were the observations that BMDMΦ contributed to the resident niche of several tissues under homeostatic and inflammatory conditions. Specifically, intestinal MΦ are continually replenished from the bone marrow and this was hypothesised to be a result of the degree of environmental exposure. Furthermore, 2 months post thioglycollate (fungal extract frequent used to induce inflammation) induced BMDMΦ recruitment to the

peritoneal cavity of *Cx3cr1*$^{creET}$*:R26-yfp* mice, RFP$^{+}$ cells could be still be detected in the cavity and they had assumed a MHC$^{lo}$F4/80$^{hi}$ phenotype characteristic of resMΦ in this tissue (Yona et al., 2013). Also, IL-4 driven proliferation was not restricted to resMΦ but was capable of inducing heightened proliferation to BMDMΦ (Jenkins et al., 2011)

Consequently, a central question in the field centred on whether tissue resMΦ and BMDMΦ, which arose from distinct lineages, possess diverse functional capabilities. Specifically, are resMΦ evolutionarily more involved in development of the embryo, tissue homeostasis and specific anti-parasitic immunity? Conversely, did monocyte-derived macrophages arise to tackle bacterial and viral infections? And can monocyte-derived macrophages, which replace resMΦ under irradiation protocols, truly recapitulate the phenotype and function of these prenatally seeded cells?

With this knowledge I embarked upon my research project, initially asking whether the expanded resMΦ population found within the pleural cavity of L. *sigmodontis* infected C57BL/6 mice described by Jenkins et al. 2011 was important in the killing of adult worms. Conversely, I wanted to ask whether BMDMΦ possess heightened bactericidal capabilities when compared to resMΦ. However, this is a field continually in flux and data is now accumulating to suggest that while many tissues are indeed seeded by prenatally derived macrophages, these cells are continually replenished with BMDMΦ at a rate, which appears to be highly tissue and context specific.

### 1.1.3 Replenishment of resMΦ populations from the bone marrow with age

Colonic lamina propria macrophages are seeded initially from the yolk sack, however these cells are no longer detectable in new-born mice (*Csf1r*-Mer-iCre-Mer mice, crossed with *Roasa26*$^{R26R\text{-}eYFP/R26\text{-}eYFP}$ with 4'OHT at E8.5), having been replaced by foetal liver (FL) derived monocytes (*Cx3cr1*$^{+/GFP}$ mice)(Bain et al., 2014). This FL-derived resMΦ population (F4/80$^{hi}$CD11b$^{lo}$) is the dominant MΦ population in the lamina propria at birth but diminishes in prominence with age due to replacement by infiltrating BMDMΦ (F4/80$^{lo}$CD11b$^{hi}$). The blood-derived monocytes, which infiltrate the colonic lamina propria to replace these resident

macrophages, form a characteristic 'monocyte waterfall' as they mature from a $Ly6C^{+}MHCII^{-}CX3CR1^{int}CCR2^{hi}$ through an intermediary $Ly6C^{hi}MHCII^{+}CXCR1^{hi}CCR2^{-}$ activation state to differentiate into cells expressing the phenotypical colonic MΦ cell surface markers $MHCII^{+}CXCR1^{hi}CCR2^{-}F4/80^{lo}CD11b^{hi}$. This study highlighted that while intestinal macrophages are prenatally seeded, these cells are relatively short lived compared with other resMΦ populations and are continually replenished from the bone marrow by monocytes (Bain et al., 2014). Circulating $Ly6C^{+}$ monocytes have now been shown to contribute to the resMΦ pool in the skin and heart under both inflammatory and homeostatic conditions (Tamoutounour et al., 2013, Epelman et al., 2014, Molawi et al., 2014). Most recently, Bain et al. highlighted that resident $F4/80^{hi}CD11b^{lo}GATA6^{+}$ resMΦ within the peritoneal and pleural spaces, while prenatally derived and detected for a period of 4 months, are gradually replenished from the bone marrow with age by $Ly6C^{+}$ monocytes which mature through an intermediary $MHC^{hi}F4/80^{lo}$ cell surface phenotype. Furthermore, this replacement was highly gender dependent with female mice displaying a higher rate of macrophage turnover (Bain et al., 2016).

### 1.1.4 Residency is a result of local conditioning signals

Consequently, opinions are divided on whether origin truly imprints any phenotypical or functional characteristics upon MΦ that cannot be impressed upon BMDMΦ. As such, light has been shed on the local environmental signals that drive tissue specific transcription factors resulting in functional differentiation of resMΦ. The transcription factor SPI-C is essential in driving the iron recycling abilities and thereby homeostatic function of red pulp macrophages (RPM) of the spleen, the absence of SPI-C results in defected RPM development and accumulation of unprocessed iron in the spleen (Kohyama et al., 2009). Heme, a product of red blood cell degradation, has been identified as the local tissue factor responsible for driving SPI-C expression within the spleen (Haldar et al., 2014). Furthermore, following drug induced-hemolysis, which results in RPM deficiency, heme can repopulate the RPM compartment through driving the functional specialisation of monocytes through inducing SPI-C expression (Haldar et al., 2014).

Microglia possess a unique hyporesponsive phenotype ($CD86^{lo}$, $MHCII^{lo}$, $CD11c^{lo}$, $CX3CR1^{hi}$), in order to prevent excessive inflammation in this highly privileged tissue, compared with other resMΦ populations. The cytokine TGF-β, which is present within the CNS during development, is essential in driving the smad TFs that maintain this activation state of microglia (Abutbul et al., 2012, Butovsky et al., 2014).

The transcription factor GATA6 controls the expression of 39% of peritoneal MΦ specific genes and is selectively expressed by resident peritoneal and pleural MΦ when compared to lung, liver, spleen, intestinal, adipose, bone marrow and foetal MΦ (Rosas et al., 2014, Okabe and Medzhitov, 2014). A reduction in total resMΦ number and loss of the characteristic $CSF1R^{+}$,$F4/80^{hi}$,$MHC^{lo}$,$CD11b^{lo}$ resMΦ phenotype was observed in MΦ-specific GATA6 KO mice (*Gata6-KO$^{mye}$* / Mac-*Gata6 KO*), highlighting the importance of this TF in maintaining resMΦ phenotype. Okabe and Medzhitov found that GATA6 expression was driven by retinoic acid, the end metabolite of vitamin A degradation, which is released by the omentum (a fat-associated lymphoid follicle of the peritoneum). Consequently, as mice on a vitamin A deficient diet aged, the dominance of the $GATA6^{+}CCR2^{-}MHC^{lo}F4/80^{hi}$ resMΦ population declined and the presence of a $GATA6^{-}CCR2^{+}MHC^{hi}F4/80^{int}$ BMDMΦ macrophage population emerged within the cavity (Okabe and Medzhitov, 2014). Okabe and Medzhitov hypothesise that vitamin A deficiency results in recruitment of inflammatory MΦ. However, given the recent work by Bain et al, the appearance of this BMDMΦ population in the peritoneum of aging mice probably reflects the influx of BMDMΦ that occurs under homeostatic conditions to replenish the resMΦ population, but in the absence of retinoic acid these cells are unable to integrate into the niche. Furthermore, the inability of small peritoneal macrophages ($F4/80^{lo}$) and inflammatory macrophages (elicited by thioglycollate injection) to upregulate GATA6 when co-cultured with ATRA (trans-retinoic acid) for 24 hours was a result of epigenetic silencing at the *gata6* locus, as noted by the presence of a Histone 3 lysine 27 trimethylation (H3K27me3)(Okabe and Medzhitov, 2014). However, Bain et al. have demonstrated that BMDMΦ which integrate into the local peritoneal and pleural MΦ populations can assume GATA6 expression (Bain et al., 2016), perhaps due to the presence of a local tissue factor able to activate the gata6 locus by

replacement of H3K27me3 with H3K4me3. Rosas et al. highlighted the role for GATA6 in enabling resMΦ to proliferate and repopulation the peritoneal cavity after acute peritonitis induced by zymosan (Martin et al., 2001, Rosas et al., 2014).

Thus local tissue factors such as heme, TGF-β and retinoic acid are capable of inducing the functional differentiation of bone marrow derived macrophages, under conditions of RPM hemolysis, *in vitro* and under homeostatic conditions, respectively. In order to address if BMDMΦ that integrate into the local niche are transcriptionally identical to their prenatal four founders Lavin et al. carried out detailed analysis of the enhancer landscape of resMΦ from WT mice and compared this to the enhancer landscape of tissue resMΦ 4 months post reconstitution of host mice after lethal irradiation. Indeed, almost all resMΦ enhancers were assumed by BMDMΦ, highlighting that tissue driven specialisation rather than origin is likely the primary driver of MΦ function (Lavin et al., 2014). Similarly, through delivery of either YS, FL or BMD MΦ/monocytes intranasally to *csf2rb*$^{-/-}$ mice, which lack the GM-CSF receptor and subsequently alveolar MΦ, van de Larr et al. illustrated that MΦ populations of distinct origin could all give rise to functional alveolar MΦ with near identical transcriptional phenotypes. Thus, experiments to date have failed to identify any functional capabilities imprinted upon a MΦ at origin that cannot be induced by the local tissue environment. However, as investigation into this field intensifies, origin specific functions may be identified. It may be that prenatally derived MΦ are essential in ensuring correct development *in utero*. Furthermore, the responsiveness of BMDMΦ, as determined by their enhancer landscape, is also important in enabling successful integration into the local MΦ compartment and also determines how this cell will respond to subsequent stimuli.

## 1.2 Macrophage Activation

A recent review article by Murray et al. suggests that the term ‘macrophage activation’ should now replace the out-dated phrase of ‘macrophage polarisation’, which was historically generated to describe the distinct MΦ activation profiles induced by IFNγ and/or TLR agonists vs. that induced by IL-4 (Murray et al., 2014). It is now appreciated that the activation profiles induced by TLR agonists, IFNγ and TLR agonists, IFNγ alone, IL-4, IL-10, glucocorticoids (GC), TGF-β, or immune

complexes are unique and distinct from one another. Consequently, attempting to arbitrarily segregate these activation profiles as either classically (M1) or alternatively activated (M2) over simplifies the complexity of MΦ activation. This results in confusion in the field as a result of inaccurate association of specific function with broadly defined activation phenotypes. Moving forward, Murray et al. suggest that the activating stimuli (e.g. M(IFNγ) vs. M(IL-4)), resultant TF activation, cytokine production, chemokine production, scavenger receptor expression and amino acid metabolism should be noted to enable true characterisation of an activation profile (Murray et al., 2014) (See Table 2 and Figure 1-2). While this model should be applied to *in vitro* research it may prove more difficult to translate into the *in vivo* setting, where a cell is rarely activated by one stimulus and indeed many of these stimuli remain unidentified.

The 'classically activated MΦ' was first noted by Mackaness in the 1960s as the enhanced bactericidal ability of MΦ upon exposure to BCG (Mackaness, 2014). Subsequently, an array of pathogen recognition receptors (PRRs) (e.g. TLRs, RLRs and NLRs)(Akira, 2011) were identified which enable MΦ to recognize pathogen associated molecular patterns (PAMPs) of bacterial and viral antigens. PRR engagement and/or stimulation with inflammatory cytokines results in the initiation of signal transduction pathways, which polarize the macrophage toward a phenotype characterised by the transcription factor STAT1, production of inflammatory cytokines TNFα, IL-6, IL-12 and activation of the enzyme inducible nitric oxide synthase 2 (iNOS). iNOS generates high concentrations of bactericidal nitric oxide (NO) within the pathogen-containing phagolysosome through degradation of L-arginine (Fang, 2004). However, it is now known that while M(LPS), M(LPS+IFNγ) and M(IFNγ) all induce $pSTAT1^{+}$,$Socs1^{+}$, $Nfkbiz^{+}$, $Nos2^{+}$, only M(LPS) and M(LPS+IFNγ) secrete TNFα, IL-6 and IL-27. Furthermore, M(LPS+IFNγ) produce IL-12a necessary for $T_H1$ $CD4^{+}$ cell induction and possess the highest degree of Nos2 activation and thus bactericidal capabilities.

The realisation that IL-4 and IL-13, the products of $CD4^{+}$ $T_H2$ cells, induced expression of the mannose receptor and increased phagocytosis of MΦ *in vitro* resulted in Stein, Doyle and colleagues to propose the assumption of an 'alternatively

activated MΦ' (AAMΦ) phenotype characterised by the expression of the mannose receptor (Stein et al., 1992, Doyle et al., 1994). Subsequent studies of the transcriptional phenotype of AAMΦ *in vivo* identified molecules RELMα (Resistin-like molecule α; aka FIZZ1), the chitinase-like molecule YM1 (Nair et al., 2003, Raes et al., 2002, Loke et al., 2002) and the enzyme arginase-1 (Arg-1)(Munder et al., 1998), which are now routinely used collectively to identify AAMΦ both *in vitro* and *in vivo*. Indeed RELMα, YM1 and Arg-1 are considered the 'Big Three' molecules of alternative activation. Today, this AAMΦ phenotype best describes M(IL-4). IL-4 binds the IL-4 receptor, a heterodimer consisting of the IL-4Rα subunit dimerised with either a γC subunit (Type I receptor) or the IL-13Rα1 subunit (Type II receptor)(Zurawski et al., 1993). Consequently, IL-4 can signal through the type I and II receptors, whereas IL-13 signals only through the type II receptor. Engagement of IL-4Rα results in activation of the transcription factor STAT6, which subsequently activates STAT6-dependent genes *Arginase-1* (Arg-1), *Chi3l3* (chitinase 3 like 3, YM1) and *Retnla* (Resistin like alpha, RELM-α).

**Table 2 Macrophage activation profiles**

Adapted from Murray et al. 2014. Shown are the functional activation profiles of murine macrophages stimulated with CSF-1 and indicated stimuli

| | M(IL-4) | M(Ic) | M(IL-10) | M(GC+TGFβ) | M(GC) | M(-) | M(LPS) | M(LPS+IFNγ) | M(IFNγ) |
|---|---|---|---|---|---|---|---|---|---|
| Transcription factors SOCS proteins | pSTAT6++++ pSTAT1-ve Ifr4 Socs2 | | pSTAT3+ Nfil3, Sbno2 Socs3 | | | Baseline gene expression dependent on culture variables | pSTAT1+ PSTAT6 –ve Socs1 Nfkbiz | pSTAT1+ PSTAT6-ve Socs1, Nfkbiz Irf5 | pSTAT1+++ Socs1 |
| Cytokines | | Il10, Il6 | Il10 | | | | Tnf, Il6, Il27 | | |
| Chemokines | Ccl17 Ccl24 Ccl22 | Cxcl13 Ccl1 Ccl20 | | | | | | | |
| Amino acid metabolism | Arg1+++ | Nos2 | | | | | Arg1+ Nos2+ | Arg1+ Nos2+++ | Ido1 Nos2+++ |
| Others | Retnla, Chi3l3, Alox15 | Retnla -ve | Il4ra | | | | | | |

## 1.2.1 RELMα

Resistin-like molecule α (RELMα) is a cysteine-rich protein that is part of a family of 'resistin-like molecules' including RELMβ, Resistin and RELMγ (Beltowski, 2003). RELMα is abundantly expressed and secreted by M(IL-4) both *in vivo* during nematode infection and in response to *in vitro* IL-4 stimulation (Loke et al., 2002,

Nair et al., 2003). While a specific role for RELMβ has been illustrated in the gut (Artis et al., 2004)(discussed later), RELMα appears to be more multifaceted in its functions having been implicated in $T_H2$ induced fibrotic conditions (Holcomb et al., 2000, Yamaji-Kegan et al., 2010, Wynn and Barron, 2010), immune suppression, active worm killing and wound repair. RELMα is highly expressed during bleomycin-induced lung fibrosis and in the absence of IL-4Rα signalling, reduced RELMα expression correlates with a significant decrease in pulmonary fibrosis (Liu et al., 2004). RELMα is produced not only by MΦ but also by eosinophils, neutrophils, DCs, and epithelial cells (Pesce et al., 2009b, Osborne et al., 2013, Holcomb et al., 2000, Munitz et al., 2009). Conversely, RELMα has been associated with the suppression of the immune response, as RELMα deficient mice present with an enhanced $T_H2$ immune response against *Schistosoma mansoni* (Pesce et al., 2009b, Nair et al., 2009). Similarly, RELMα positive DCs promote IL-10 production by T cells (Cook et al., 2012). An active role for RELMα in worm killing has been suggested through its chemotactic (Munitz et al., 2009) and potential metabolic properties (Ruckerl and Allen, 2014). While, the absence of RELMα results in an enhanced $T_H2$ immune response against *Schistosoma mansoni,* these mice also present with exacerbated lung pathology (Pesce et al., 2009b, Nair et al., 2009). Recently a direct role for RELMα has been illustrated in coordinating collagen deposition during wound healing, though inducing fibroblast production of lysyl hydroxylase-2, which subsequently mediates a pro-fibrotic type of collagen cross-linking (Knipper et al., 2015). Consequently, the exacerbated pathology observed by Pesce et al. and Nair et al. may have, in part, been a result of defective healing of wounds caused by tissue migrating larvae. Thus, multiple functions have been attributed to RELMα. Whether these functions of RELMα are reflective of diverse cellular sources or infection-stage specific function remains to be explored.

### 1.2.2 YM1

YM1 is a chitinase-like–protein (CLP) induced through IL-4Rα signalling and which is highly associated with type 2 immunity and pathologies such as asthma and allergy (Loke et al., 2002, Webb et al., 2001, Welch et al., 2002). Chitinase molecules function in degrading chitin, a central component of the extracellular structure of many pathogens, including worms and fungi. Production of AMCase, an active

chitinase, by AAMΦ within the brain of *Toxoplasma gondii* infected mice is essential in controlling the cyst burden in the brain (Nance et al., 2012). Furthermore, blocking AMCase results in reduced airway inflammation and associated eosinophil accumulation in the lung (Sutherland et al., 2011). Thus, the data is suggestive of chitinases being involved in modulating the immune response against chitin containing pathogens. In contrast to enzymatically active chitinases, CLPs are enzymatically inactive and do not bind chitin. YM1 while unable to bind chitin has been shown to bind heparin sulphate, an extracellular matrix protein (Chang et al., 2001). Secreted YM1 proteins readily form crystal structures in the lung and it has been suggested that these structures once ingested would damage the helminth parasite (Ruckerl and Allen, 2014). An active role for YM1 has been suggested in promoting the DC induction of $T_H2$ cell responses (Arora et al., 2006, Cai et al., 2009, Cook et al., 2012). Furthermore, recent work by the Allen lab has demonstrated that YM1 contributes to parasite control through driving γδ T cell expansion and subsequent IL-17-dependent neutrophil recruitment (Sutherland et al., 2014). However as frequently observed in anti-parasite immunity there is a trade-off as YM1 activation recruits neutrophils, which also contribute to lung pathology (Sutherland et al., 2014). In summary direct roles for YM1 have been illustrated, though it is hypothesised that like RELMα and arginase-1, YM1 possess an array of functions that are far-reaching and highly context specific.

### 1.2.3 Arginase 1

The final of the 'Big Three' molecules associated with alternative activation is Arginase-1 (Arg-1). Expression of the enzyme Arg-1 or iNOS nicely demonstrates the mutual exclusivity of between M(IFNγ+LPS) and M(IL-4) as these enzymes compete for their common substrate L-arginine (Munder et al., 1998). This is further exemplified by the suppression of iNOS by Arg-1 (Wijnands et al., 2014). Arg-1 metabolism of L-arginine results in the production of L-Ornithine and urea. L-ornithine is further metabolised by ornithine decarboxylase and ornithine aminotransferase to generate polyamines and prolines (Yeramian et al., 2006, Bronte and Zanovello, 2005). Prolines are essential for the synthesis of collagen and polyamines are needed for cell proliferation and growth (Albina et al., 1993, Igarashi and Kashiwagi, 2000). These data, together within the finding that arginase

expression is often associated with fibrosis, has resulted in M(IL-4) being highly implicated in wound healing (Wynn and Barron, 2010). Indeed, MΦ expressing Arg-1 are implicated in the progressive fibrotic phase of bleomycin induced pulmonary fibrosis (Gibbons et al., 2011). Conversely, through depletion of local L-arginine necessary for cellular proliferation, Arg-1 has been shown to inhibit T cell proliferation (Rodriguez et al., 2007). Following on from this, macrophage-specific depletion of Arg-1 during *S. mansoni* infection resulted in increased mortality as a result of an uninhibited $T_H2$ immune response in the presence of excess L-arginine, which would otherwise be consumed by M(IL-4) (Pesce et al., 2009a). Thus, like RELMα and YM1, Arg-1 is capable of exerting regulatory functions over the $T_H2$ immune response. However an active role in worm killing has also been demonstrated; Arg-1 expressing M(IL-4) coordinate with antigen specific IgG during secondary *Heligmosomoides polygyrus* infection to trap and kill invading larvae (Esser-von Bieren et al., 2013). Importantly, work by Pesce et al. in the lab of Tom Wynn has suggested that arginase expression by MΦ during *S. mansoni* infection is responsible for immunoregulation whereas Arg-1 expression by fibroblast may be more important for wound healing (Pesce et al., 2009a). Consequently, future studies will hopefully elucidate the importance of cellular source as regards the functional impact of Arg-1 expression.

### 1.2.4 Bone-marrow derived and resident derived-M(IL-4) possess distinct activation phenotypes

In addition to driving STAT6 activation, IL-4Rα engagement induces proliferation of MΦs; both local tissue resMΦ and BMDMΦ that have infiltrated into the site of infection (Jenkins et al., 2011). The proliferative program induced by IL-4/IL-13 exceeds that permitted by CSF-1, which controls homeostatic proliferation of resMΦ, thereby allowing the accumulation of a large number of macrophages within tissues during $T_H2$ driven inflammation (Jenkins et al., 2013). In order to determine if distinct profiles of alternative activation are assumed by MΦ generated via local proliferation vs. those recruited into the site of infection Gundra et al. carried out a detailed microarray analysis of MΦ isolated from the peritoneal cavity of IL-4c injected mice and compared these to MΦ isolated from the peritoneal cavity of IL-4c+thioglycollate injected mice (Gundra et al., 2014). While both alternatively

activated resMΦ and BMDMΦ expressed RELMα, YM1 and Arg-1 in response to IL-4 stimulation, they otherwise possessed distinct transcriptional and cell surface phenotypes (See Figure 1-2). Specifically, markers such as PD-L2 and the enzyme Raldh that have long been associated with alternative activation were defined as specific markers of BMDAAMΦ. Furthermore, expression of the mannose receptor, another historic marker of alternative activation, was expressed on BMDMΦ independently of IL-4 exposure. The gene for Uncoupling Protein 1 (UCP-1) was identified as being highly upregulated and specific to resident derived M(IL-4). UCP-1 has previously been thought to be specific to brown adipocytes in where it is important in thermogenesis (Nedergaard and Cannon, 2013, Fedorenko et al., 2012). Functionally, both BMDM(IL-4) and resM(IL-4) inhibited naïve T cell proliferation *in vitro*, however only BMDM(IL-4) were capable of inducing $FOXP3^+$ T regulatory cells and this was a result of Raldh expression. This publication was the first to demonstrate that IL-4 can induce distinct transcriptional programs on differing MΦ populations. Furthermore, the functional capabilities of the macrophage population in response to IL-4 were dictated by their origin.

As aforementioned Bain et al, have recently highlighted that peritoneal and pleural resMΦ populations, while initially seeded prenatally, are continually replenished from the bone marrow. Consequently, I propose that the distinct M(IL-4) activation phenotypes assumed by BMDMΦ vs. resMΦ are a reflection of the effect of IL-4 upon MΦ populations with distinct enhancer landscapes rather than a reflection of origin specific activation phenotypes. Furthermore, the MΦ enhancer landscape prior to stimulation is determined by where a MΦ is in its lifecycle, i.e. – monocyte, intermediate –MoMΦ or resMΦ. These publications have highlighted the diversity of M(IL-4) activation phenotype. Furthermore, the importance of investigating the expression of molecules outside of RELMα, YM1 and Arg-1 when attempting to correlate the M(IL-4) activation phenotype with a specific function is clear.

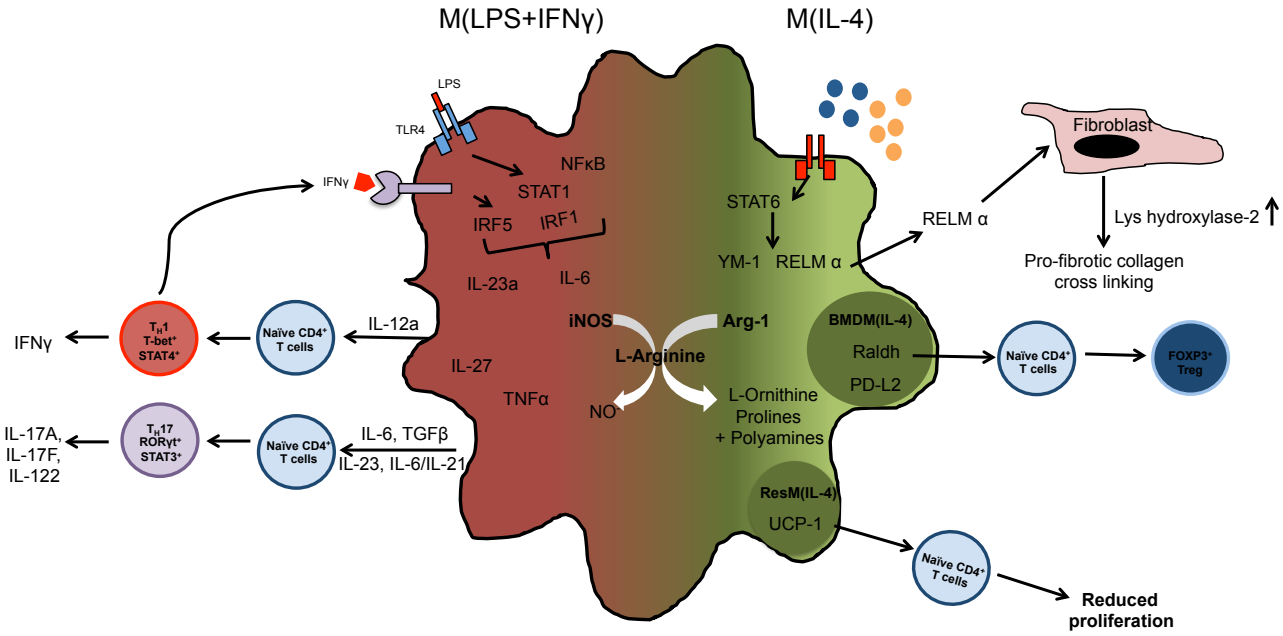


## Figure 1-2 Macrophage activation phenotypes

Activating stimuli such as IL-4 or LPS+IFNγ induce signal transduction cascades within the MΦ resulting in transcription factor activation. Signalling via the IL-4Rα subunit results in STAT6 activation and subsequent expression of molecules RELMα, YM1 and Arg-1. MΦ secreted RELMα is essential in directing wound healing through stimulating fibroblast production of Lys-hydroxylase-2. Arg-1 competes with iNOS for the substrate L-arginine, to generate L-ornithine and polyamines, which are also implicated in wound healing. The transcriptional profile induced by STAT6 is dependent upon the enhancer landscape of a MΦ at the time of activation. For example, IL-4Rα activation of recently recruited BMDMΦ results in the upregulation of the enzyme Raldh and cell surface molecule PD-L2. Furthermore, AABMDMΦ have been shown to both inhibit proliferation and induce FOXP3 expression of naïve T cells *in vitro*. In contrast, IL-4Rα activation of resMΦ results in the expression of the protein UCP-1 and *in vitro* AAresMΦ are associated with the inhibition of T cell proliferation. In contrast to IL-4, MΦ activation via LPS binding to TLR4 results in the expression of transcription factors STAT1 and NFkB which induce the transcription and production of pro-inflammatory cytokines IL-12a, IL-6, TGF-β, IL-23 and IL-21. Depending on the combination of cytokines secreted by the MΦ a naïve T cell can be polarized toward a $T_H1$ or a $T_H17$ phenotype.

## 1.3 Macrophage Function

### 1.3.1 Development

Prenatally derived MΦ are centrally involved in development as evidenced by the severe phenotypes of *Csf$^{op}$/Csf$^{op}$* and *Csf1r-/Csf1r-* mice, which possess inactivating mutations in the CSF-1 gene and the CSF-1R gene, respectively (Cecchini et al., 1994, Dai et al., 2002). These mice are osteopetrotic, increased bone density resulting in brittle bones, due to a lack of osteoclasts which function in hollowing out bone to generate the space in which haematopoiesis initiates (Marks and Lane, 1976). In addition to incomplete bone formation *Csf$^{op}$/Csf$^{op}$* mice are toothless, deaf, present with fertility complications and do not possess tissue resident macrophages including brain microglia (Dai et al., 2002, Erblich et al., 2011). The absence of brain microglia in *Csf1r$^{-/-}$* mice results in defective development of the brain and olfactory system (Erblich et al., 2011). Microglia instruct brain development through phagocytizing synaptic material and pruning synapses post birth (Paolicelli et al., 2011). The central role of phagocytic macrophages in embryonic development is also highlighted by the incomplete removal of the space between digits upon limb budding in *Csf1r-/Csf1r-* mice (Dai et al., 2002). Macrophages are also involved in angiogenesis during development. In retinal development, MΦ limit excessive angiogenic branching of vessels through production of Flt1, the inhibitor of vascular endothelial growth factor (VEGF)(Rao et al., 2007, Stefater et al., 2011).

Development later in life is also highly dependent on macrophages. Mammary gland development at puberty and during pregnancy requires the recruitment of macrophages to the rudimentary mammary duct, where they facilitate outgrowth through phagocytosis of apoptotic epithelial cells (Pollard, 2009).

### 1.3.2 Homeostasis

Within tissues macrophages carry out specialised functions to maintain homeostasis. A central function of the spleen is the recycling of red blood cells to maintain iron homeostasis and this function is carried out by resident red pulp macrophages. As aforementioned, this tissue specific function of red pulp macrophages is driven by heme, which induces the transcription factor SPI-C (Kohyama et al., 2009, Haldar et al., 2014). While the Kupffer cells in the liver are essential in iron recycling under

homeostatic conditions, a recent publication has highlighted that Ly6C monocytes rapidly infiltrate into the liver in response to erythrocyte damage. Within the liver these so called monocyte derived transient macrophages (tMΦ) upregulate ferroportin 1 and function in emergency iron recycling (Theurl et al., 2016). Interestingly, these tMΦ assume a Kupffer cell phenotype but once the stressed erythrocytes are removed, they disappear and the resident prenatally derived Kupffer cells proliferate to reseed the tissue niche (Theurl et al., 2016).

Under homeostatic conditions microglia function in the remodelling of synapses that is necessary for learning (Parkhurst et al., 2013). Microglia possess a quiescent phenotype in order to prevent inflammation-associated damage in the brain. This quiescent phenotype is a result of TGF-β driven SMAD activation and results in the inhibition of phagocytosis and cytokine secretion (Abutbul et al., 2012). Alveolar macrophages (AMΦ), the resident MΦ in the lung are functionally specialised to remove pulmonary surfactant, which is secreted by alveolar epithelia cells to aid gas exchange. The absence of AMΦ macrophages results in the development of pulmonary alveolar proteinosis (PAP), a disease in which individuals struggle to breathe due to in-efficient gas exchange as a result of excess surfactant in the lung (Dranoff et al., 1994).

Within the gut, intestinal macrophages possess an anti-inflammatory phenotype in order to prevent the generation of an immune response against microbiota and food antigens. This anti-inflammatory phenotype is characterised by the secretion of IL-10 and unresponsiveness in the face of TLR engagement (Bain et al., 2013). Breakdown in this intestinal tolerance results in the generation of food allergies or inflammatory bowl disease. In contrast, splenic marginal zone MΦ are specialised in sensing blood borne pathogens, through their expression of PRRs MACRO and SIGN-RI (N et al., 2013).

In recent years, it has come to light that macrophages are important in maintaining insulin sensitivity in white adipose tissue (WAT) and in enabling the thermogenic function of brown adipose tissue (BAT). MΦ in the WAT and BAT of lean individuals possess an alternatively activated phenotype, which is driven by eosinophil derived IL-4, characterised by the transcription factors PPAR-γ, PPAR-δ

and KLF4, expression of $Arg1^+$, $CD206^+$, $CD301^+$ and production of the anti-inflammatory cytokine IL-10 (Lumeng et al., 2007, Wu et al., 2011, Odegaard et al., 2007). In contrast, overconsumption and resultant obesity is marked by the influx of bone marrow derived macrophages into the adipose tissue (Lumeng et al., 2007, Weisberg et al., 2003). These recruited macrophages possess an inflammatory phenotype, characterised by the expression of the enzyme iNOS and production of TNF-α and IL-6, which contribute to insulin resistance through reducing adipocyte expression of glucose transporter 4 (GLUT4) and thereby subsequent uptake of glucose by adipocytes (Lumeng et al., 2007). Production of IL-10 by alternatively activated adipose tissue MΦ can suppress the inflammatory effects of TNF-α on adipocytes, through preventing GLUT4 downregulation and maintaining glucose adsorption (Lumeng et al., 2007). However, in obese mice BMD inflammatory MΦ outweigh the anti-inflammatory derived MΦ resulting in obesity induced diabetes. Exposure to cold environments, results in lipolysis of WAT and induction of thermogenic genes in BAT. Historically it was believed that cold induced thermogenesis was controlled by hypothalamic sensing and subsequent noradrenaline activation of $\beta_3$-adrenergic receptors on WAT and BAT (Lowell and Spiegelman, 2000). However, it is now realised that upon exposure to cold environments adipose tissue macrophages undergo rapid alternative activation and consequently produce catecholamines that drive the expression of thermogenic genes in BAT (*Ppargc1a, ucp1* and *Acsl1*) and lipolysis in WAT(Nguyen et al., 2011). Therefore, macrophages appear to play a homeostatic role in maintaining host sensitivity to insulin and enabling rapid activation of the thermogenic response. Conversely, macrophages are also highly implicated in the low-grade inflammation associated with obesity.

### 1.3.3 Antibacterial immunity

Since the late 1990s it has been known that macrophages and dendritic cells possess an array of cell surface (TLR, CLR) and intracellular pathogen recognition receptors (PRRs; TLRs, RLRs, NLRs) that enable specific pathogen recognition and induction of signalling pathways which results in the secretion of cytokines responsible for polarisation of the subsequent immune response.

TOLL-Like-Receptor-4 (TLR4) that recognises lipopolysaccharide (LPS), the major component of the extracellular coat of gram-negative bacteria, was the first identified pathogen recognition receptor (PRR) (Poltorak et al., 1998). LPS is bound by LPS-binding protein (LBP) in serum that anchors to CD14 on the surface of MΦ and DCs (Wright et al., 1990, Hailman et al., 1994). The LPS-LBP-CD14 complex, subsequently activates TLR-4, which is associated with surface bound MD-2, ultimately resulting in secretion of pro-inflammatory cytokines by the MΦ (Shimazu et al., 1999). Since the discovery of TLR-4, 13 TLRs varying in location (membrane/cytosol) and antigen specificity (bacterial/viral) have been identified. TLR-1, 2, 4, 5 and 6 are specialised in recognising bacterial pathogen associated molecular patterns (PAMPs) whereas TLR-3, 7, 8 and 9 are involved in recognition of viral PAMPs. TLRs are type 1 transmembrane proteins, possessing a leucine rich extracellular horse-shoe shaped domain responsible for antigen recognition and an cytosolic TIR (Toll-interleukin (IL)-1 receptor) domain which propagates antigen binding through induction of intracellular signal transduction pathways. Antigen binding by monomeric TLRs, results in dimerization and recruitment of adaptor proteins MyD88 and/or TRIF to the TIR domain of the cytosolic TLR tail. Recruitment of MyD88 and TRIF cumulates in the activation of transcription factors NF-κB, AP-1 and IRF3 which direct transcription of cytokines, chemokines and anti-viral type I interferons (Akira, 2011). *Salmonella* Typhimurium lipoproteins can be recognised by TLR1/2/6 heterodimers, LPS is recognised by TLR4, TLR-5 recognises the flagella protein Fli C(Broz et al., 2012).

The nucleotide-binding domain (NOD)-like receptors (NLRs) are responsible for the detection of intracellular bacteria. NOD-1 and NOD-2 bind muramyl dipeptide (MDP) of bacterial peptidoglycan resulting in NF-κB activation (Inohara et al., 2003, Pauleau and Murray, 2003). The NODs have received attention due to the association of familial mutations with susceptibility to Crohn's disease; the molecular mechanism underlining this association is not yet understood (Hugot et al., 2001). Conversely, the degree of MΦ activation elicited by MDP activation of NOD2 is considerable lower than that elicited by TLR engagement, suggesting that NOD2 plays a minor role in bacterial detection. Dectin-1 is a cell surface receptor specific for β-glucan the primary component of fungal and yeast cell walls. Dectin-1 is a C-

type lectin receptor (CLR) which possesses an extracellular carbohydrate-recognizing C-type lectin domain and an intracellular ITAM domain which induces signal transduction of NF-κB activation (Kerscher et al., 2013).

Activation of transcription factors NF-κB, AP-1 and IRF results in the secretion of pro-inflammatory cytokines (TNF-α, IL-1, IL-6, IL-12, IL-10), chemokines (MIP-1α, CXCL8), type 1 interferons (IFN-α and IFN-β) and the upregulation of cell surface co-stimulatory molecules necessary for naïve T cell stimulation. Neutrophils are rapidly recruited by the chemokine CXCL8 to the site of infection, where they function to ingest and degrade bacteria.

The production of IL-12 in combination with upregulation of CD80/86 and ICAM by DCs results in polarisation of naïve $CD4^+$ T helper cells toward a $T_H1$ phenotype characterised by the transcription factors T-bet and STAT4 and production of IFN-γ. During *Salmonella* infection monocyte-derived DCs are essential in driving $T_H1$ cell polarisation in lymph nodes (Flores-Langarica et al., 2011). $T_H1$ cell-derived IFN-γ subsequently acts on MΦ and neutrophils resulting in a heightened bactericidal ability through activation of NADPH oxidase and iNOS that generate reactive oxygen species (ROS) and reactive nitrogen species (RNS), respectively. Assembly of NADPH oxidase results in an increase in superoxide ($O_2^-$) within the phagolysosome, which is converted into hydrogen peroxide ($H_2O_2$) by superoxide dismutase. $H_2O_2$ subsequently gives rise to $^{\bullet}OH$, $OCl^-$ and $OBr^-$ (Ischiropoulos et al., 1992, Miller and Britigan, 1997). *Salmonella* Typhimurium genes encoded on *Salmonella* Pathogenicity Island-2 (SPI-2) prevent assembly of NADPH on the salmonella containing vacuole and thereby enable intracellular bacterial survival (Vazquez-Torres et al., 2000).

In addition to promoting bactericidal capabilities of macrophages, $T_H1$ cell derived IFN-γ promotes in antibody class switching toward IgG2a and IgG3 isotypes. Antigen specific antibodies further enhance anti-bacterial immunity through opsonizing extracellular bacteria and activating macrophages and neutrophils via their Fc receptors.

### 1.3.4 Anti-helminth immunity

Helminths are large multicellular parasites of mammals. The term helminth encompasses the platyhelminth and nematode phyla, which split from their common metazoan ancestor over 1 billion year ago. Despite the length of evolutionary divergence between these phyla, all helminths induce a type-2 immune response upon infection of their mammalian host. The nematodes are round worms that can be further subdivided into hookworms, whipworms and filarial taxa. The platyhelminthes are subdivided into cestodes and trematodes (Jenkins and Allen, 2010).

In contrast to type-1 immunity, less is understood about how the innate immune system senses helminth associated molecular patterns and drives the polarisation of the adaptive immune response toward IL-4, IL-13 and IL-5 producing $CD4^+$ $T_H2$ cells. The eggs of schistosome parasites are one of the most potent drivers of type 2 immunity and soluble egg antigen (SEA) promotes $T_H2$ cell induction by DCs. SEA has been shown to bind the C-type lectin receptors DC-SIGN and MGL (van Liempt et al., 2007). Furthermore, SEA has been illustrated to induce the production of innate IL-4 from basophils (Schramm et al., 2003). Indeed basophils have been suggested to be the dominant source of innate IL-4 driving $T_H2$ cell differentiation (Perrigoue et al., 2009). However this data is controversial and does not hold up in *Schistosoma mansoni* infection in which basophil depletion does not affect $T_H2$ cell induction (Phythian-Adams et al., 2010).

Consequently, it has been realised that epithelial cells (ECs) are important players in the initiation and polarisation of the immune response at mucosal surfaces during $T_H2$ immunity against helminthic parasites. ECs produce central cytokines TSLP, IL-25 and IL-33 in response to helminth antigens and tissue damage (Rimoldi et al., 2005, Zeuthen et al., 2008, Angkasekwinai et al., 2007, Humphreys et al., 2008). In response to the intestinal dwelling whipworm *Trichuris muris* ECs produce IL-33 and TSLP (Taylor et al., 2009, Humphreys et al., 2008). IL-25, IL-33 and TSLP promote the generation of a $T_H2$ immune response through activation of innate lymphoid cells (ILCs) that produce polarising cytokines IL-4, IL-13, IL-5, and IL-9 upon activation (Fallon et al., 2006, Moro et al., 2010, Neill et al., 2010, Price et al.,

2010). The protective role of ILC2s against helminthic parasites was first illustrated in *il25*$^{-/-}$ mice, in which the absence of IL-25 prevented ILC2 expansion, $T_H2$ cell induction and consequently expulsion of the parasitic worm *Nippostrongylus brasiliensis* (Fallon et al., 2006).

Engagement of IL-4Rα on intestinal epithelial cells by IL-13/IL-4 increases mucin production (Hasnain et al., 2011) and promotes IEC differentiation into RELMβ producing goblet cells (Artis et al., 2004, Herbert et al., 2009). *In vitro* RELMβ binds to the chemosensory organs of *T. muris* resulting in reduced parasitic movement (Artis et al., 2004). Furthermore, IL-4Rα engagement also promotes increased EC proliferation, resulting in an enhanced turnover rate of intestinal epithelial cells (Akiho et al., 2002, Cliffe et al., 2005). This shedding of the intestinal lining results in displacement of gastrointestinal nematodes from their preferred niche and ultimately results in their expulsion. Furthermore, during *Trichinella spiralis* infection mast cells degrade epithelia cell tight junctions (McDermott et al., 2003), thereby increasing the movement through the gut. Collectively within the gastrointestinal tract IL-4Rα engagement promotes the 'weep and sweep' action of the intestinal lining, which promotes parasitic expulsion.

*H. polygyrus* is a natural murine parasite, which provides a model for intestinal helminthiasis. Infective L3 *H. polygyrus* larvae invade and reside within the intestinal mucosa from day 4-8 pi. By day 8 pi the larvae have moulted to L5 and enter the lumen as adults which subsequently mate and produce eggs that are transmitted through the faeces. During secondary infection with *H. polygyrus,* $CD4^+$ $T_H2$ cell-derived IL-4 drives the accumulation of AAMΦ that provide protective immunity through encysting mucosal tissue invading larvae and promoting their demise in an Arginase-1 dependent mechanism (Anthony et al., 2006). Subsequently, antigen specific IgG antibodies and complement have been shown to mediate the attachment of macrophages and subsequent entrapment of *H. polygyrus* larvae (Esser-von Bieren et al., 2013). These attached Mϕ express Arg-1 resulting in the production of L-ornithine which assists in larval killing through inhibiting worm motility (Esser-von Bieren et al., 2013). Similarly, destruction of *Strongyloides stercoralis* larvae is achieve through the collaborative efforts of MΦ, neutrophils,

complement and antigen specific IgM (Bonne-Annee et al., 2013). These publications were some of the first to demonstrate a role for complement enabling parasite destruction via collaboration with innate immune cells. The complement system encompasses over 30 proteins, primarily inactive proteases produced by the liver and constitutively present in serum. Activation of the complement cascade can occur via one of three pathways and ultimately cumulates in the formation of a membrane attack complex which inserts into bacterial membranes promoting bacterial lysis. Outside of anti-bacterial immunity complement is essential in the clearance of apoptotic bodies and conversely has been highly implicated in the progression of many autoimmune disease (Holers, 2014). Work carried out by Dr. Graham Thomas while a PhD student in the Allen Lab demonstrated that F4/80$^{hi}$ Mϕ isolated from the peritoneal cavity of *Brugia malayi* infected mice highly upregulate C3, the central protein of the complement cascade. This finding was the motivation for our investigation into the phenotype of C3 deficient mice during *L. sigmodontis* infection carried out in Chapter 4.

In contrast to the soil transmitted helminths, vector transmitted filarial nematodes reside in the tissues and are the causative agents of Elephantiasis (lymphatic filariasis) (Evans et al., 1993) river blindness and skin disease (Onchocerciasis)(Davies, 1994). Filarial nematodes are further subdivided based on their tissue niche; lymphatics (*Wuchereria bancrofti* and *Brugia malayi*), subcutaneous tissues (*Onchocerca volvulus* and *Loa loa*) and serous cavities (*Mansonella).*

Infective L3 larvae are transmitted to their human host by either a mosquito or blackfly vector when taking a blood meal. Infective L3 larvae subsequently migrate to their niche tissue where they moult through an L4 stage into adulthood. Within the tissues, adult filariae mate and produce L1 larvae/ microfilaria (mf) that are subsequently transferred to their vector host when taking a blood meal. Within the vector L1 larvae mature into L3 and the cycle continues.

Once established filarial nematodes can persist within their mammalian host for more than 10 years. Currently there are approximately 120 million individuals infected with filarial nematodes, highlighting the global burden of these often neglected

tropical disease (Mendoza et al., 2009). The immune response against filarial nematodes has been a long-standing interest in the Allen lab. Initial investigations into the immune response against filarial nematodes utilized the human filarial *B. malayi.* In this model microfilaria (mf) or adult worms can be directly implanted into the peritoneal cavity of mice and the stage specific immune response examined (Lawrence et al., 1994). However, *B. malayi* cannot mature beyond its implantation stage in the murine host therefore examination of the complete immune response against filarial nematodes was hindered in this model. In 1992, it was discovered that *Litomosoides sigmodontis,* a filarial nematode of the cotton rat, is capable of infecting several murine strains and completes its life cycle in susceptible BALB/c mice, thereby providing an invaluable tool for studying the immune response against filarial nematodes.

## 1.4 *Litomosoides sigmodontis* Infection

*L. sigmodontis* is a filarial nematode of the cotton rat *Sigmodon hispidus* and is a member of the Onchocercidae family (Hoffmann et al., 2000), which includes the human filariae *W. bancrofti, L. loa , Brugia* and *Onchocerca* spp. (Xie et al., 1994, Blaxter and Koutsovoulos, 2015). In 1992 it was discovered by Petit et al. that *L. sigmodontis,* can complete its life cycle in a susceptible murine strain, the BALB/c mouse (Petit et al., 1992) (Figure 1-3). Within this strain, infective L3 larvae migrate from the skin via the lymphatics to the thoracic cavity by day 4 post infection (pi). By day 28 pi L3 larvae have developed into sexually mature adult worms that subsequently mate and produce blood circulating mf that are detectable from day ~55-77 pi. The presence of blood circulating mf is deemed patency, i.e. an infection has reached patency when mf are present in the blood. Adult worms decline in the BALB/c mouse ~ day 80 pi (Graham et al., 2005). Within the C57BL/6 mouse L3 larvae mature to adulthood but are killed ~day 55 pi, prior to the production of mf, consequently the C57BL/6 strain is considered semi-resistant to infection (Graham et al., 2005).

A quantitative analysis of over 85 experiments (approx. 700 mice) highlighted that differences in recovery rate between susceptible BALB/c and resistant C57BL/6 mice are present from day 10 pi, however due to variation in the system this is rarely

evident in a single experiment (Graham et al., 2005). In addition, Graham et al. highlighted a previously unappreciated sex difference in susceptibility to *L.* sigmodontis, with female BALB/c mice displaying a significantly greater worm recovery over BALB/c males from day 10-70 post infection (Graham et al., 2005). Furthermore, the data illustrated that female BALB/c mice were four times more likely to become microfilaremic compared to male BALB/c mice, and adult worms are detectable for at least 10-days longer in the female mice (80 vs 90 days pi) (Graham et al., 2005). Both male and female C57BL/6 mice displayed a significantly lower worm recovery rate when compared to BALB/c from day 10 pi and the same sex-dependent difference in susceptibility was observed at early time points with female C57BL/6 mice being less resistant than males. Following this study our lab have solely used female mice due to their enhanced susceptibility on both strains.

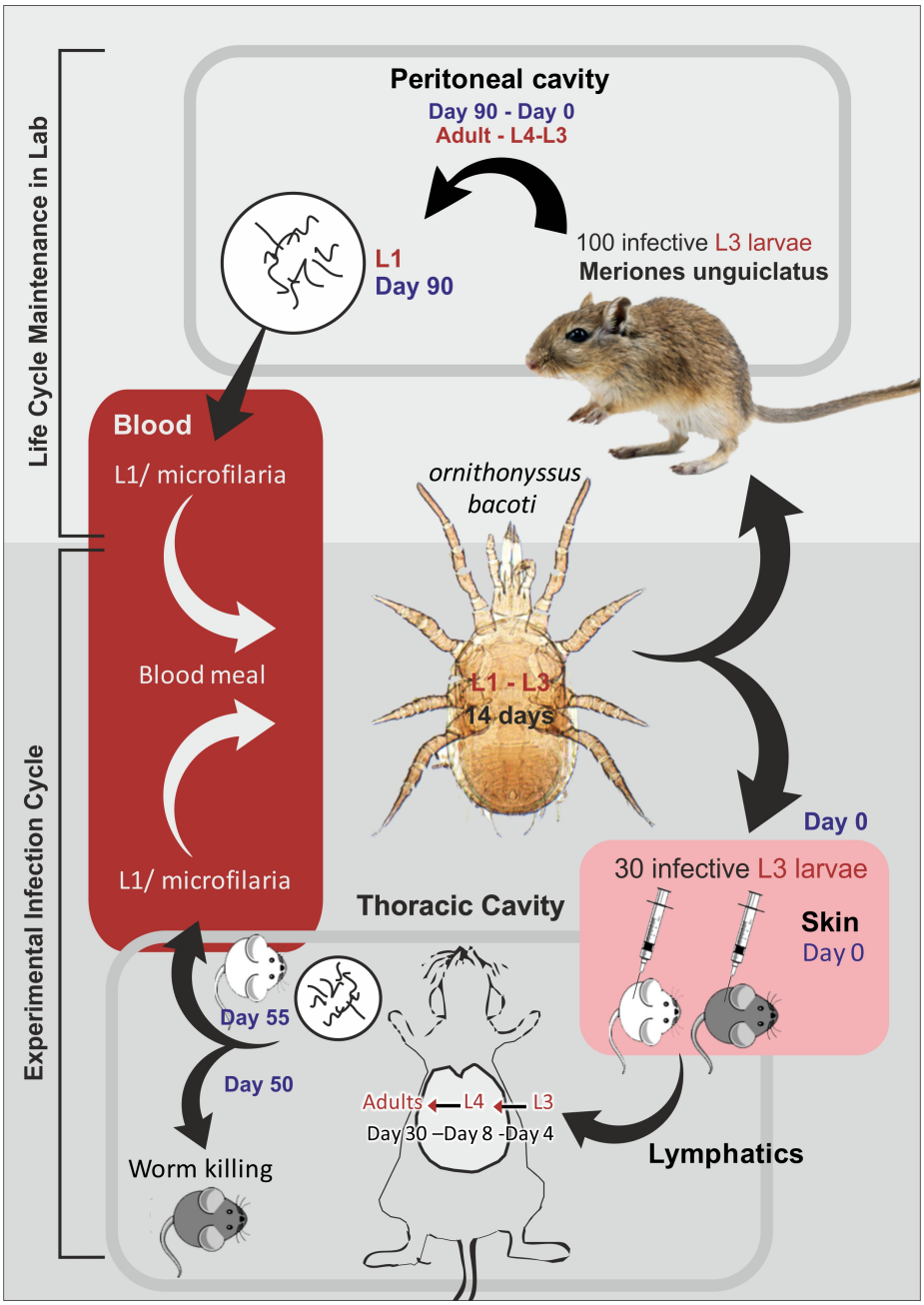


**Figure 1-3 *Litomosoides sigmodontis* life cycle**

The figure illustrates the method used to maintain the *L. sigmodontis* lifecycle in the lab and also the experimental infection of resistant C57BL/6 and susceptible BALB/c mice. Infective L3 larvae are isolated through manual crushing of the mite vector. 100 L3s are used to infect the permissive gerbil host i.p. After 90 days microfilaria can be detected in the bloodstream of infected gerbils. The mite vector is allow take a blood meal for 18 hours, during which microfilaria are acquired. Within the mite vector the microfilaria develop to the infective L3 stage over a period of 14 days. The mites are kept in a temperature and humidity controlled incubator for this period. The mites are then crushed to isolate the L3s. 30 L3s are picked for infection of C57BL/6 or BALB/c mice. The C57BL/6 mice clear infection ~day 50 pi, whereas microfilaria are present in the bloodstream from ~day 55 in the BALB/c strain.

The canonical $T_H2$ cytokine IL-4 is central in resistance to *L. sigmodontis* as IL-4 deficient C57BL/6 mice are susceptible to patent infection with a recovery rate similar to that of BALB/c mice from day 40 pi and blood mf detectible in at day 60 pi (Le Goff et al., 2002). In contrast, IL-4 deficiency on the BALB/c strain does not affect worm development, as recovery rate was unchanged, however the intensity of patent infection is greater in the absence of IL-4, with blood mf counts 100-fold great in IL-$4^{-/-}$ vs. WT BALB/c (Volkmann et al., 2001). These publications highlighted that the mechanism of worm killing in resistant and susceptible strains are likely to be distinct, with the C57BL/6 strain highly dependent upon IL-4, whereas in the BALB/c strain IL-4-effector mechanisms function primarily in reducing female production of mf rather than contributing to worm killing at earlier stages. The IL-4Rα-induced response within tissues is considerable different to that of the gastrointestinal tract; immune cells function in trapping and killing of worms rather than clearance. It is becoming increasingly clear that myriad of immune cells involved in worm killing is likely to be highly parasite, tissue and strain specific. Indeed, eosinophils along with MΦ are a major component of granulomas that form around young adult worms in C57BL/6 mice, with very few neutrophils present(Attout et al., 2008). In contrast, granuloma formation occurs later in the BALB/c strain and encapsulates mature adult worms that are often still alive; neutrophils contribute more than eosinophils to granuloma formation in susceptible BALB/c mice (Attout et al., 2008).

During *L. sigmodontis* infection IL-4 drives the generation of M(IL-4), which express Arg-1 and secrete RELMα and YM1. Subsequent work in the Allen lab discovered that IL-4 is responsible for the MΦ accumulation observed within the thoracic cavity of resistant C57BL/6 mice at day 11 pi, through inducing proliferation of the local tissue resident MΦ population (Jenkins et al., 2011). Studies in $Rag^{-/-}$ mice showed that an adaptive immune cell is the source of IL-4 responsible for alternative activation and macrophage proliferation (Jenkins et al., 2013).

In contrast to IL-4, IL-5 has been implicated in the later worm killing observed in susceptible BALB/c mice, with a 4-fold increased in adult worm numbers in anti-IL-5 treated BALB/c mice compared to controls at day 80 pi. No difference in recovery

rate was observed at day 28 pi in anti-IL-5 treated mice vs. controls, demonstrating the late acting role of IL-5 in worm killing in BALB/c mice (Martin et al., 2000). IL-5 depletion resulted in a decrease in thoracic cavity eosinophils and neutrophils at day 80 pi (Martin et al., 2000). Eosinophils are essential in vaccine-mediated protection against *L. sigmodontis* in both C57BL/6 and BALB/c mice, through rapid destruction of skin invading larvae (Martin et al., 2000, Le Goff et al., 2000). However, eosinophils are unlikely to be involved in primary killing in resistant C57BL/6 mice as IL-5 deficiency has no effect on worm recovery at day 20-40-pi (Le Goff et al., 2000). In susceptible BALB/c mice, IL-5 mediates worm killing through increasing the pleural concentrations of TNF-α, G-CSF and IL-8 resulting in neutrophil recruitment and encapsulation of live worms, eventually causing in worm death (Al-Qaoud et al., 2000). The involvement of neutrophils over eosinophils in worm killing suggested a mixed contribution of both $T_H1$ and $T_H2$ effector mechanism in the eventual death of adult worms in the BALB/c host. Indeed $IFN\gamma^{-/-}$ mice present with 2-fold greater adult worm number at day 80 pi compared to WT mice and fewer worms are encapsulated and this was associated with fewer, less activated neutrophils within the cavity (Saeftel et al., 2001). Furthermore, the increased worm burden of double knockout $IL\text{-}5^{-/-}IFN\gamma^{-/-}$ mice compared to single knockout $IL\text{-}5^{-/-}$ or $IFN\gamma^{-/-}$ mice highlighted that IL-5 and IFNγ work synergistically to promote worm killing (Saeftel et al., 2003). Thus, the later worm killing in susceptible BALB/c mice is a result of IL-5 and IFNγ activation and recruitment of neutrophils that function in encapsulating and killing adult worms. However, the mixed $T_H1/T_H2$ immune response is not specific to the susceptible phenotype with both mice strains presenting with mixed cytokine and antibody responses at day 30 pi(Babayan et al., 2003). Of note however, while mixed, the immune response in resistant C57BL/6 mice is more $T_H2$ skewed with great pleural IL-4, IL-5, IL10 and IgG2 at day 30 pi compared to BALB/c (Babayan et al., 2003).

The dependence of the resistant phenotype upon IL-4 and the central role for IL-4 in alternative activation and proliferation of macrophages, would suggest that macrophages are protective in against *L. sigmodontis* in the resistant C57BL/6 strain. This, hypothesis is consistent with data from secondary *H. polygyrus* infection in which antigen specific IgG bound to MΦ via Fc receptors collaborate with

complement to collectively trap invading larvae (Esser-von Bieren et al., 2013). Similarly during *S. stercoralis* infection MΦ, complement and neutrophils work together to killing the worm (Bonne-Annee et al., 2013). Recent data from our lab has highlighted that during *L. sigmodontis* infection pleural cavity B cells, located within fat associated lymphoid follicles, proliferate and produce antigen specific IgM (Jackson-Jones L et al., Nat Comm in press) and the numbers of FALCs and antigen-specific IgM is greater in resistant C57BL/6 and than susceptible BALB/c mice until day 18 pi (Jackson-Jones L et al., Nat. Comm in press). This data gives credence to the hypothesis that MΦ and antigen specific antibodies collaborate to trap and kill worms within resistant C57BL/6 mice.

In contrast, a detrimental role for B cells during chronic *L. sigmodontis* infection of susceptible BALB/c mice has been illustrated with $JH^{-/-}$ and $\mu MT^{-/-}$ BALB/c mice failing to develop patent infection (Martin et al., 2001) (Knipper JA et al., unpublished data). The contribution of B cells to the resistant and susceptible phenotypes and how antibodies might interact with MΦ to elicit worm killing during *L. sigmodontis* infection requires further study. MΦ have been implicated in mediating the immunosuppressive phenotype that accompanies chronic filarial infection (Loke et al., 2000). As such, MΦ isolated from the pleural cavity of susceptible BALB/c at both day 40 and 60 pi inhibit T cell proliferation *in vitro (Taylor et al., 2006)*. The transgenic overexpression of IL-10 by MΦ on the FVB background, which is normally resistant to *L. sigmodontis* results in this strain becoming susceptible with patent infection pursuing (Specht et al., 2012). Hoffman et al. have also demonstrated that IL-10 is a critical susceptibility factor and that B cells may be a major IL-10 source (Hoffmann et al., 2001). Thus, unravelling the role of B cells in *L. sigmodontis* infection is complicated by the potential of B cells to play potentially conflicting roles.

Immunosuppression within the BALB/c strain in addition to the presence of immunosuppressive MΦ is marked by the emergence of a hyporesponsive T cell phenotype during patency (Taylor et al., 2006). Using IL-4gfp 4get mice, to track antigen specific $T_H2$ cells, van der Werf et al., demonstrated that between day 20 and day 60 post infection in BALB/c mice antigen specific $T_H2$ cells loose their ability to

produce IL-4, IL-5 and IL-2(van der Werf et al., 2013). This hyporesponsive phenotype is correlated with the increased expression of programed death -1 (PD-1) on T cells. Furthermore using anti-PD-L1/anti-PD-L2 antibodies, PD-L2 was identified as being responsible for the induction of this phenotype. However, the PD-L2 expressing cell that induces PD-1 expression, and the subsequent hyporesponsive T cell phenotype has not been identified (van der Werf et al., 2013).

In summary, the mechanisms of worm killing are likely to be quite different between resistant C57BL/6 and susceptible BALB/c mice. The data would suggest that IL-4 and by association MΦ are important in worm killing and prevention of patency on the C57BL/6 background (Le Goff et al., 2002). Conversely, IL-4 does not appear to play a role in worm development in the susceptible strain and to date an immunosuppressive function has been assigned to MΦ in this strain (Volkmann et al., 2001) (Taylor et al., 2006).

## 1.5 Aims of Thesis

While the knowledge surrounding macrophage function is steadily increasing, the relationship between macrophage origin and function during helminth infection has remained unexplored. To date the literature has demonstrated that there is a proliferative burst of the resMΦ population, which is derived prenatally, by day 11-post infection with *L. sigmodontis* (Jenkins et al., 2011, Yona et al., 2013). This proliferative burst is followed by a proliferative crash, in which proliferation is below homeostatic levels, until day 28 pi (Graham Thomas –PhD thesis 2013). Yet, Babayan et al. have documented the peak of MΦ accumulation within the pleural cavity as occurring at day 30 pi. This peak in pleural cell accumulation at day 30 pi was evident in both resistant and susceptible strains, with a trend toward enhanced numbers in the resistant C57BL/6 strain (Babayan et al., 2003). Thus, the peak of cellular accumulation correlates with worm killing in the resistant C57BL/6 strain, which is most evident between day 20 and 40 pi (Le Goff et al., 2000). However, the composition of the MΦ compartment in both resistant and susceptible strains remains unexplored. Additionally, a protective role for MΦ in resistance to filarial infection has yet to be illustrated. More broadly, the functional consequences of MΦ dynamics and source, during tissue nematode infection has yet to be fully understood in either susceptible or resistant host.

Consequently, the core aim of this thesis has been to investigate and compare the mechanisms of MΦ accumulation and MΦ origin within the pleural cavity of resistant C57BL/6 versus susceptible BALB/c mice with the ultimate aim of understanding the functional consequences of diverse mechanisms of MΦ accumulation or source.

Findings that emerged during this thesis led to two additional sub aims:

1. Is complement involved in the resistant phenotype of C57BL/6 mice?
2. Does the macrophage disappearance reaction reflect functional differences in bactericidal capabilities between BMDMΦ and resMΦ?

# Chapter 2 Macrophage dynamics are central to understanding resistance and susceptibility to *Litomosoides sigmodontis* infection

## 2.1 Summary

Infection with the filarial nematode *Litomosoides sigmodontis* results in IL-4 driven proliferative expansion of resident pleural cavity macrophages (MΦ) in a process independent of bone marrow derived macrophage (BMDMΦ) recruitment. Resident macrophage (resMΦ) populations within the serous cavities are derived prenatally from the foetal liver, independent of haematopoietic stem cells from the bone marrow. Consequently, I became interested in the functional importance of resMΦ proliferation vs. BMDMΦ recruitment to worm clearance and ultimate outcome of *L. sigmodontis* infection. C57BL/6 mice are resistant to *L. sigmodontis* infection as adult worms are killed prior to sexual maturity, in contrast BALB/c mice are susceptible with adult worms successfully mating and producing circulating microfilaria ~ day 55-post infection (pi). In order to investigate the contribution of resMΦ proliferation vs. BMDMΦ recruitment to resistance and susceptibility I analysed the pleural exudate cells of infected C57BL/6 and BALB/c mice over the course of infection. Resistance was associated with resMΦ proliferation, resulting in a significantly greater accumulation of pleural macrophages in resistant C57BL/6 mice vs. BALB/c from day 11 pi. Importantly, the resMΦ population in both naïve and infected animals was continually replenished from the bone marrow with age, highlighting the successful integration of BMDMΦ into the resident niche in this strain. In contrast, susceptibility was marked by an influx of monocytes and their conversion into F4/80$^{lo}$ (MoMΦ) from day 35. These infiltrating BMDMΦ did not successfully integrate into the resident resMΦ pool and resulted in a decline in its dominance within the pleural space. Ultimately, these data highlight the diverse MΦ dynamics present in the pleural cavity of both naïve and infected C57BL/6 and BALB/c mice and suggest opposing roles for resMΦ and BMDMΦ in worm killing.

## 2.2 Introduction

*L. sigmodontis* is the only filarial nematode capable of completing its life cycle in a susceptible laboratory mouse strain (BALB/c) and thus providing a model in which

to study the immune response to human filarial worms such as *Onchocerca volvulus* and *Wuchereria bancrofti* (Hoffmann et al., 2000).

*L. sigmodontis* L3 larvae which are isolated from infected mites and injected subcutaneously (30 L3/mouse) migrate via the lymphatics to the pleural cavity by ~day 4 pi. Larvae in the pleural cavity undergo two moults developing into sexually mature adults. In susceptible BALB/c mice the adult female worms produce microfilaria (mf), which enter the blood stream from day 55-60 pi. Once mf are circulating in the blood the infection is said to have become patent or to have reached patency. In contrast to BALB/c mice, C57BL/6 mice are resistant; the adult worms are killed prior to sexual maturity, patency never develops and the number of worms recoverable from the pleural cavity declines from ~day 22-55 pi (Hoffmann et al., 2000, Graham et al., 2005)

I am interested in the role that macrophages (MΦ) contribute to the resistant and susceptible phenotypes, through participating in worm killing or immunosuppression, during *L. sigmodontis* infection, specifically focusing on the influence of origin and residency upon disease outcome. In recent years, it has come to light that certain resident macrophage (ResMΦ) populations (microglia, liver Kupffer cells, epidermal Langerhans cells, splenic red pulp macrophages, peritoneal, and lung alveolar macrophages) are initially derived from F4/80$^{hi}$ yolk-sac and foetal liver MΦ independent of the establishment of haematopoietic stem cells (HSCs) (Yona et al., 2013, Schulz et al., 2012, Ginhoux et al., 2010). These ResMΦ populations are long-lived and capable of self-maintenance through in situ proliferation driven by colony stimulating factor 1 (CSF-1) or IL-34 (Hashimoto et al., 2013, Schulz et al., 2012). HSCs give rise to F4/80$^{lo}$ bone marrow derived monocytes (BMDMs) that continually replenish short-lived resident macrophage populations such as those in the gut (Bain et al., 2014). Furthermore, F4/80$^{lo}$ BMDMs infiltrate into tissues upon an inflammatory insult, such as bacterial infection, often causing the disappearance of the ResMΦ population (Barth et al., 1995). Despite their disappearance it has been shown that after an acute inflammatory insult, surviving ResMΦ undergo a CSF-1 driven proliferative burst to restore the ResMΦ pool (Davies et al., 2011).

In a genome wide expression array, F4/80$^{hi}$ and F4/80$^{lo}$ macrophages from naïve animals at embryonic day 16.5 clustered separately, illustrating that ontogeny has a direct impact upon MΦ function. F4/80$^{hi}$ macrophages were enriched in transcripts *Maf, Cx3cr1* and *Csf1r*, whereas F4/80$^{lo}$ MΦ displayed a transcriptional phenotype associated with BMDMs (*Gata2, Ccr2, Flt3*) (Schulz et al., 2012). These data suggested that F4/80$^{hi}$ tissue ResMΦ possess an underlying transcriptional profile determined by their origin, which would dictate their functional capabilities. Beyond the importance of origin, tissue specific transcription factors are implicated in driving further tissue MΦ differentiation. *Sall1* has been identified as a transcription factor enriched in microglia, *Car4* in lung macrophages, *Clec4f* in Kupffer cells and *Spi-c*, and G*ata6* in red pulp MΦ and peritoneal MΦ respectively (Lavin et al., 2014, Yang et al., 2013, Kohyama et al., 2009, Okabe and Medzhitov, 2014).

The local microenvironmental signals which drive these tissue-specific transcription factors have remained elusive until recent years. Within the spleen, heme has been shown to mediate *Spi-c* expression, thereby driving the efficient iron recycling function of splenic red pulp MΦ (Kohyama et al., 2009, Haldar et al., 2014). Similarly, TGF-β is necessary for the development of microglia and promotes the specific transcriptional profile associated with this resMΦ population (Abutbul et al., 2012, Butovsky et al., 2014). Within the peritoneal cavity, the transcription factor GATA6 has been identified as an essential regulator of resMΦ phenotype (Rosas et al., 2014, Okabe and Medzhitov, 2014). GATA6 expression is regulated by omentum-released retinoic acid, derived from dietary vitamin A. A subset of 44 genes were identified as being specific to peritoneal macrophages when compared to lung, liver, spleen, intestine and adipose tissue MΦ. Expression of 39 % of these 44 genes is GATA6-dependent. This illustrates that, while the vitamin A- retinoic acid-GATA6 axis is one dimension of control, additional transcription factors must be responsible for the regulation of the remaining 61 % of peritoneal MΦ specific genes. One such GATA6-indepenent gene is *Cd102*, which encodes the cell surface integrin CD102/ICAM2 (Okabe and Medzhitov, 2014).

TIM4 is a type 1 transmembrane protein responsible for binding phosphatidylserine on the surface of apoptotic cells that has also been used to identify resMΦ in the

peritoneal cavity (Miyanishi et al., 2007, Davies et al., 2011). The GATA6 dependence of TIM4 expression is unclear. The total number of $TIM4^{+}$ resMΦ are significantly decreased in mice which specifically lack GATA6 in the myeloid compartment. However this could be reflective of the total decrease in MΦ number also observed (Rosas et al., 2014). Furthermore, *Tim4* does not appear in a list of the 44 most changed genes in myeloid specific GATA6 KO mice (Okabe and Medzhitov, 2014).

It remains controversial whether origin is the determining factor in enabling a population to carry out its specific function or whether BMDMΦs can acclimatise and replace prenatally derived resMΦ i.e. during infection or with age. Recently some progress has been made on this front; BMDMΦs transplanted into lethally irradiated hosts assumes an enhancer profile of the host embryonically derived macrophages in a tissue-specific manner. This included the *Gata6* locus for peritoneal macrophages (Lavin et al., 2014). The development of a $Kit^{MercreMer}$ fate-mapping mouse has illustrated that most tissue resident macrophage populations, with the exception of microglia and dermal Langerhans cells, are derived from HSC (Sheng et al., 2015). Macrophages of yolk sack, foetal liver, and bone marrow origin have been shown to differentiate into functional alveolar macrophages (AMΦ) when transferred into GM-CSF knock out mice, which lack AMΦ due to their developmental dependence on this cytokine (van de Laar et al., 2016). Once isolated, the AMΦ of distinct ontogenies had assumed a near identical transcriptional profile to that of wild type AMΦ and few ontogeny related transcripts could be described (van de Laar et al., 2016). Thus local conditioning factors and perhaps to a lesser degree origin can shape the transcriptional status of a mature MΦ population. This status is likely to determine the functional response of the population upon exposure to inflammatory stimuli such as TLR agonists or polarising cytokines.

IL-4 is the central cytokine of type 2 immunity. In its absence resistant C57BL/6 mice are rendered susceptible to *L. sigmodontis* infection, with blood mf detected at day 60 pi (Le Goff et al., 2002). IL-4 induces proliferation of resMΦ, enabling a large increase in local pleural MΦ number by day 11 pi with *L. sigmodontis* (Jenkins et al., 2011). Through the use of clodronate-loaded liposomes and bone marrow

chimeric mice, this local expansion was shown to be independent of F4/80$^{lo}$ blood monocytes. The proliferative program induced by IL-4 supersedes homeostatic proliferation permitted by CSF-1(Jenkins et al., 2013).

In addition to proliferation, IL-4 polarises macrophages toward an M(IL-4) activation phenotype, characterised by expression of RELMα, Ym1, and arginase-1. Gundra et al. has demonstrated that while both recently recruited BMDMΦ and resMΦ populations can assume an M(IL-4) activation phenotype (Arg1$^{+}$, Ym1$^{+}$, RELMα$^{+}$), these two populations are otherwise phenotypically and functionally distinct (Gundra et al., 2014). Microarray analysis clearly illustrated that M(IL-4) derived from the BM and resMΦ possess diverse transcriptional profiles and subsequently cell surface phenotypes (Gundra et al., 2014). Thus, these data suggests that the function of a cellular population in response to polarising stimuli is affected by origin.

Macrophage numbers increase greatly in the pleural space during *L. sigmodontis* infection, making them one of the most abundant cell types in both resistant and susceptible strains. While a dominant cell in the pleural space of both strains, previous studies have highlighted a trend toward greater total MΦ number in the resistant C57BL/6 strain over the BALB/c at day 30 pi (Babayan et al., 2003). Given our increased knowledge of macrophage origin and proliferation, I decided to investigate if the mechanisms of macrophage accumulation are equal between strains. In particular I wanted to ask if the resident macrophage population generated via local proliferation was involved in worm killing or if there was a need for an influx of monocytes, with greater anti-helminthic capabilities, from the bone marrow. Conversely, I was interested in how the MΦ dynamics in the susceptible strain may differ from that in the resistant C57BL/6 mice.

To address these questions I have examined the dynamics of pleural cell accumulation over the course of *L. sigmodontis* infection in both C57BL/6 and BALB/c mice, focusing specifically on the macrophage compartment. I chose to look at day 11, 28, 35 and 50- post infection in both strains. Previous work in the lab has identified day 11 as the peak of macrophage proliferation, prior to day 30 pi. In order to address the developmental progress of the worm between strains, I chose day 28 pi; a time point at which the worm should be moulting into adulthood. The peak of

pleural cell accumulation has previously been noted to occur ~day 35, thus I chose this date in the hope of identifying differences in the cellular infiltrate which may correlate with worm killing. Lastly, I chose to investigate day 50 pi as this is prior to the onset of patency in the BALB/c (~day 55 pi) strain and the infection should still be active in the C57BL/6 strain.

Expression of colony stimulating factor receptor 1 (CSF-1R) and CD11b were used to identify the total macrophage population. CX3CR-1, also known as the fractalkine receptor, is a chemokine receptor expressed by monocytes, DCs, subsets of NK cells and T cells but not by most differentiated macrophage populations. In CX3CR1-GFP reporter mice the resident macrophage population are $CX3CR1^{-}GFP^{-}$, which express high levels of the cell surface marker F4/80 and low levels of MHC II (Jung et al., 2000). Furthermore, through the use of partial-bone marrow chimeric mice our lab has verified $F4/80^{hi}$ as a resolute marker for resident macrophages. The remaining $F4/80^{lo}$ population constitutively represents 10-20% of the MΦ compartment, express a high level of MHC II and label $CX3CR1\text{-}GFP^{hi}$, illustrating the bone marrow origin of this population (Ghosn et al., 2010, Jung et al., 2000). Due to the influx of monocytes into the macrophage compartment during infection I further divided the $F4/80^{lo}$ cells into MoMΦ ($F4/80^{lo}MHC^{hi}Ly6C^{-}$), and recently recruited monocytes ($F4/80^{lo}MHC^{lo\text{-}hi}Ly6C^{+}$). I stained for the transcription factor GATA6 and the cell surface molecules CD102 and TIM4 in order to look at tissue-specific markers of residency. These markers have been described for the peritoneal cavity and pleural cavities (Rosas et al., 2014, Bain et al., 2016).

## 2.3 Results

### 2.3.1 Differences in worm recovery and pleural cell accumulation are evident from day 11 post infection.

WT C57BL/6 and BALB/c female mice were infected with 30 L3s subcutaneously into the scruff. In order to quantify worm recovery the pleural cavity was washed at each time point pi. As expected, a greater degree of worm killing was seen in the C57BL/6 strain over the time course. From day 11 pi there was already a trend toward fewer worms being recovered from infected C57BL/6 mice versus BALB/c, this trend continued and enhanced worm killing in the C57BL/6 strain resulted in significant differences in recovery rate at day 35 and day 50 pi compared to BALB/c mice (Figure 2-1A). It must be noted that the data represented here are a combination of two separate experiments; one with time points day 11 and 28 pi and the second with time points day 35 and 50 pi. A single experiment with all four time points was carried out (See Appendix 1), however due to the time it takes to count infectious doses and infect 48 animals, this experiment was inconsistent. Consequently I decided to combine two of the most representative experiments for presentation here. As a result, the apparent 'increase' in recovery rate between day 28 and 35 pi in the susceptible BALB/c strain is a reflection of experimental variance; worm number cannot increase within the host (Figure 2-1A). By day 50 pi, the number of recoverable worms from the C57BL/6 strain had decreased to ~7% (~2 worms/mouse) of the initial dose. In contrast, ~37% (~11 worms/mouse) were still recovered in BALB/c mice (Figure 2-1A). In addition, by day 35 worm growth was stunted within the C57BL/6 host compared to BALB/c mice, with shorter male and female worms recovered from the pleural space (Figure 2-1B). Differences in female worm length were still observed at day 50 pi (Figure 2-1B). However differences in male worm length were not always significant (See Appendix 2). Variation in worm width was only seen between female worms at day 35 pi with narrower worms recovered from the C57BL/6 host. While this difference in worm recovery rate and worm health at day 35 and 50 is consistent with a meta-analysis of strain differences, previous studies failed to obtain statistically significant differences at day 30 pi from a single experiment (Graham et al., 2005, Babayan et al., 2003).

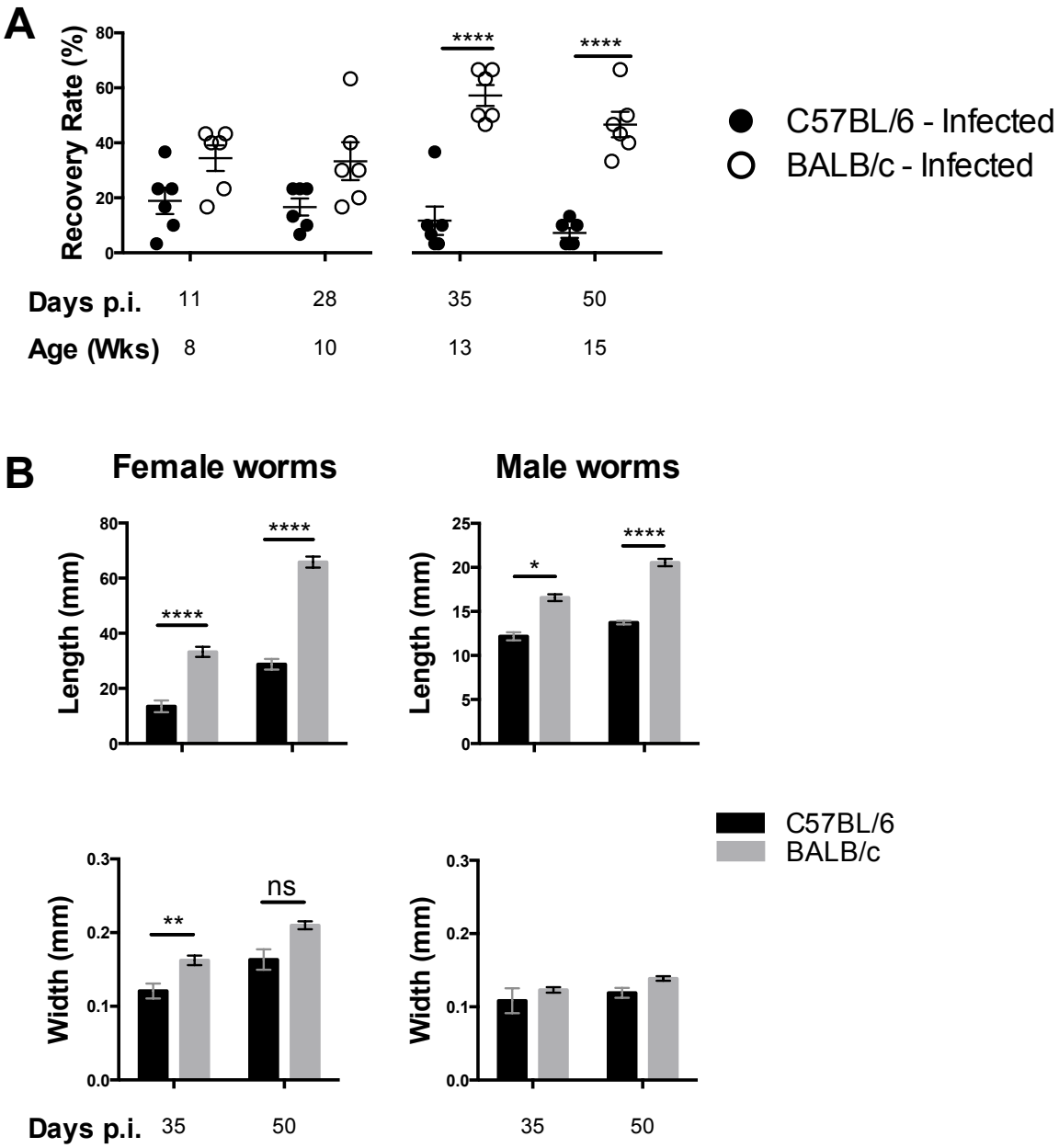


## Figure 2-1 Differences in worm survival and health are evident from day 35 pi

C57BL/6 and BALB/c female mice, aged 6-8 weeks, were infected with 30 infective *L. sigmodontis* L3 larvae subcutaneously (s.c) and sacrificed on days 11, 28, 35 and 50 pi via anaesthetic overdoes followed by cutting of the brachial artery. The pleural cavity was washed with 10 ml RPMI (1 % pen-strep, 1 % L-glutamine) to isolate the pleural cells and surviving worms **(A)** Percentage of the worms recovered from the pleural space upon necroscopy. **(B)** Length and width of the female and male worms isolated from the pleural cavity of infected C57BL/6 and BALB/c hosts at day 35 and 50 pi. The worm recovery data is representative of three independent experiments, with 6 mice per time point. The break in graph **(A)** illustrates that two separate experiments are presented. Significance was determined via 2-way ANOVA and Bonferroni's test.

In addition to worm recovery, the pleural cavity was washed to obtain the pleural exudate cells (PLEC) for quantitative analysis via multiparameter flow cytometry. The staining and gating strategy illustrated in Figure 2-2 was used to determine which cellular populations contributed to the heightened cell number in C57BL/6 mice. Overall, significantly more total cells were isolated from the pleural cavity of infected C57BL/6 compared to BALB/c mice from day 11-35 pi (Figure 2-3A). There were a greater number of neutrophils present in cavity of C57BL/6 mice at day 28 and 35 pi, however this cell type accounts for <1% of the total cells present at these time points (Note scale at $10^5$) (Figure 2-3B). T cell number did not differ until day 50 pi, with greater numbers of T cells isolated from BALB/c mice (Figure 2-3C). B cell numbers, peak in the cavity at day 28 and while the trend of B cell accumulation was similar between strains, the number found in C57BL/6 mice was twice that found in the BALB/c mice between day 28-50 pi (Figure 2-3D). Eosinophils were the cell type that increased most relative to naïve animals. Differences in eosinophil number were not observed at day 28/35 pi, however greater numbers were present in the C57BL/6 strain at day 11 and significantly more were isolated from the BALB/c strain at day 50 (Figure 2-3E).

The most striking finding was the difference in macrophage cell numbers over the course of infection (Figure 2-3F). By day 11 pi there was a 18-fold increase in the number of macrophages in infected C57BL/6 mice relative to naïve, compared to a 4-fold increase in the BALB/c strain. This initial difference in macrophage accumulation resulted in six times the number macrophages in the C57BL/6 strain as there was in the BALB/c mice at day 11 pi (Figure 2-3F). A considerable difference in macrophage number between strains was maintained throughout the time course (Figure 2-3F).

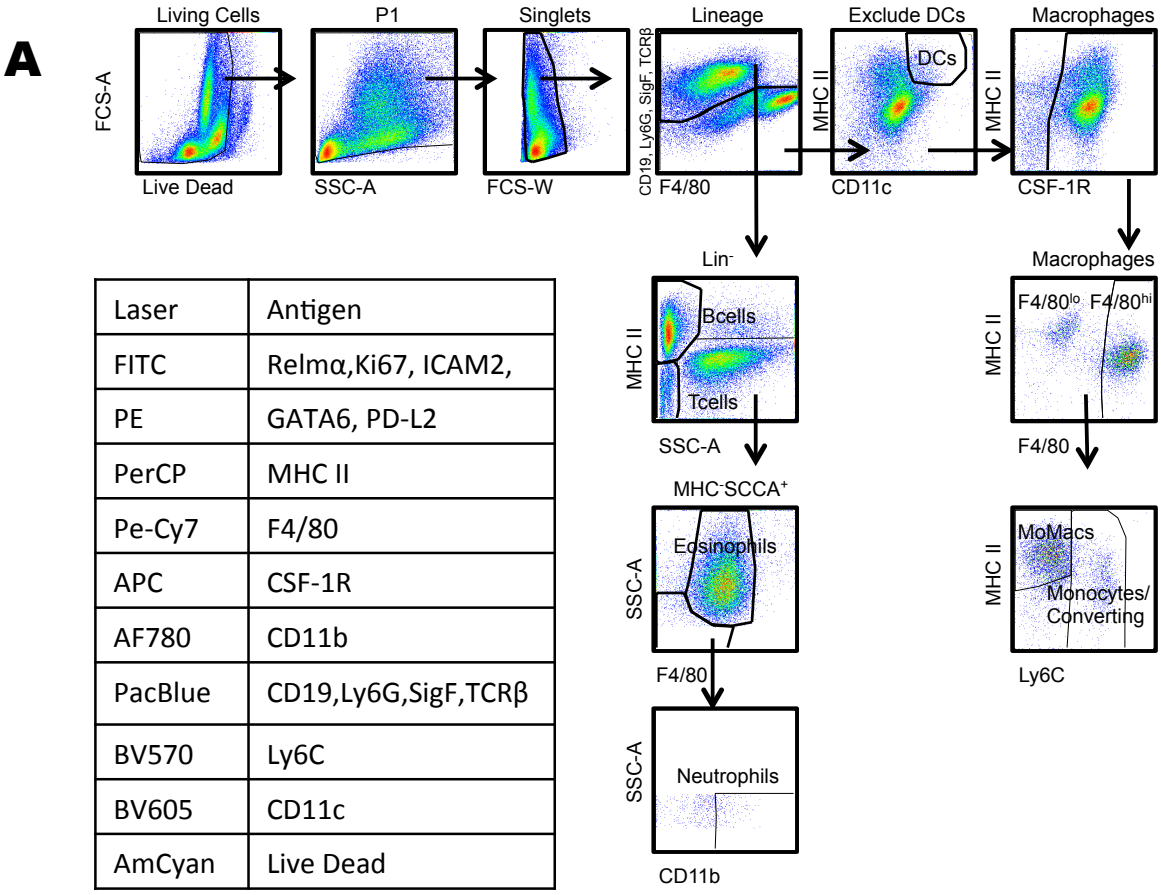


| Laser | Antigen |
|---|---|
| FITC | Relmα,Ki67, ICAM2, |
| PE | GATA6, PD-L2 |
| PerCP | MHC II |
| Pe-Cy7 | F4/80 |
| APC | CSF-1R |
| AF780 | CD11b |
| PacBlue | CD19,Ly6G,SigF,TCRβ |
| BV570 | Ly6C |
| BV605 | CD11c |
| AmCyan | Live Dead |

**Figure 2-2 Gating strategy used to identify pleural leukocyte populations.**

C57BL/6 and BALB/c female mice, aged 6-8 weeks, were infected with 30 infective *L. sigmodontis* L3 larvae subcutaneously (s.c). Mice were sacrificed on days 11, 28, 35 and 50 pi via an anaesthetic overdoes followed by cutting of the brachial artery. The pleural cavity was washed with 10 ml RPMI (1 % pen-strep, 1 % L-glutamine) to isolate the pleural exudate cells (PLEC) and surviving worms. The PLEC was plated at $1X10^6$ cells/200 µl / well and washed twice in PBS prior to incubation with an Aqua Live Dead Stain, a blocking reagent and surface staining antibodies. Following staining for surface antigens the cells were permeabilized overnight in 100 µl of 1X permeablization buffer, eBioScience. Samples were subsequently acquired on an LSR II **(A)** The gating strategy and various antibody-staining panels used to identify the cellular populations within the PLEC.

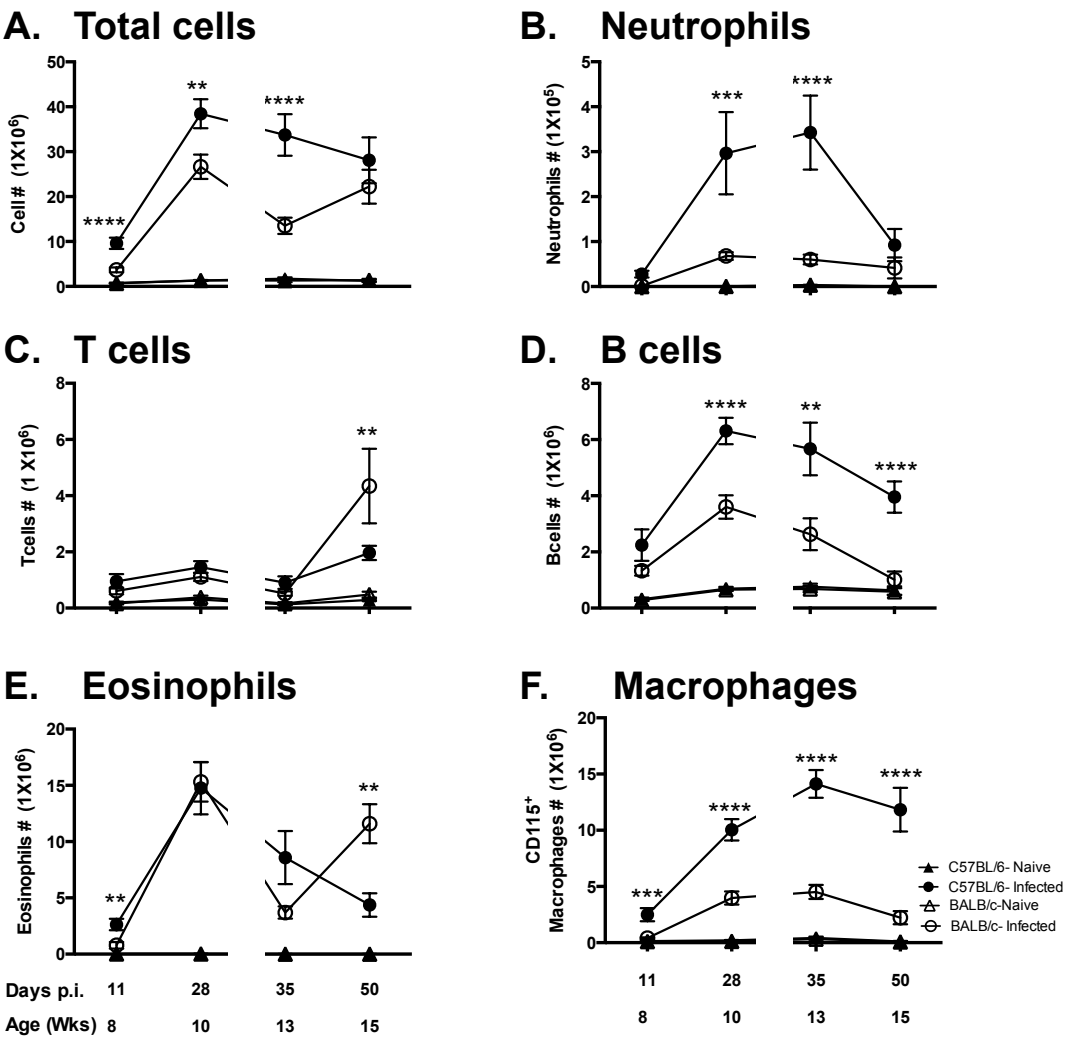


## Figure 2-3 Enhanced MΦ and B cell numbers are associated with resistance

C57BL/6 and BALB/c female mice, aged 6-8 weeks, were infected with 30 infective *L. sigmodontis* L3 larvae subcutaneously (s.c). Mice were sacrificed on days 11, 28, 35 and 50 pi via an anaesthetic overdoes followed by cutting of the brachial artery. At each time point the pleural cavity was washed out with 10 ml RPMI (1% LG, 1% PS). The pleural cell populations were identified via flow cytometry using the vigorous gating strategy illustrated in Fig2-2. **(A)** Total cells **(B)** neutrophils **(C)** T cell **(D)** B cells **(E)** Eosinophils **(F)** Macrophages. Data are representative of three independent experiments with 6 mice/group/time point. The break in the graphs illustrates that animals from day 11&28 were infected on a single day and animals from day 35 & 50 were infected on a separate day. A 2-way ANOVA was carried out at each time point. * P<0.05, ** P<0.01, ***P<0.0001,**** P<0.00001. Bars are representative of the mean ± SEM

### 2.3.2 Failure to expand and maintain a resident cell population distinguishes susceptibility from resistance

To determine the contributions of resident and bone marrow derived macrophage populations to the overall macrophage number during infection, I divided the compartment into three sub-populations; F4/80$^{hi}$, MoMΦ and Monocytes (Figure 2-4A). This revealed that the difference in total MΦ number between strains was a result of heightened F4/80$^{hi}$ cells in C57BL/6 mice (Figure 2-4B&C). There were more MoMΦ in the C57BL/6 strain at day 11 pi however; numbers did not differ throughout the remainder of the time course (Figure 2-4D). A significant influx of bone marrow derived Ly6C$^{+}$ monocytes was seen in the cavity of the BALB/c strain at day 35 and day 50 pi that was not observed in the C57BL/6 mice. (Figure 2-4E).

In naïve C57BL/6 controls the F4/80$^{hi}$ population (Blue) constituted 80-90% of the total MΦ population (Figure 2-5A). The remaining 10-20 % of the MΦ compartment was composed of MoMΦ (Green). There was negligible contribution of monocytes to the MΦ population in the C57BL/6 strain (Red) (Figure 2-5A). In naïve and infected BALB/c mice, the F4/80$^{hi}$ population represented 70-80 % of the MΦ compartment at day 11 pi, slightly lower than what was observed in the C57BL/6 strain (Figure 2-5B). There was a trend toward a decline in the percentage of F4/80$^{hi}$ cells contributing to the MΦ pool in naïve C57BL/6 mice with age and this was prevented by infection (Figure 2-5A). A similar, yet more pronounced decline in the percentage of the F4/80$^{hi}$ population contributing to the MΦ compartment was observed in naïve and infected BALB/c mice (Figure 2-5B). This decline is marked by a corresponding increase in percentage of bone marrow derived MoMΦ in the cavity. Infection in BALB/c mice did not prevent this age related decrease in F4/80$^{hi}$ cell percentage but exacerbated their decline through recruitment of monocytes from the bone marrow (Figure 2-5B). Infection driven expansion of the F4/80$^{hi}$ MΦ population in the BALB/c strain was less than a third of that seen in the C57BL/6 strain (Figure 2-5C&D). Consequently, by day 50 pi in the BALB/c strain, MoMΦ and Monocytes represent >50 % of the macrophage pool (Figure 2-5B&D).

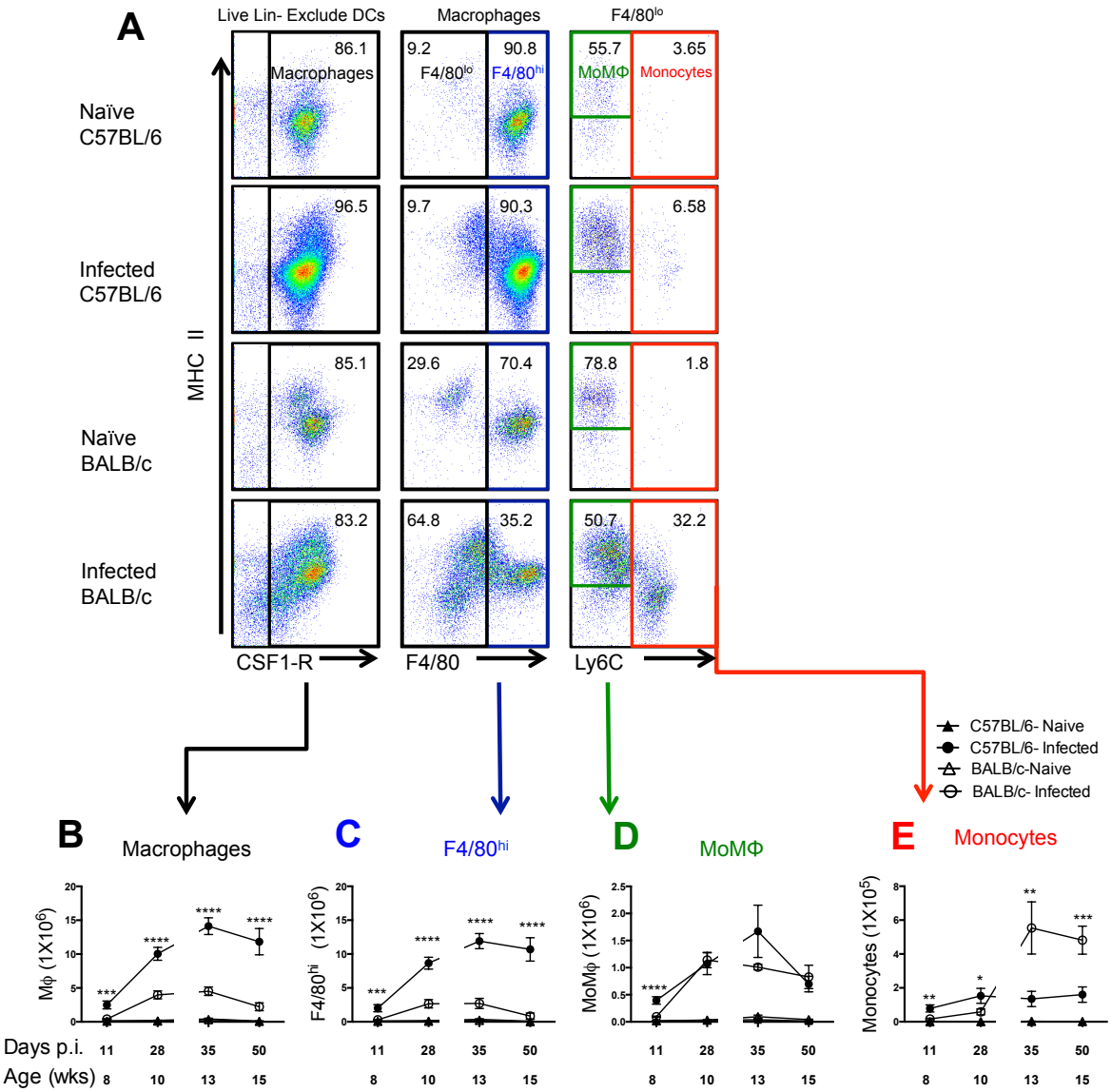


## Figure 2-4 Differences in MΦ numbers is a result of heightened F4/80$^{hi}$ cells in the C57BL/6 strain

C57BL/6 and BALB/c female mice, aged 6-8 weeks, were infected with 30 infective L3 *L. sigmodontis* larvae subcutaneously (s.c). Mice were sacrificed on days 11, 28, 35 and 50 pi and the pleural cavity was washed out with 10 ml RPMI (1% LG, 1% PS) to isolate the PLEC and surviving worms. **(A)** representative FACS plots from day 35 pi showing the gating strategy to identify and divide the macrophage population (CSF-R1$^{+}$) into subpopulations. The increase in **(B)** total macrophage **(C)** F4/80$^{hi}$ **(D)** MoMΦ (F4/80$^{lo}$MHC$^{+}$Ly6C$^{-}$) and **(E)** monocytes (F4/80$^{lo}$Ly6C$^{+}$) cell number over the course of infection in C57BL/6 and BALB/c mice. A 2-way ANOVA was carried out on each time point. Bars represent the mean +/- the SEM and data are representative of three independent experiments, with 6 mice per group/time point. The break in the graphs illustrates that animals from day 11&28 were infected on a single day and animals from day 35&50 were infected on a separate day. * P<0.05, ** P<0.01, ***P<0.0001,**** P<0.00001.

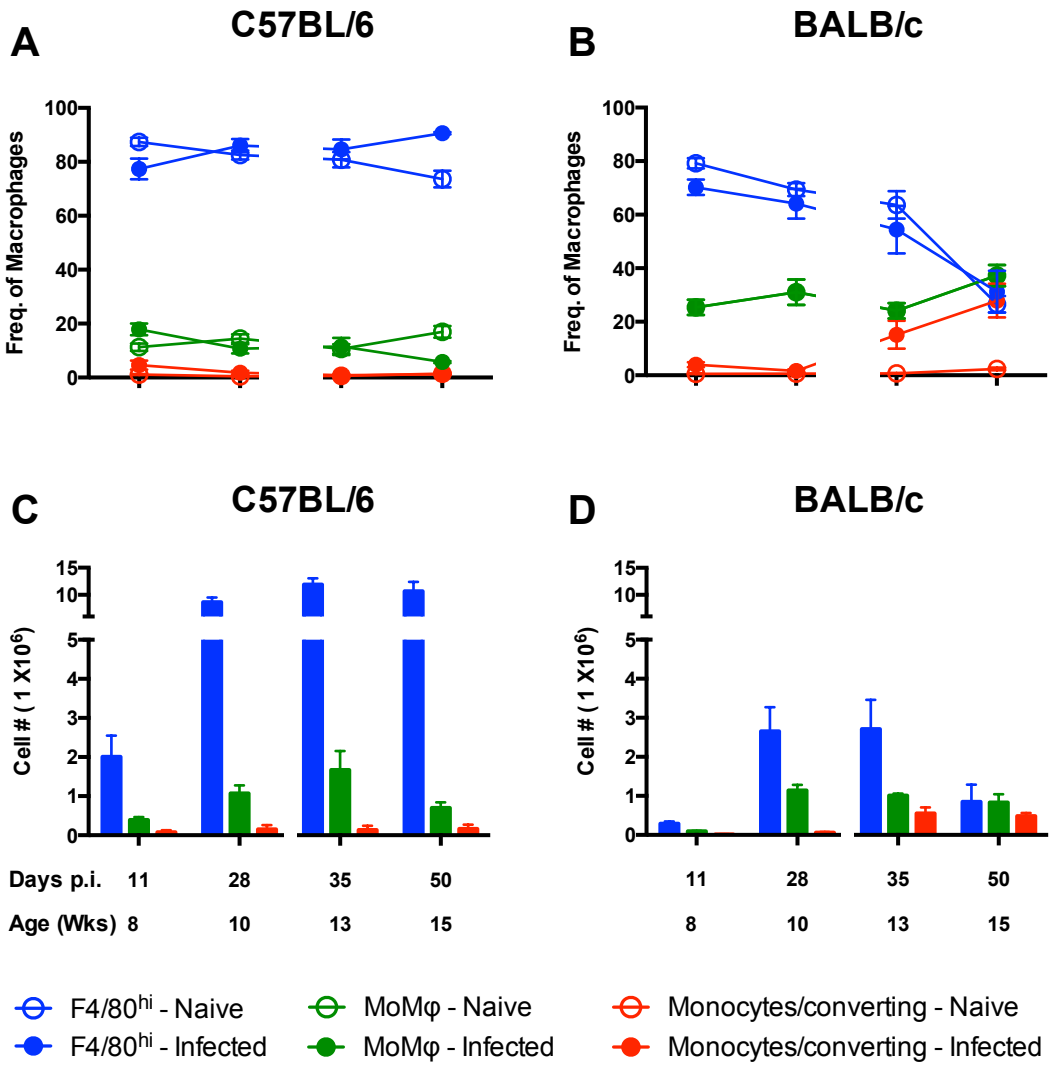


**Figure 2-5 Dynamics of the MΦ compartment are distinct between strains**

C57BL/6 and BALB/c female mice, aged 6-8 weeks, were infected with 30 infective L3 *L. sigmodontis* larvae subcutaneously (s.c). Mice were sacrificed on days 11, 28, 35 and 50 pi and the pleural cavity was washed with 10ml RPMI (1 % L-Glut, 1 % Pen-Strep) to isolate the pleural exudate cells (PLEC) and surviving worms. At each time point post *L. sigmodontis* infection the macrophage population was subdivided into F4/80$^{hi}$, MoMΦ and monocytes using the gating strategy illustrated in Figure 2-4. The percentage contribution of each subpopulation to the MΦ compartment as a whole within naïve and infected **(A)** C57BL/6 and **(B)** BALB/c mice. Actual numbers of each subpopulation within naïve and infected **(C)** C57BL/6 and **(D)** BALB/c mice. The break in the graphs illustrates that animals from day 11&28 were infected on a single day and animals from day 35&50 were infected on a separate day.

The transcription factor GATA6 and the cell surface marker CD102 have been identified as markers of residency expressed by the F4/80$^{hi}$ population within the peritoneal and pleural spaces (Okabe and Medzhitov, 2014, Rosas et al., 2014). In alignment with this, the F4/80$^{hi}$ population of naïve C57BL/6, naïve BALB/c mice and infected C57BL/6 mice, were more that 90 % positive for GATA6 and CD102 (Figure 2-6A&B). Additionally, neither MoMΦ nor Monocytes express GATA6 or CD102 in naïve animals (Figure 2-6A&B). There was a decline in the percentage of the F4/80$^{hi}$ population within infected BALB/c mice expressing GATA6 and CD102 by day 50 pi (Figure 2-6B). This did not reach significance but is reflective of the migration of MoMΦ into the F4/80$^{hi}$ MΦ gate.

The age related decline in the percentage of F4/80$^{hi}$ cells contributing to the MΦ pool in naïve C57BL/6 mice and the corresponding increase in MoMΦ, resulted in a decline in GATA6 but not CD102 expression by the total MΦ pool between day 11 and day 50 pi (Figure 2-6C&D). As infection within the C57BL/6 mice prevented this age-related decline in F4/80$^{hi}$ cell contribution at day 50 pi, GATA6 and CD102 expression were maintained at > 90 % by the MΦ compartment as a whole (Figure 2-6C). This resulted in significantly greater GATA6 expression by the infected MΦ compartment of C57BL/6 mice at day 50 pi relative to their naïve controls (Figure 2-6C).

The decreased F4/80$^{hi}$ cell contribution to the MΦ compartment in the BALB/c strain from 8 weeks of age (day 11 pi) was reflected in a significantly lower percentage of the MΦ pool staining positive for GATA6 and CD102 compared to C57BL/6 naïve controls (Figure 2-6C&D). Furthermore as BALB/c mice age and the percentage of F4/80$^{hi}$ cells contributing to the MΦ compartment declines, the expression of GATA6 and CD102 by the MΦ compartment decreases also (Figure 2-6C&D). Ultimately, this increases the difference in GATA6 and CD012 expression between naïve C57BL/6 and BALB/c mice (Figure 2-6C&D). As infection does not prevent the age related decline in F4/80$^{hi}$ cell contribution in the BALB/c strain, there is significantly less GATA6 and CD102 expression by the total macrophage compartment of infected BALB/c mice vs. C57BL/6 mice at day 11 and 50 pi (Figure 2-6C&D)

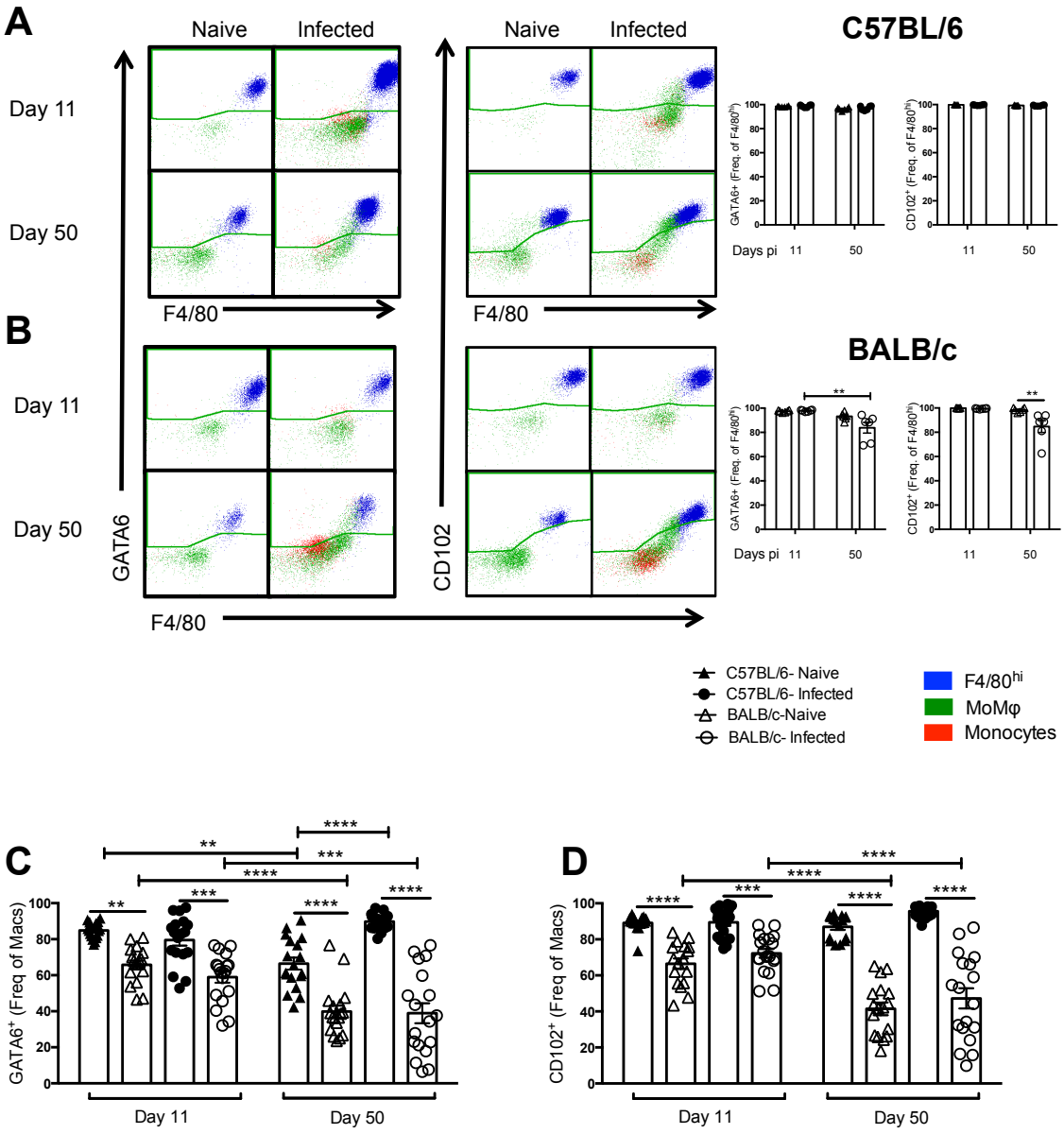


**Figure 2-6 Influxing bone marrow derived cells result in a global decrease in GATA6 and CD102 expression by macrophages in susceptible BALB/c mice**

C57BL/6 and BALB/c female mice, aged 6-8 weeks, were infected with 30 infective *L. sigmodontis* L3 larvae subcutaneously (s.c). Mice were sacrificed on days 11, 28, 35 and 50 pi and the pleural cavity was washed with 10 ml RPMI (1 % L-Glut, 1 % Pen-Strep) to isolate the pleural exudate cells (PLEC) and surviving worms. At each time point post *L. sigmodontis* infection the macrophage population was subdivided into F4/80$^{hi}$, MoMΦ and monocytes using the gating strategy illustrated in Figure 2-4. Representative FACS plots of GATA6 and CD102 expression by F4/80$^{hi}$, MoMΦ and monocytes in **(A)** C57BL/6 and **(B)** BALB/c mice at day 11 and 50 pi **(C)** GATA6 and **(D)** CD102 expression by the macrophages compartment in naïve and infected C57BL/6 and BALB/c mice at day 11 and day 50 pi. Data are representative of three pooled experiments. * P<0.05, ** P<0.01, ***P<0.0001,**** P<0.00001 as determined by a 2 way ANOVA. Error bars are the mean ± SEM.

In the gut and recently the peritoneum, Ly6C$^{+}$ monocytes have been shown to infiltrate tissues under homeostatic conditions and mature via a 'monocyte waterfall' to replenish the resident MΦ population (Bain et al., 2014). Bain et al have recently extended this finding to the peritoneal and pleural spaces of C57BL/6 mice, illustrating that F4/80$^{lo}$ BMDMΦ contribute to the resMΦ population in naïve mice as they age (Bain et al., 2016). In our experiments, there appears to be a 'monocyte waterfall' within the MΦ compartment of infected BALB/c mice, with monocytes (Ly6C$^{+}$MHC$^{-}$) appearing to mature into MoMΦ (F4/80$^{lo}$MHC$^{hi}$Ly6C$^{-}$) through sequential loss of Ly6C and acquisition of MHC expression (Figure 2-7A). Furthermore, in many samples there was a suggestion of MoMΦ migrating into the F4/80$^{hi}$ gate and an increase in MHC II expression by the F4/80$^{hi}$ population, potentially suggestive of complete replenishment of the resident population in this strain by BMDMΦ. The continual decline the in percentage of F4/80$^{hi}$ MΦ in both naïve and infected BALB/c mice suggests that recruited BMDMΦ fail to integrate into the resident niche at a rate sufficient to maintain the F4/80$^{hi}$ population at 80 % of the MΦ compartment (Figure 2-5B). While some of the MoMΦ population upregulate F4/80 and consequently migrate into the F4/80$^{hi}$ gate (Figure 2-7A), these cells fail to assume GATA6 and CD102 expression, as indicated by a decline in these markers by the F4/80$^{hi}$ population by day 50 pi (Figure 2-6B).

To address whether proliferation could be solely responsible for the large increase in F4/80$^{hi}$ cell number seen during infection, the percentage of F4/80$^{hi}$ cells expressing high levels of Ki67 was assessed at each time point. Expression of Ki67 can be used to identify cells in active cell cycle, and we have shown that cells expressing high levels of Ki67 overlap with BrdU positive events, following a 3 hours BrdU pulse (Jenkins et al., 2013). Day 11 pi was the only time point at which proliferation peaked above homeostatic levels in either strain (See appendix 4). At this time point, the level of F4/80$^{hi}$ cell proliferation was significantly greater in the C57BL/6 strain compared to the BALB/c at day 11 (Figure 2-7B).

Unpublished data in the lab has revealed that proliferation can be shut off very rapidly, thus it is possible that we missed subsequent proliferative bursts outside of the time points examined. To indirectly address this issue we asked if the degree of

macrophage accumulation is intact in *Ccr2*$^{-/-}$ mice, in which monocyte recruitment is absent due to an inability of monocytes to egress from the bone marrow (Tsou et al., 2007). Unfortunately, due to failures in the rederivation process I was unable to obtain *Ccr2*$^{-/-}$ mice on the BALB/c background. Nonetheless, *Ccr2*$^{-/-}$ mice on the C57BL/6 background were infected with *L. sigmodontis* for 28 days and the PLEC was then isolated. The number of eosinophils, dendritic cells and MΦ detected in the pleural cavity at day 28 pi was significantly decreased in *Ccr2*$^{-/-}$ vs. WT mice (Figure 2-8A&C). This difference in MΦ number was primarily reflective of the significant decrease in MoMΦ and monocytes within the infected cavity. However, while not significant there was a slight decline in F4/80$^{hi}$ cell number in the *Ccr2*$^{-/-}$ mice vs. WT (Figure 2-8D&F). Parallel to reduced F4/80$^{hi}$ cells, a similar decline in the number of GATA6 and CD102 positive cells was observed in the *Ccr2*$^{-/-}$ mice compared to WT (Figure 2-8G&H). The decrease in eosinophils, DC, and BMDMs did not significantly affect the worm recovery rate at day 28 pi (Figure 2-8I). This data suggests that at day 28 pi the majority of the expanded of F4/80$^{hi}$ population in the C57BL/6 strain is a result of resMΦ proliferation, with room to speculate that a small degree of bone marrow derived MΦ recruitment contributes to the total MΦ number.

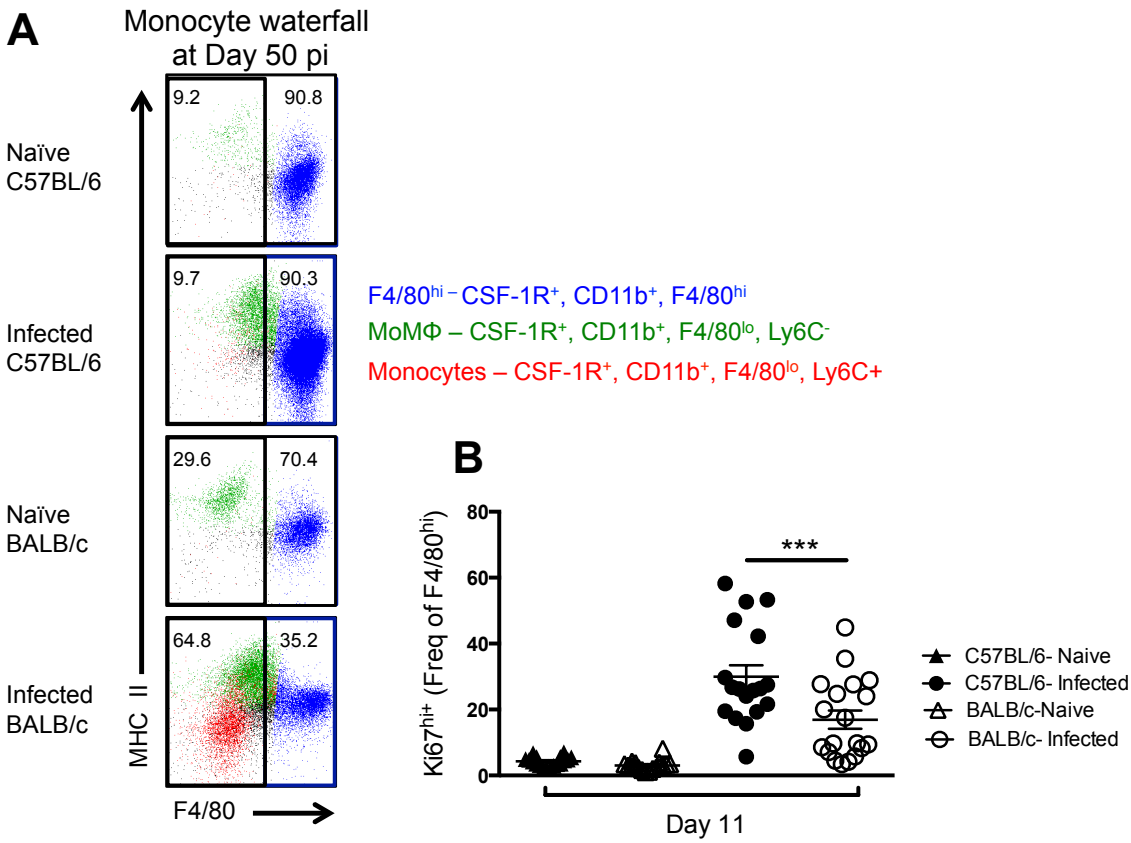


**Figure 2-7 BMDMΦ form a 'monocyte waterfall' with resMΦ in susceptible BALB/c mice, whereas resistance is marked by F4/80$^{hi}$ cell proliferation**

C57BL/6 and BALB/c female mice, aged 6-8 weeks, were infected with 30 infective *L. sigmodontis* L3 larvae subcutaneously (s.c). Mice were sacrificed on days 11, 28, 35 and 50 pi and the pleural cavity was washed with 10 ml RPMI (1 % L-Glut, 1 % Pen-Strep) to isolate the pleural exudate cells (PLEC) and surviving worms. F4/80$^{hi}$, MoMΦ and monocyte populations were using gating strategy illustrated in Fig 2-4A **(A)** movement of monocytes, MoMΦ and F4/80$^{hi}$ subpopulations through the MΦ compartment of naïve and day 50 pi C57BL/6 and BALB/c mice. Data are representative of 3 independent experiments with 6 mice/group. **(B)** Detection of F4/80$^{hi}$ cells expressing high levels of Ki67 at day 11 pi in C57BL/6 and BALB/c mice. Data are representative of three pooled experiments. ***P<0.0001 as determined by a 2 way ANOVA. Error bars are the mean ± SEM.

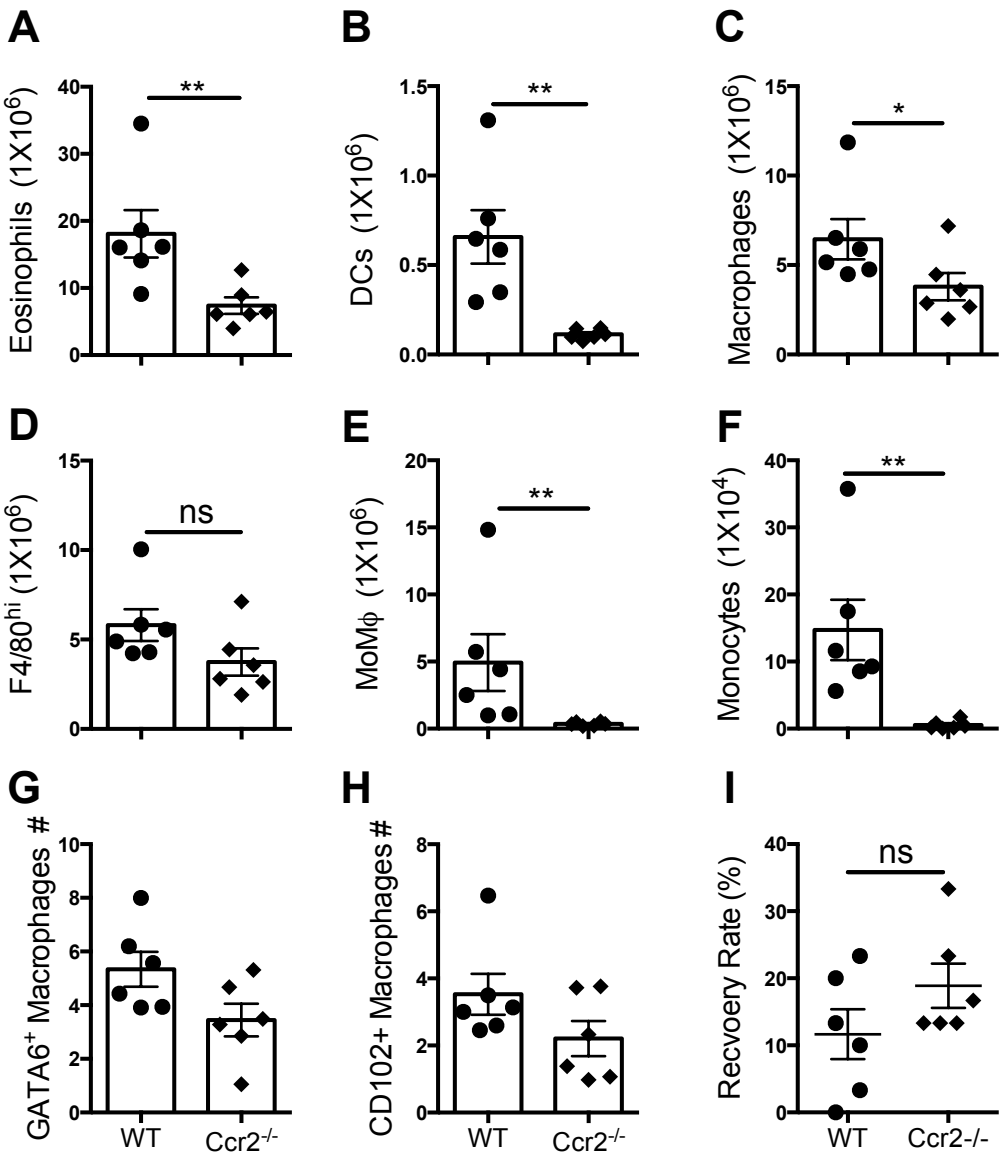


**Figure 2-8 F4/80$^{hi}$ cell expansion displays independence from BMDMΦ at day 28 pi**

*Ccr2*$^{-/-}$ C57BL/6 and Charles River WT control female mice were infected with 30 *L. sigmodontis* L3 larvae subcutaneously. The animals were sacrificed 28 days post infection, worm recovery and pleural cells were isolated through washing of the pleural cavity with 10 ml RPMI (1 % L-Glut, 1 % Pen-Strep). Graphs are representative plots from infected animals **(A)** eosinophils **(B)** dendritic cells **(C)** CD115$^{+}$ Macrophages **(D)** F4/80$^{hi}$ **(E)** MoMΦ **(F)** monocytes. Percentage of MΦ expressing **(G)** GATA6 and **(H)** CD102. **(I)** Recovery rate. Bars represent mean ± SEM and are representative from two independent experiments, each with 6 mice/group. * P <0.05, ** P<0.001 as determined by Student's t test and Mann Whitney test.

### 2.3.3 Integration into the resident macrophage compartment rather than origin underlines the resistant phenotype

Day 11 pi was the only time point at which we observed proliferation above homeostatic levels. The data from *Ccr2*$^{-/-}$ C57BL/6 mice suggested that expansion of the F4/80$^{hi}$ resMΦ population can occur independently of recruitment of bone marrow derived cells, presumably through IL-4 driven proliferation. Knockout mice are an invaluable tool in immunological research, however the lack of CCR2 from birth may have global effects upon development. Thus in order to definitely prove that the enhanced F4/80$^{hi}$ cell numbers in the resistant C57BL/6 strain are a result of proliferation of a resMΦ population we generated partial bone marrow chimeric mice, in which recruitment of cells from the bone marrow can still occur.

To do this, the lower limbs of CD45.1$^{+/+}$ C57BL/6 females were lethally irradiated, the upper body and thereby the pleural space is protected by a lead block (Figure 2-9A). The partially irradiated hosts are subsequently injected i.v with 5X10$^{6}$ bone marrow cells from donor CD45.2$^{+/+}$ mice, to reconstitute the bone marrow of the lower limbs. The degree of donor cell contribution to any tissue population can then be calculated by dividing the percentage of CD45.2$^{+}$ cells in the tissue by that observed in the blood (Figure 2-9B). By generating partial bone marrow chimeric mice we can ask to what degree bone marrow derived cells contribute to the expanded F4/80$^{hi}$ population observed in the pleural cavity during *L. sigmodontis* infection. The animals were assessed on days 35 and 50 pi. These mice were allowed to reconstitute for 9 weeks prior to infection and thus were on average 9 weeks older than those in previous experiments. If the expanded F4/80$^{hi}$ cells were a result of IL-4 driven expansion of a resident population, this F4/80$^{hi}$ population would be greater than 95 % CD45.1$^{+}$.

As in previous experiments many of the C57BL/6 mice had cleared infection by day 50 (Figure 2-10A). The level of F4/80$^{hi}$ cell contribution was maintained at 80-90 % of the total MΦ compartment and (Figure 2-9D) similar numbers of F4/80$^{hi}$ cells were isolated (Figure 2-10B). The donor CD45.2$^{+}$ cells comprised on average 15% of the circulating blood monocytes at 5 and 8 weeks post irradiation, this degree of blood chimerism was maintained until days 35 and 50 pi (Figure 2-9C). Surprisingly,

the percentage of F4/80$^{hi}$ cells derived from the bone marrow at day 35 pi in naïve and infected animals was ~50 % and this increased further by day 50 pi to ~80 % (Figure 2-10C). There was no difference in the level of chimerism observed between naïve and infected animals at either day 35 or 50 pi, suggesting that the increased contribution of BMDM to the F4/80$^{hi}$ pool is an age related phenomena, which is not accelerated by nematode infection (See schematic Figure 2-12). This data is supported by a very recent publication by Bain et al (Bain et al., 2016). showing a gradual replenishment of the pleural F4/80$^{hi}$ population by BMDMΦ with age. Bain et al, showed that by 19 weeks of age, the level of bone marrow cell contribution to the pleural macrophage compartment is ~50 %. My experimental mice were approximately 18 weeks of age at the time of infection. Thus by the time the mice were infected, 50 % of the F4/80$^{hi}$ population had already been replenished from the BM. The fact that host and donor cell contribution to the F4/80$^{hi}$ pool remained constant between naïve and infected animals at day 35 and day 50 despite a 27-fold increase in cell number is supportive of proliferation of the pre-existing resident F4/80$^{hi}$ population independent of their origin (Schematic Figure 2-12). Furthermore, the data suggests that there is no difference in the proliferative capabilities of donor and host derived cell F4/80$^{hi}$ cells. Indeed, host and donor derived F4/80$^{hi}$ MΦ illustrated no difference in the percentage of Ki67 positivity in either naïve controls or at day 35/50 pi (Figure 2-11.). However, the percentage of Ki67 positive cells in the infected mice at day 35 and 50 pi was significantly lower than what was observed in naïve controls, suggestive of a post-proliferative shut-down (Figure 2-11). Consequently these data support the recent publication by Bain et al in showing equal capabilities of donor and host derived resMΦ to proliferate during homeostasis and extend these observations to the infection driven expansion of the F4/80$^{hi}$ population seen during *L. sigmodontis* infection.

The transcription factor GATA6 and cell surface markers CD102 and TIM4 have previously been used to identify the resMΦ population (Okabe and Medzhitov, 2014, Rosas et al., 2014, Davies et al., 2011). Consistent with that, >95% of the F4/80$^{hi}$ population in C57BL/6 mice was positive for GATA6 and CD102 in all experiments carried out (Figure 2-6A&B). Here, using protected bone marrow chimeras, I asked the question whether origin influences the ability of a cell to become resident through

expression of these markers. At day 35 and 50 pi in the chimeric mice >95% of the F4/80$^{hi}$ population was GATA6$^{+}$, 50 % of this population were of donor origin at day 35 pi and this increased to ~80 % by day 50 pi (Figure 2-10D&G). Similarly, while >98 % of the F4/80$^{hi}$ population was positive for CD102 at day 35 and day 50 pi, 50% of these cells were donor derived by day 35, however this did not increase further at day 50 pi (Figure 2-10E&H). Previous reports have illustrated >90% of the F4/80$^{hi}$ population in naïve animals to be TIM4 positive (Davies et al., 2011). However, we found that TIM4 was only expressed by ~50% of the F4/80$^{hi}$ population in naïve animals (Figure 2-10F&I). The percentage of cells expressing TIM4 mirrored the level of chimerism found in the F4/80$^{hi}$ population; indicative of TIM4 being a true marker of host derived MΦ (Figure 2-10C). However, while 80 % of the TIM4$^{+}$ population was of host origin, 20% of the TIM4$^{+}$ F4/80$^{hi}$ cells were BMD (Figure 2-10I). Thus, while BMDMΦ are capable of assuming a TIM4$^{+}$ phenotype it would appear to occur at a slower rate than GATA6 and CD102 acquisition. Interestingly, the percentage of TIM4$^{+}$ cells remained at 50% from 23-35 weeks of age, but the percentage of BMDM incorporation had increased during this time period. Furthermore, there was an increase in the percentage of cells expressing TIM4 upon infection (70-80 %)(Figure 2-10F).

Thus, partial bone marrow chimeric mice have revealed that bone marrow-derived macrophages successfully integrate into the resident F4/80$^{hi}$ population in both naïve and infected animals, assuming high levels of F4/80$^{hi}$ expression and markers such as GATA6 and CD102. These data suggest that TIM4 is not a robust marker of residency as only 50% of the F4/80$^{hi}$ population were TIM4 positive in aged naïve animals. Furthermore, TIM4 is a gene which has been identified as being highly sensitive to IL-4Rα signalling (Gundra et al., 2014), thereby explaining the sharp increase in the percentage of TIM4 positive MΦ upon infection.

Ultimately, these data reveal mechanistic differences in macrophage dynamics between naïve C57BL/6 and the BALB/c mice; there is continual recruitment and successful integration of BMDMΦ into the resMΦ pool in the C57BL/6 mice, in contrast, recruited BMDMΦ in the BALB/c strain do not upregulate F4/80, GATA6 or CD102, at a rate sufficient to integrate into the resMΦ population and maintain a

resMΦ dominated MΦ compartment as seen in the C57BL/6 strain. Furthermore, infection driven macrophage accumulation differs between the strains, with proliferation largely contributing to the enhanced numbers in the C57BL/6 and recruitment driving the expansion in BALB/c mice.

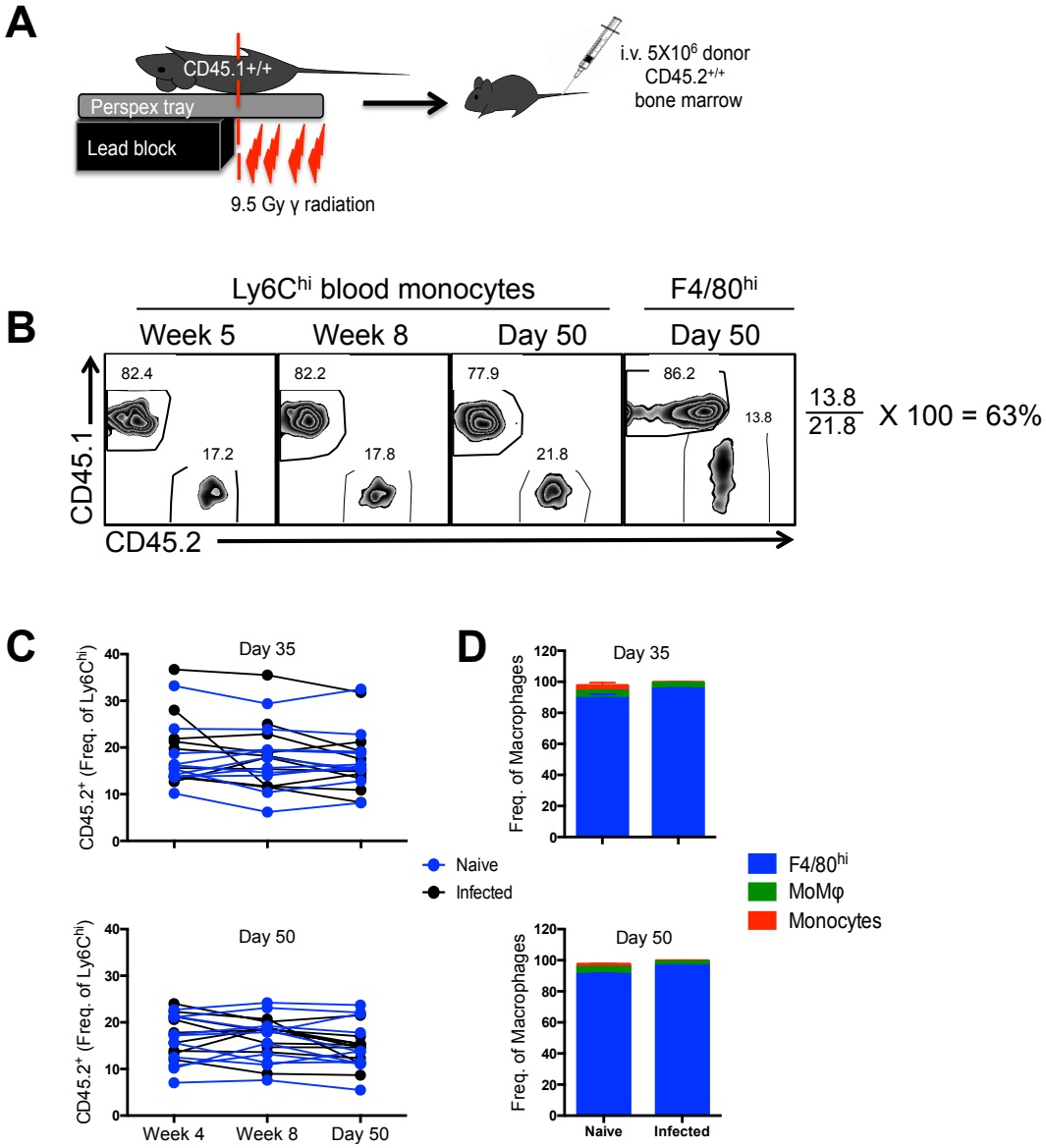


## Figure 2-9 Generation and infection of partial bone marrow chimeric C57BL/6 mice

Partial bone marrow chimeric C57BL/6 female mice were generated as depicted in Fig 2-8. **(A)** CD45.1$^{+/+}$ C57BL/6 hosts were irradiated in the lower limbs and subsequently administered donor CD45.2$^{+/+}$ bone marrow i.v. 9 weeks after reconstitution the mice were infected with 30 L. sigmodontis L3 larvae s.c. The animals were sacrificed on day 35 and 50 pi and the pleural cavity was washed with 10 ml RPMI (1 % L-Glut, 1 % Pen-Strep) to isolate the PLEC and surviving worms. The MΦ compartment was analysed using the gating strategy illustrated in Fig2-2. **(B)** Degree of bone marrow derived macrophage contribution to the pleural F4/80$^{hi}$ population was calculated by dividing the percentage of CD45.2$^{+}$ F4/80$^{hi}$ cells by the percentage of CD45.2$^{+}$ Ly6C$^{hi}$ monocytes in the peripheral blood. **(C)** Blood chimerism at 4 and 8 weeks post irradiation and 50 days pi. **(D)** Contribution of MΦ subpopulations to MΦ compartment as whole at day 50 pi. Data are representative of two independent experiments with 10 mice/group/experiment.

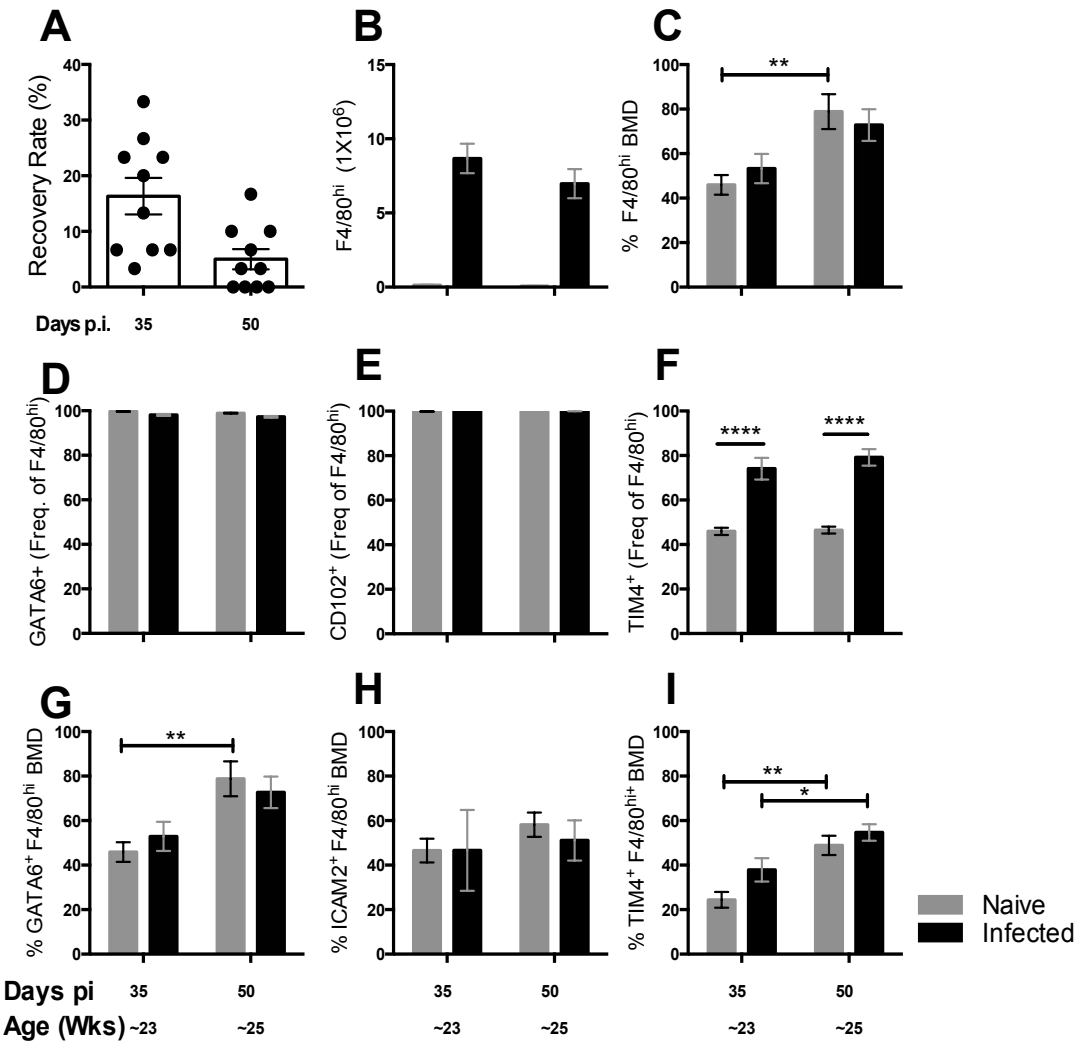


## Figure 2-10 Bone marrow derived cells successfully integrate into the resident F4/80$^{hi}$ MΦ population

Partial bone marrow chimeric C57BL/6 female mice were generated as depicted in Fig 2-8. 9 weeks after reconstitution the mice were infected with 30 L. sigmodontis larvae s.c. The animals were sacrificed on day 35 and 50 pi and the pleural cavity was washed with 10 ml RPMI (1 % L-Glut, 1 % Pen-Strep) to isolate the PLEC and surviving worms. The MΦ compartment was analysed using the gating strategy illustrated in Fig2-2. **(A)** Worm recovery rate at day 35 and day 50 post infection in partial bone marrow chimeric C57BL/6 mice. **(B)** F4/80$^{hi}$ cell number **(C)** Percentage of the F4/80$^{hi}$ cells which are bone marrow derived. Expression of **(D)** GATA6 **(E)** CD102 and **(F)** TIM4 by F4/80$^{hi}$ MΦ. **(G-I)** Percentage of **(G)** GATA6$^{+}$, **(H)** ICAM2$^{+}$ **(I)** TIM4$^{+}$ F4/80$^{hi}$ cells which are BMD in naïve and infected animals at day 35 and day 50 post infection. Data are representative of two independent experiments with 10 mice/group/experiment. *P<0.05, ** P<0.01, **** P<0.00001 as determined by a 2 way ANOVA. Error bars are the mean ± SEM

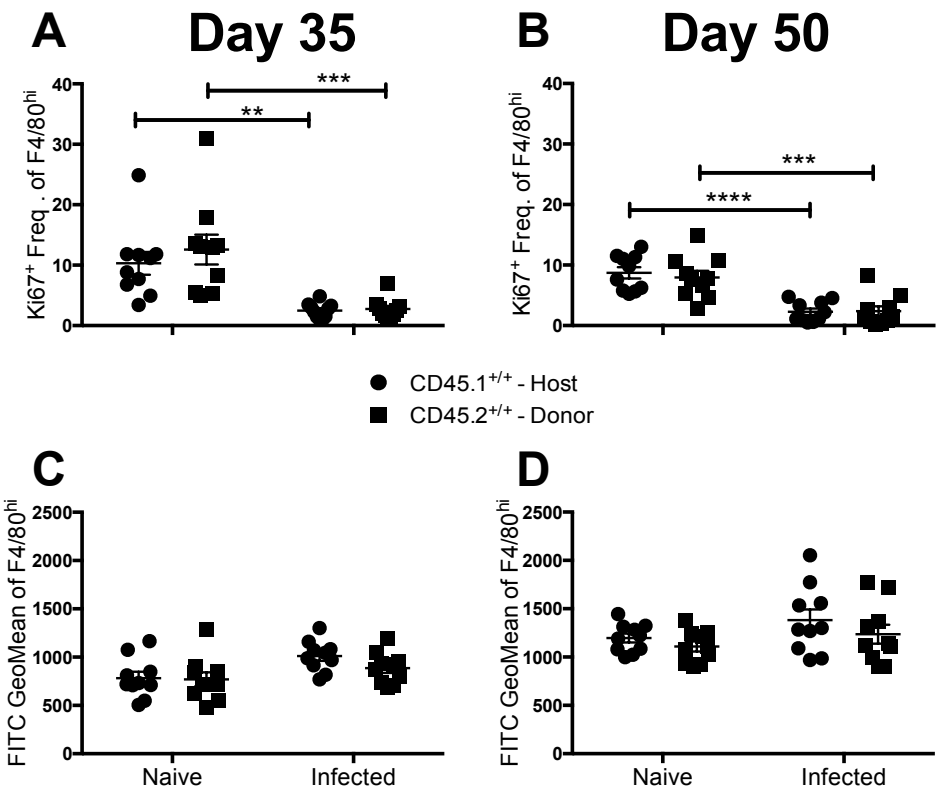


**Figure 2-11 Host and donor F4/80$^{hi}$ cells possess equal proliferative capabilities during both homeostasis and infection**

CD45.1$^{+/+}$ C57BL/6 hosts were irradiated in the lower limbs and subsequently administered donor CD45.2$^{+/+}$ bone marrow i.v. 9 weeks after reconstitution the mice were infected with 30 *L. sigmodontis* larvae s.c. and the pleural MΦ compartment was analysed at day 35 and 50 pi. **(A&B)** Percentage of Ki67 positive CD45.1$^{+/+}$ or CD45.2$^{+/+}$ F4/80$^{hi}$ MΦ **(C&D)** Ki67 Geometric mean of the CD45.1$^{+/+}$ or CD45.2$^{+/+}$ F4/80$^{hi}$ populations at day 35 and day 50 pi in infected and naïve controls. Data are representative of two independent experiments with 10 mice/ group/ experiment. $P<0.05$, ** $P<0.01$, ***$P<0.0001$,**** $P<0.00001$ as determined by a 2 way ANOVA. Error bars are the mean ± SEM.

## 2.4 Discussion

Macrophages are one of the most abundant cellular populations present in the pleural space during infection with *L. sigmodontis*. Despite this, surprisingly little is known about how exactly these cells may be involved in worm killing. Previous work in our lab illustrated that IL-4 drives the proliferation of the resMΦ population within the pleural space resulting in a large increase in macrophage cell number by day 11 post infection (Jenkins et al., 2011). Subsequently, the peritoneal macrophage population was shown to be derived prenatally independent of HSC in the BM (Schulz et al., 2012). Furthermore, BMDMs and resMΦ take on distinct transcriptional profiles when exposed to IL-4 (Gundra et al., 2014). With this new perspective on macrophage origin and activation, we decided to reassess the macrophage compartment in resistant C57BL/6 and susceptible BALB/c mice during *L. sigmodontis* infection. A large disparity in macrophage number between infected C57BL/6 and BALB/c mice at day 30 pi has been noted previously (Babayan et al., 2003). I hypothesised that this difference may be explained by variation in resMΦ proliferation and/or BMDMΦ recruitment between strains.

Significantly less worms were recovered from resistant C57BL/6 mice from day 35 pi, with a trend evident as early as day 11 pi. This difference in worm recovery was accompanied by significantly greater pleural cell accumulation in the C57BL/6 strain, which peaked between day 28-35 pi the time points were active worm killing is occurring. While, a trend toward lower worm recovery in the C57BL/6 strain at day 10 and 30 pi has been previously documented by others (Babayan et al., 2003), never has this differences reached statistical significance in a single experiment. However, a meta-analysis of 85 experiments, previously carried out in our lab, demonstrated that a real decrease in worm recovery is present in the C57BL/6 strain from day 10 pi onward (Graham et al., 2005).The detection of differences in worm recovery from day 10 pi is supportive of enhanced larval killing in the skin or reduced migration of larvae from the skin to the pleural cavity in resistant C57BL/6 mice. To determine if there are differences in skin killing/ migration through the host to the cavity, one could investigate worm recovery between strains at day 4 pi, the time point at which L3 larvae arrive to the pleural cavity. However, given the number of animals need (~ 80/group) to detect a significant difference in worm

killing at day 10 pi, we hypothesise that the contribution of worm killing in the skin/during migration to the resistant phenotype is minimal and that the majority of the worms are killing within the pleural cavity. Here I report significant differences in worm burden at day 35 pi, which we and others have failed to previously obtain in a single experiment. Our laboratory has strived to continually improve the *L. sigmodontis* life cycle over the past 10 years. Consequently, the health of the L3 larvae is higher than in earlier reports. I believe that the detection of significant differences in recovery rate at day 35 pi in the experiments presented here is a reflection of the refinement of the lifecycle.

B cells and MΦs accounted for the greater total cell number observed in the resistant strain. Detailed analysis of the macrophage compartment revealed the enhanced numbers in the C57BL/6 strain was a reflection of an expanded F4/80$^{hi}$ MΦ population, which continually represented >80% of the MΦ compartment and maintained an F4/80$^{hi}$MHC$^{lo}$GATA6$^{+}$CD102$^{+}$ phenotype at all time points examined. Furthermore, there was negligible influx of monocytes observed in the C57LB/6 mice. This data suggested that there was an expansion and maintenance of the resMΦ population, potentially due to IL-4 driven proliferation of the resMΦ population in the C57BL/6 host. Previous work has highlighted that there is significantly more IL-4 detectable in the pleural wash of C57BL/6 vs. BALB/c mice (Babayan et al., 2003). Indeed a greater degree of proliferation was detected in the C57BL6/ strain at day 11 pi. As enhanced proliferation was not detected at any of the other time points examined, we hypothesised additional proliferative bursts occurring between the time points examined may be responsible for the enhanced F4/80$^{hi}$ MΦ number. Support for the proliferative expansion of the F4/80$^{hi}$ population independently of BMDMΦ recruitment was gleaned from experiments in *Ccr2*$^{-/-}$ animals, in which there was no significant difference in F4/80$^{hi}$ MΦ number at day 28 pi.

The large contribution of BMD macrophages to the F4/80$^{hi}$ population observed through partial bone marrow chimeric mice initially surprised us. However, because the degree of BMDMΦ contribution to the F4/80$^{hi}$ population in infected mice was equivalent to that seen in naïve animals this suggested that incorporation of BMDMΦ to the F4/80$^{hi}$ pleural ResMΦ pool occurs under homeostatic conditions

and is an age related phenomena. Bain et al. recently demonstrated that the pleural macrophage population is continually replenished by BMDMΦ and that this contribution increases with age. In this study by 18 weeks of age 50 % of the pleural F4/80$^{hi}$ population had been derived from the bone marrow (Bain et al, 2016). I take this as strong evidence that considerable BMDMΦ incorporation would have occurred by 19 weeks; the age of my animals upon infection. Thus, the equal degree of BMDMΦ contribution between naïve and infected animals at day 35 pi, despite a 27-fold difference in cell number illustrates that both prenatally seeded and BMD F4/80$^{hi}$ populations within the pleural space are equally capable of proliferating locally during infection (see schematic Figure 2-12). A greater degree of BMDMΦ contribution to the F4/80$^{hi}$ population of infected animals compared with naïve would have indicated that infection was driving recruitment, whereas had host derived cells possessed inherent proliferative capabilities above that of F4/80$^{hi}$ cells of bone marrow origin, the degree of BMDMΦ contribution would have been lower in infected animals. Bain et al. demonstrated that host F4/80$^{hi}$ MΦ possess a lower level of homeostatic proliferation, as measured by Ki67 positivity, when compared to donor F4/80$^{hi}$ cells within the peritoneal space. This decreased *in-situ* self-renewal of host MΦ correlated with decreased expression of the CSF-1R. However, upon exogenous CSF1 administration these cells were capable of proliferating to a degree equal to that of recently recruited BMD F4/80$^{hi}$ peritoneal macrophages (Bain et al., 2016). In contrast to Bain et al. we did not observe decreased homeostatic proliferation of host F4/80$^{hi}$ MΦ compared to donor derived F4/80$^{hi}$ MΦ, as there was no difference in the Ki67 positivity of CD45.1$^{+}$ F4/80$^{hi}$ and CD45.2$^{+}$ F4/80$^{hi}$ cells within naïve mice at day 35 or 50 pi, suggesting equal capacity to proliferate regardless of origin. Furthermore, the degree of proliferation detected in the F4/80$^{hi}$ population of infected animals is significantly lower than that detected in naïve animal. This is suggestive of a shutdown in homeostatic levels of proliferation often seen after proliferative bursts.

Interestingly, there is an increase in donor contribution to the F4/80$^{hi}$ pool between 23-25 weeks of age. This is easily explained by continual replacement of the resident population by BMDMΦ with age. However, the increase in chimerism in the F4/80$^{hi}$ pool of infected animals between day 35 and 50 pi is less easily explained because of

the decrease in cell numbers between these time points. This increase in chimerism could be a result of preferential survival of the pre-existing donor cells, increased recruitment of donor MΦ, or increased cell death of host MΦ. I believe that increased recruitment is a not likely to explain the enhanced chimerism, due to the decrease in total F4/80$^{hi}$ number. Thus, the increased chimerism in the F4/80$^{hi}$ MΦ pool by day 50 is a reflection of preferential survival of pre-existing donor derived cells and death of host derived cells (See schematic Figure 2-12). The consistency of macrophage kinetics between naïve controls and infected animals suggests that nematode infection somehow maintains the normal homeostatic process of ageing without limiting cell number.

The chimeric data also highlighted the seamlessness with which BMDMΦ are capable of assuming a resident macrophage phenotype as evidenced by the up-regulation of GATA6 and CD102. The transcription factor GATA6 has been identified as a master regulator responsible for the transcriptional, functional and phenotypic differentiation of peritoneal MΦ (Okabe and Medzhitov, 2014, Rosas et al., 2014). GATA6 has been linked to the proliferative renewal of resMΦ and I believe that this is reflected in the ability of GATA6$^{+}$ donor derived F4/80$^{hi}$ MΦ to proliferate and contribute to the expanded resMΦ population to a degree equal to that of host derived GATA6$^{+}$ F4/80$^{hi}$ MΦ (Rosas et al., 2014). Through total irradiation studies Okabe et al. demonstrated that BMDMΦ could give rise to bona fide resident peritoneal macrophages in a gata6-dependent manner. The percentage of resMΦ in the peritoneal cavity of vitamin A deficient mice decreases with age, while the percentage of BMDMΦ increases (Okabe and Medzhitov, 2014). I believe that this was not reflective of inflammation but rather the age related increase in BMDMΦ contribution to the resMΦ population and that the absence of vitamin A derived retinoic acid results in an inability of these cells to integrate into the resident niche (Okabe and Medzhitov, 2014). CD102 is a retinoic acid-independent marker of resident macrophages within the peritoneal cavity. The expression of both GATA6 and CD102 by BMDMΦ in the F4/80$^{hi}$ population of both naïve and infected C57BL/6 mice supports complete integration of these cells into the resident niche. However, to definitively prove that BMDMΦ are capable of assuming a transcriptional profile indistinguishable from that of resident derived F4/80$^{hi}$ MΦ it

would be necessary to carry out microarray analysis of host vs. donor F4/80$^{hi}$ MΦ. This would be extremely challenging due to the fact that only 15 % of blood derived monocytes express CD45.2, thus the remaining 75% of blood monocytes are CD45.1$^{+}$ and would be indistinguishable from host CD45.1$^{+}$ F4/80$^{hi}$ cells. However, my conclusion is supported by work from others in which BMDMΦ administered to lethally irradiated hosts assume an enhancer profile nearly identical to that of peritoneal resMΦ from non-irradiated controls and this included the *gata6* locus (Lavin et al., 2014). Further, BMDMΦ transferred into GM-CSF knockout mice are capable of differentiating into functional aMΦ, with a transcriptional profile near identical to that of WT aMΦ (van de Laar et al., 2016). Ultimately, we have shown that large expansion of F4/80$^{hi}$ macrophages associated with resistant C57BL/6 mice is a result of proliferative expansion of the resMΦ population present in the pleural space at the time of infection, independent of their origin. Furthermore, there is a continual increase in the contribution of BMDMΦ to the resident pool with age and nematode infection does not alter this process, but merely lifts the homeostatic controls on numbers.

The degree of macrophage accumulation in the BALB/c mice over the course of infection was only a third of that seen in C57BL/6 mice and this was a result of significantly less F4/80$^{hi}$ cells from day 11 pi. This suggested less MΦ proliferation in this host, which was confirmed through Ki67 staining at day 11 pi. Outside the F4/80$^{hi}$ MΦ expansion the macrophage compartment dynamics were strikingly different to those observed in the C57BL/6 mice. There was an increasing percentage of BMDMΦ contributing to the MΦ compartment of naïve and infected BALB/c mice and this resulted in a decline in the percentage of resMΦ. Given the recent data by Bain et al, on the replenishment of resMΦ by F4/80$^{lo}$ BMDMΦs (Bain et al., 2016), the continual decline of F4/80$^{hi}$ cells in the BALB/c strain was suggestive of an inability of BMDMΦ to efficiently integrate into the resident niche and this was reflected in the global decrease in GATA6 and ICAM2 expression by the macrophage pool by day 50 pi (25 weeks of age). In the infected animals there was migration of the MoMΦ population into the F4/80$^{hi}$ gate resulting in a decline in ICAM2 positivity in the F4/80$^{hi}$ resMΦ population at day 50, indicating that the rate of conversion in the BALB/c strain is inefficient to successfully convert influxing

cells into resMΦ (Fig. 9B). The failure of these BMDMΦ to successfully integrate into the F4/80$^{hi}$ population may be a reflection of a deficit in local retinoic acid or epigenetic silencing at the gata6 locus, which has been noted for thioglycollate elicited macrophages (Okabe and Medzhitov, 2014).

There was a striking influx of Ly6C$^{+}$ monocytes into the pleural cavity of susceptible BALB/c mice at day 35 and 50 pi. There may be several factors which drive this monocytic influx. In the naïve BALB/c mice there is a continual decline the percentage of F4/80$^{hi}$ cells within the macrophage compartment and a corresponding increase in MoMΦ. It may be that nematode infection accelerates this rate of homeostatic recruitment, resulting in increased monocyte recruitment, which would normally occur at a slower rate. Alternatively, as the adult worms are considerably longer at day 35 pi in the BALB/c mice they are more likely to induce tissue damage, thereby driving monocyte recruitment. During *S. mansoni* infection an influx of monocytes is observed at 7 weeks pi in the liver, this influx correlates with female production of eggs and subsequent egg-induced inflammation (Pearce and MacDonald, 2002, Nascimento et al., 2014). It is possible that the monocyte influx observed at day 35 pi of *L. sigmodontis* BALB/c mice is a result of early reproductive secretions by the adult worms which are reaching sexual maturity and mating within the BALB/c host at this time point, however this is this influx is too early to correlate with mf production which does not occur until day 55 pi(Hoffmann et al., 2000).

Large differences in B cell numbers were also noted throughout the time course, with significantly more B cells present in the pleural space of resistant C57BL/6 mice from day 28- 50 pi. B cells and their antibody products play a central role in anti-parasitic immunity (Esser-von Bieren et al., 2013, Rajan et al., 2005, Carter et al., 2007). During secondary *H. polygurus* infection MΦ work collaboratively with antibodies to trap and kill invading larvae (Esser-von Bieren et al., 2013). During *L. sigmodontis* infection, B cells within the fat associated lymphoid structures of the pleural space proliferate and produce antigen specific IgM; this is true of both susceptible BALB/c and resistant C57BL/6 mice up until day 18 pi (Jackson-Jones L et al., unpublished data). Given the greater number of total B cells, I suspect that

there is much more IgM present in the pleural space of C57BL/6 mice relative to BALB/c. This is suggestive of a protective role for antibodies early during *L. sigmodontis* infection and I would hypothesise that local IgM and MΦ populations work collaboratively to form granulomas, eventually leading to death of the *L. sigmodontis* worm in resistant C57BL/6 mice. In contrast, a detrimental role for B cells during chronic *L. sigmodontis* infection of susceptible BALB/c mice has been illustrated with $JH^{-/-}$ and $\mu MT^{-/-}$ BALB/c mice failing to develop patent infection (Martin et al., 2001) (Knipper JA et al., unpublished data). The contribution of B cells to the resistant and susceptible phenotypes and how antibodies might interact with macrophages to elicit worm killing during *L. sigmodontis* infection requires further study.

To summarise, in this chapter I have carried out the first detailed side-by-side comparison of the macrophage compartment in naïve and *L. sigmodontis* infected C57BL/6 and BALB/c mice and highlighted the fundamental differences in MΦ kinetics between these two commonly used laboratory strains. In the C57BL/6 host, the $F4/80^{hi}$ cell number increases significantly over that seen in the BALB/c primarily through proliferation of a resident macrophage population alongside continual slow integration of bone marrow derived macrophages. In contrast, the MΦ compartment in the BALB/c host displays a program of recruitment and failed integration rather than proliferation of a resident population. Worm killing in the C57BL/6 strain is a gradual process that is most effective between day 35 and day 50. At these time points the composition of the macrophage compartments between C57BL/6 and BALB/c is vastly different, with the C57BL/6 host containing a highly resident compartment and the BALB/c host possessing a MΦ population which is ~50% composed of cells displaying a classic BMD phenotype. Gundra et al. have demonstrated that MΦ displaying a classical $F480^{lo}$ phenotype take on an alternatively activated phenotype which is distinct from that of resident $F4/80^{hi}$ MΦ in response to IL-4Rα signalling. Bone marrow derived alternatively activated macrophages express high levels of the marker PD-L2 and the retinoic acid regulating enzyme Raldh2; neither of these markers are expressed by $F4/80^{hi}$ cells at day 11 pi with *L. sigmodontis* in C57BL/6 mice (Gundra et al., 2014). PD-L2 and Raldh2 have been implicated in the induction of hyporesponsive and regulatory T

cell phenotype, which are known to delay worm killing in the BALB/c strain (van der Werf et al., 2013). Chapter 3 investigates the functional consequences of distinct macrophage compartment dynamics when these cells become alternatively activated during *L. sigmodontis* infection.

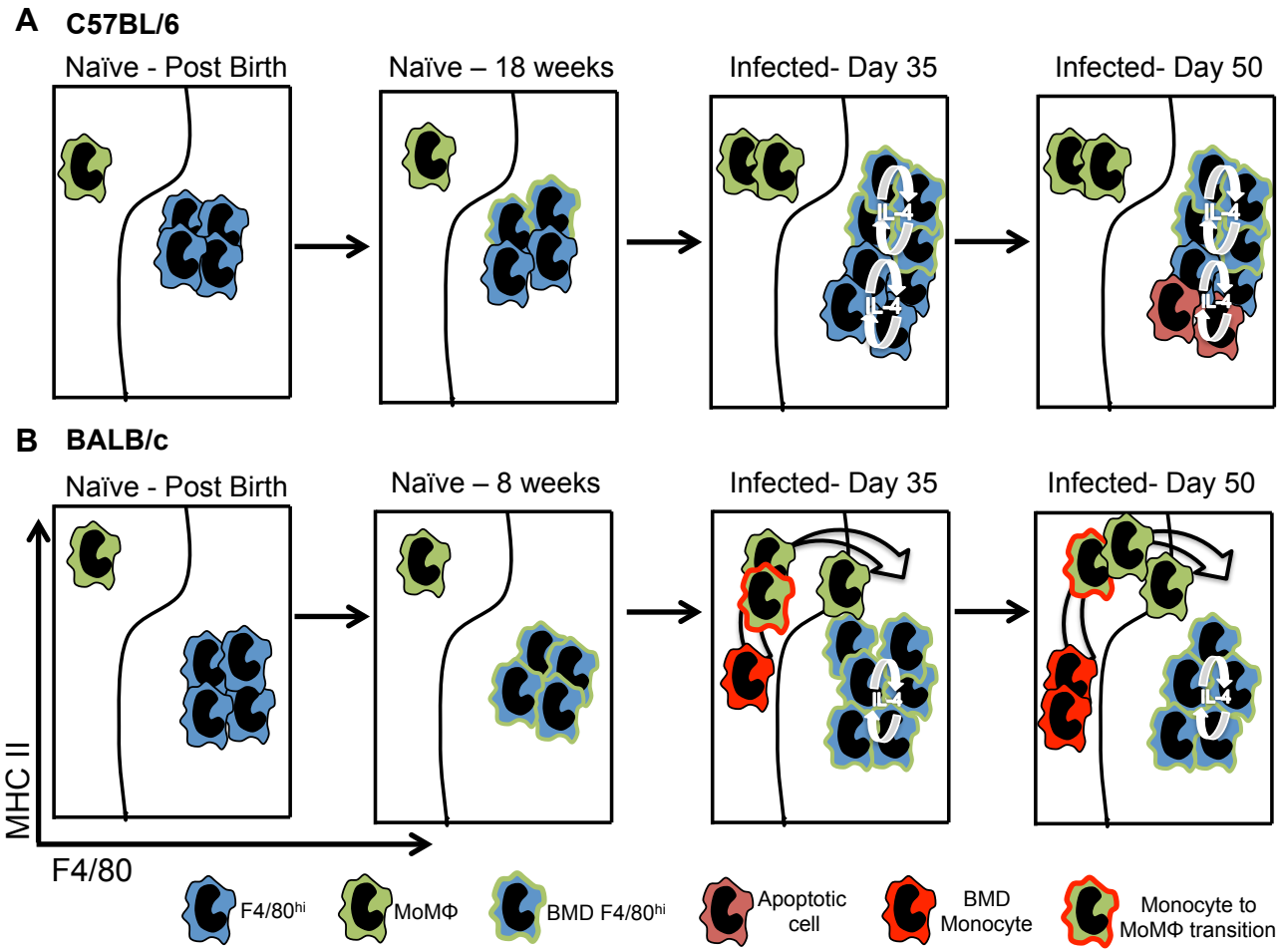


**Figure 2-12 Proposed mechanism of macrophage expansion in resistant C57BL/6 and susceptible BALB/c mice**

**A)** C57BL/6 - Resident pleural F4/80$^{hi}$ macrophages are continually replenished by BMDMΦ with age, maintaining the F4/80$^{hi}$ population at 80 % of the MΦ pool. Upon infection F4/80$^{hi}$ MΦ proliferate to generate an expanded F4/80$^{hi}$ population. Host and donor derived F4/80$^{hi}$ MΦ display equal proliferative capabilities by 23 weeks of age/ day 35 pi. By day 50 pi (25 weeks) of age the percentage of BMDMΦ contribution to the MΦ pool increases and this is a result of death of host derived F4/80$^{hi}$ MΦ and preferential survival of BMD F4/80$^{hi}$ MΦ. **(B)** BALB/c- The percentage of F4/80$^{hi}$ cells contributing to the MΦ pool declines with age and the percentage of MoMΦ increases. Upon infection there is early proliferation of the F4/80$^{hi}$ population and an influx of bone marrow derived monocytes, which mature into F4/80$^{lo}$MHC$^{hi}$Ly6C$^{-}$ MoMΦ. By day 50-post infection BMD monocytes and MoMΦ constitute 50 % of the MΦ compartment, these cells fail to integrate into the resident niche through upregulation of GATA6 and CD102.

# Chapter 3 Functional relevance of distinct macrophage compartments during *Litomosoides sigmodontis* infection

## 3.1 Summary

Chapter 2 highlighted the distinct MΦ dynamics occurring within naïve and infected C57BL/6 and BALB/c mice; resistance was associated with an expanded F4/80$^{hi}$ resMΦ population of mixed origin whereas susceptibility was marked by an increasing percentage of BMDMΦ and decline in resMΦ dominance. Outside of RELMα, YM-1 and Arg-1 expression, ResMΦ and BMDMΦ assume vastly different transcriptional and cell surface phenotypes in response to IL-4 stimulation, reflecting the functional consequences of alternative activation of MΦ with distinct phenotypes. This chapter highlights a greater rate of MΦ turnover in susceptible BALB/c mice and confirms a mechanism of continual recruitment and inefficient integration of BMDMΦ into the resMΦ niche. The MΦ compartment of susceptible BALB/c mice contains a large proportion of BMDMΦ by day 50 pi that once alternatively activated is highly positive for the immunosuppressive marker PD-L2. Depletion of monocytes prior to day 35 pi confirmed an immunosuppressive role for BMD AAMΦ in this strain, however this was independent of PD-L2. PD-L2 expression on the resMΦ compartment of resistant C57BL/6 mice was negligible and depletion of the expanded F4/80$^{hi}$ population in this strain was indicative of an active role for AAMΦ possessing a resMΦ phenotype in parasite killing. The results from this chapter highlight a distinct role for recently recruited alternatively activated macrophages in suppression the $T_H2$ immune response and an opposing role of alternative activated macrophages possessing a resMΦ phenotype in active worm killing.

## 3.2 Introduction

The accumulation of large number of alternatively activated macrophages is a hallmark of type 2 immunity. AAMΦ are generated through signalling from the IL-4Rα subunit, resulting in STAT6 activation and expression of the molecules; RELMα, YM1 and arginase-1 (Stein et al., 1992, Doyle et al., 1994, Loke et al.,

2002). Despite the large accumulation of these cells during parasite infection, their precise function is still largely unknown.

MΦ depletion during primary *Nippostrongylus brasiliensis* and secondary *Heligmosomoides polygyrus* infection resulted in reduced resistance, thereby illustrating an active role for MΦ in worm killing (Anthony et al., 2006, Zhao et al., 2008). AAMΦ bind parasite specific IgG antibodies during challenge infection with *H. polygyrus*, resulting in Arg-1 expression and subsequent trapping and killing of larvae. Complement component 3 was also necessary for the antibody-MΦ mediated larval trapping, illustrating that worm killing is a concerted effort between multiple players of the immune system (Esser-von Bieren et al., 2013). Another example of the multidisciplinary action necessary for worm killing can be seen during *Strongyloides stercoralis* infection in which MΦ, neutrophils and complement work collaboratively to kill the larvae (Bonne-Annee et al., 2013).

Conversely, AAMΦ are also highly implicated in the regulation and suppression of the $T_H2$ immune response. RELMα and Arg-1 have both been shown to suppress $CD4^+$ T cell production of IL-4, IL-5 and IL-13, illustrating an immunosuppressive role for these characteristic molecules of alternative activation (Nair et al., 2009, Pesce et al., 2009b). However, while RELMα deficiency during *N. brasiliensis* infection resulted in increased resistance (Pesce et al., 2009b) its absence during *Schistosoma mansoni* infection cumulated in exacerbated pulmonary fibrosis and enhanced susceptibility (Nair et al., 2009, Pesce et al., 2009b). A critical role for RELMα has been demonstrated in directing collagen deposition and successful wound repair (Knipper et al., 2015), thus the enhanced pulmonary fibrosis observed during *S. mansoni* infection likely reflects this deficit in wound repair. Similarly, macrophage specific depletion of Arg-1 during *S. mansoni* infection resulted in increased liver fibrosis and $T_H2$ related pathology(Pesce et al., 2009a), whereas in the context of secondary *H. polygyrus* infection Arg-1 expression was necessary for the larval trapping by the macrophage-antibody-complement complexes (Esser-von Bieren et al., 2013). Interestingly, Bone-Annee et al. demonstrated that expression of RELMα and Arg-1 was dispensable for the MΦ-neutrophil-complement mediated killing of *S. stercoralis* larvae and Esser-von Bieren et al. found that while IL-4 was

not necessary for the macrophage-antibody-complement trapping of *H. polygyrus* larvae, it was important in driving the local MΦ accumulation. Collectively, these data highlight that the role of AAMΦ and their associated molecules is highly context and parasite specific and illustrates the need for a greater understanding of the AAMΦ phenotype in disease settings.

The realisation that IL-4 induces the proliferative expansion of local prenatally derived resMΦ, which may be completely distinct from BMDMΦ (Jenkins et al., 2011), added an additional layer of complexity to the investigation of AAMΦ function in worm killing. Specifically the question arose as to whether differences exist in the modes of alternative activation assumed by BMDMΦ versus resMΦ upon exposure to IL-4 and whether these differences could resolve the discrepant findings regarding AAMΦ function in worm killing vs. immunosuppression.

In order to address the effect of IL-4 on MΦ populations of diverse origin, Gundra et al. induced the accumulation of alternatively activated macrophages of bone marrow origin (BMD AAMΦ) in the peritoneal cavity, through injection of thioglycollate and IL-4c, and compared the proliferation, alternative activation and transcriptional landscape of these cells to AAMΦ generated from resident cell proliferation, injection of IL-4c alone. IL-4 induced proliferation of both BMD and resMΦ, however the resMΦ population proliferated to a significantly greater degree. Furthermore, while both BMDMΦ and resMΦ upregulated RELMα, YM1 and Arg-1 in response to IL-4Rα stimulation, microarray analysis revealed an otherwise diverse transcriptional and cell surface phenotype between these populations. In particular, PD-L2 and Raldh were identified as specific markers of BMD AAMΦ. Whereas, uncoupling protein 1 (UCP-1), involved in thermogenesis was identified as being selectively expressed by resident derived AAMΦ. AAMΦ in the liver of *S. mansoni* infected animals were shown to be derived from the bone marrow and express high levels of PD-L2 (Nascimento et al., 2014, Gundra et al., 2014). Conversely, the expanded resident derived AAMΦ population in the pleural cavity of *L. sigmodontis* infected C57BL/6 mice was PD-L2 negative (Gundra et al., 2014). While both BMD and resident derived AAMΦ inhibited $CD4^+$ cell proliferation *in vitro*, only BMD AAMΦ polarised T cells toward a $FoxP3^+$ $CD4^+$ phenotype and this was through

expression of the enzyme Raldh (Gundra et al., 2014). Raldh is the rate-limiting enzyme in the oxidation of the vitamin A derivative retinal to retinoic acid (RA). In the gut expression of Raldh by $CD103^+$ DCs and local TGF-β results in the induction of inducible Tregs (iTregs), which are necessary for tolerance against food antigens (Sun et al., 2007). PD-L2 is a ligand for the T cell receptor programed death 1(PD-1), involved in T cell inhibition in the periphery (Liang and Sha, 2002). PD-1 knockout mice develop spontaneous autoimmunity. Expression of PD-L2 on AAMΦ is stat6 dependent (Loke and Allison, 2003) and result in the inhibition of T cell proliferation (Huber et al., 2010).

Prior to the appreciation that resMΦ and BMDMΦ have distinct origins, PD-L2 and raldh expression, in conjunction with their inhibitory effects, were assigned to AAMΦ. Gundra et al. have revealed that these immunosuppressive functions of AAMΦ are specific to BMDMΦ and in doing so the questions arises if AAMΦ of bone marrow origin are immunosuppressive and whether AAMΦ derived from resident cell proliferation are constructive to an effective $T_H2$ immune response and worm killing.

Chapter 2 highlighted the distinct mechanisms of MΦ accumulation between resistant and susceptible strains during *L. sigmodontis* infection. In resistant C57BL/6 mice MΦ accumulated through local proliferation of the resMΦ population, which is continually replenished from the bone marrow with age. In contrast, in the susceptible BALB/c strain there is a large influx of BMDMΦ, which diminish the dominance of the resMΦ population and fail to integrate into the local niche through up regulation of GATA6 and CD102. Chronic *L. sigmodontis* infection of susceptible BALB/c mice is characterised by the induction of a hyporesponsive T cell phenotype, whereby antigen specific $CD4^+$ $T_H2$ cells express PD-1 and diminished production of IL-4, IL-5 and IL-2 (van der Werf et al., 2013). The induction of this hyporesponsive T cell phenotype was reversed through the administration of an anti-PD-L2 antibody and patent infection failed to develop in these normally susceptible BALB/c mice. Furthermore, the onset of this hyporesponsive T cell phenotype was identified as occurring between day 20-60 post

infection (van der Werf et al., 2013), mirroring the window in which I observed and influx of BMD monocytes into the pleural cavity of infected BALB/c mice.

Thus in Chapter 3, I address whether the influx BMD monocytes seen in the BALB/c strain assume an immunosuppressive AAMΦ phenotype and thereby contribute to the susceptibility of the BALB/c strain, specifically asking if these cells are PD-L2$^{+}$ and responsible for the induction of a hyporesponsive T cell phenotype. Conversely, through depletion of the resident derived AAMΦ population in the C57BL/6 strain, I investigate if this population is actively contributing to worm killing.

## 3.3 Results

### 3.3.1 Differences in alternative activation of the MΦ compartment confirm distinct dynamics between strains

WT C57BL/6 and BALB/c mice were infected with *L. sigmodontis* s.c, and sacrificed on day 11, 28, 35 and 50 pi. The pleural cavity was washed to isolate the PLEC and the MΦ compartment was analysed via intracellular flow cytometry for expression of markers of alternative activation; RELMα and PD-L2.

The strains illustrated equal capacity to express RELMα upon infection, with ~99 % of the MΦ population staining positive from day 11-50 pi (Figure 3-1A), furthermore there was no difference in the mean fluorescent intensity of the infected MΦ compartments (Figure 3-1B). However, due to the large disparity in total MΦ number between the strains, there was significantly more RELMα positive MΦ in the C57BL/6 strain over the BALB/c at day 11, 35 and 50 pi (Figure 3-1C).

Administration of IL-4c to WT mice, results in the majority of the pleural MΦ compartment expressing RELMα, this expression is diminished in IL-4Rα$^{-/-}$ mice, illustrating the direct role for IL-4 in RELMα induction(Jenkins et al., 2011). Thus, we expected no detectable expression of RELMα in naïve controls and were surprised to observe ~80 % RELMα positivity in the MΦ compartment of BALB/c mice and 50 % in C57BL/6 at 10 weeks of age (Figure 3-1A). The percentage of RELMα positive cells was significantly higher in the BALB/c mice compared to C57BL/6 at 10 weeks. Despite the majority of the MΦ compartment expressing RELMα in naïve animals (Figure 3-1A), the mean fluorescence intensity of the MΦ population was significantly lower when compared to that of infected mice at day 11, 28 and 35 pi (Figure 3-1B). The low geometric mean of the MΦ population in naïve animals suggests that each cell expresses many fewer RELMα molecules when compared to their counterparts in infected animals.

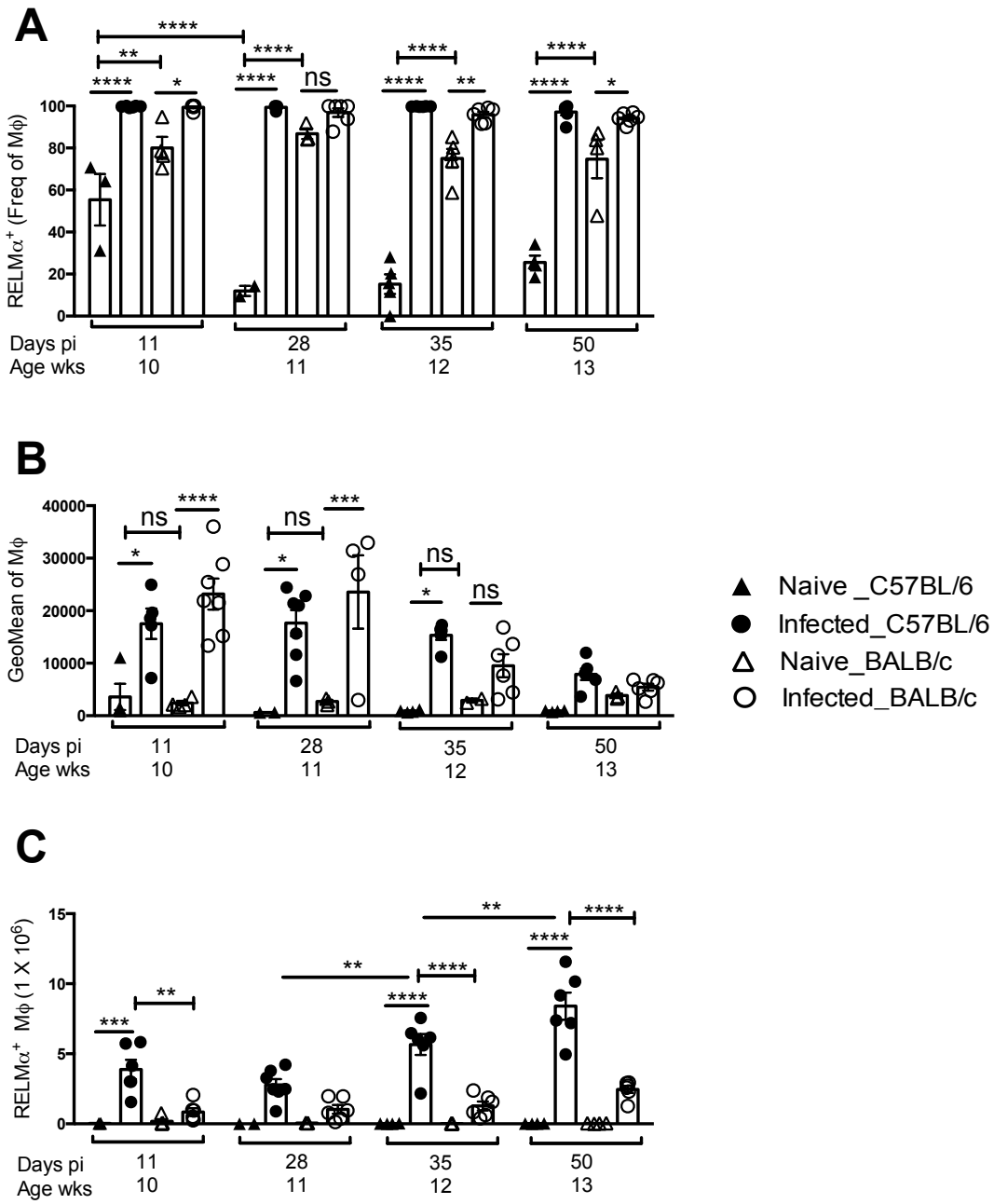


**Figure 3-1 RELMα expression by the MΦ compartment highlights differential homeostatic mechanisms between strains, but equal capacities during infection**

C57BL/6 and BALB/c female mice aged 6-8 weeks were infected with 30 *L. sigmodontis* L3 larvae s.c. The animals were sacrificed on days 11, 28, 35 and 50 pi and the pleural cavity was washed with 10 ml RPMI (1 % L-Glut, 1 % Pen-Strep) to isolate the PLEC and surviving worms. The total MΦ population was identified using the gating strategy illustrated in Fig2-2. **(A)** The percentage of MΦ expressing RELMα **(B)** Geometric mean of the MΦ population. **(C)** Total number of RELMα positive MΦ. Bars are representative of mean ± SEM, data are representative of 3 independent experiments with 2-6 mice/group. * P<0.05, ** P<0.01, ***P<0.0001,**** P<0.00001 as determined by a 2 one way ANOVA.

At 10 weeks of age, the F4/80$^{hi}$ population dominates the MΦ compartment in both strains; in C57BL/6 mice the F4/80$^{hi}$ population maintains its presence with age and infection, whereas in the BALB/c the percentage of F4/80$^{hi}$ cells gradually declines (Chapter 2- Fig. 5A&B). Consequently, the percentage of MΦ expressing RELMα at 10 weeks is reflective of the expression levels within the F4/80$^{hi}$ compartment at this time point (Figure 3-2A). There was a significant decline in the percentage of MΦ expressing RELMα in naïve C57BL/6 mice between 10 and 11 weeks of age, and this was reflective of the shutdown in RELMα expression in the F4/80$^{hi}$ population (Figure 3-1A & Figure 3-2B). In contrast, the F4/80$^{hi}$ population of naïve BALB/c mice remained ~80 % RELMα positive at 11 weeks of age and declined gradually to 50 % by 13 weeks (Figure 3-2A). The percentage of RELMα expression by the MoMΦ population was maintained at ~60 % and ~85 % in C57BL/6 and BALB/c mice respectively at all time points examined (Figure 3-2B).

Due to lack of events at day 11 and 28 post infection and from naïve animals, data for the expression of RELMα by monocytes at these time points could not be generated. However, ~85 % of monocytes that had infiltrated into the pleural cavity at day 35 were RELMα positive and this declined to ~55 % by day 50 pi (Figure 3-2C). Thus, during infection the MΦ population in C57BL/6 and BALB/c strains were equally capable of assuming an alternatively activated MΦ phenotype through RELMα induction. In order to further validate the differences in MΦ dynamics observed in Chapter 2, I decided to assess expression of PD-L2 in the MΦ compartment of infected C57BL/6 and BALB/c mice at day 50-post infection. Expression of PD-L2 has been identified as a marker of alternatively activated macrophages of bone marrow origin (Gundra et al., 2014).

A striking difference in the percentage of PD-L2 positive MΦ was observed between infected C57BL/6 and BALB/c mice; with a significantly greater percentage PD-L2$^{+}$ MΦ in the BALB/c strain (Figure 3-3A). Acquisition of PD-L2 expression occurred as cells migrated through the monocyte-MoMΦ maturation waterfall, with MoMΦ expressing more PD-L2 than monocytes (Figure 3-3B&C). Importantly this was true of both strains, though expression was always significantly less in the C57BL/6 mice (Figure 3-3B&C). Furthermore, in the BALB/c mouse PD-L2 expression was not

restricted to the monocyte and MoMΦ populations with a considerable percentage of the F4/80$^{hi}$ population expressing PD-L2 at day 50 pi (Figure 3-3D). The representative flow cytometric plots highlight the increased movement of the PD-L2$^{+}$ cells through the macrophage compartment of BALB/c vs. C57BL/6 mice (Figure 3-3E). Expression of PD-L2 on the F4/80$^{hi}$ population of infected BALB/c mice highlights the bone marrow origin of these cells and is supportive of BMDMΦ recruitment and delayed integration into the resident niche through down regulation of PD-L2 and assumption of a GATA6$^{+}$CD102$^{+}$ phenotype.

In the C57BL/6 partial bone marrow chimeric mice we observed that ~80 % of the F4/80$^{hi}$ population in both naïve and infected animals at day 50/25weeks of age were derived from the donor MΦ, supporting integration of BMDMΦ into the resMΦ pool. In these experiments the bone marrow derived macrophages were capable of assuming a resident F4/80$^{hi}$,GATA6$^{+}$, CD102$^{+}$ phenotype. Here we detect ~30% PD-L2 expression on the MoMΦ population (Figure 3-3C) in the C57BL/6 mice, whereas <4% of the F4/80$^{hi}$ population is PD-L2$^{+}$ (Figure 3-3D), this suggests that in the C57BL/6 mice as MoMΦ assume a resMΦ phenotype PD-L2 expression is lost. In order to investigate this hypothesis further, I co-stained the MΦ population at day 50 pi for both CD102 and PD-L2 (Figure 3-3F).

There was a significantly greater percentage of CD102$^{-}$PD-L2$^{-}$ cells in both naïve C57BL/6 and BALB/c mice compared to their infected counterparts (Figure 3-1G). These cells represent the BMD MoMΦ that normally constitute 20 % of the MΦ compartment in an 8-week-old naïve mouse and increase in dominance in aged BALB/c mice (Chapter 2_Fig5B). Consequently, a significantly greater percentage CD102$^{-}$PD-L2$^{-}$ cells were present in the MΦ compartment of naïve BALB/c than naïve C57BL/6 mice at 12-14 weeks of age (Figure 3-3G). Approximately 50 % of the MΦ compartment in infected BALB/c was CD102$^{-}$PD-L2$^{+}$, a significantly greater percentage than that detected in the MΦ compartment of naïve controls or infected C57BL/6 mice (Figure 3-3H). Furthermore, a significantly greater percentage of double positive CD102$^{+}$PD-L2$^{+}$ cells were detected in the MΦ compartment of infected BALB/c mice vs. naïve controls or infected C57BL/6 mice (Figure 3-3I). In both naïve and infected C57BL/6 mice, more than 80 % of the MΦ compartment was

$CD102^{+}PD\text{-}L2^{-}$ and this was significantly greater than the percentage of $CD102^{+}PD\text{-}L2^{-}$ cells in the MΦ compartment of naïve and infected BALB/c mice (Figure 3-3J). Despite the high degree of BMDMΦ contribution to the resMΦ compartment of C57BL/6 mice, which was revealed by bone marrow chimeric studies, there was negligible detection of $CD102^{+}PD\text{-}L2^{+}$ cells in this strain. The absence of $CD102^{+}PD\text{-}L2^{+}$ cells in the C57BL/6 strain suggests that bone marrow derived macrophages rapidly transit through a $PD\text{-}L2^{+}$ intermediate before adapting to local niche factors and assuming a $F4/80^{hi}$, $GATA6^{+}$, $CD102^{+}$, $PD\text{-}L2^{-}$ resMΦ phenotype. Additionally, these data reiterate that in the BALB/c strain there is an increasing percentage of BMDMΦ to the MΦ compartment of naïve mice, resulting in an increase in $CD102^{-}PD\text{-}L2^{-}$ cells and a decrease in resident $CD102^{+}PD\text{-}L2^{-}$ cells, this BMDMΦ recruitment and decline in resMΦ was initially suggestive of an inability of BMDMΦ to integrate into the resident niche. While the majority of recruited BMDMΦ assume an alternatively activated $CD102^{-}PD\text{-}L2^{+}$ phenotype upon infection in the BALB/c strain, a smaller percentage of $CD102^{+}PD\text{-}L2^{+}$ expressing cells were detected. The presence of $CD102^{+}PD\text{-}L2^{+}$ expressing cells in the MΦ compartment of the BALB/c strain highlights that BMDMΦ can assume a resident MΦ phenotype, but that the rate of recruitment is greater than the rate of conversion in the BALB/c strain.

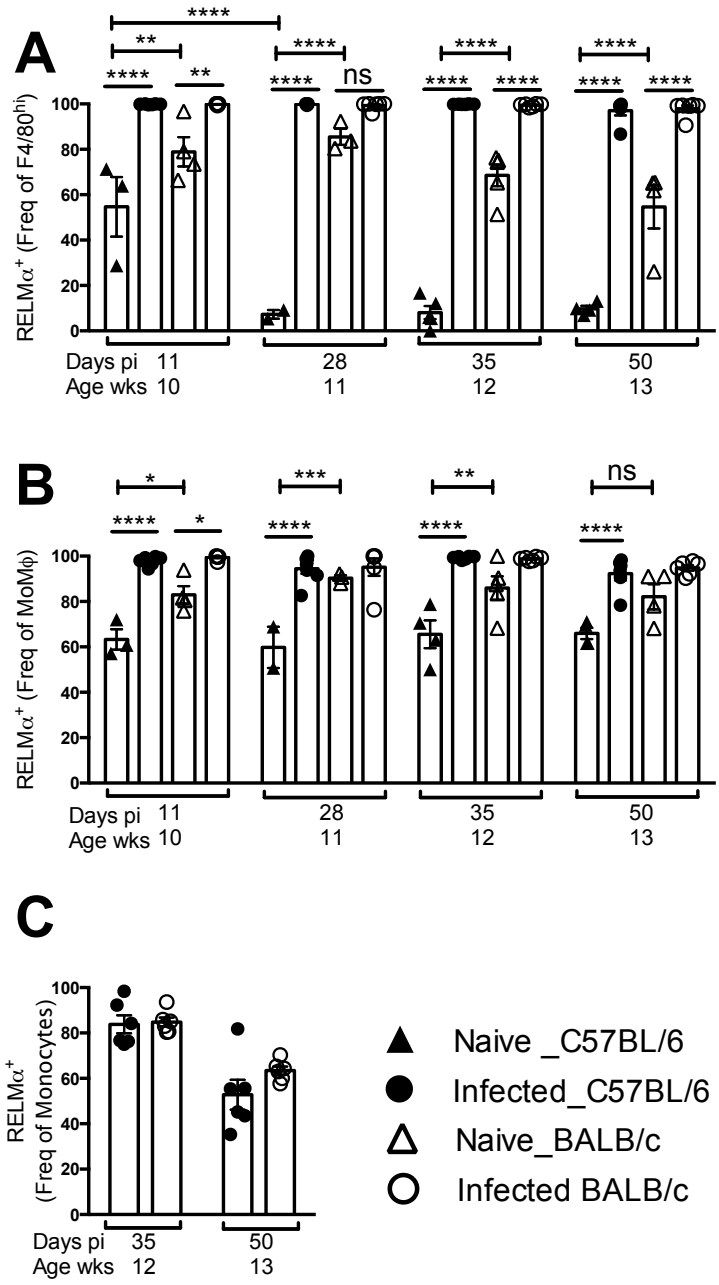


## Figure 3-2 RELMα expression by MΦ subpopulations

C57BL/6 and BALB/c females were infected with 30 L3 *L. sigmodontis* larvae s.c. C57BL/6 and BALB/c female mice aged 6-8 weeks were infected with 30 *L. sigmodontis* L3 larvae s.c. The animals were sacrificed on days 11, 28, 35 and 50 pi and the pleural cavity was washed with 10 ml RPMI (1 % L-Glut, 1 % Pen-Strep) to isolate the PLEC and surviving worms. Flow cytometric staining strategy depicted in Fig2-2 was used to identify the MΦ subpopulations **(A-C)** The percentage of **(A)** F4/80$^{hi}$ **(B)** MoMΦ and **(C)** monocytes expressing RELMα within the pleural cavity of naïve and infected C57BL/6 and BALB/c mice.

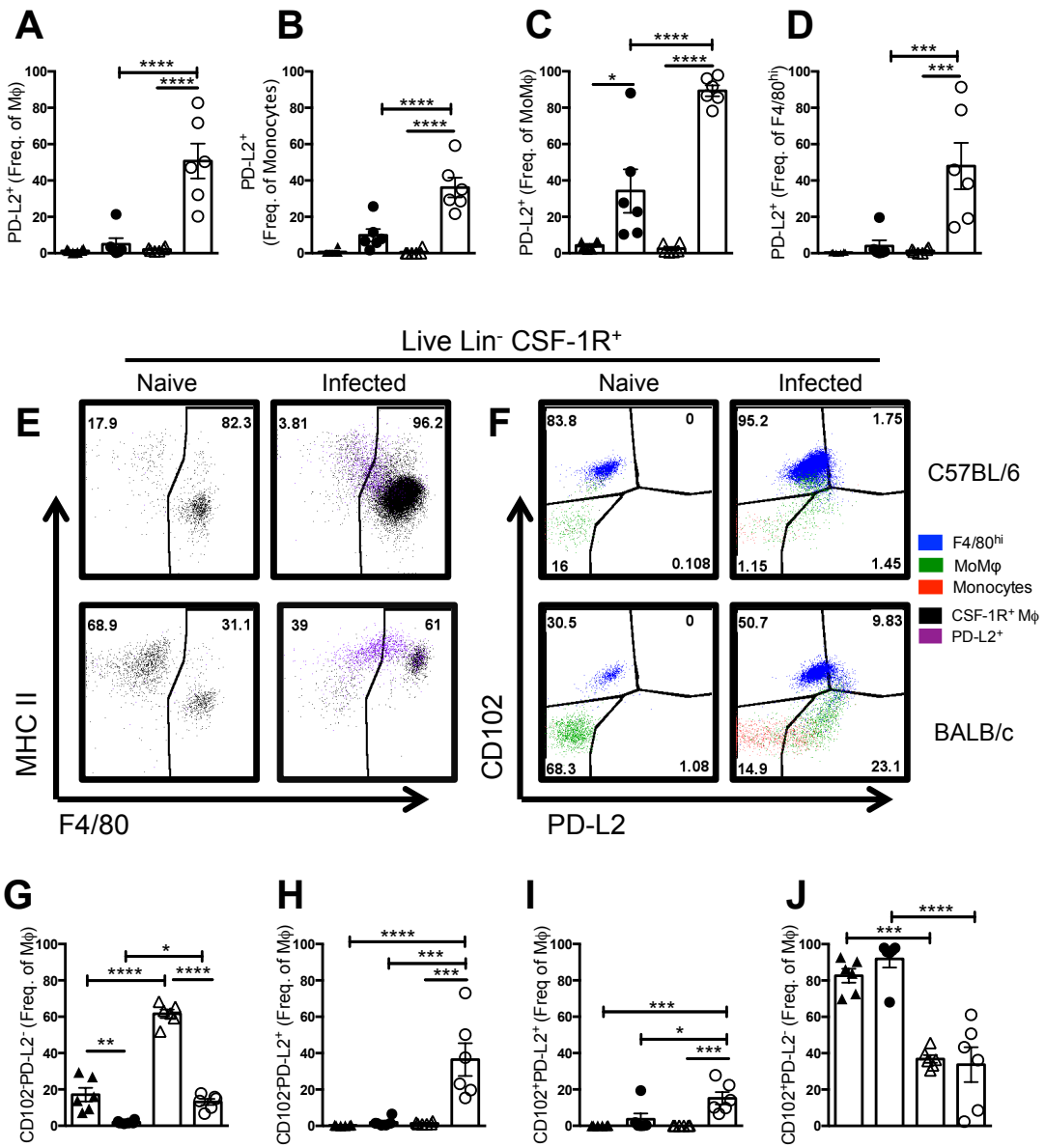


**Figure 3-3 MΦ expression of PD-L2 and CD102 reveal mechanistic differences in alternative activation and conversion between strains**

C57BL/6 and BALB/c female mice aged 6-8 weeks were infected with 30 *L. sigmodontis* L3 larvae s.c. The animals were sacrificed on day 50 pi and the pleural cavity was washed with 10 ml RPMI (1 % L-Glut, 1 % Pen-Strep) to isolate the PLEC. The total MΦ population was identified using the gating strategy illustrated in Fig2-2. **(A-D)** PD-L2 expression by **(A)** total MΦ **(B)** monocytes **(C)** MoMΦ and **(D)** F4/80$^{hi}$ **(E&F)** Representative plots illustrating **(E)** PD-L2 expression throughout the MΦ compartment and **(F)** expression of PD-L2 and/or CD102 by the MΦ subpopulations. **(G-J)** Expression or lack thereof CD102 and PD-L2 by MΦ compartment. Bars are representative of mean ± SEM, data are representative of three independent experiments with 6 mice/group. * P<0.05, ** P<0.01, ***P<0.0001,**** P<0.00001 as determined by a 2 one way ANOVA.

### 3.3.2 BMDMΦ are detrimental to worm killing an a PD-L2-independent manner at day 35 pi in susceptible BALB/c mice

The time course analysis carried out in Chapter 2 highlighted that one of the most striking differences between resistant C57BL/6 mice and susceptible BALB/c mice was the presence of a large expanded F4/80$^{hi}$ resMΦ population in C57BL/6 mice and the influx of monocytes into the susceptible strain. These influxing bone marrow derived monocytes form a 'monocyte waterfall' throughout the MΦ compartment and express high levels of PD-L2. During *L. sigmodontis* infection of susceptible BALB/c mice, antigen specific CD4$^{+}$ $T_H2$ cells are conditioned toward a hyporesponsive T cell phenotype, characterized by expression of PD-1 and diminished production of IL-4, IL-5 and IL-2 (van der Werf et al., 2013). Administration of an anti-PD-L2 antibody restored T cell function and patent infection failed to develop in these normally susceptible BALB/c mice. The onset of this hyporesponsive T cell phenotype was identified as occurring between day 20-60 post infection (van der Werf et al., 2013). Here I aim to assess whether monocytes, which infiltrate into the pleural space of susceptible BALB/c mice are detrimental to worm killing, through induction of a hyporesponsive T cell phenotype via PD-L2 expression.

First, I sought to characterise and correlate the MΦ and T cell dynamics at day 50 pi. As in previous experiments there was a higher degree of BMDMΦ contribution to the MΦ compartment of BALB/c mice compared to C57BL/6 mice (Figure 3-4A). Within the pleural cavity a trend toward a greater $T_H2$ response in the C57BL/6 strain was observed, with slightly more of the CD4$^{+}$ T cells expressing the $T_H2$ master transcription factor GATA3 than in the BALB/c strain (Figure 3-4B). The $T_H2$ response in the draining parathymic lymph nodes was significantly greater in infected C57BL/6 mice compared to BALB/c (Figure 3-4C). Of note however, is that the frequency of $T_H2$ cells is unchanged between naïve and infected BALB/c mice, suggestive of a shutdown back to basal levels. Furthermore, there is a trend toward a greater frequency of $T_H2$ cells in the parathymic lymph nodes of naïve BALB/c mice compared to C57BL/6. There was a greater percentage of PD-L2$^{+}$ cells in all MΦ sub-populations of the BALB/c strain vs. C57BL/6 (Figure 3-3B-D) and this

translated numerically to a much greater proportion of the BALB/c MΦ being PD-L2$^+$ (Figure 3-4D&E), thereby increasing the likelihood of a PD-L2$^+$ MΦ interacting with a GATA3$^+$CD4$^+$ T cell and inducing a hyporesponsive T cell phenotype. Taken together, this data confirms a greater percentage of PD-L2$^+$ MΦ and a weaker $T_H2$ response can be seen in the susceptible BALB/c mice at day 50 pi when compared to resistant C57BL/6 mice. When a correlation analysis of the percentage of PD-L2$^+$ MΦ and the worm recovery rate was carried out a strong correlation with a spearman co-efficient of 0.749 was obtained (Figure 3-4F). As illustrated in Chapter 2 (Chapter 2 Fig. 3), MΦ and B cells are the two cell types, which are most different between resistant C57BL/6 and susceptible BALB/c mice. Previous work has hypothesised the B cells may be the cell type responsible for inducing the hyporesponsive T cell phenotype during *L. sigmodontis* infection (van der Werf et al., 2013). Here I found that there were many more PD-L2$^+$ MΦ in the cavity than there were PD-L2$^+$ B cells (Figure 3-4G) and therefore continued to investigate the detrimental role of BMDMΦ to worm killing in the susceptible BALB/c mice.

The influx of monocytes into the pleural cavity of BALB/c mice was observed from day 35 post infection, a time point at which active worm killing is occurring in the C57BL/6 strain. In order to prevent this monocyte influx and determine if doing so resulted in enhanced worm killing, an anti-CCR2 or control rat IgG antibody was administered daily intraperitoneally from day 31-34-post infection and the animals were sacrificed on day 35 (Figure 3-5A). This experiment was carried out four times and the prevention of the monocyte infiltration was successful in three of these experiments. As in previous experiments, a considerable influx of monocytes was detected in the MΦ compartment of control rat IgG treated mice, resulting in a decline in the percentage of F4/80$^{hi}$ MΦ (Figure 3-5B). Successful prevention of the monocyte influx was determined by the absence of monocytes and the maintenance of the F4/80$^{hi}$ population at ~80 % of the total MΦ compartment. In one of the four experiments carried out, the monocyte influx had occurred prior to the administration of the anti-CCR2 antibody, enabling the monocytes to mature into MoMΦ and escape depletion (Figure 3-5B). This resulted in significantly more MoMΦ in the cavity of these mice and significantly less F4/80$^{hi}$ MΦ (Figure 3-5B). Thus, I chose to exclude this experiment from further analysis.

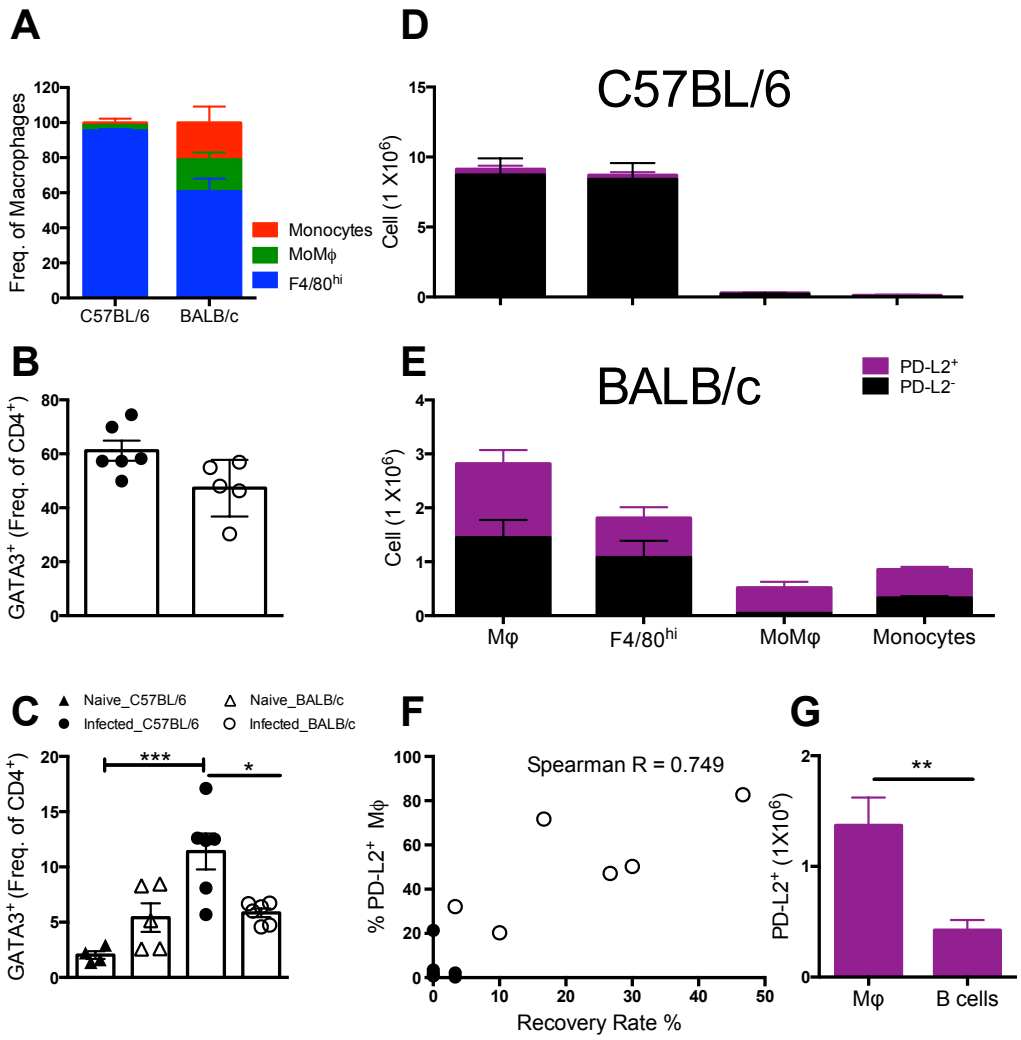


**Figure 3-4 PD-L2 expression in susceptible BALB/c mice correlates with reduced worm killing and a hyporesponsive $T_H2$ cell phenotype**

C57BL/6 and BALB/c female mice aged 6-8 weeks were infected with 30 *L. sigmodontis* L3 larvae s.c. The animals were sacrificed on day 50 pi and the pleural cavity was washed with 10 ml RPMI (1 % L-Glut, 1 % Pen-Strep) to isolate the PLEC and the draining parathymic lymph nodes were also isolated. The total MΦ population was identified using the gating strategy illustrated in Fig2-2 and T cell compartment identified using staining panel outlined in Materials and Methods Table 6. **(A)** Contributions of MΦ subpopulations to MΦ as a whole. **(B&C)** Percentage of $CD4^+$ cells expressing GATA3 in the **(B)** PC and **(C)** dLN. **(D&E)** Total number of PD-$L2^+$ macrophages across the macrophage subpopulations in **(D)** C57BL/6 and (E) BALB/c mice. **(F)** Correlation of the percentage of MΦ expressing PD-L2 and worm recovery rate **(G)** comparison of total PD-$L2^+$ MΦ and B cells in the PC at day 50 pi. Bars are representative of mean ± SEM, data are representative of three independent experiments with 6 mice/group. * $P<0.05$, ***$P<0.0001$ as determined by a 2 one way ANOVA

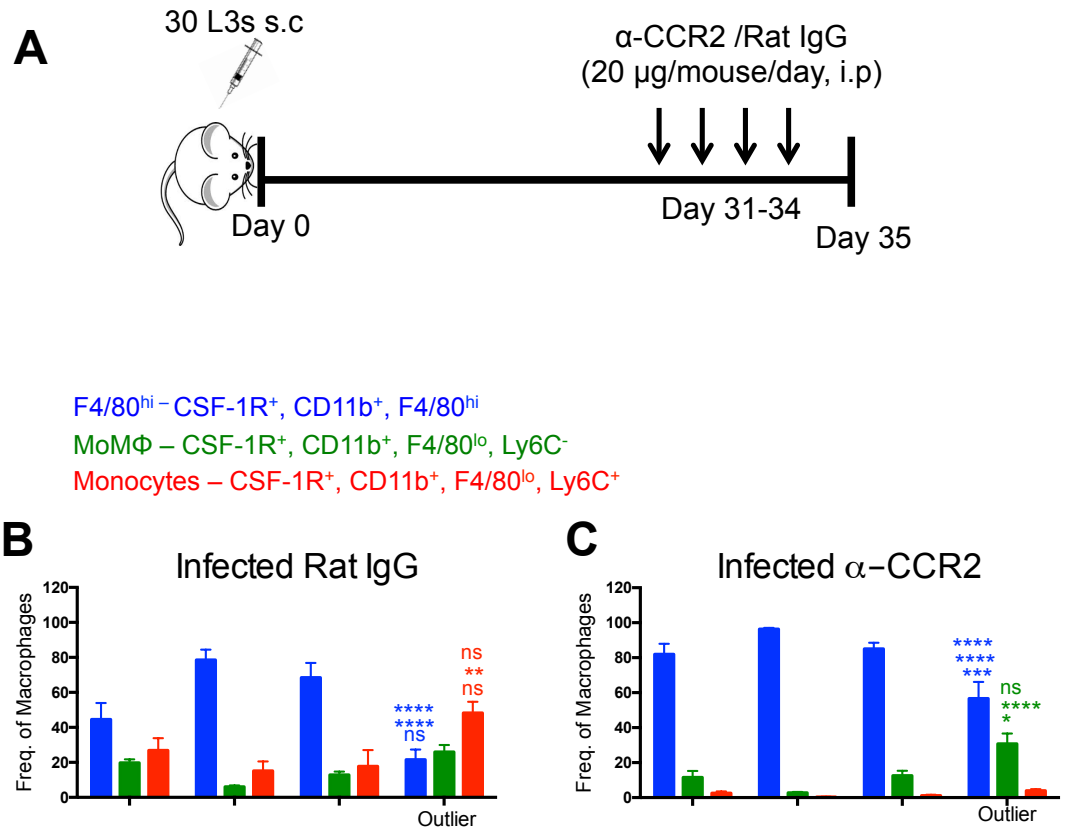


**Figure 3-5 Anti-CCR2 treatment successfully depletes Ly6C$^{+}$ monocytes but not MoMΦ or F4/80$^{hi}$ MΦ**

BALB/c female mice were infected s.c. with 30 *L. sigmodontis* L3s and treated with a monocyte depleting anti-CCR2 a mAb or control from day 31-34 pi. The animals were sacrificed on day 35 pi and the pleural cavity was washed with 10 ml RPMI (1 % L-Glut, 1 % Pen-Strep) to isolate the PLEC. The total MΦ population was identified using the gating strategy illustrated in Fig2-2. **(A)** Schematic illustrating anti-CCR2 administration. **(B-C)** Percentage of F4/80$^{hi}$, MoMΦ and monocytes contributing to the macrophage compartment at day 35 within infected **(B)** control Rat IgG and **(C)** anti-CCR2 treated mice. Bars are representative of mean ± SEM, **(B-C)** representative of 4 independent experiments with 5,10,6 and 6 mice per group **(B&C)** * P<0.05, ** P<0.01, ***P<0.0001,**** P<0.00001 as determined by a 2 way ANOVA.

When the influx of monocytes into the pleural space was successfully prevented this resulted in a significant increase in worm killing (Figure 3-6A). While the difference in worm recovery between Rat IgG and anti-CCR2 treated mice does not appear striking, it is extremely unusual to have BALB/c mice which have cleared the worm by day 35 pi. In the anti-CCR2 treated group 29 % of the mice had cleared the worm compared to 5% in the rat IgG treated group (Figure 3-6A). Anti-CCR2 treatment did not affect the number of F4/80$^{hi}$ MΦ in the cavity (Figure 3-6B), but successfully depleted MoMΦ (Figure 3-6C) and monocytes (Figure 3-6D). This difference in worm killing could not readily be attributed to PD-L2 expression on the MΦ compartment as there was no significant difference in the number of PD-L2$^{+}$ MΦ between anti-CCR2 treated and Rat IgG treated controls (Figure 3-6E). There was also no difference in the number of $T_H2$ cells between control and monocyte depleted mice in the pleural cavity at day 35 pi (Figure 3-6F). However, the quality of the local $T_H2$ response in the pleural cavity of monocyte-depleted mice was significantly greater with more of the $T_H2$ cells producing IL-4 (Figure 3-6G) and a trend toward greater IL-5 (Figure 3-6H) and IFNγ production (Figure 3-6I). Within the draining lymph nodes, there was no detectable difference in number of $T_H2$ cells (Figure 3-6J) or their production of IL-4 (Figure 3-6K) or IL-5 (Figure 3-6L) between control Rat IgG and anti-CCR2 treated mice. There was however an increase in IFNγ production by GATA3$^{+}$ CD4$^{+}$ cells within the draining lymph nodes upon monocyte depletion (Figure 3-6M).

These data confirm that the influx of bone marrow derived macrophages into the pleural space of susceptible BALB/c mice is detrimental, resulting in decreased worm killing and a weakened $T_H2/T_H1$ response, that is essential for worm killing in susceptible BALB/c mice (Saeftel et al., 2003). However, we failed to see an effect of monocyte depletion on the percentage or number of PD-L2$^{+}$ MΦ, thus the detrimental role of monocytes on worm killing is likely PD-L2-independent at day 35 pi. The percentage of PD-L2 expression observed in both Rat IgG controls and anti-CCR2 treated mice at day 35 pi was considerably lower than what had previously been observed at day 50. Analysis of the PD-L2 expression on the MΦ compartment at day 11, 28, 35 and 50 pi revealed that induction of PD-L2 on the MΦ compartment did not peak until between day 35 and day 50 post infection (Figure

3-7A&B). Thus, while the monocyte influx occurs at day 35 pi, these cells do not become alternatively activated and up-regulate PD-L2 until day 50 pi.

In order to determine if PD-L2$^{+}$ MΦ are involved in the induction of the hypo-responsive T cell phenotype at day 50 pi, we administered the anti-CCR2 antibody from day 31-34 post infection and subsequently isolated the PLEC at day 50 pi (Figure 3-7C). Monocyte depletion prior to day 35 pi did not result in increased worm killing by day 50 pi in BALB/c mice (Figure 3-7D). This was not too surprising as analysis of the MΦ compartment revealed that monocyte depletion was only transient. By day 50, there was an influx of monocytes into the pleural cavity of several of the anti-CCR2 treated mice (Figure 3-7E) and while no difference in MoMΦ was detected (Fig. 7F), the percentage of F4/80$^{hi}$ MΦ had declined to ~30 %, similar to what was seen in Rat IgG treated mice (Fig. 7G). However, in both the Rat IgG and anti-CCR2 treated groups, the mice that had cleared the worms (green) were those in which monocytes had not infiltrated (Fig. 7E), the F4/80$^{hi}$ population remained dominant (Figure 3-7G) and maintained a resident CD102$^{+}$ phenotype (Figure 3-7H). Furthermore, there was a greater degree of PD-L2 expression on the MΦ compartment of the mice with the highest worm burden (red) (Figure 3-7I) and a trend toward less IL-5 and IFNγ production by GATA3$^{+}$CD4$^{+}$ in the pleural space (Figure 3-7J&K).

Collectively, these data confirm an immunosuppressive role for monocytes within the susceptible BALB/c strain and highlight that in the absence of monocytes the mixed $T_H1/T_H2$ immune response within the BALB/c strain is sufficient to clear the worm at earlier time points.

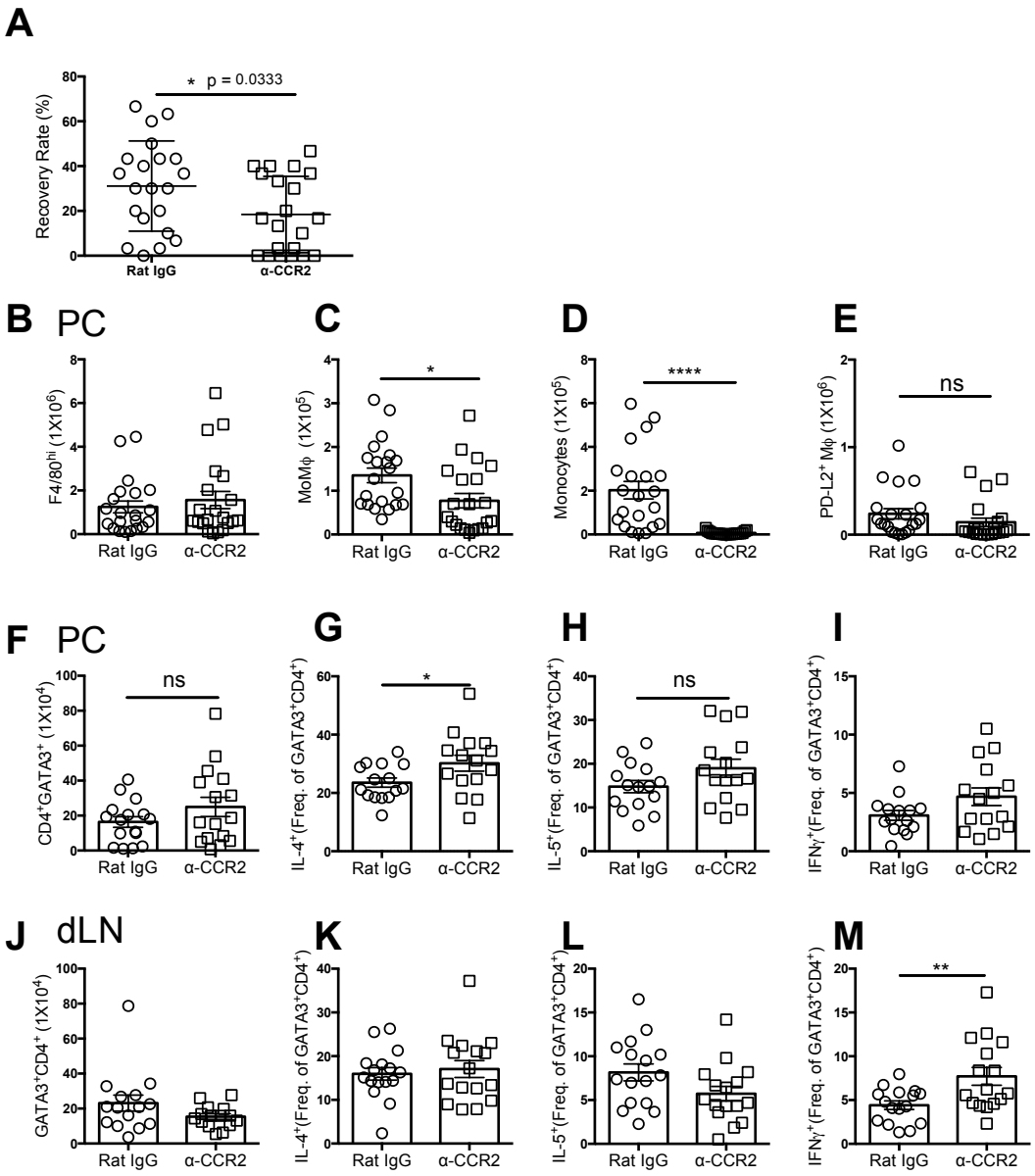


## Figure 3-6 Monocyte depletion prior to day 35 promotes worm killing, independent of MΦ PD-L2 expression, through enhancing local $T_H2$ quality

*L. Sigmodontis* infected BALB/c mice were treated with a monocyte depleting anti-CCR2 mAb from day 31-34 pi. The MΦ compartment and T cell quality in the PC and dLN were assessed on day 35 pi. **(A)** Worm burden. **(B-E)** Total number of **(B)** $F4/80^{hi}$ **(C)** MoMΦ **(D)** Monocytes **(E)** $PD\text{-}L2^+$ MΦ and **(F)** $CD4^+$ $GATA3^+$ T cells in the PC. **(G-H)** The percentage PC $GATA3^+CD4^+$ cells expressing **(G)** IL-4, **(H)** IL-5 and **(I)** IFNγ. **(J)**Total number of $CD4^+$ $GATA3^+$ T cells in the draining parathymic lymph nodes. **(K-M)** The percentage dLN $GATA3^+CD4^+$ cells expressing **(K)** IL-4, **(L)** IL-5 and **(M)** IFNγ. Bars are represent mean ± SEM **(A-E)** are representative of three independent experiments with 5, 10 and 6 mice/group **(F-M)** are representative of two independent experiments with 10 and 6 mice per group. * $P < 0.05$ as determined by an unpaired Student's t test with Welch's correction.

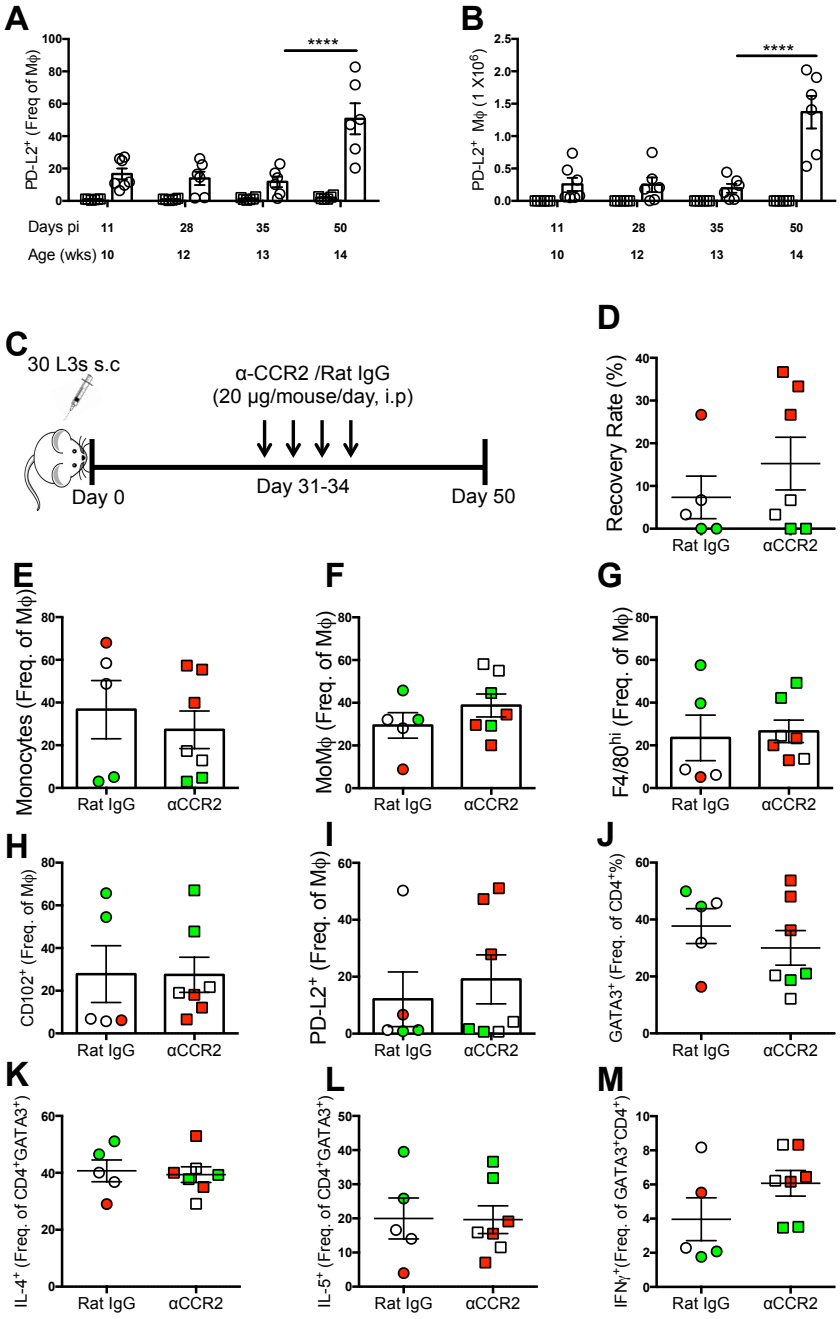


**Figure 3-7 Sustained monocyte depletion is associated with heightened worm killing and decreased PD-L2 expression by MΦ**

BALB/c mice were infected with 30 *L. sigmodontis* larvae and **(A&B)** PD-L2 expression by the PC MΦ compartment was assessed at day 11, 28, 35 and 50 pi. **(A)** The percentage of MΦ expressing PD-L2 **(B)** total number of PD-L2$^{+}$ MΦ at each time point. **(C-D)** an anti-CCR2 mAb was administered from day 31-34 pi, the PC was subsequently assessed at day 50 pi. **(C)** Schematic showing experimental plan. (**D) R**ecovery rate. **(E-G)** Frequency of **(E)** F/80$^{hi}$, **(F)** MoMΦ and **(G)** monocytes of total MΦ compartment. MΦ expression of **(H)** CD102 and **(I)** PD-L2 **(J)** percentage of CD4$^{+}$ cells expressing GATA3 within PC **(K-M)** expression of IL-4, IL-5 and IFNγ by GATA3$^{+}$CD4$^{+}$ cells in the PC. Bars are representative of mean ± SEM **(A-M)** are results from a single experiment with 6/7 mice/group.,**** P<0.00001 as determined by a 2 way ANOVA

### 3.3.3 Depletion of resident macrophages in resistant C57BL/6 mice is suggestive of an active role in worm killing

A large expansion of the F4/80$^{hi}$ resMΦ population was the defining characteristic of the PLEC from resistant C57BL/6 mice during *L. sigmodontis* infection. Consequently I hypothesised that resMΦ are involved in active worm killing in the C57BL/6 mice.

In order to address this, we depleted resMΦ during *L. sigmodontis* infection through administration of clodronate-loaded liposomes directly into the thoracic cavity. Liposomes are spherical vesicles composed of a phospholipid bilayer encasing an aqueous compartment. The uptake of liposomes containing dissolved clodronate, a non-toxic bisphosphonate, results in high concentrations of intracellular clodronate and the subsequent induction of apoptosis in these cells (van Rooijen et al., 1996). Clodronate liposomes or control PBS was administered on day 27 and 29 pi and the animals were sacrificed on day 33 (only received clodronate on day 27), 35 and 39 pi (Figure 3-8A). We had originally hoped to take the day 33 and day 39 time points out until day 50; a point at which many C57BL/6 mice have cleared the worm, in the hope of seeing a statistically significant difference in worm killing in the absence of resMΦ, however due to ill-health of the animals we had to terminate the experiments early.

The representative flow cytometric plots clearly illustrate that administration of clodronate-loaded liposomes resulted in successful depletion of F4/80$^{hi}$ MΦ within the pleural cavity with the caveat of inducing the recruitment of BMD monocytes (Figure 3-8B). The successful resMΦ depletion was evident in the decreased number (Figure 3-8C) and percentage of F4/80$^{hi}$ MΦ (Figure 3-8D) present in the pleural space at day 33, 35 and day 39 pi. While the number and percentage of MoMΦ remained unchanged (Figure 3-8E&F) there was a large influx of monocytes into the cavity at all time points (Figure 3-8G&H). The successful depletion of the F4/80$^{hi}$ MΦ and influx of monocytes resulted in a decrease in the percentage of MΦ expressing CD102 (Figure 3-9A) and an increase in those expressing PD-L2 within the cavity (Figure 3-9B). Clodronate liposome treatment at day 27 and analysis of worm recovery on day 33 did not reveal any difference in worm burden (Figure

2-9C) However, analysis of worm burden at day 35 and 39 revealed a trend toward less worm killing in mice that had been depleted of F4/80$^{hi}$ MΦ (Figure 3-9D&E).

While MΦ are the most phagocytic cell present in the pleural space and therefore most likely to ingest the clodronate liposomes, these vesicles are not specific to MΦ and thus may also be taken up both other cell types. At day 33 and 35 post infection, clodronate liposomes did not appear to deplete any other cells within the pleural space, specifically B cells, eosinophils, DCs or T cells (Figure 3-10A-E). However, by day 39 pi the numbers of B cells were also significantly reduced (Figure 3-10A). It is difficult to decipher if the decrease in B cells was a direct result of clodronate liposomes ingestion or a result of decreased signalling from the resMΦ population. Furthermore, it is impossible to say if the decrease in worm killing observed at day 39 pi was a result of successful depletion of the F4/80$^{hi}$ MΦ or depletion of B cells also. Depletion of the F4/80$^{hi}$ MΦ did not affect the $T_H2$ immune response at any of the time points examined, the percentage of $T_H2$ cells remained constant (Figure 3-10E) as did the production of IL-4, IL-5 and IFNγ by these cells (Figure 3-10F-H).

At each time point 200 ul of clodronate loaded liposomes were delivered into the pleural space. This is a relatively high does, however we felt it an appropriate amount to target the ~1X10$^7$ MΦ present in the pleural space from day 28 post infection. Due to the need for high numbers I excluded naïve control groups, additional experiments by a post-doc in the lab have highlighted that the adverse affects of intrapleural clodronate-loaded liposomes administrations are only seen in the infected-clodronate treated group, not the naïve-clodronate treated control group, indicative of a protective role for MΦ during infection. However, upon necroscopy clodronate liposomes were isolated from the pleural space of several animals, indicating an overdoes of clodronate. Furthermore, these mice also presented with fibrotic livers.

Thus, we while we successfully depleted F4/80$^{hi}$ MΦ through direct delivery of clodronate-loaded liposomes into the pleural space we failed to obtain a difference in worm recovery between liposome-treated and PBS-treated mice. Despite our inability to obtain a difference in worm burden, I am intrigued by the slight trend toward decreased worm killing in clodronate treated mice. To truly investigate the

role of the resMΦ population in worm killing a more direct and specific method of MΦ depletion would need to be employed.

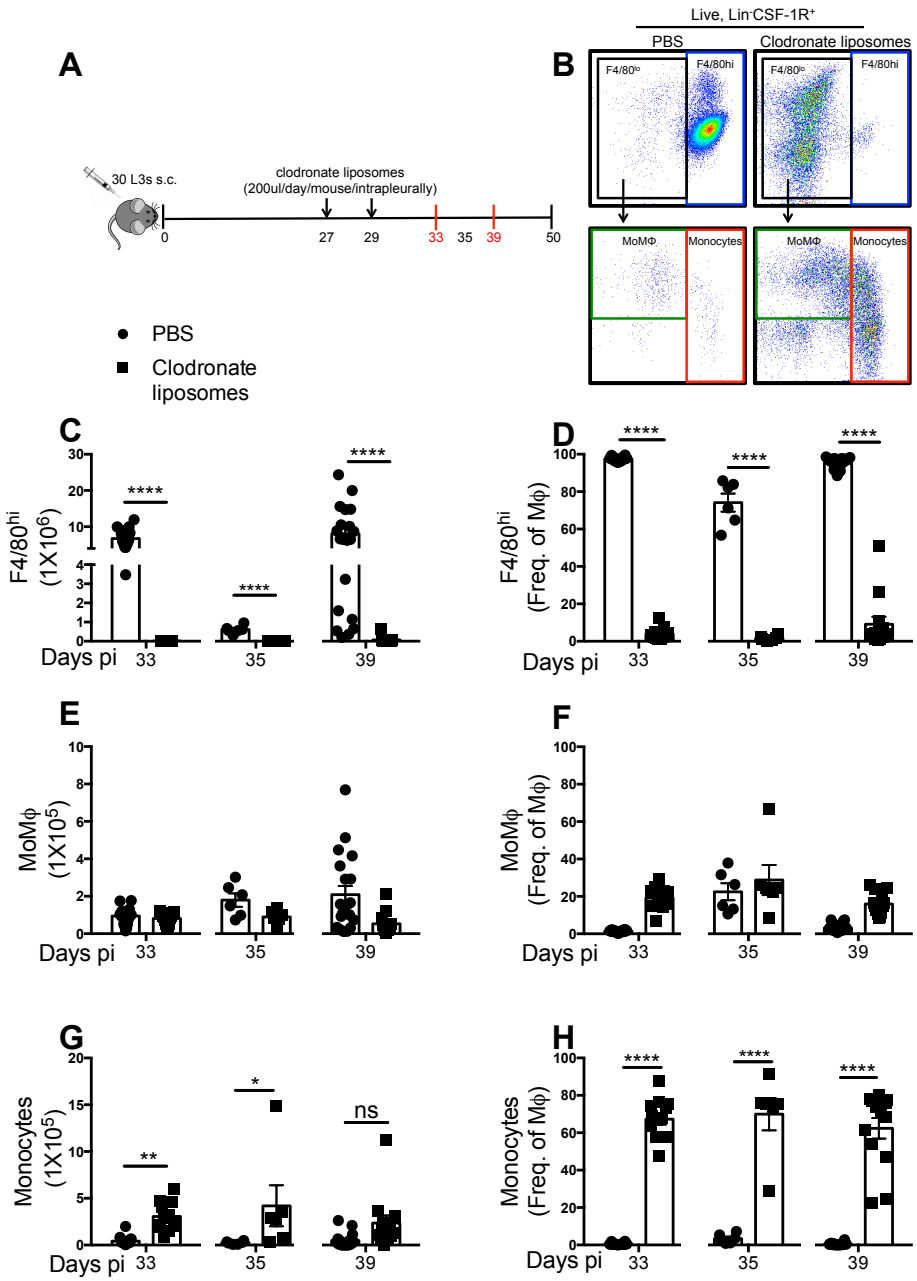


**Figure 3-8 Intrapleural administration of clodronate successfully depletes F4/80$^{hi}$ resMΦ and induces monocyte recruitment**

C57BL/6 female mice were infected s.c. with 30 *L. sigmodontis* L3s and subsequently injected intrapleurally on day 27 and/or day 29 pi with clodronate liposomes or control PBS. Animals were sacrificed on days 33, 35 and 39 pi at which point the pleural cavity was washed with 10 ml RPMI (1 % Pen-Strep, 1 % L-Glut) to isolate the pleural exudate cells. **(A)** Schematic of experimental outline and necessary endpoints due to ill-health of animals (**B)** representative flow cytometric plots illustrating successful depletion of F4/80$^{hi}$ MΦ and subsequent monocyte influx. Number and percentage of F4/80$^{hi}$ MΦ **(C&D),** MoMΦ **(E&F)** and monocytes **(G&F)** within the pleural space of clodronate or PBS treated animals on day 33,35 and 39 pi**.** Bars are representative of mean ± SEM, each time point is representative of 1 independent experiment with 6 (day 35) – 20 mice/ group. * P<0.05, ** P<0.01, ***P<0.0001,**** P<0.00001 as determined by a 2 way ANOVA

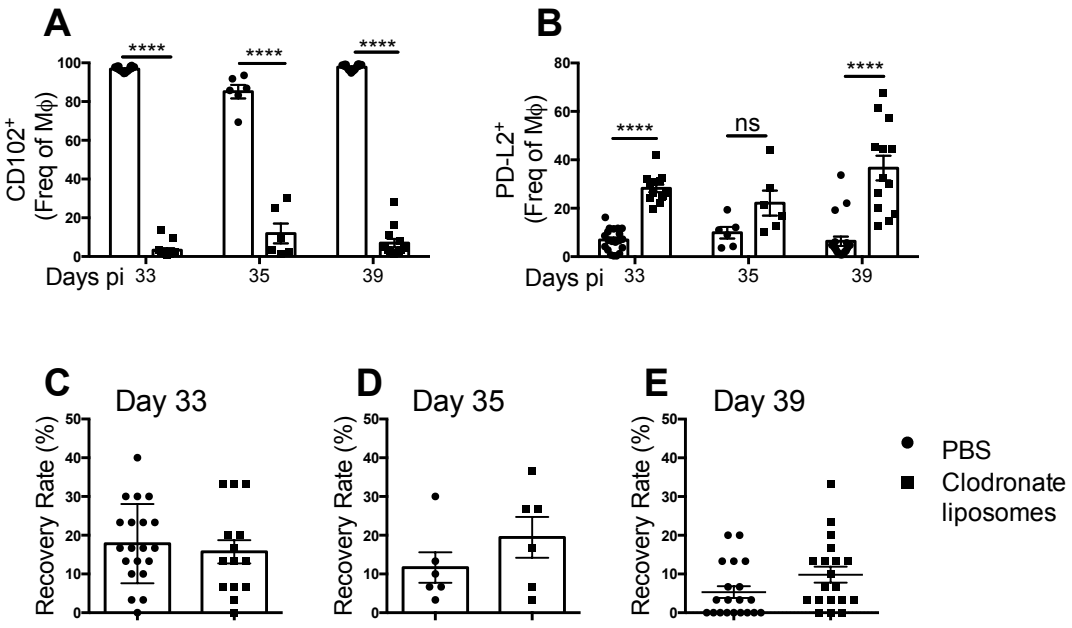


**Figure 3-9 Clodronate depletion of F4/80$^{hi}$ resMΦ in resistant C57BL/6 mice is suggestive of a protective role in worm killing**

C57BL/6 female mice were infected s.c. with 30 *L. sigmodontis* L3s and subsequently injected intrapleurally on day 27 and/or day 29 pi with clodronate liposomes or control PBS. Animals were sacrificed on days 33, 35 and 39 pi at which point the pleural cavity was washed with 10 ml RPMI (1 % Pen-Strep, 1 % L-Glut) to isolate the pleural exudate cells and surviving worms. The cellular populations were identified using the gating strategy illustrated in Fig2-2. Percentage of MΦ expressing **(A)** CD102 or **(B)** PD-L2 within the pleural space of clodronate or PBS treated animals on day 33, 35 and 39 pi**.** Recovery rate at **(C)** day 33 **(D)** day 35 **(E)** day 39 pi. Bars are representative of mean ± SEM, each time point is representative of 1 independent experiment with 6 (day 35) – 20 mice/ group. * P<0.05, ** P<0.01, ***P<0.0001,**** P<0.00001 as determined by a 2 way ANOVA.

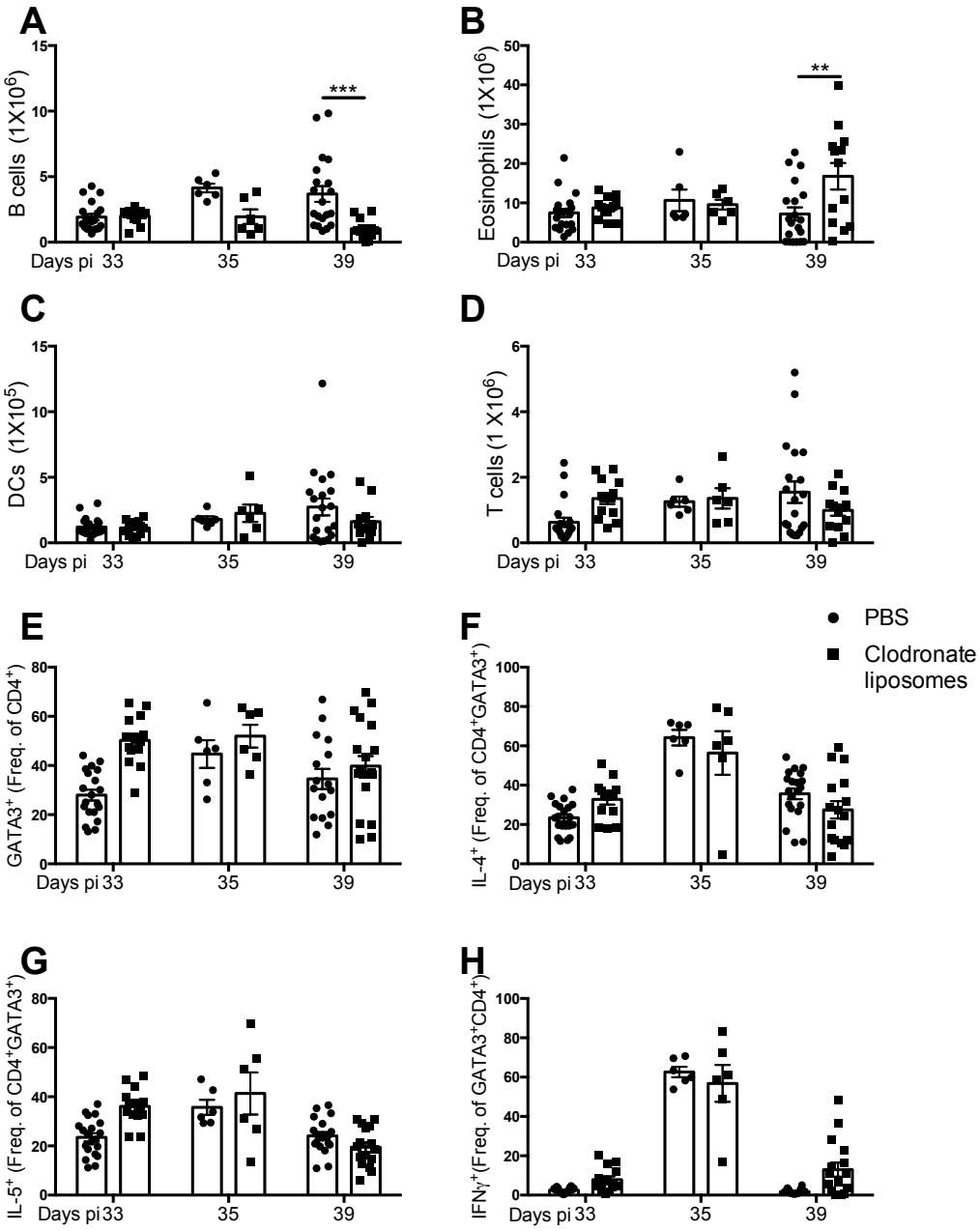


**Figure 3-10 Clodronate depletion of F4/80$^{hi}$ MΦ is specific at early time points but affects B cell and eosinophil numbers by day 39 pi**

C57BL/6 female mice were infected s.c. with 30 *L. sigmodontis* L3s and subsequently injected intrapleurally on day 27 and/or day 29 pi with clodronate liposomes or control PBS. Animals were sacrificed on days 33, 35 and 39 pi at which point the pleural cavity was washed with 10 ml RPMI (1 % Pen-Strep, 1 % L-Glut) to isolate the pleural exudate cells and surviving worms. The cellular populations were identified using the gating strategy illustrated in Fig2-2. Total number of **(A)** B cells **(B)** Eosinophils **(C)** DCs and **(D)** T cells **(E)** percentage of $CD4^+$ cells expressing GATA3 **(F-H)** Expression of IL-4, IL-5 and IFNγ by $GATA3^+$ $CD4^+$ cells in the PC at time points examined. Bars are representative of mean ± SEM, each time point is representative of 1 independent experiment with 6 (day 35) – 20 mice/ group. * P<0.05, ** P<0.01, ***P<0.0001,**** P<0.00001 as determined by a 2 way ANOVA.

## 3.4 Discussion

Alternatively activated macrophages have been implicated in the antagonistic activities of worm killing and suppression of the $T_H2$ immune response, consequently deciphering their exact function in anti-parasitic immunity has been complicated. The realisation that BMDMΦ are distinct from resMΦ in their origins and assume an alternatively activated phenotype which is more immunosuppressive, offered some insight into these conflicting findings. Chapter 2 revealed that resistance to *L. sigmodontis* is associated with proliferation of the resMΦ compartment, which is itself continually replenished from the bone marrow by MoMΦ. In contrast, susceptibility was marked by the influx of BMDMΦ, which displace the resMΦ pool. I hypothesised that the distinct dynamics seen between C57BL/6 and BALB/c mice would result in differences in alternative activation and ultimately illustrate polarising roles for these MΦ in worm killing.

While both MoMΦ and F4/80$^{hi}$ MΦ displayed equal propensities to induce RELMα upon infection, a significantly greater number of RELMα positive MΦ were present within the pleural space of resistant C57BL/6 mice throughout the course of infection. Despite this, a significantly greater percentage of $T_H2$ cells were detected in the draining lymph nodes of C57BL/6 compared to BALB/c mice and a similar trend was observed in the pleural cavity, suggesting a heightened type 2 immune response in the resistant strain. Thus, this data would suggests that during *L. sigmodontis* infection the hyporesponsive T cell phenotype of BALB/c mice is independent of the reported immunosuppressive functions of RELMα (Nair et al., 2009, Pesce et al., 2009b).

Bain et al. have recently highlighted that in naïve mice, RELMα is expressed by BMD precursors (F4/80$^{lo}$MHCII$^{+}$CSF1R$^{+}$) to the F4/80$^{hi}$ resident MΦ pool, thereby underlining a role for this molecule in the maturation of monocytes through the MΦ compartment. Furthermore, RELMα positive cells within the F4/80$^{hi}$ population of naïve mice were suggested to be recent immigrants into the resident niche (Bain et al., 2014). Thus, the high percentage of RELMα expression in the MoMΦ population (which was defined as F4/80$^{lo}$MHCII$^{+}$CSF1R$^{+}$Ly6C$^{-}$) of naïve C57BL/6 and BALB/c mice reported here are reflective of the continual replenishment of the resident

F4/80$^{hi}$ population by bone marrow derived macrophages. A significantly greater percentage of the MoMΦ and F4/80$^{hi}$ populations are RELMα positive in the BALB/c strain compared with the C57BL/6, emphasising a greater degree of resident cell turnover in this strain. The shutdown in RELMα expression from ~50 -10 % positive seen in the F4/80$^{hi}$ population of naïve C57BL/6 mice between the ages of 10 -11 weeks is indicative of considerable integration of BMDMΦ into the resident MΦ population at this age, prior to a switch to a more gradual process of BMDM integration. BMD monocytes do no contribute to resident Kupffer or arterial macrophage populations during adulthood (Gomez Perdiguero et al., 2015, Schulz et al., 2012, Yona et al., 2013). However recent studies have show that immediately after birth BMD monocytes integrate into these populations and self maintain(Ensan et al., 2016, Scott et al., 2016). Consequently, a recent review on MΦ ontogeny has suggested that a tissue may be temporarily 'open' to reconstitution by BMDMΦ at birth and remain 'closed' throughout adulthood (Ginhoux and Guilliams, 2016). I suggest that the increase in RELMα positivity seen in the naïve C57BL/6 mice at 10 weeks of age is representative of an 'opening' of the compartment to BMDMΦ integration prior to the assumption of a more gradual process of replenishment. Precisely why the rate of macrophage turnover is so drastically different between C57BL/6 and BALB/c mice remains unknown. However, given the suggestion that microbiome may influence the turnover rate (Sheng et al., 2015), I am curious if the MΦ compartment of the BALB/c mice would resemble that of the C57BL/6 if these mice were also housed in open top cages from birth.

Chapter 2 highlighted the delayed acquisition of residency marker, GATA6 and CD102, by BMDMΦ that had entered the F4/80$^{hi}$ gate within infected BALB/c mice (Chapter 2_Fig 6A&B). The detection of PD-L2$^{+}$ cells within the F4/80$^{hi}$ population of infected BALB/c mice further supports a model of inefficient integration of BMDMΦ into the resident MΦ niche in this strain. Negligible detection of PD-L2 expression by the F4/80$^{hi}$ population of C57BL/6 mice at day 50 pi, despite being ~80 % BMD is evidence that successful integration into the resident niche involves down regulation of PD-L2. Indeed, BMDAAMΦ (PD-L2$^{+}$) transferred into IL-4$^{-/-}$ mice down regulated PD-L2 expression and assumed a resident MΦ phenotype 8 weeks post transfer (Unpublished data Loke P). Furthermore, these BMD F4/80$^{hi}$ MΦ could

proliferate in response to exogenous IL-4 administration but failed to upregulate PD-L2 again (Unpublished data Loke P). Thus, I propose that PD-L2 is not a bone-fide marker of alternatively activated MΦ of bone marrow origin but rather a marker of alternatively activated monocytes and F4/80$^{lo}$ MΦ prior to their integration into the resident MΦ niche. Integration into the resident MΦ niche results in the upregulation of GATA6, and consequently the assumption of a transcriptional profile, which dictates ones response to environmental stimuli. An outstanding question in the field is whether maturation into a resident F4/80$^{hi}$ MΦ results in restricted plasticity of this cell type. Indeed prenatally seeded cardiac macrophages loose their inherent proliferative capabilities with age, such that bone marrow derived monocytes are required to maintain the resident MΦ pool (Molawi et al., 2014). Similarly, in the peritoneal cavity, recently recruited donor derived F4/80$^{hi}$ MΦ possess higher levels of surface CSF-1R, suggesting that these BMD resMΦ possess a proliferative advantage (Bain et al., 2016). Furthermore, it will be interesting to address whether the macrophage disappearance reaction and subsequent reseeding of the resident pool is truly a result of proliferative expansion of the initial population or a reflection of death of incompetent cells and reseeding of the niche by BMDMΦ.

Through monocyte depletion prior to day 35 pi we revealed a suppressive role for BMDAAMΦ during *L. sigmodontis* infection, with an enhanced $T_H2$ and trend toward greater $T_H1$ immune response evident in their absence. The eventual clearance of adult worms in susceptible BALB/c mice (~day 90 pi) is a result of a mixed $T_H1/T_H2$ immune response, with IFNγ and IL-5 working synergistically to recruit and activate neutrophils that encapsulate and kill adult worms (Saeftel et al., 2003). Here we highlight that an effective mixed $T_H1/T_H2$ immune response is present within the pleural cavity as early as day 35 pi, but in the presence of immunosuppressive monocytes it is not effective. I believe it would be interesting to know about the composition of the MΦ compartment ~day 90 pi, when the adult worms are normally killed, have the immunosuppressive monocytes dissipated by this time point? A similar immune-suppressive yet host protective role of BMD alternatively activate monocytes has been illustrated in *S. mansoni* infection, were monocyte depletion resulted in a stronger $T_H2$ immune response at the cost of overall host wellbeing (Nascimento et al., 2014, Girgis et al., 2014). This highlights the

delicate balance which must be struck between pathogen elimination and host protection, as such I hypothesise that the immunosuppressive phenotype assumed by BMD AAMΦ upon infiltration into an inflammatory milieu containing IL-4 is a mechanism to prevent the generation of an over zealous immune response which would likely result in excessive damage to self. Here, due to the limitations of using a depleting antibody (which can only be administered for five days prior to appearance of neutralising antibodies) only a short window of monocyte depletion was examined during *L. sigmodontis* infection of BALB/c mice, consequently whether exacerbated pathology would ensue during prolonged monocyte depletion as result of an enhanced $T_H1/T_H2$ immune response, remains unknown. Furthermore, while we successfully demonstrated a detrimental role for BMD AAMΦ in killing of *L. sigmodontis* worms, we were unable to correlate this effect to decreased PD-L2 expression on the MΦ compartment.

Given that >98 % of the MΦ compartment in infected BALB/c mice is RELMα positive from day 11 pi, and that *In vitro* IL-4 stimulation of inflammatory macrophages, results in > 95% of cells expressing PD-L2 within 24 hours (Huber et al., 2010), I assumed that BMDMΦ would immediately upregulate PD-L2 upon entry into the pleural cavity of infected BALB/c mice and would therefore be PD-$L2^+$ on day 35. The realisation that the jump in PD-L2 expression, from ~20 - ~60 % PD-$L2^+$, does not occur until after day 35 pi despite > 80 % of MoMΦ and monocytes being positive for RELMα, reveals a disconnection between the assumption of these two markers of alternative activation. Interestingly, while induction of both RELMα and PD-L2 is dependent on intrinsic STAT6 signalling, there is no STAT6 binding domain upstream of PD-L2 (Loke and Allison, 2003, Huber et al., 2010). Thus, how exactly downstream STAT6 signalling induces PD-L2 expression is unknown. In an attempt to illustrate a specific role for PD-L2 on BMD AAMΦ in hyporesponsive T cell induction at day 50 pi and given the aforementioned limitations of using the anti-CCR2 antibody, we decided to prevent pleural monocyte infiltration prior to day 35 pi in infected BALB/c mice in the hope that this would be sufficient to prevent further monocyte infiltration until day 50 pi. Unfortunately, this was not the case and by day 50 pi, monocytes had infiltrated into the pleural space of some mice, causing disappearance of the resident cells and upregulation PD-L2. However, this data

reveals that monocyte recruitment from day 35 pi is a continual process and further investigation is necessary to identify the immunological or worm derived factors inducing this recruitment.

To definitively illustrate a role for PD-L2 on monocytes in the induction of a hyporesponsive T cell phenotype within the BALB/c strain, we would need to create mice which lack PD-L2 specifically on bone marrow derived macrophages. To do this, we would carry out full body irradiation of $CCR2^{-/-}$ host BALB/c mice and then reconstitute with an 80:20 mix of $CCR2^{-/-}$ : $PD\text{-}L2^{-/-}$ donor bone marrow. In this way, any cells dependent on CCR2 would be derived from the $PD\text{-}L2^{-/-}$ fraction of bone marrow and all other cell types would have intact PD-L2 expression. B cells and dendritic cells are also capable of PD-L2 expression during *L. sigmodontis* infection of BALB/c mice and thus the possibility that these cell types are responsible for the induction of hyporesponsive T cells should not be over looked. Both B cell and PD-L2 deficient mice on the BALB/c background possess heightened resistance against *L. sigmodontis,* however mice deficient of PD-L2 specifically on B cells display susceptibility equal to that of WT mice (Knipper JA, Taylor MD Unpublished data). This data strengthens my current hypothesise that BMD AAMΦ are involved in regulating the $T_H2$ immune response via PD-L2.

Here we demonstrate that intrapleural injection of clodronate-loaded liposomes can successfully deplete resident $F4/80^{hi}$ MΦ, for at least 10 days. However, from 6 days post-clodronate loaded liposomes administration a population of BMD monocytes have infiltrated into the pleural space, illustrating that the compartment is being reseeded from the bone marrow and the ultimately short-term effect of resident cell depletion. Ten days was the longest period of resident cell depletion achieved and by this time point (day 39 pi) a clear indication toward decreased worm killing in macrophage-depleted mice was evident. While, this decreased worm killing may be reflective of $F4/80^{hi}$ resMφ depletion we cannot rule out the possibility that it is the influx of immunosuppressive $PD\text{-}L2^{+}$ monocytes which are preventing worm killing. Furthermore, the number of B cells were also affected by 10 days post clodronate administration, suggesting that MΦ communicate with and B cells to maintain numbers within the pleural space, alternatively the decrease in B cells could suggest

death via ingestion clodronate-loaded liposomes. During secondary *H. polygyrus* infection macrophage and antibodies work collaboratively to trap and kill the invading larvae (Esser-von Bieren et al., 2013). I suspect that antigen specific IgM produced by pleural B cells, binds to Fc receptors of the expanded resident MΦ population and unleashes the antibody-dependent cell-mediated cytotoxicity of macrophages on adult worms, aiding granuloma formation and worm killing.

To further investigate the role of resident pleural macrophages in destruction of *L. sigmondontis* worms and eliminate the possible immunosuppressive effects of monocytes in this setting, a more specific method of resident cell depletion combined with an inability to recruit monocytes would need to be employed. Simultaneously, Rosas et al. and Okabe and Medzhitov generated mice that are deficient of the transcription factor GATA6 in macrophages, resulting depletion of resident macrophages within the peritoneal cavity and pleural cavities (Rosas et al., 2014, Okabe and Medzhitov, 2014). I believe that crossing of this Gata6-KO$^{mye}$ C57BL/6 mouse with CCR2$^{-/-}$ C57BL/6 mice would generate a genetically modified model on which C57BL/6 mice would appear susceptible to *L. sigmodontis* infection. Furthermore, in order to investigate the B cell – MΦ interaction during *L. sigmodontis* infection, detailed histology would need to be carried out on granulomas isolated from the pleural space of infected mice. The granulomas isolated from the pleural space of infected mice are free-floating and extremely small, making mounting, sectioning and staining extremely difficult. I have however, developed a protocol for the staining of these granulomas and preliminary staining, places B cells at the interface between worm and macrophages. Future work in the lab will investigate granuloma formation and how the structures may differ between C57BL/6 and BALB/c mice.

In conclusion, through this Chapter we have further confirmed and advanced upon the dynamics of the macrophage compartments observed in Chapter 2. Assessment of RELMα expression by the macrophage compartment of naïve animals revealed that the resident MΦ pool of naïve BALB/c mice displays a greater rate of replenishment from the bone marrow compared to naïve C57BL/6 mice. Detection of PD-L2 expression by F4/80$^{hi}$ macrophages of infected BALB/c mice further

supported the replenishment of the resident pool by BMDMΦ and also recapitulated the delay in successful integration of these cells into the resident niche, as observed through GATA6 and CD102 negativity in Chapter 2. The continual infiltration of BMDMΦ, their alternative activation and inefficient integration into the resident MΦ niche results in a large percentage of PD-L2 positive macrophages within the pleural cavity of infected BALB/c mice. Monocyte depletion experiments illustrated that these cells are indeed suppressive to the $T_H2$ immune response at day 35 pi, however the mechanism at this time point remains unknown. In contrast to the BALB/c mice, the inability to detect PD-L2 on the F4/80$^{hi}$ population of infected C57BL/6 mice is reflective of the successful integration of BMDMΦ into the resident niche in this strain. Depletion of the expanded F4/80$^{hi}$ resident MΦ population in infected C57BL/6 mice was met with technical challenges, ultimately however the results are supportive of an active role for F4/80$^{hi}$GATA6$^{+}$CD102$^{+}$PD-L2$^{+}$ MΦ in the killing of *L. sigmodontis* worms.

# Chapter 4 The role of complement in resistance to *Litomosoides sigmodontis* infection

## 4.1 Summary

The complement component 3 (C3) encoding gene is one of the most upregulated genes by F4/80$^{hi}$ peritoneal cavity Mφ in response to *Brugia malayi* infection of BALB/c mice. *B. malayi* infection of IL-4$^{-/-}$ BALB/c mice demonstrated that C3 expression was IL-4 dependent. Furthermore, recent data has demonstrated that C3 is essential in the killing of *Strongylides stercoralis* and *H. polygyrus* larvae during primary and secondary infection, respectively. C3 deficient C57BL/6 mice were made readily available to us and thus we investigated whether C3 may be important in the resistant phenotype against *L. sigmodontis* infection. C57BL/6 mice deficient in C3 were infected with *L. sigmodontis* for 28 or 35 days. There was no difference in the clearance of *L. sigmodontis* worms by C3 deficient C57BL/6 mice and their WT littermate controls at either day 28 or 35 post infection. Interestingly however there was a significant decline in the number of F4/80$^{hi}$ Mφ accumulated within the pleural space by day 35 post infection of resistant C57BL/6 mice. Thus we have highlighted that worm killing in resistant C57BL/6 mice occurs independent of C3 at the time points examined.

## 4.2 Introduction

The complement system consists of over 30 soluble proteins, which are produced primarily by the liver and constitutively present in serum. The majority of the complement system proteins are proteases, which upon activation cleave and activate the next protein in the cascade. There are three pathways of complement activation; classical, alternative and lectin. Classical activation occurs when C1q recognises the Fc receptor of antibodies bound to antigen; antigen binding results in a conformational change in antibody structure, which enables C1q recognition. C1q undergoes autocleavage resulting in C1s release, C1s cleaves downstream of C4 and C2 resulting in C3 convertase formation. Activation of the lectin pathway occurs when collectins such as mannose binding lectin and ficolin recognise their bacterial or viral substrates and the alternative pathway of complement activation is a result of spontaneous C3 assembly. While each pathway differs in the initial steps of

activation, all combine upon the formation C3 convertase, a proteolytic complex that cleaves C3 into C3a and C3b. The cleavage of C3 marks the commitment of the system to form the membrane attack complex, which integrates into pathogen membranes and thereby causing death by lysis (Holers, 2014).

Historically, complement has been implicated in antibacterial, viral and fungal immunity. However, recent reports have highlighted a previously unappreciated role for complement in anthelminthic immunity. C3 is essential in MΦ and NΦ mediated killing of *Strongylides stercoralis* larvae during primary infection both *in vitro* and *in vivo* (Bonne-Annee et al., 2013). Furthermore, complement is necessary for trapping *H. polygyrus* larvae during challenge infection through mediating attachment of antibody – macrophage complexes to the larval surface (Esser-von Bieren et al., 2013). Previous work by the Allen lab has highlighted the complement cascade as the most differentially regulated pathway when comparing AAMΦ retrieved from *B. malayi* infected BALB/c mice to thioglycollate elicited MΦ, with C3 highly upregulated in NeMΦ (Figure 4-1) (Thomas et al., 2012). Similar to *L. sigmodontis* infection, BALB/c mice are more susceptible to *B. malayi* infection than are C57BL/6 mice (Rajan et al., 2002), thus it is possible that C3 upregulation by F4/80$^{hi}$ MΦ is detrimental to worm killing rather than protective. However, given the recent publications on the contribution of complement to killing of *Strongylides stercoralis* and *H. polygyrus* larvae (Bonne-Annee et al., 2013, Esser-von Bieren et al., 2013) and the large accumulation of MΦ, B cells and antigen specific IgM (Jackson-Jones et al., 2016) within the pleural space resistant C57BL/6 mice during *L. sigmodontis* infection, we hypothesised that complement may be involved in resistant phenotype against *L. sigmodontis,* potentially through mediating antibody dependent effector functions of MΦ. This chapter contains preliminary experiments to investigate into the role of complement during *L. sigmodontis* infection. Future work in the lab may build on this data.

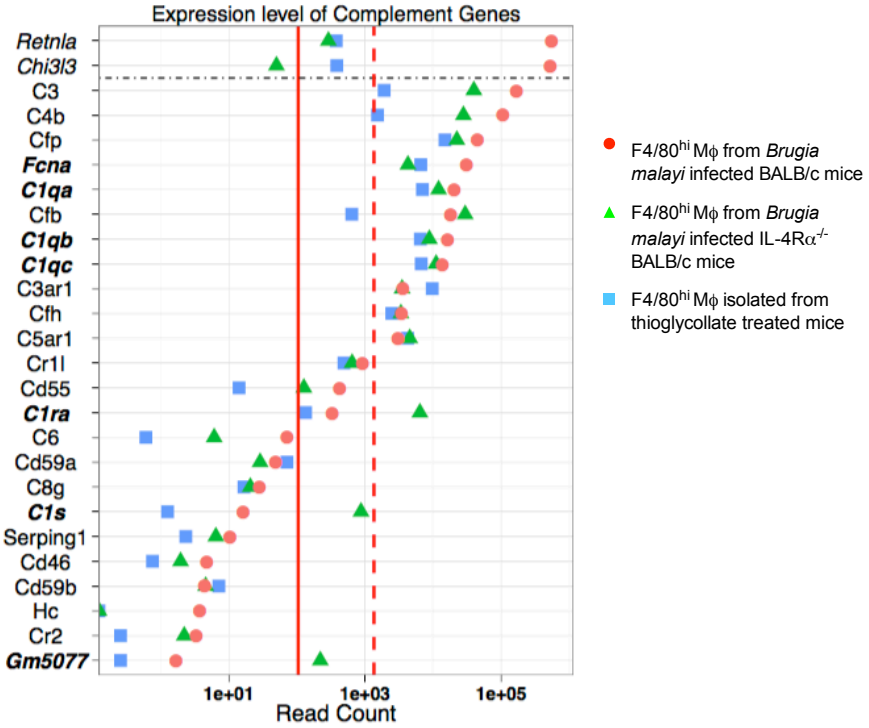


**Figure 4-1 Differential expression of complement and coagulation cascade genes between WT infected MΦ and thioglycollate elicited MΦ**

WT and IL-4Rα-/- BALB/c mice were infected with *B. malayi* through implantation of adult worms into the peritoneal cavity in order to generate nematode elicited MΦ that were isolated on day 21 pi. Injection of thioglycollate intraperitoneally and isolation of the PEC on day 3 was utilised as a method of generating a large number of bone marrow derived macrophages. The F4/80$^{hi}$ Mϕ population was isolated from each of the groups and gene expression analysed via RNA sequencing.

## 4.3 Results

### *4.3.1* The role of complement in resistance to *L. sigmodontis.*

In order to investigate the role that complement may play in the resistant phenotype we decided to infect C57BL/6 mice that are deficient in complement component 3 (C3) All experimental mice were generated from heterozygote breeding pairs enabling comparison of $C3^{-/-}$ mice with their WT littermates. Because C3 is central to all three activation pathways, the complement cascade is non-functional in these mice. At day 28-post infection no difference in recovery rate was detected between WT and C3-/- mice (Figure 4-2 A). There was however more granulomas retrieved from the pleural space of C3-/- at this time point (Figure 4-2B). A trend toward less total living cells (Figure 4-2C), B cells (Figure 4-2 D), T cells (Figure 4-2E), Eosinophils (Figure 4-2F) and MΦ (Figure 4-2H) was observed in the C3 deficient mice relative to WT. No difference in the number of dendritic cells in the pleural cavity was observed (Figure 4-2G). It is important note that having so few samples per group at this time point (2/3mice/group) impacted upon the ability to detect significant differences in cell numbers. By day 35 pi no differences were detected in recovery rate (**Error! Reference source not found.**A), granuloma number (**Error! ference source not found.**B), total cells (Figure 4-4C), B cells (**Error! Reference source not found.**D), T cells (**Error! Reference source not found.**E), Eosinophils (**Error! Reference source not found.**F) or dendritic cells (**Error! Reference source not found.**G). There was however significantly fewer macrophages present in the pleural space of C3 deficient mice at day 35 pi compared to WT.

The trend toward fewer macrophages at day 28, was a result of both decreased $F4/80^{hi}$ and MoMΦ numbers but no difference in monocytes was detected at this time point (Figure 4-4A-C). At day 35 pi, the significant decline in macrophage numbers observed in the $C3^{-/-}$ mice was a reflection of decreased $F4/80^{hi}$ MΦ accumulation. Neither MoMΦ nor monocytes were significantly different between $C3^{-/-}$ and WT mice at this time point (Figure 4-4D-F). At day 28 and 35 pi, the macrophage compartment of $C3^{-/-}$ mice was equally capable of inducing RELMα expression upon infection as WT mice (Figure 4-5A&D). At day 28 and 35 pi there was an increase in the percentage of GATA6 positive MΦ upon infection, in both

WT and $C3^{-/-}$ mice, consistent with data from chapter 1 highlighting that infection prevents an age related decline in $F4/80^{hi}$ population and subsequent decline in GATA6 positivity (Figure 4-5B&E). There was a trend toward a greater induction of PD-L2 positivity of the MΦ compartment at day 28 pi, but no difference could be detected at day 35 post infection (Figure 4-5C&F).

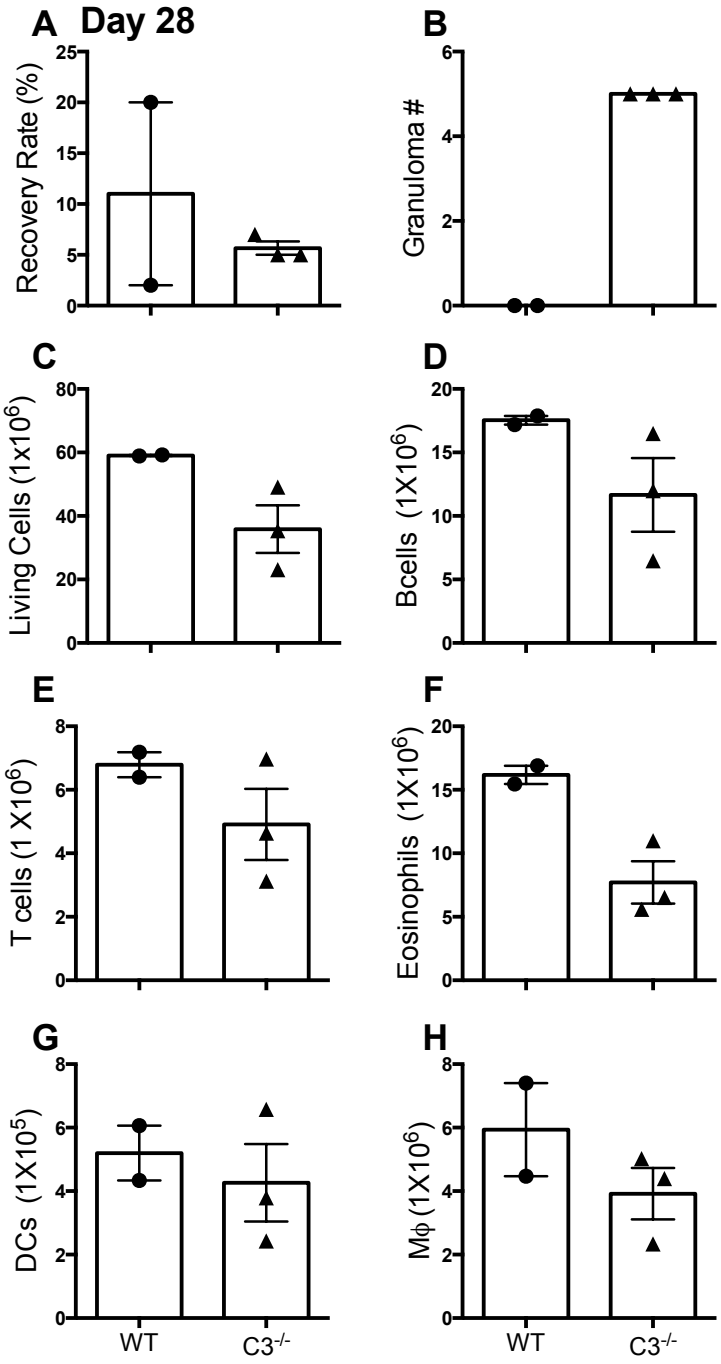


**Figure 4-2 C3 deficiency in resistant C57BL/6 mice does not affect worm burden at day 28 post infection**

$C3^{-/-}$ mice and their WT littermate controls were infected with 30 *L. sigmodontis* larvae s.c. and the pleural compartment was washed with 10 ml RPMI (1 % L-Glut, 1 % Pen-Strep) at day 28 pi to isolate the worms, granulomas and pleural exudate cells for analysis by multiparameter flow cytometry. **(A)** Worm recovery rate, **(B)** Granulomas isolated from pleural space. The cellular populations were identified using the gating strategy illustrated in Fig2-2 **(C)** total number of living cells **(D)** B cells **(E)** T cells **(F)** Eosinophils **(G)** dendritic cells **(H)** Macrophages. Bars are representative of Mean ± SEM. Data were generated from one experiment.

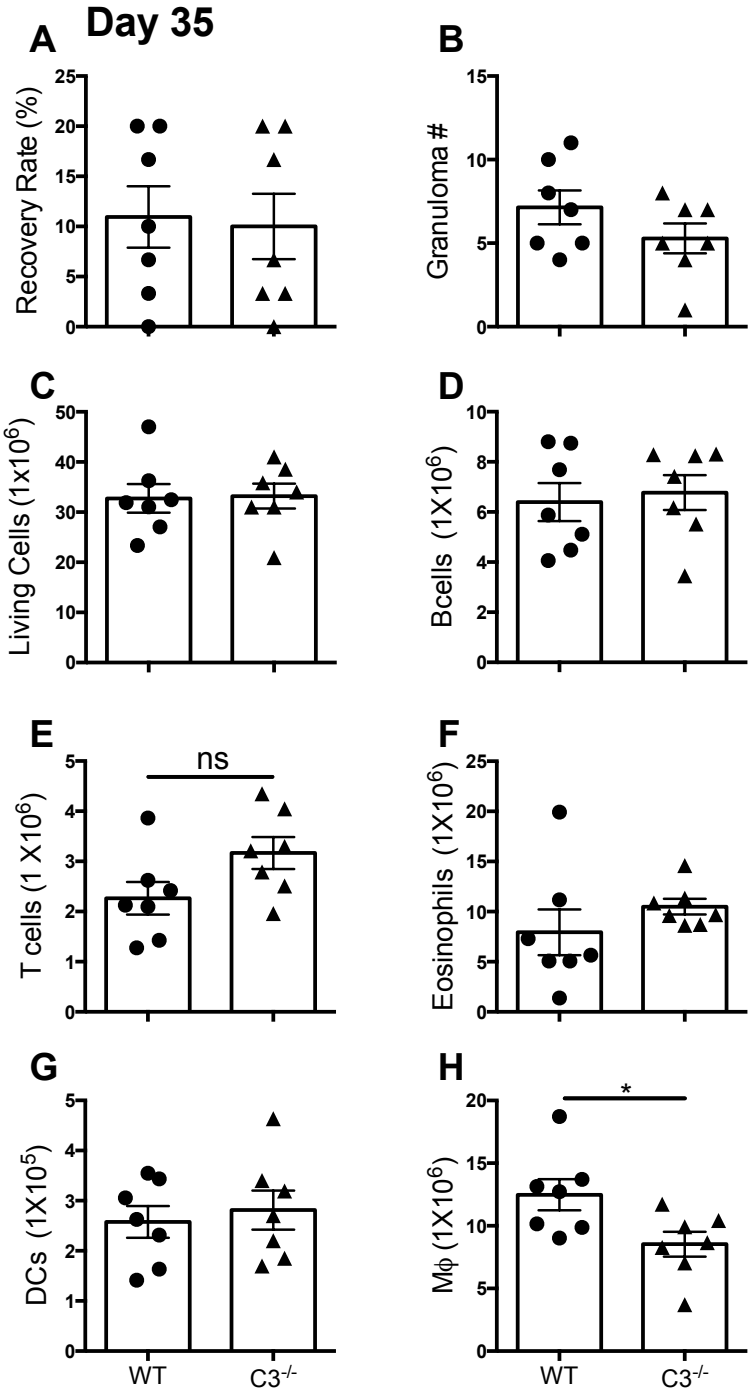


**Figure 4-3 C3 deficiency results in decreased MΦ number but does not affect worm burden at day 35 post infection**

$C3^{-/-}$ mice and their WT littermate controls were infected with 30 *L. sigmodontis* larvae s.c. and the pleural compartment was washed with 10 ml RPMI (1 % L-Glut, 1 % Pen-Strep) at day 35 pi to isolate the worms, granulomas and pleural exudate cells for analysis by multiparameter flow cytometry **(A)** Worm recovery rate, **(B)** Granulomas isolated from pleural space. The cellular populations were identified using the gating strategy illustrated in Fig2-2 **(C)** total number of living cells **(D)** B cells **(E)** T cells **(F)** Eosinophils **(G)** dendritic cells **(H)** Macrophages. Bars are representative of Mean ± SEM. * P <0.05, ** P<0.001 as determined by Student's t test and Mann Whitney test. Data were generated from one experiment.

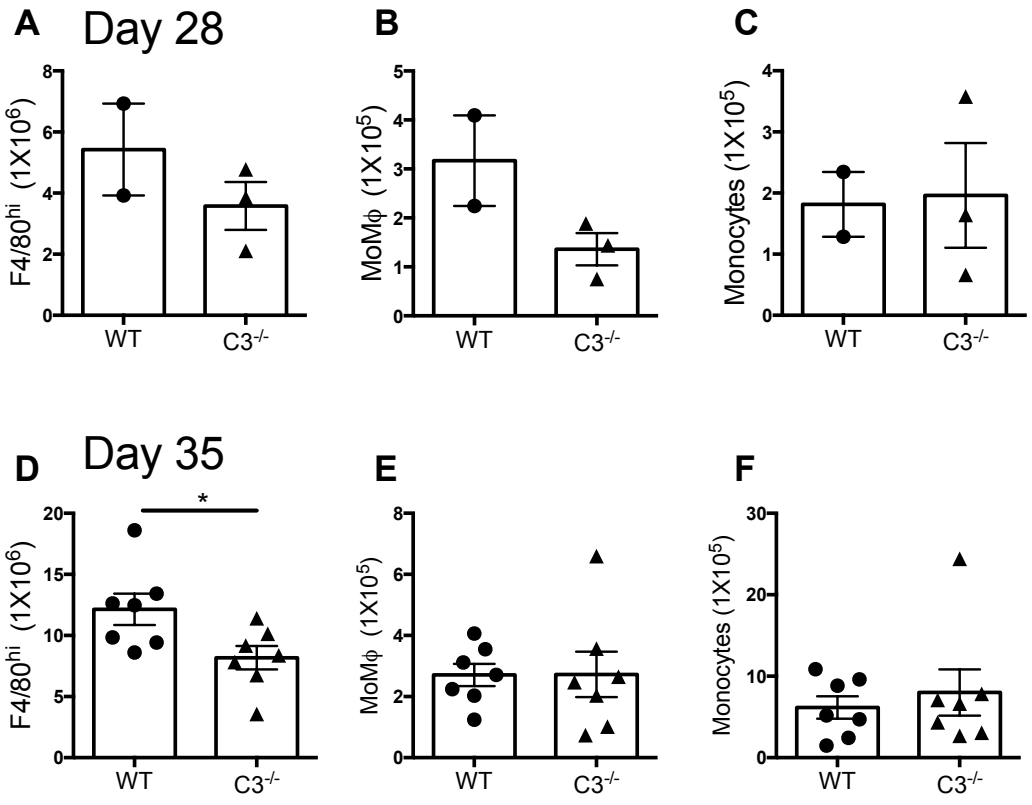


**Figure 4-4 Decreased MΦ numbers in C3$^{-/-}$ mice at day 35 post infection is reflective of decreased number of F4/80$^{hi}$ resMΦ**

C3$^{-/-}$ mice and their WT littermate controls were infected with 30 *L. sigmodontis* larvae s.c. The animals were sacrificed on days 28 and 35- pi, the pleural compartment was washed with 10 ml RPMI (1 % L-Glut, 1 % Pen-Strep) to isolate the pleural exudate cells for analysis by multiparameter flow cytometry. The Mϕ subpopulations were identified using the gating strategy illustrated in Fig2-2. **(A&D)** Total number of F4/80$^{hi}$ **(B&E)** MoMΦ and **(C&E)** Monocytes at day 28 **(A-C)** and day 35 **(D-F)** post infection, respectively. Bars are representative of Mean ± SEM. * P <0.05, as determined by Student's t test and Mann Whitney test. Data were generated from one experiment.

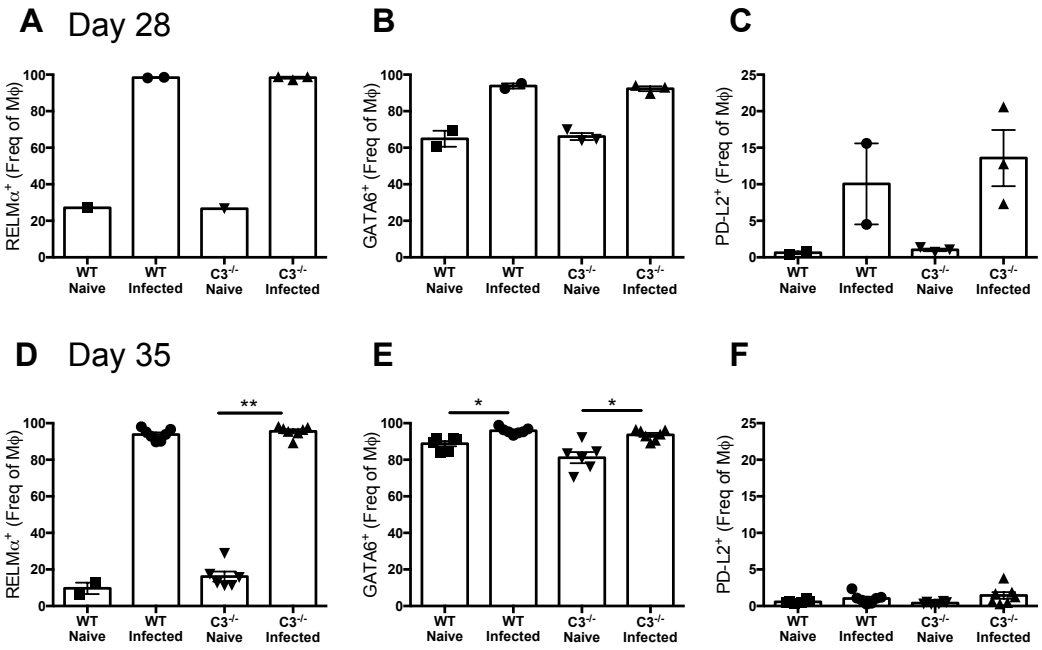


## Figure 4-5 Alternative activation and residency are maintained in C3 deficient C57BL/6 mice at day 28 and 35 post infection

$C3^{-/-}$ mice and their WT littermate controls were infected with 30 *L. sigmodontis* larvae s.c. The animals were sacrificed on days 28 and 35- pi, the pleural compartment was washed with 10 ml RPMI (1 % L-Glut, 1 % Pen-Strep) to isolate the pleural exudate cells for analysis by multiparameter flow cytometry. The Mϕ population was identified using the gating strategy illustrated in Fig2-2. Percentage of MΦ expressing **(A&D)** RELMα **(B&E)** GATA6 **(C&F)** PD-L2 at day 28 **(A-C)** and 35 **(D-F)** pi in WT and $C3^{-/-}$ mice. Bars are representative of Mean ± SEM* P <0.05, ** P<0.001 as determined by Student's t test and Mann Whitney test. Data were generated from one experiment.

## 4.4 Discussion

Complement has been implicated in mediating binding of antibody-macrophage complexes to larval surfaces, thereby enabling trapping and killing (Esser-von Bieren et al., 2013, Bonne-Annee et al., 2013). The large number of macrophages, B cells and parasite specific IgM which accumulate in the pleural space of *L. sigmodontis* infected C57BL/6 mice has led us to postulate that antibody mediated attachment and activation of macrophages is a potential mechanism of worm killing in this strain, which may involve complement. Consequently, we decided to investigate the role of complement in worm killing in this normally resistant strain.

No difference in worm killing was observed at either day 28 or 35 pi in C57BL/6 mice deficient in complement component C3, highlighting that at these time points complement is not actively involved in parasite killing. At day 28 post infection, there was a trend toward less cellular recruitment in the $C3^{-/-}$ mice, potentially reflecting the deficit in chemotactic C3a and C5a. However, by day 35 post infection any deficit in cellular recruitment is no longer evident. A significant decline in $F4/80^{hi}$ cell number by day 35 pi is suggestive of a role for complement in the accumulation of the expanded pleural $F4/80^{hi}$ resMΦ population. How precisely complement aids the expansion of the resMΦ population remains unknown, potentially through promoting *in situ* MΦ proliferation. Alternatively complement may be involved in lifting the homeostatic controls on cell number within the cavity.

While, complement deficiency did not affect worm survival at day 28 or day 35 post infection it is possible that complement is essential at later points of infection. Consequently, investigation into the immune response at day 50 pi in $C3^{-/-}$ mice would be necessary to rule-out a role for complement in the ultimate clearance of the worm. As illustrated in Chapter 2, the expanded $F4/80^{hi}$ population observed in the pleural cavity of *L. sigmodontis* infected C57BL/6 mice is generated through proliferation of the resident cell population, which is continually replenished from the bone marrow. Esser-von Bieren et al. illustrated the collaboration between alternatively activated macrophages, IgG and complement in the gut to efficiently trap invading larvae. Macrophages in the gut are rapidly replenished from the bone marrow, consequently, I hypothesise that these BMD AAMΦ would possess a

transcriptional profile distinct from that of resident derived AAMΦ in the pleural space of *L. sigmodontis* infected mice. Furthermore, both *B. malayi* infection and studies by Bonne-Annee et al. on the destruction of *S. stercoralis* larvae involve implantation of either adult worms or a cell-impermeable diffusion chamber into the peritoneal cavity. The physical act of surgical implantation into the peritoneal cavity would result in recruitment of BMDMΦ, which would subsequently assume an alternatively activated phenotype as a result of the subsequent $T_H2$ immune response. Thus, I hypothesise a possible reason that C3 does not appear to influence infection outcome in the C57BL/6 mice in *L. sigmodontis* infection may be that C3 production is a signature of BMD AAMΦ, rather than the expanded resident F4/80$^{hi}$ population. Analysis of microarray data comparing resident derived AAMΦ vs. AAMΦ derived from the bone marrow, revealed that IL-4 induced increased C3 expression in both BMD and resident derived MΦ. However, there was a greater increase in C3 production by BMD AAMΦ (9-fold) compared to resident derived AAMΦ (5-fold)(Gundra et al., 2014). The granulomas which form around young adult worm in the C57BL/6 strain consist largely of MΦ and eosinophils, whereas those which form in the BALB/c strain around fully mature adult worms are composed of neutrophils and MΦ (Attout et al., 2008). The killing of *S. stercoralis* larvae in the peritoneal cavity is achieved through collaboration of MΦ, antibodies, neutrophils and complement (Bonne-Annee et al., 2013). Consequently, it may be that complement is necessary for worm killing only in collaboration with neutrophils. Thus, I hypothesise that complement plays a role in the worm killing mechanism employed against *L. sigmodontis* in infected BALB/c mice, but perhaps not, or to a lesser degree, in the C57BL/6 mice.

In this chapter, I have presented preliminary work to highlight that complement does not play a major role in the resistance of C57BL/6 mice against *L. sigmodontis* infection. However, the complement system may promote proliferation of the F4/80$^{hi}$ resident macrophage population. Due to the apparent lack of impact of complement deficiency on infected C57BL/6 mice, future work in the lab may focus more on the role of complement in the immune response of BALB/c mice against *L. sigmodontis*.

# Chapter 5 Macrophage origin correlates with distinct bactericidal functionality *in vitro* but not *in vivo*

## 5.1 Summary

*Salmonella* infection results in the infiltration of monocytes from the blood into the peritoneal cavity. Monocytes mature into MoMΦ through sequential loss of Ly6C expression and acquisition of MHC II expression. This infiltration and maturation of monocytes-MoMΦ results in the displacement of the resMΦ population; this phenomenon has been described as the macrophage disappearance reaction (MDR). In recent years it has come to light that resMΦ in the peritoneal cavity are of a distinct developmental origin to bone marrow derived monocytes and MoMΦ. Thus, I am interested in whether the MDR reflects a difference in functional capability between the two subsets, which ultimately is related to ontogeny. In order to address this question, I generated an *in vitro* system to assess the interaction of MoMΦ and resMΦ with *Salmonella enterica* serovar Typhimurium SL3261. I found that *in vitro* MoMΦ are infected by and/or ingest SL3261 to a much greater degree than resMΦ. The resMΦ population is less efficient at both controlling the spread of and killing intracellular SL3261 overtime, compared to the MoMΦ population. *In vivo* however, there appears to be no difference in the ability of the monocyte derived MoMΦ population and the prenatally seeded F4/80$^{hi}$ resMΦ to be infected by/ingest SL3261, nor is there a difference in their bactericidal ability. Ultimately, my work illustrates that *in vitro* bone marrow derived MoMΦ and prenatally-derived cells exhibit distinct bactericidal functional capabilities. However, these functional differences do not translate to the *in vivo* setting. This is likely due to differences in numbers between the systems as well as local niche factors influencing macrophage function.

## 5.2 Introduction

*Salmonella enterica* serovar *typhi* (*S. typhi*) is a gram negative, facultative intracellular bacterium that causes more than 27 million cases of typhoid fever per annum, resulting in 217,000 deaths. Infection by *S. typhi* is limited to humans and transmission is primarily a result of contaminated water sources and a lack of sanitation in less developed countries. *Salmonella enterica* subspecies *enterica*

serovar Typhimurium is a non-typhoidal *Salmonella* serovar, *S.* Typhimurium from here on, that causes acute intestinal inflammation and self-limiting diarrhoea in humans. In mice however, *S.* Typhimurium results in systemic disease similar to that seen in Typhoid patients (Broz et al., 2012). Hence, oral and intraperitoneal infection of mice with *S.* Typhimurium is a widely used model to study typhoid fever.

Once ingested, the bacterium passes through the mucus layer of the intestinal lumen and avoids antimicrobial proteins through expression of the Pho-PhoQ signal transduction system. Subsequent access to the underlying Peyer's patches may occur via three routes; 1) Bacteria-mediated uptake through the injection of proteins, encoded on the Salmonella Pathogenicity Island-1 (SPI-1), into non-phagocytic cells of the epithelial barrier (Bueno et al., 2010). 2) Uptake and translocation through M cells within the epithelial barrier (Vazquez-Torres and Fang, 2000). 3) Uptake by CX3CR1-expressing DCs/Macrophages, which extend projections into the intestinal lumen(Vazquez-Torres et al., 1999).

The immune response to *S.* Typhimurium is strongly pro-inflammatory, characterized by cytokines IL-6, IL-1β, TNF-α, IFNγ(de Jong et al., 2012). This type-1 immune response is initiated by engagement of *S.* Typhimurium lipopolysaccharide, peptidoglycan and flagellin with their respective TLRs (TLR-4, TLR-2, TLR-5)(Broz et al., 2012). Accumulation of MoMΦ within the peritoneal cavity in response to *S.* Typhimurium infection is thought to be a mechanism to protect against potential gut leakage and resulting sepsis.

Within macrophages, *S.* Typhimurium expresses SPI-2 encoded genes that result in the formation of the Salmonella containing vacuole (SCV), a replicative niche within the macrophage. SPI-2 encoded proteins can also inhibit NADPH Oxidase formation, enabling bacterial survival (Vazquez-Torres et al., 2000). Within the SCV, *Salmonella* can replicate before exiting the cell through an ill-defined mechanism that frequently cumulates in macrophage death.

Here, I will model infection through intraperitoneal infection with *S. Typhimurium* SL3261, subsequently referred to as SL3261. SL3261 is a non-virulent strain generated through the insertion of a tetracycline-resistance transposon into the Aro

gene. Disruption of the Aro gene results in blockade of the aromatic biosynthetic pathway, causing the bacterium to become auxotrophic for aromatic amino acids not available in mammalian tissues(Hoiseth and Stocker, 1981).

Intraperitoneal infection with *S.* Typhimurium results in the influx MoMΦ and the disappearance of the resMΦ population. I wanted to ask whether this dynamic could be explained by a greater ability of the MoMΦ population to phagocytose and kill intracellular *S.* Typhimurium.

## 5.3 Results

### 5.3.1 MoMΦ preferentially take up/are infected by *S.* Typhimurium compared to resMΦ

In order to ask if the MDR reflects a complete dysfunction of the resMΦ population in response to *S*. Typhimurium, I generated an *in vitro* system in which to study the initial interaction between MΦ and SL3261. The peritoneal exudate cells (PEC) were isolated from the either naïve animals or those injected with thioglycollate as a source of resMΦ and MoMΦ respectively. Whole PEC from naïve or thioglycollate injected animals were used, I did not adherence purify. Thus from here on out, unless otherwise stated, resMΦ and MoMΦ will be used to reflect total PEC from naïve and thioglycollate injected animals, respectively. ResMΦ and MoMΦ were co-cultured and infected with SL3261 at a multiplicity of infection of 1 or 5 (MOI 1/5) for 1 hour; any remaining bacteria were eradicated by means of gentamicin treatment for 1 hour. The cells were then stained for flow cytometric detection of intracellular LPS. At this time point, a greater percentage of the MoMΦ population were positive for LPS when compared to resMΦ (Figure 5-1A). Furthermore, there were more bacteria within an individual MoMΦ when compared to resMΦ, as evidenced by the greater geometric mean (Figure 5-1B). In the co-culture system, MoMΦ and resMΦ are at a 1:1 ratio and this co-culturing ensures that each population receive an equal infectious dose and stimulation. To exclude the possibility that the low level of uptake by the resMΦ population was as result of competition between the populations, this experiment was repeated with individually cultured MoMΦ and resMΦ populations. Similar to the co-culture system, a greater percentage of MoMΦ were $LPS^+$ 1-hour post infection (Figure 5-1C). However, when MoMΦ and resMΦ were separately cultured the geometric mean of MoMΦ was not greater than that of resMΦ (Figure 5-1D)

Additionally, there was an increased number of CFU on agar plates which had been streaked with MoMΦ infected for 1 hour compared to resMΦ infected for the same period of time (Figure 5-1E). The greater percentage of MoMΦ containing $LPS^+$ bacteria 1-hour post infection may reflect enhanced bacterial uptake by MoMΦ or preferential targeting of the MoMΦ population by the bacterium.

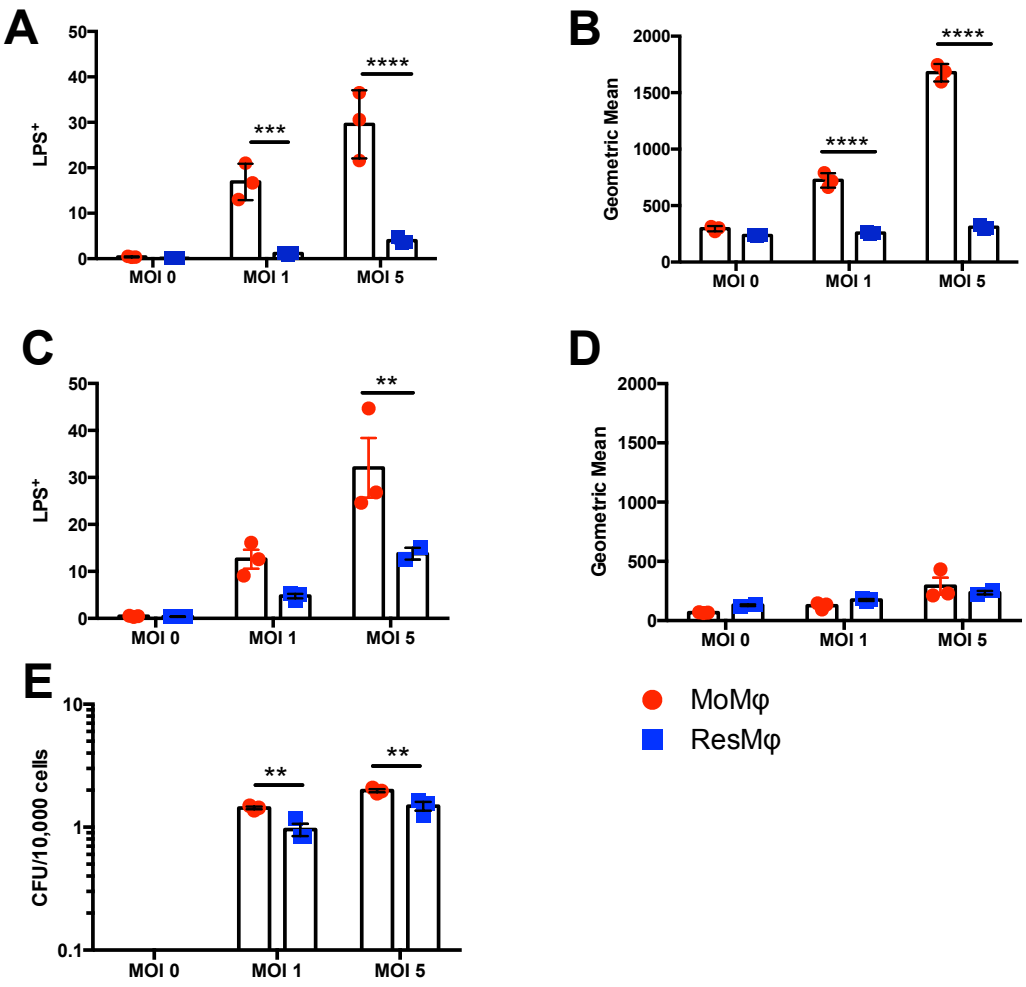


## Figure 5-1 Uptake of SL3261 by MoMΦ and resMΦ in vitro

MoMΦ and resMΦ, were cultured ex vivo separately **(A&B)** or together **(C-E)** ($4X10^5$ cells/ 100 µl/ well). The cells were infected with *S.* Typhimurium SL3261 (50 µl) for 1 hour, extracellular SL3261 was thereafter removed via Gentamicin treatment (200 µg/ml, 50 µl). Bacterial uptake was determined by measuring the percentage of the macrophage population positive for LPS after an additional hour of incubation, via flow cytometry **(A-D)** or via colony counts **(E)**. **(A)** Percentage of MoMΦ and resMΦ positive for LPS when the populations are co-cultured, **(B)** geometric mean of co-cultured populations. **(C)** Percentage of MoMΦ and resMΦ positive for LPS when the populations are separately cultured, **(D)** geometric mean of the separately cultured populations. **(E)** Separately infected MoMΦ and resMΦ were plated on agar plates and CFU/10,000 cells 1Hr post infection was determined. Results are mean of 3 biological replicates and representative of 3 independent experiments, significance was determined via 2-way ANOVA and Bonferroni's test.

### 5.3.2 Preferential uptake by MoMΦ does not correlate with enhanced cell surface marker expression

We were surprised to find such a marked difference in the initial macrophage-*salmonella* interaction between resMΦ and MoMΦ populations. The next logical step was to ask if this difference was a result of differentially expressed cell surface molecules associated with bacterial uptake. ResMΦ and MoMΦ were isolated from the peritoneal cavity of naïve and thioglycollate injected animals, respectively. The expression of cell surface markers previously associated with bacterial uptake was analysed via flow cytometry. Of the α-integrins analysed (CD11a, CD11b, CD11c) CD11c was the only marker preferentially expressed by the MoMΦ population. Additionally, there was no difference in the expression of the β-integrins, CD18 or the TLR4 co-receptor, CD14 (Figure 5-2A). TLR4 is the Toll-Like Receptor that binds to bacterial lipopolysaccharide. To investigate the role of TLR4 in bacterial uptake, resMΦ and MoMΦ were isolated from the peritoneal cavity of TLR4 KO animals and the uptake of the bacterium by the macrophage populations was compared to WT. TLR4 deficiency did not alter bacterial uptake, as measured by the percentage of $LPS^+$ MΦ, by either MoMΦ or resMΦ populations (Figure 5-2B). Hence, the enhanced bacterial uptake by the MoMΦ population cannot be attributed to a greater level of expression of the cell surface markers examined here.

Pre-treatment of the MoMΦ population with cytochalasin D, 1 hour prior to infection with SL3261 resulted in a significant reduction of bacterial uptake by this population (Figure 5-2C). Thus, the uptake/infection of the macrophages is partially dependent on rearrangement of the actin cytoskeleton.

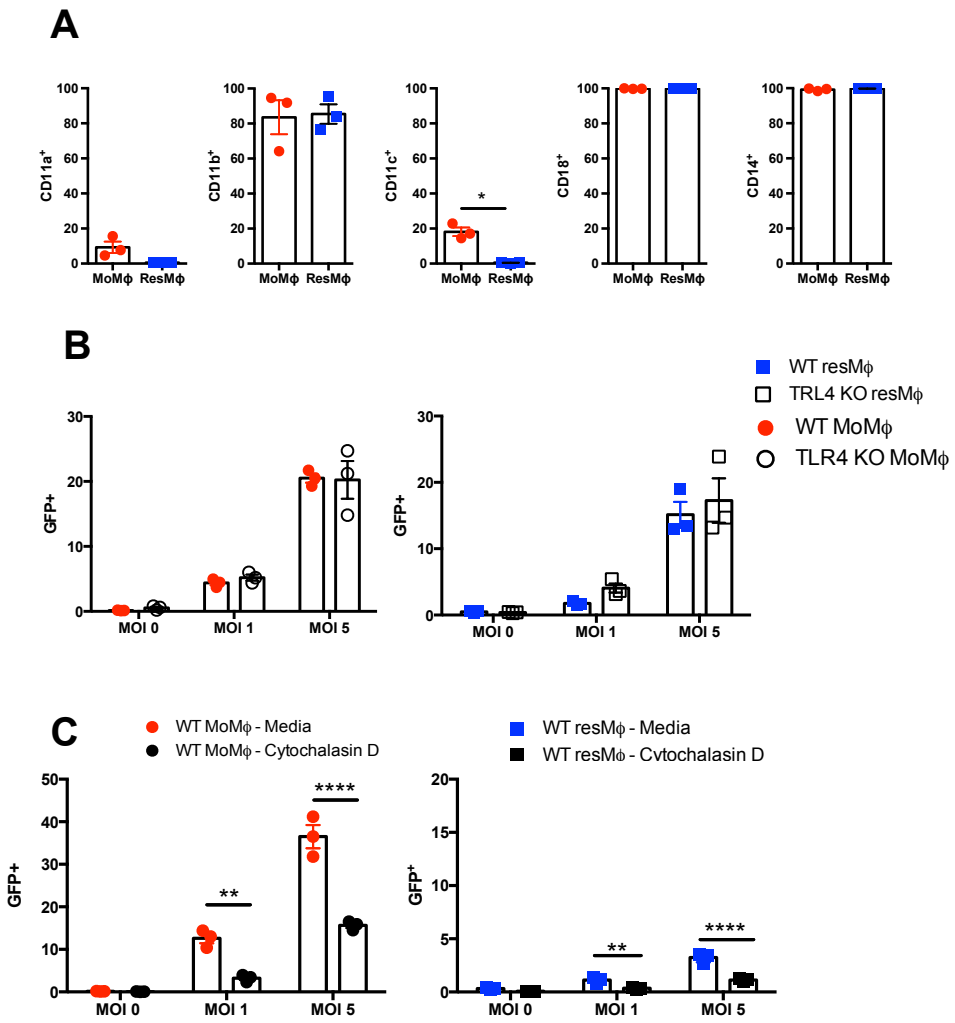


## Figure 5-2 Expression of Cell surface markers related to bacterial uptake by MoMΦ and resMΦ

Peritoneal exudate cells from were isolated from naïve (resMΦ) or thioglycollate (MoMΦ) injected WT C57BL/6 females. **(A)** The expression of cells surface markers previously associated with Salmonella uptake by WT MoMΦ ( ● ) and resMΦ ( ■ ) populations within the PLEC. **(B)** Total PLEC from naïve and thioglycollate injected WT and TLR4 KO animals were cultured *in vitro* for 3 hours prior to infection with *S.* Typhimurium GFP for 1 hour. Bacterial uptake was measured via the percentage of the MΦ subpopulation staining positive for GFP.**(C)** Total PLEC from naïve and thioglycollate injected WT C57BL/6 females were separately cultured and pre-treated with either media or cytochalasin D for 1 hour prior to bacterial infection. Bacterial uptake was measured via the percentage cells staining positive for GFP. Data are representative of 3 independent experiments, significance was determined via 2-way ANOVA and Bonferroni's test, error bars are mean ± SEM of 3 biological replicates. ** P<0.01, **** P<0.0001.

### 5.3.3 MoMΦ display enhanced bactericidal capabilities compared to resMΦ

The initial *in vitro* data led to two hypotheses; **1)** the MoMΦ population possess heightened *Salmonella* phagocytizing abilities, which may reflect enhanced bactericidal capabilities over resMΦ. **2)** The bacterium preferentially targets the MoMΦ population to access a MoMΦ-specific intracellular replicative niche. In order to ascertain whether *S.* Typhimurium is killed more rapidly or survives better within MoMΦ compared to resMΦ, the cells were infected *in vitro* for 1, 24 and 48 hours, before being streaked on agar plates and the resultant CFU counted.

Reinforcing the initial uptake/infection data, a greater number of CFU were detected on agar plates streaked with MoMΦ 1-hour post infection, compared to those streaked with resMΦ 1-hour post infection. This was significant at an MOI 1 and MOI 5 (Figure 5-3A). However, the reverse was found when comparing the number of CFU on agar plates streaked with MoMΦ/ResMΦ 24 hours post infection. At 24 hours there was a trend toward more CFU on plates streaked with resMΦ compared to MoMΦ at an MOI 1 and this reached significance at an MOI 5 (Figure 5-3B). Furthermore, there were no CFU detectable on plates that received MoMΦ infected for 48 hours, and while there was CFU on plates that received resMΦ infected for 48 hours, this did not reach statistical significance (Figure 5-3C). This data would support hypothesis 1, in that the MoMΦ population take-up more of the bacterium and kill it more rapidly than do the resMΦ population over time. In these experiments whole PEC from thioglycollate treated or naïve mice, rather than adherence purified MoMΦ and resMΦ, were plated. Thus, it is possible that additional immune cell populations, such as neutrophils, are contributing to the enhanced uptake and killing carried out by the thioglycollate elicited PEC. In order to demonstrate a specific role for MΦ in the uptake and killing of *S.* Typhimurium this experiment was repeated using flow cytometry.

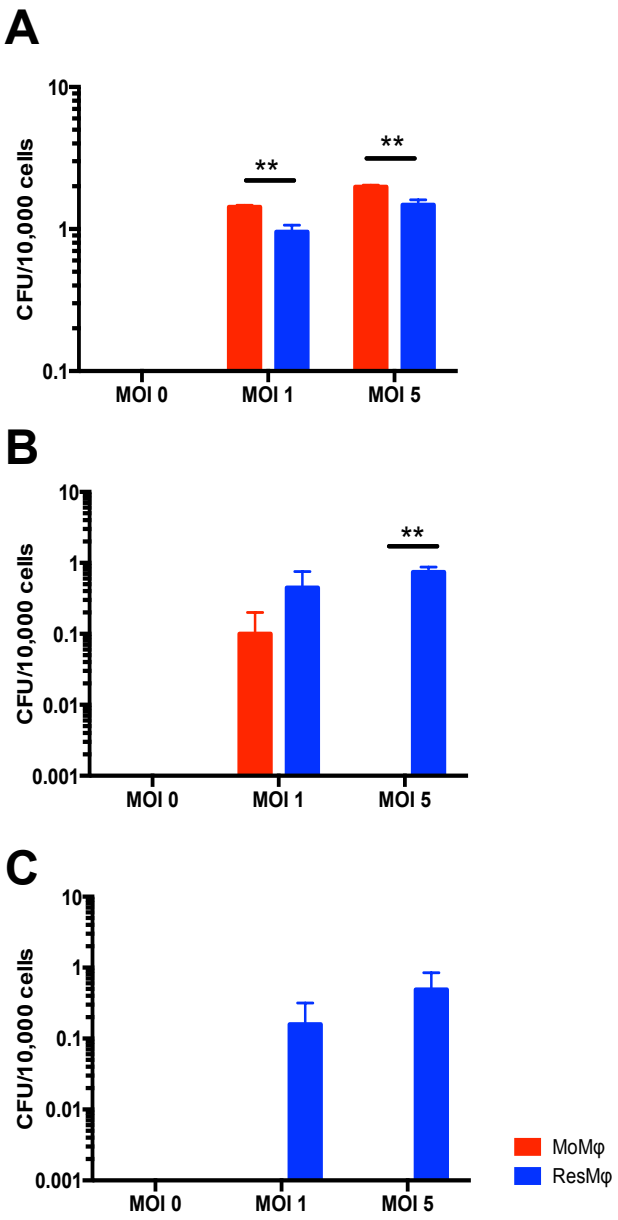


**Figure 5-3 Dynamics of Salmonella growth and control from colony forming units**

Peritoneal exudate cells isolated from naïve (resMΦ) or thioglycollate (MoMΦ) injected WT C57BL/6 females were cultured *ex vivo* separately ($4X10^5$ cells/ 100 µl/ well). The cells were infected with *S.* Typhimurium SL3261 (50 µl) for 1 hour; extracellular SL3261 was thereafter removed via gentamicin treatment (200 µg/ml, 50 µl). 1, 24 and 48 hours post stimulation the cells were plated on agar plates and CFU/10,000 cells was determined. Results are mean of 3 biological replicates and representative of 2 independent experiments. Significance was determined via 2-way ANOVA and Bonferroni's test. ** $P<0.01$. Bars are representative of the mean ± SEM

### 5.3.4 ResMΦ act as vehicle for dissemination

The CFU data was highly suggestive of a difference in the killing of SL3261 by MoMΦ and resMΦ over time. However, when plating MoMΦ and resMΦ whole PEC from thioglycollate/naïve mice was plated. In order to definitively pinpoint MoMΦ as being responsible for the enhanced bacterial killing, resMΦ and MoMΦ were analysed via flow cytometry for the detection of intracellular LPS 1, 24 and 48 hours post gentamicin treatment.

The initial spread of the bacterium through the macrophage population can be determined by looking at the fold change in the percentage of the population that is $LPS^+$ from 1 hour to 24 hours. Additionally, the fold change between 24 and 48 hours reflects spread of the bacterium over time.

At 24 hours post gentamicin treatment the fold change of the resMΦ population was significantly greater than that of the MoMΦ population (Figure 5-4A). This was true at an MOI 1 and MOI 5 (Figure 5-4A&C). At 48 hours post gentamicin treatment there was no difference in the fold change of the two populations positive for LPS relative to that at 24 hours (Figure 5-4A&C). This data suggests that once ingested *Salmonella* can rapidly spread through the resMΦ population. In contrast, there was little spread of the bacterium through the MoMΦ population after initial uptake, suggesting better containment of *Salmonella* by MoMΦ. The inability to detect differences in the fold change between MoMΦ and resMΦ populations at 48 hours suggested that resMΦ begins to control the bacterium by this time point, alternatively it is indicative of the bacterium having reached a threshold number within the population.

The fold change in the geometric mean of the MoMΦ and resMΦ populations is a representation of the change in the number of intracellular LPS per individual cell. The antibody against LPS does not discriminate between live and dead bacteria; therefore the geometric mean is reflective of the number of bacteria per individual cell, independent of live/dead status.

At a MOI 1 the MoMΦ exhibited a greater fold change in geometric mean between 1-24 hours post stimulation (Figure 5-4B). This data can be interpreted in two ways

**1)** that while MoMΦ can contain the bacterium, it does replicate within the cell or **2)** the MoMΦ population contain more dead *Salmonella* at 24 hours either through direct killing of *S.* Typhimurium or ingestion of *S.* Typhimurium-containing apoptotic cells. However, by there was no difference in the geometric mean of the MoMΦ and resMΦ populations at an MOI 1 between 48 and 24 hours post infection (Figure 5-4B). Furthermore, at an MOI 5 no difference was detected in the geometric mean of MoMΦ when compared to resMΦ at either 24 or 48 hours post infection (Figure 5-4D).

Similar results were obtained when MoMΦ and resMΦ were cultured and infected separately prior to flow cytometric analysis. A greater fold change in the percentage of $LPS^+$ positive MΦ was seen in the resMΦ population compared to the MoMΦ population at 24 hours post infection at an MOI 1 and MOI 5 (Figure 5-5A&C). However, no difference in the geometric mean was observed between separately infected MoMΦ / resMΦ at either 24/48 hours post infection at either an MOI 1 or MOI5 (Figure 5-5B&D).

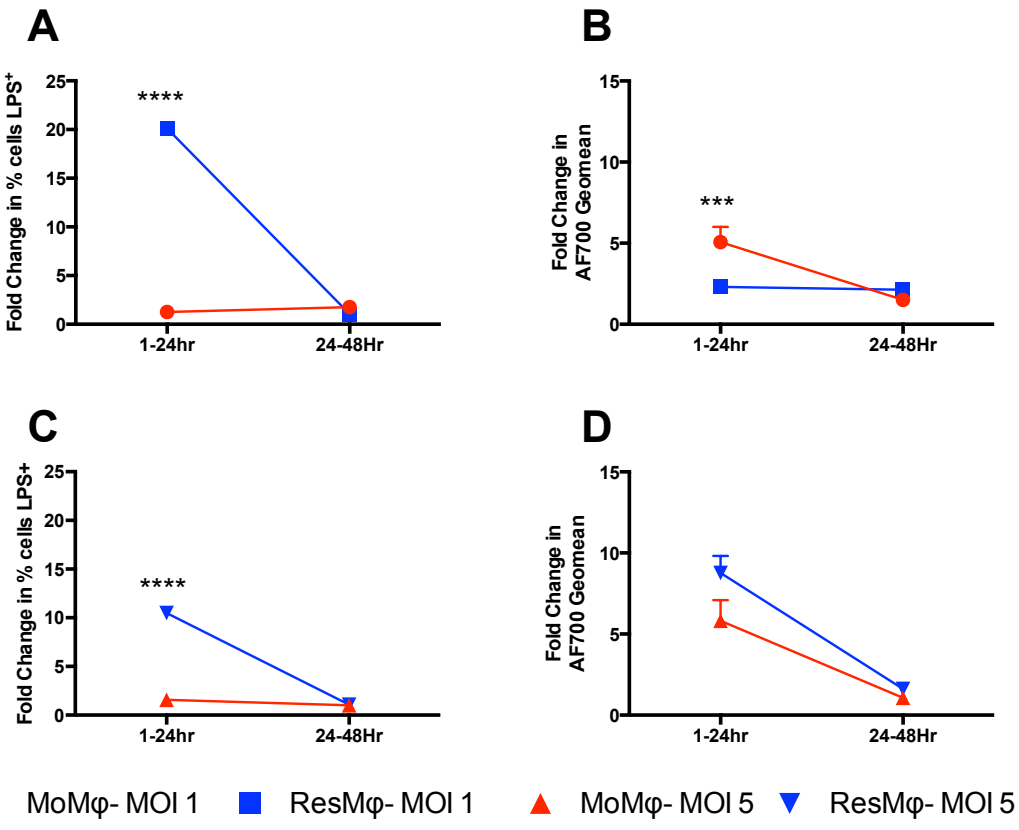


**Figure 5-4 Dynamics of Salmonella growth and control within co-cultured MoMΦ and resMΦ**

Peritoneal exudate cells were isolated from naïve (resMΦ) or thioglycollate (MoMΦ) injected WT C57BL/6 females and co-cultured *in vitro* ($4X10^5$cells/well) for 2 hours prior to infecting with *S.* Typhimurium (SL3261) for 1 hour. Extracellular SL3261 was removed via gentamicin treatment. The cells were incubated for a further 1, 24, or 48 hours and subsequently stained for flow cytometric analysis. **(A&C)** Representative plots showing the fold change in the percentage of the MoMΦ and resMΦ populations positive for LPS between 1-24 hours post infection and 24-48 hours post infection at an MOI 1 **(A)** and MOI 5 **(C)**. **(B)** Representative plots showing the fold change in the geometric mean of the MoMΦ and resMΦ populations between 1-24 hours post infection and 24-48 hours post infection. Results are mean of 3 biological replicates ± SEM and representative of 3 independent experiments, significance was determined via a 2-way ANOVA and Bonferroni's test. ***P<0.0001,**** P<0.00001.

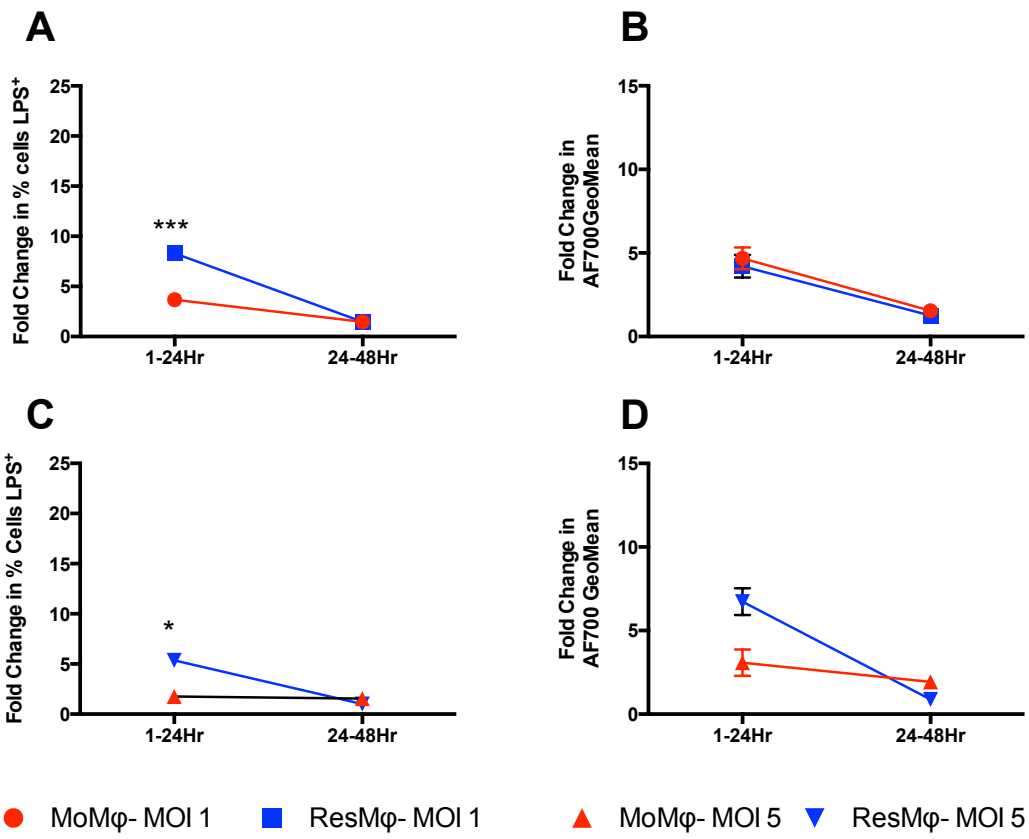


**Figure 5-5 Dynamics of Salmonella growth and control within separately cultured MoMΦ and resMΦ**

Peritoneal exudate cells were isolated from naïve (resMΦ) or thioglycollate (MoMΦ) injected WT C57BL/6 females and separately cultured *in vitro* (4X10$^5$cells/well) for 2 hours prior to infecting with *S.* Typhimurium (SL3261) for 1 hour. Extracellular SL3261 was removed via gentamicin treatment. The cells were incubated for a further 1, 24, or 48 hours and subsequently stained for flow cytometric analysis. **(A&C)** Representative plots showing the fold change in the percentage of the MoMΦ and resMΦ populations positive for LPS between 1-24 hours post infection and 24-48 hours post infection at an **(A)** MOI 1 and **(C)** MOI 5. **(B&D)** Representative plots showing the fold change in the geometric mean of the MoMΦ and resMΦ populations between 1-24 hours post infection and 24-48 hours post infection at an **(C)** MOI 1 and **(D)** MOI 5. Results are representative of 2 independent experiments, significance was determined via 2-way ANOVA and Bonferroni's test. * P<0.05, ***P<0.0001. Bars are representative of the mean ± SEM.

### 5.3.5 *In vitro, Salmonella*-macrophage dynamics do not translate to the *in vivo* setting.

In the steady state the ratio of F4/80$^{hi}$ resMΦ to MHC$^{hi}$F4/80$^{lo}$ MoMΦ within the peritoneal cavity of 8-week-old C57BL/6 mice is approximately 9:1. In order to investigate if the 10 % of MHC$^{hi}$F4/80$^{lo}$ MoMΦ within the peritoneal cavity display bactericidal capabilities similar to their *in vitro* counterparts, WT C57BL/6 female mice were infected i.p. with $10^6$ *S.* Typhimurium SL3261 which constitutively expresses GFP. The PEC was isolated 1, 3, 6 and 24 hours post infection for flow cytometric analysis. The advantage of the GFP *S.* Typhimurium SL3261, subsequently referred to as SL3261 GFP, is that when alive the bacterium will stain GFP$^+$LPS$^+$ and upon death the bacterium will loose GFP and thus stain GFP$^-$LPS$^+$. Unfortunately, due to technical issues I was never able to get this co-staining to work *in vitro* and therefore could not definitively comment on the killing ability of either cell type. *In vivo* however, the staining works well.

At 1-hour post infection, macrophages are the cell type within the peritoneal cavity containing the most Salmonella (Figure 5-6A). Additionally, at this time point a greater percentage of macrophages are GFP$^+$ compared any other population, although the percentage of dendritic cells (DCs) GFP$^+$ is also relatively high (Figure 5-6B). Through looking at the percentage of a population GFP$^+$ you can infer the efficiency with which this population takes up the bacterium or is infected by the bacterium.

In order to account for influxing monocytes, I divided the macrophage compartment into three subsets MHC$^-$F480$^{lo}$ cells, which are likely monocytes, MHC$^{hi}$F4/80$^{lo}$ MoMΦ and F4/80$^{hi}$ resMΦ. The MHC$^-$F480$^{lo}$ cells represent bone marrow derived monocytes which influx into the cavity at approx. 3 hours post insult. At 1-hour post infection there is a decrease in the number of F4/80$^{hi}$ resMΦ, however these cells still vastly outnumber the MHC$^{hi}$F4/80$^{lo}$ MoMΦ (Figure 5-6C). In contrast to my in vitro data, a greater number of F4/80$^{hi}$ resMΦ are GFP$^+$ 1 hour post infection (Figure 5-6D). There is, however, no difference in the percentage of MHC$^{hi}$F4/80$^{lo}$ MoMΦ and F4/80$^{hi}$ resMΦ GFP$^+$ (Figure 5-6E) at this time point.

By 3 hours post infection there is an influx of $MHC^{-}F4/80^{lo}$ cells in both naïve PBS injected controls and infected mice (Figure 5-7A&B). In the infected animals the number and percentage of $MHC^{-}F4/80^{lo}$ MΦ increases steadily and this correlates with the disappearance of the resMΦ population (Figure 5-7B&D). In contrast, 24 hours post PBS injection the composition of the macrophage compartment has nearly returned to homeostasis (Figure 5-7C), although the number of $F4/80^{hi}$ resMΦ is still lower than the initial numbers a 1 hour (Figure 5-7A). These graphs quite nicely illustrate that the MDR begins as rapidly as 1-hour post infection.

Through examining the fold change in the percentage of each MΦ subpopulation positive for both GFP and LPS vs. LPS alone, I was able to compare the bacterial growth and killing within each population. There was negligible detection of live $GFP^{+}LPS^{+}$ bacteria in any of the MΦ subpopulation at 1 hour post infection, subsequently the fold change in macrophages containing $GFP^{+}LPS^{+}$ bacteria at 3, 6 and 24 hours post infection was less than 1 % (Figure 5-8A). However, by 3 hours post infection there was a 2-fold increase in the percentage of cells containing dead bacteria ($GFP^{-}LPS^{+}$) and this was equal across all MΦ subpopulations. The peak in macrophages containing dead bacteria was reached at 6 hours post infection after which the detection declined, indicative of LPS degradation (Figure 5-8B).

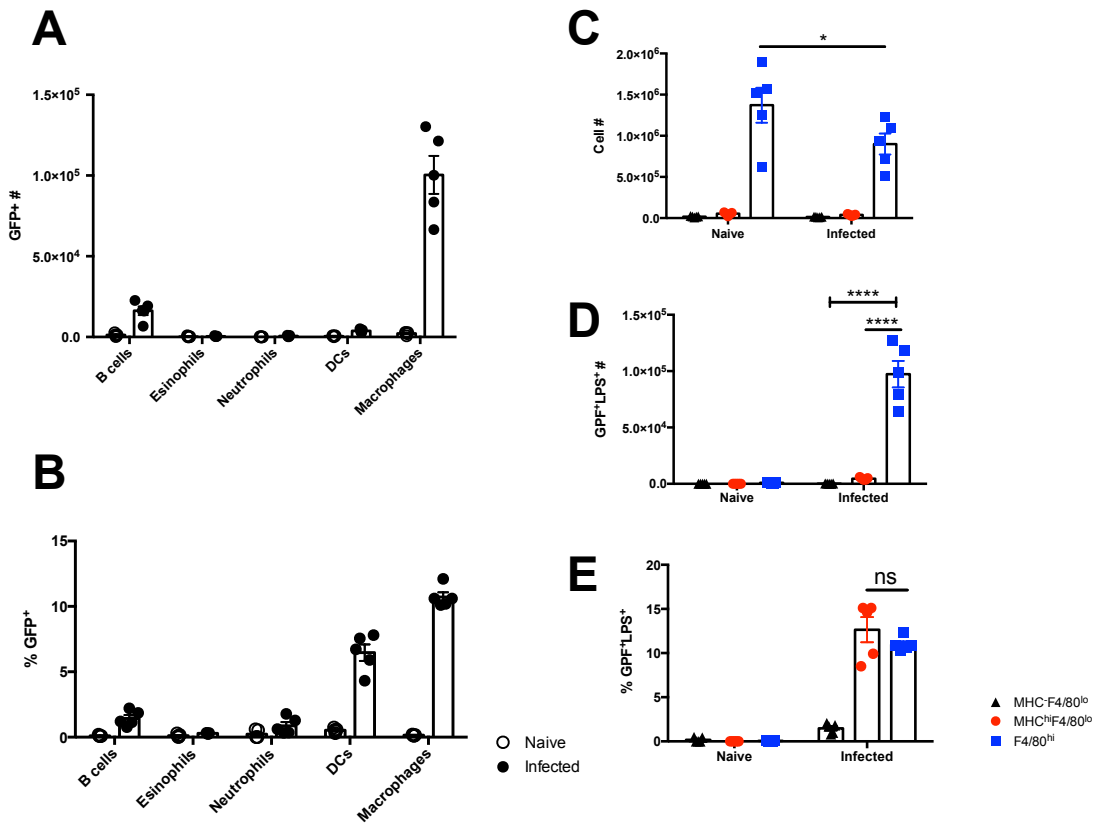


## Figure 5-6 In vivo uptake of GFP S. Typhimurium (SL3261)

C57BL/6 female mice, aged 6-8 weeks, received SL3261 GFP ($1X10^6$ CFU/200ul) or PBS intraperitoneally for 1 hour, after which they were culled via $CO_2$ and the peritoneal exudate cells (PEC) isolated for flow cytometric analysis. **(A)** The number of $GFP^+$ cells within the peritoneal cavity. **(B)** The percentage of each cellular population which contains GFP Salmonella. **(C)** The number of $MHC^-F4/80^{lo}$ vs. $F4/80^{lo}$ vs. $F4/80^{hi}$ MΦ within the cavity. **(D)** Number of $GFP^+$ $MHC^-$ $F4/80^{lo}$ vs. $GFP^+$ $F4/80^{lo}$ (MoMΦ) vs. $F4/80^{hi}$ (resMΦ). **(E)** % of $GFP^+$ $MHC^-F4/80^{lo}$ vs.$GFP^+$ $F4/80^{lo}$ (MoMΦ) vs. $GFP^+F4/80^{hi}$ (resMΦ). Data are representative of two independent experiments with 6 mice/group, significance was determined via 2-way ANOVA and Bonferroni's test. * P<0.05,***P<0.0001 Bars are representative of the mean ± SEM

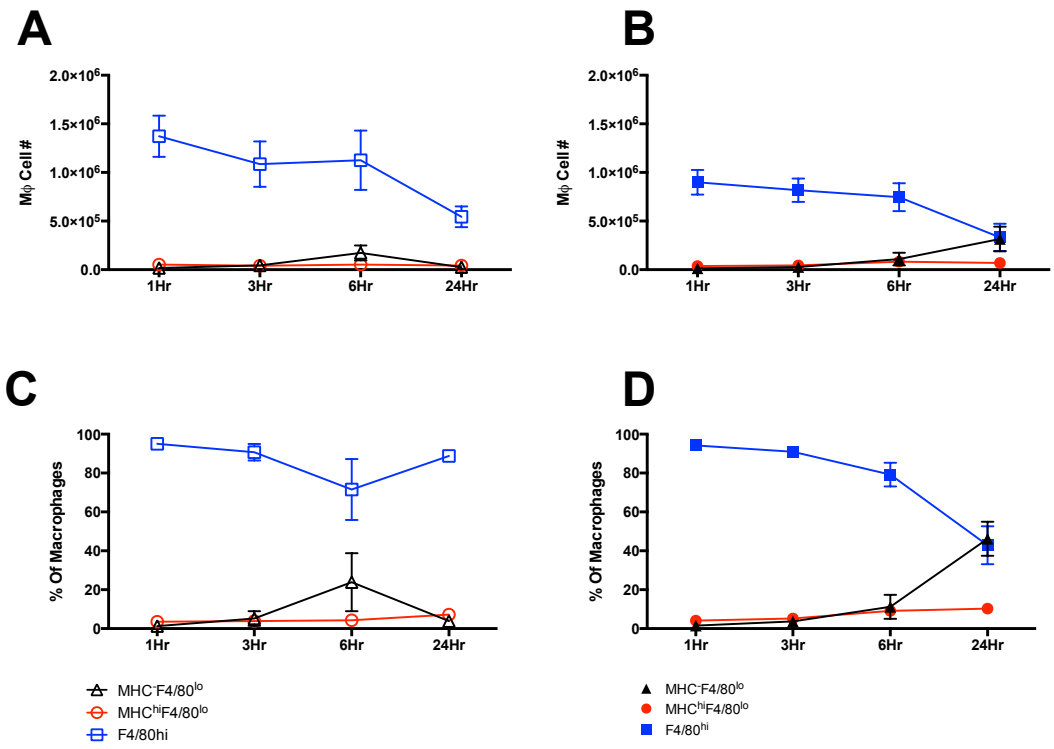


**Figure 5-7 Dynamics of the peritoneal macrophage population upon SL3261 GFP infection in vivo**

C57BL/6 female mice, aged 6-8 weeks, received SL3261 GFP ($1X10^6$ CFU/200ul) or PBS i.p. for 1, 3, 6 or 24 hours, after which they were culled via $CO_2$ and the peritoneal exudate cells (PEC) isolated for flow cytometric analysis. **(A & B)** Changes in number of $MHC^-F4/80^{lo}$, $MHC^{hi}F4/80^{lo}$ and $F4/80^{hi}$ cells within the peritoneal cavity upon PBS injection **(A)** or SL3261 GFP infection **(B)**. **(C & D)** % of the macrophage population composed of $MHC^-F4/80^{lo}$, $MHC^{hi}F4/80^{lo}$ and $F4/80^{hi}$ macrophages upon PBS injection **(C)** or SL3261 GFP infection **(D)**. Data are representative of two independent experiments with 6 mice/group.

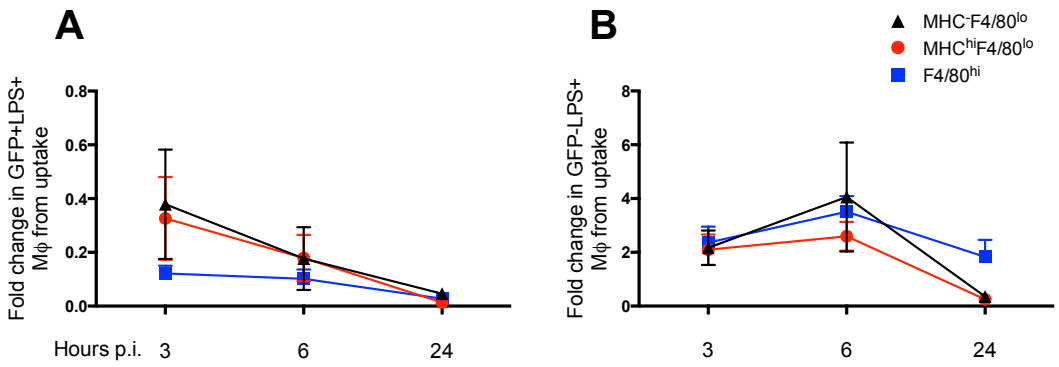


## Figure 5-8 *In vivo* killing of S. Typhimurium (SL3261)

C57BL/6 female mice, aged 6-8 weeks received SL3261 GFP (1X10$^6$ CFU/200ul) or PBS i.p. for 1, 3, 6, or 24 hours, after which they were culled via $CO_2$ and the peritoneal exudate cells (PEC) isolated for flow cytometric analysis. **(A)** Fold change in the percentage of each MΦ subpopulation containing live (GFP$^+$LPS$^+$) bacterial relative to the percentage positive at 1hr post infection. **(B)** Fold change in the percentage of each MΦ subpopulation containing dead (GFP$^-$LPS$^+$) bacterial relative to the percentage positive at 1hr post infection. Data are representative of two independent experiments with 6 mice/group.

## 5.4 Discussion

We have characterised the functional differences between MoMΦ and resMΦ in response to *S.* Typhimurium both *in vitro* and *in vivo*. Our findings strongly support the emerging literature on macrophage function being the outcome of a complex local tissue environment.

Infection of co-cultured MoMΦ and resMΦ for 1 hour revealed a greater number of bacteria was contained within the MoMΦ population in comparison to the resMΦ. This was a somewhat surprising result, given that resMΦ are highly adapted to preferentially phagocytose apoptotic bodies over MoMΦ and the current literature primarily describes bacterial uptake by macrophages to be phagocytosis dependent (Uderhardt et al., 2012, Broz et al., 2012, de Jong et al., 2012). However, this increased bacterial uptake up/targeting of MoMΦ supports the overall hypothesis that this population arose (independently of tissue resident macrophages) to function against intracellular pathogens in a type 1 immune setting.

I next sought to investigate if the observed difference in bacterial uptake/infection of MoMΦ was a result of differentially expressed cell surface receptors involved in *Salmonella* internalisation between the MoMΦ and resMΦ populations. Vazquez-Torres et al showed that *Salmonella* that are SPI-1 deficient, and hence unable to invade epithelia cells, could still cross the intestinal barrier. This was attributed to $CD18^{+}$ phagocytes at the intestinal epithelial barrier (Vazquez-Torres et al., 1999). CD18 is a β integrin, which possesses a binding site for LPS and forms heterodimers with the α-integrins CD11a, CD11b and CD11c, to form lymphocyte function-associated antigen 1 (LFA-1), complement receptor 3 (CR3) and CR4 respectively(Samuel D.Wright, 1989, Solovjov et al., 2005). Furthermore, CR3 has been shown to be essential for the uptake of unopsonized *Salmonella* by neutrophils (van Bruggen et al., 2007). Other receptors which we hypothesized might be involved in this differential uptake were TLR4 which recognises bacterial LPS and its co-receptor CD14(Wright et al., 1990). However, analysis of CD18, CD11a, CD11b and CD14 via flow cytometry revealed that the expression of these markers is not significantly different between MoMΦ and resMΦ. The expression of CD11c was significantly greater on the MoMΦ population. CR4 (CD11c:CD18) was the first

of the αβ integrins shown to induce intracellular signalling in response to LPS. This was independent of serum proteins and cumulated in NFκβ activation (Ingalls and Golenbock, 1995). LFA-1 and CR3 were also shown to induce similar signalling. However, TLR4, CD14 and LPS binding protein are now known to form the main protein complex responsible for LPS binding (Flaherty et al., 1997, Lien et al., 2000). Thus the recognition of LPS by CR4 may be of a much lower affinity than that of the LPS binding complex. Furthermore, given that bacterial uptake by TLR4 KO MoMΦ/resMΦ is unchanged when compared to WT, it is unlikely that LPS binding by CR4 explains the enhanced bacterial uptake by the MoMΦ population. As with all the integrins, CR4 is involved in cellular migration. Therefore, the heightened CD11c expression may simply reflect the fact that these thioglycollate elicited MoMΦ have recently arrived from the bone marrow. In support of this monocyte recruitment in atherosclerotic lesions is reduced in mice lacking CD11c ($\alpha X^{-/-}apoE^{-/-}$ vs $apoE^{-/-}$)(Wu et al., 2009).

Active invasion of macrophages by *Salmonella* in a SPI-1 dependent manner has also been described (Drecktrah et al., 2006, Bueno et al., 2010). Thus, SPI-1 proteins specifically targeting receptors, which are expressed to a higher degree on MoMΦ, could explain the heightened bacterial numbers within the MoMΦ population. Cholesterol has previously been shown to be important in the uptake of *Salmonella* by its target cell and recent work has shown this binding to be dependent of the effector protein sipB (Santos et al., 2013, Garner et al., 2002). Additionally, the amount of cell surface cholesterol was shown to increase throughout the cell cycle, with the concentration at mitosis twice that at G1(Santos et al., 2013). This finding has led me to hypothesis that the difference in bacterial numbers within the MoMΦ and resMΦ could be a result of different cell surface cholesterol levels. Perhaps MoMΦ, which are derived from the bone marrow, and thus have divided more recently than resMΦ, have more cell surface cholesterol.

The MoMΦ population also killed intracellular SL3261 at a faster rate did the resMΦ population over time. The CFU data clearly illustrates a more rapid decline in intracellular bacterial numbers within the MoMΦ population. While the antibody against LPS binds both live and dead bacteria, making a conclusion regarding

bacterial killing difficult, what is clear is that SL3261 more rapidly spreads throughout the resMΦ population, whereas MoMΦ appear more capable of controlling the cell-cell spread of the bacterium. The greater geometric mean of the MoMΦ population at 24 hours when the populations are co-cultured suggested that the MoMΦ are potentially re-infected by bacteria, which have moved through the more permissive resMΦ population. While I was carrying out these experiments, Burton et al. nicely illustrated that in the spleen inflammatory macrophages are more efficient at killing *Salmonella* than are resident red pulp macrophages, in which the majority of the salmonella resided. The bactericidal ability of the inflammatory monocytes was shown to be the result of a lethal oxidative burst induced by NADPH oxidase and myeloperoxidase activation (Burton et al., 2014). In contrast the resident macrophage population do not possess myeloperoxidase and kill the bacterium to a lesser degree in a NADPH oxidase independent manner (Burton et al., 2014). The inflammatory macrophages observed here, at day 4 post *Salmonella* infection, would be akin to the thioglycollate elicited MoMΦ used in my experiments. Additionally, like the resMΦ in the peritoneal cavity, the resident red pulp macrophage of the spleen are prenatally-derived (Yona et al., 2013, Schulz et al., 2012).

*In vivo,* macrophages are the cell population, which take up the most *Salmonella* within 1 hour of infection. However, in comparison to the *in vitro* data, *in vivo* the F4/80$^{hi}$ population contain significantly more GFP SL3261 than the F4/80$^{lo}$ population, although this was not surprising given the vast imbalance in F4/80$^{lo}$ to F4/80$^{hi}$ numbers in the peritoneal cavity. There was however, no difference in the ability of the MoMΦ and resMΦ populations to ingest *Salmonella,* as determined by the percentage of each population positive for GFP. Thus I would like to hypothesis that the MoMΦ population are better at *Salmonella* uptake *in vivo*, however their low numbers severely reduces their likelihood of interacting with the bacterium. Another possibility is that local tissue factors such as retinoic acid and CSF-1 have conditioned the F4/80$^{lo}$ monocyte-derived population within the cavity, such that their initial bactericidal ability has been dampened. An emerging concept in the field is that tissue specific factors imprint distinct transcriptional profiles upon local macrophage populations, thus altering tissue specific function (Gautier et al., 2012, Hashimoto et al., 2011). In alignment with this hypothesis it is not that surprising that

there was no difference observed in the killing ability of the F4/80$^{lo}$ and F4/80$^{hi}$ cells *in vivo*.

During both *Salmonella* infection and sterile inflammation the MDR begins within 1 hour of insult. Between 3-6 hours there is an initial influx of monocytes into the cavity in both PBS injected controls and infected animals. By the time these cells have arrived there is little extracellular bacteria remaining (data not shown). Consequently, if these cells possess heightened bacterial uptake and killing capabilities, similar to that observed for thioglycollate elicited MoMΦ *in vitro*, we were not able to detect it here. By 24 hours, the monocyte population have disappeared in the control animals but increase to represent 50 % of the population in the *Salmonella* infected animals. Work by Dr. Dominik Rückler in our lab has illustrated that by 5 days post *Salmonella* infection, the F4/80$^{hi}$ resMΦ has been entirely replaced by F4/80$^{lo}$ monocyte-derived macrophages. Interestingly, the existing MHC$^{hi}$F4/80$^{lo}$ MoMΦ within in the cavity do not vary over the time course suggesting that they are not sensitive to the same migratory factors as the F4/80$^{hi}$ population.

In this chapter, we investigated the functional difference between bone-marrow derived macrophages (MoMΦ) and tissue macrophages (resMΦ) which are initially derived prenatally, in the context of *S.* Typhimurium infection. Our results show that *in vitro* MoMΦ are functionally more capable of ingesting, containing and killing SL3261 than are resMΦ. However, these *in vitro* functional differences did not translate to the *in vivo* setting. I hypothesise that this is a consequence of the low F4/80$^{lo}$ MoMΦ numbers within the peritoneal cavity as well as the conditioning of this population by tissue specific niche factors. Finally, the MDR reaction is a rapid response to injury, initiated within 1 hour of infection, which appears to only drive the disappearance of the F4/80$^{hi}$ population.

# Chapter 6 General Discussion

The realisation that many tissue resident macrophage populations are established prenatally revolutionized the field of MΦ biology (Ginhoux et al., 2010, Schulz et al., 2012, Yona et al., 2013). Prenatally-derived MΦ were illustrated to be long-lived and capable of *in situ* self-renewal (Hashimoto et al., 2013), suggestive of stem cell-like properties. Furthermore, during helminth infection tissue resident MΦ proliferate to generate an expanded resMΦ population, which is independent of bone marrow derived MΦ recruitment (Jenkins et al., 2011). In contrast, an inflammatory insult results in the disappearance of these cells and infiltration of BMDMΦ, yet during the resolution of the inflammatory response resMΦ proliferate to re-seed the tissue niche (Davies et al., 2013). All of the above data was highly suggestive of prenatally derived resMΦ and BMDMΦ possessing distinct developmental origins and as a result specific functional capabilities with regard to Type 2 and Type 1 immunity.

This thesis has investigated the functional relevance of MΦ origin in relation to resistance and susceptibility to a filarial nematode and also the bactericidal capabilities of these populations in response to *Salmonella* Typhimurium infection. Whilst the overarching focus has been on MΦ function during infection, analysis of the MΦ compartment of naïve partial bone marrow chimeric mice has provided some key additional insights that have enabled alignment of this data with the currently evolving field. As such it has become increasingly clear, that while many of these resMΦ populations are initially derived from embryonic sources, they can by replaced/replenished by bone marrow derived macrophages, which are capable of successfully recapitulating the functional capabilities of their prenatally-derived founders (Bain et al., 2014, Molawi et al., 2014, Sheng et al., 2015, Bain et al., 2016). Consequently, a great research effort is currently on going to understand the local tissue specific signals which condition infiltrating MΦ (either during development or later in life) toward a highly specialised resMΦ phenotype.

Chapter 2 began by examining the accumulation of immune cells within the pleural cavity of resistant and susceptible mice during infection with the filarial nematode *L. sigmodontis.* The results demonstrated that resistance was associated with a greater degree of pleural cell accumulation, which reflected greater B cell and MΦ cell

numbers. Interestingly both AAMΦ and B cells have been attributed with pro- and anti-worm killing functions (Taylor et al., 2006, Anthony et al., 2006, Zhao et al., 2008, Al-Qaoud et al., 1998, Martin et al., 2001), highlighted that cellular function is extremely complex. The specific role of a cellular population also is also likely infection-stage specific. Further analysis of the MΦ compartment revealed that an expanded F4/80$^{hi}$ resMΦ population in resistant C57BL/6 mice accounted for the difference in total MΦ number between the strains. Previous data in the lab has shown that a peak in MΦ proliferation occurs at day 11-post infection, followed by a proliferative crash, in which proliferation is below homeostatic levels until day 28 post infection. Indeed, of the time points examined (Day 11, 28, 35 and 50 pi) proliferation above homeostatic levels was only detected at day 11. Consequently, we questioned whether the continual increase in MΦ number observed from day 11-50 post infection was a result of BMDMΦ recruitment and integration into the resMΦ niche or proliferation between the examined time points. Experiments in CCR2 deficient animals, in which BMDMΦ recruitment cannot occur, suggested that the expanded F4/80$^{hi}$ resMΦ population was independent of BMDMΦ recruitment until day 28 pi. Subsequent studies in partial bone marrow chimeric animals, illustrated that the expanded F4/80$^{hi}$ population in the pleural space of resistant C57BL/6 mice must indeed be generated through local proliferation of the resMΦ population in-between the examined time points. However, the data also confirms recent work by Bain et al., regarding the longevity of the resMΦ population within the pleural space, highlighting that the population is replenished from the bone marrow with age (Bain et al., 2016). Moreover, the data leads to a fascinating insight: that the proliferative program induced by IL-4 enables the exponential expansion of the resMΦ population while maintaining the rate of homeostatic integration of BMDMΦ into the resident niche.

Within the peritoneal and pleural cavities retinoic acid has been identified as a key modulator of the resident macrophage phenotype, through inducing a transcriptional program controlled by the transcription factor GATA6 (Okabe and Medzhitov, 2014, Rosas et al., 2014). Furthermore, the cell surface marker CD102 has been identified as a peritoneal/pleural MΦ specific marker which is controlled by a yet-to-be-identified tissue factor (Okabe and Medzhitov, 2014). Chapter 2 highlighted that

there is a 27-fold increase in F4/80$^{hi}$ MΦ cell number by day 30 pi in the resistant C57BL/6 strain, half of this increase is a result of BMDMΦ integration into the resMΦ niche. The ability of these BMDMΦ to successfully integrate into the local niche suggests both an abundance of local niche factors, such as retinoic acid and illustrates the responsiveness of incoming cells toward conditioning factors. The latter statement stems from data presented by Okabe and Medzhitov in which overnight culturing of BMDMΦ with a retinoic acid derivative did not induce GATA6 or CD102 expression, and this was a result of transcriptional silencing at the GATA6 locus (Okabe and Medzhitov, 2014). Thus, I hypothesise that additional tissue specific signals present *in vivo* 'prime' infiltrating BMDMΦ such that they are open to conditioning by factors such as retinoic acid.

One of the core findings in Chapter 2 was that resistance was strongly associated with an expanded F4/80$^{hi}$ MΦ population generated through *in situ* proliferation. This led me to my hypothesis that the expanded resMΦ population is actively involved in the killing of *L. sigmodontis* worms within the pleural cavity. This hypothesis is well founded given that immunity against secondary *H. polygyrus* infection is mediated by an expanded population of alternatively activated resMΦ, generated by $T_H2$ derived IL-4 (Anthony et al., 2006). This MΦ mediated protection during secondary *H. polygyrus* infection is through larval trapping in collaboration with antibodies and complement (Esser-von Bieren et al., 2013). Furthermore, IL-4c results in expansion of resident peritoneal cavity MΦ, which are positive for RELMα and dependent upon fatty acid oxidation (Huang et al., 2014). This IL-4c expanded peritoneal MΦ population are protective during primary *H. polygyrus* infection, resulting in reduced, although not significantly so, worm recovery and egg out-put by day 14 pi (Huang et al., 2014). Similarly, IL-4 induced AAMΦ during primary infection with *N. brasiliensis* mediate smooth muscle hypercontractility essential for worm expulsion (Zhao et al., 2008). The expanded resMΦ population within the gut of *H. polygyrus* and *N. brasiliensis* infected animals are likely generated through proliferation of recently recruited BMDMΦ. Indeed Anthony et al., described the expanded AAMΦ population as CD206 positive, a marker now know to be specific to BMD AAMΦ (Gundra et al., 2014). AAMΦ within the gastrointestinal tract are BMD and would possess an M(IL-4) activation phenotype distinct to that of AAMΦ

generated through local proliferation of ResMΦ, as seen in *L. sigmodontis* infection (Gundra et al., 2014). Thus it is possible that the killing mechanisms orchestrated by these BMD AAMΦ in the gut are completely distinct from those mediated by AAresMΦ in the pleural space.

However in addition to MΦ, there were vastly more B cells within the pleural space of resistant C57BL/6 compared to BALB/c mice, suggesting that a MΦ-antibody collaboration may be involved in worm killing within this strain. Data from an additional project in the lab, carried out by Dr. Lucy Jackson-Jones, further supports this hypothesis. Resident pleural cavity B cells, that reside in the fat associated lymphoid follicles (FALCs) of the pericardium and mediastinum, proliferate *in situ* during *L. sigmodontis* infection and secreted large amounts of antigen specific IgM locally (Jackson-Jones et al., 2016- Nature Communications-in press). The production of antigen specific IgM by pleural cavity B cells was observed in both strains, however to a significantly greater degree in the resistant C57BL/6 strain (Jackson-Jones et al., 2016- Nature Communications-in press). Thus, I hypothesise that expanded resMΦ and IgM function in trapping and killing adult worms in the C57BL/6 strain. In Chapter 3, in an attempt to illustrate a protective role of F4/80$^{hi}$ resMΦ in worm killing, I depleted the population through administration of clodronate containing liposomes directly into the pleural cavity. The longest period of MΦ depletion achieved was 12 days, from day 27-39 pi, given the protracted affair that is worm killing this was a relatively short time frame. Nonetheless, we achieved promising results with a trend toward greater worm recovery in the absence of resident F4/80$^{hi}$ population. Additional experiments examined the pleural cavity at 4 and 6 days post clodronate-liposome administration. At these time points (day 33 and day 35 pi) the F4/80$^{hi}$ population was successfully depleted, with no affect upon other pleural cell populations or difference in worm recovery evident. In contrast, following 14 days of F4/80$^{hi}$ MΦ depletion, a significant decrease the number of B cells and eosinophils was observed within the pleural cavity. Consequently, this data is suggestive of eosinophils, B cells and MΦ working collaboratively to kill the worm in the resistant strain. Indeed eosinophils have previously been identified as a major component the granulomas which form around young adult worms in the C57BL/6 strain (Attout et al., 2008).

Macrophage-mediated killing of *H. polygyrus* and *Strongyloides stercoralis* larvae occur in collaboration with antibodies and also complement proteins (Esser-von Bieren et al., 2013, Bonne-Annee et al., 2013). Given the dominance of MΦ and B cells within the pleural space of C57BL/6 mice and the realisation that B cells are producing antigen specific IgM, we decided to investigate if complement was involved in the resistance phenotype. We infected mice deficient in C3, the central component of all three pathways of complement activation, to determine if this cascade is also involved in the coordination of the immune-mediated killing of adult worms in the resistant C57BL/6 strain. While complement deficiency did not influence worm killing observed at either day 28 or 35 post infection a significant decrease in F4/80$^{hi}$ resMΦ was observed, suggestive of a supportive role for complement in MΦ proliferation.

Chapter 2 illustrated that the F4/80$^{hi}$ population consistently represented ~90 % of the total MΦ compartment in the C57BL/6 strain, with the remaining 10 % consisting of CSF1$^{+}$F4/80$^{lo}$MHC$^{hi}$ cells, referred to as MoMΦ in this thesis. This MoMΦ population is akin to the previously described small peritoneal macrophage population within the peritoneal cavity that are recently recruited from the BM (Ghosn et al., 2010). Furthermore, recent work by Bain et al has illustrated that RELMα expressing cells within this MoMΦ population represent monocyte-derived precursors to the F4/80$^{hi}$ resMΦ population under homeostatic conditions (Bain et al., 2016). Chapter 2 demonstrated that susceptibility within the BALB/c strain was marked with significantly less F4/80$^{hi}$ MΦ proliferation at day 11 pi and an influx of BMD Ly6C$^{+}$ monocytes at day 35-50 post infection. In both naïve and infected BALB/c mice the percentage of F4/80$^{hi}$ resMΦ declined with age and the proportion of MoMΦ and monocytes increased. As such by day 50 pi, the pleural MΦ compartment of susceptible BALB/c mice was composed of 50 % BMDMΦ and 50 % resMΦ. This data is indicative of an inability of infiltrating BMDMΦ to integrate into the local pleural cavity niche within the susceptible BALB/c strain, either due to a deficiency in retinoic acid or another niche factor responsible for priming the cells. Okabe et al., placed C57BL/6 mice on a Vitamin A deficient diet, thereby reducing retinoic acid, and observed a continual decline in the percentage of F4/80$^{hi}$ resMΦ and an increase in BMD MoMΦ and monocytes within the peritoneal space by 12

weeks of age. The representative flow cytometric plots from this paper (Okabe and Medzhitov, 2014) are strikingly similar to the 'monocyte waterfall' that I have observed in infected BALB/c mice. Consequently, I hypothesize that a relative lack of retinoic acid in the BALB/c strain contributes to susceptibility through a failure to maintain the resMΦ population, which in the context of a $T_H2$ immune response is critical in worm killing.

A strong $T_H2$ immune response and generation of M(IL-4) is a hallmark of *L .sigmodontis* infection in both resistant and susceptible strains (Babayan et al., 2003). However, in the susceptible strain as infection progresses immunosuppression dominates permitting microfilaria production and preventing worm clearance until ~day 90 pi (Taylor et al., 2007).

In addition to immunosuppression, previously active antigen-specific $T_H2$ cells lose their ability to secrete cytokines IL-4, IL-5 and IL-2 between day 20 and day 60-post infection. This is referred to as a hyporesponsive T cell phenotype akin to anergic or exhausted T cells (van der Werf et al., 2013). The induction of this hyporesponsive T cell phenotype is associated with PD-L2 induced PD-1 expression on $T_H2$ cells (van der Werf et al., 2013). PD-L2 expression has long been associated with alternative activation and its expression has contributed considerably to the reputation of AAMΦ or AADCs as immune suppressors rather than effectors during the type 2 immune response (Loke and Allison, 2003, Huber et al., 2010, Terrazas et al., 2005, Colley et al., 2005). Through *in vitro* co-culture experiments van der Werf et al., investigated the role of AAMΦ in the maintenance of the hyporesponsive T cell phenotype during *L. sigmodontis* infection (van der Werf et al., 2013). AAMΦ from day 60 infected BALB/c mice inhibit the proliferation of day 60 pi $T_H2$ cells in response to *L. sigmodontis* antigen, however this effect was not reversed through the addition of PD-L1/PD-L2 blocking antibodies (van der Werf et al., 2013). Thus, this paper concluded that AAMΦ are not responsible for induction of the hyporesponsive T cell phenotype via PD-L2. However, in these co-culture experiments only $F4/80^{hi}$ MΦ were used and the publication by Gundra et al. have demonstrated that PD-L2 expression is limited to AAMΦ possessing a bone marrow derived MΦ phenotype; $F4/80^{lo}$, $MHC^{hi}$ (Gundra et al., 2014). Thus, I decided to readdress the potential of the

MΦ compartment of susceptible BALB/c mice, which is 50 % BMD by day 50 pi, to induce the hyporesponsive T cell phenotype.

The data presented in Chapter 3 illustrated that a high percentage of MΦ in the BALB/c strain are positive for PD-L2, the expression of which correlated with a greater adult parasite recovery rate and a weakened immune response when compared to resistant mice. The detection of PD-L2 positive F4/80$^{hi}$ MΦ within the susceptible strain strongly suggests that BMDMΦ can integrate into F4/80$^{hi}$ resMΦ niche and this was further supported by the detection of CD102$^{+}$PD-L2$^{+}$ events. The continual decline in the percentage of F4/80$^{hi}$ cells contributing to the MΦ compartment is indicative that the rate of BMDMΦ integration into the resMΦ niche is insufficient to match the rate of influx in this strain. Monocyte depletion prior to day 35 post infection resulted in an enhanced $T_H2$ immune response and greater worm clearance in the susceptible strain, confirming an immunosuppressive and detrimental role for these cells in worm killing. However at day 35-post infection, this immunosuppressive role of monocytes could not be attributed to PD-L2 expression. Examination of PD-L2 acquisition by the MΦ compartment showed that PD-L2 induction is not observed until between day 35-50-post infection. Thus, the window of PD-L2 induction on the MΦ compartment is in alignment with the onset of $T_H2$ cell hyporesponsiveness. In order to address if monocytes are involved in the hyporesponsive T cell phenotype at day 50 pi, the anti-CCR2 antibody was administered prior to day 35 pi and the MΦ compartment was examined at day 50 pi. This strategy also failed to illustrate a role for PD-L2 in the induction of the hyporesponsive $T_H2$ cell phenotype, but this was likely a result of monocyte depletion being transient. A monocytic influx had occurred in many of the anti-CCR2 treated animals by day 50 pi, resulting in a decrease in F4/80$^{hi}$ MΦ and increase in PD-L2$^{+}$ BMDMΦ within the pleural space. Consequently, I remain confident that BMDMΦ infiltrate into the pleural cavity of susceptible mice, become alternatively activated (PD-L2$^{+}$) and subsequently induce the hyporesponsive $T_H2$ cell phenotype. I had hoped to infect *Ccr2*$^{-/-}$ BALB/c mice to investigate the susceptibility and dynamics of the MΦ compartment in this strain. However, due to complications with the re-derivation process in the animal facility here at the University of Edinburgh I was unable to carry out these experiments.

B cells within the pleural space of *L. sigmodontis* infected BALB/c mice also highly upregulate PD-L2 (van der Werf et al., 2013). Thus, work carried out by a postdoc within the Institute of Immunology and Infection Research at Edinburgh University has followed on from this preliminary data generated by Nienke van der Werf. Through the generation of mix bone marrow chimeric animals, in which PD-L2 deficiency was restricted to the B cell compartment, Dr. Johanna Knipper in Matthew Taylor's group has concluded that B cells, while immunosuppressive also, are not responsible for the induction of the hyporesponsive T cell phenotype (Knipper & Taylor, unpublished data). To conclusively illustrate a role for PD-L2 expression on BMDMΦ in the induction of hyporesponsive $T_H2$ cells I believe the generation of mice with PD-L2 deficiency restricted to BMDMΦ would be necessary.

Collectively, the data from Chapter 2-4 has highlighted that the functional capabilities of a MΦ with regard to worm killing is independent of ontogeny, but is the result of the maturation state (monocyte-MoMΦ-resMΦ) of the MΦ upon IL-4 stimulation. MΦ possessing a resMΦ phenotype assume an M(IL-4) activation state that within the pleural space is likely to be constructive to worm killing. In contrast, MΦ possessing a monocyte/ MoMΦ phenotype assume an M(IL-4) activation state which is more immunosuppressive and in the context of *L. sigmodontis* infection within the BALB/c strain contributes to delayed worm clearance. Recruitment of MΦ from the bone marrow is a signature of pro-inflammatory type 1 immune responses mounted against bacterial and viral pathogens. In general, bacterial and viral pathogens pose a more imminent threat to the host than do multicellular parasites and consequently, the type 1 immune response functions to rapidly contain and kill such pathogens often at the expense of host health, in the short term. In contrast, helminth parasites can survive within their hosts for decades; consequently mounting a pro-inflammatory immune response with the potential for prolonged self-damage would not be in the overall interest of the host. Consequently, I hypothesise that the immunosuppressive phenotype assumed by BMDMΦ as they infiltrate into an immune milieu dominated by the type 2 cytokine IL-4 is an evolutionary mechanism to prevent against self-harm. Indeed, BMD AAMΦ recruited to the liver during *S. mansoni* infection are PD-$L2^+$ and their depletion while enabling in an enhanced $T_H2$

immune response ultimately resulted in the mice succumbing to infection (Nascimento et al., 2014, Girgis et al., 2014).

Worm killing in the susceptible BALB/c strain eventually occurs ~day 80-90 pi and has been associated with a mixed $T_H1/T_H2$ immune response (Saeftel et al., 2003) and the integration of neutrophils into granulomas that form around fully developed adult worms(Attout et al., 2008). Given that day 50 pi was the latest date investigated in this thesis, the role that MΦ play in the eventual killing of worms in the BALB/c strain remains unexplored. Consequently, I believe that it would be interesting to investigate how the MΦ compartment changes between day 50-80/90 pi, specifically do the BMDMΦ assume a more resident phenotype, involving PD-L2 down regulation, which is constructive to worm killing?

Detailed immunohistochemical analysis of granulomas isolated from the pleural space will enable a greater understanding of how different immune cells populations collaborate to trap and kill *L. sigmodontis* worms. Specifically, it would be interesting to examine what makes direct contact with the worm, do antibodies bind directly to the worm and facilitate MΦ and eosinophil/neutrophil attachment. Do MΦ and neutrophils form extracellular traps, as demonstrated in *S. stercoralis* infection to further trap the worms?

The data in Chapters 2-4 demonstrate that an expanded resMΦ population are beneficial to worm killing, whereas BMDMΦ were detrimental. An influx of BMDMΦ is characteristic of bacterial infections and often results in the disappearance of the resMΦ population. I was therefore interested in addressing whether BMDMΦ display enhanced bactericidal capabilities when compared to resMΦ. This question was the focus of Chapter 5, in which an *in vitro* system was employed to overcome the *in vivo* disappearance reaction. The peritoneal exudate cells (PEC) from naïve animals and thioglycollate-injected animals, both of which contain a high proportion of MΦ, were cultured *in vitro* and infected with *Salmonella* Typhimurium. BMDMΦ contain significantly more *Salmonella* Typhimurium 1-hour post *in vitro* infection, demonstrating a heightened ability to ingest or be infected by *Salmonella* Typhimurium. Furthermore, by 24 hours pi fewer bacteria are detected on agar plates that were streaked with thioglycollate infected PEC vs. naïve infected

PEC. This data demonstrated that thioglycollate-elicited PEC more rapidly kills *Salmonella* Typhimurium when compared to naïve PEC. While MΦ are the primary component of PEC, we cannot rule out the possibility that neutrophils also played a role. The *in vitro* findings did not translate to the *in vivo* setting were both populations displayed equal capabilities regarding bacterial uptake. Of note however is that *in vivo* the MΦ compartment of C57BL/6 mice is only 10 % MoMΦ. Consequently, the equal percentage of BMDMΦ and resMΦ containing bacteria in vivo despite a 9-fold difference in cell number is suggestive that BMD MoMΦ may possess heightened bactericidal uptake capabilities *in vivo.* Through infection with $GFP^+$ *Salmonella* Typhimurium and co-staining for LPS, we had hoped to detect a difference in worm killing between MoMΦ and resMΦ. However, by 6 hours post infection there was no difference in the percentage of $GFP^+$ vs. $GFP^+LPS^+$ MoMΦ or resMΦ, thus no differences in the *in vivo* killing abilities of BMDMΦ and resMΦ were detected. Of note however, is that a relatively low dose of *Salmonella* Typhimurium was used in these experiments. It is possible that a higher infection dose would give better resolution.

In conclusion, this project began with the knowledge that IL-4 drives the expansion of resident pleural macrophages, which were thought to be independent of BMDMΦ, during *L. sigmodontis* infection of resistant C57BL/6 mice. I decided to investigate contribution of this expanded resMΦ population to the phenotype of resistant C57BL/6 and susceptible BALB/c mice during *L. sigmodontis* infection. As a result I have discovered that expansion of the resMΦ population in the resistant C57BL/6 strain is a result of both local proliferation and integration of BMDMΦ. Importantly, integration of BMDMΦ also occurs under homeostatic conditions demonstrating that the resident cells of the pleural cavity are not independent of the bone marrow. Furthermore, resMΦ depletion during *L. sigmodontis* infection was supportive of a proactive role for $F4/80^{hi}$ MΦ in worm killing. Given the enrichment of MΦ and B cells, which are capable of secreting antigen-specific IgM, in resistant C57BL/6 mice compared to BALB/c, I hypothesise that a MΦ-antibody mechanism of worm killing is at play within this strain. Future work in the lab might investigate the interaction of these immune players in the formation of granulomas around adult worms. In contrast, I have found that susceptibility in the BALB/c mice was marked by a deficit

in F4/80$^{hi}$ resMΦ expansion and an influx of BMDMΦ. Depletion experiments strongly suggested a detrimental role for BMDMΦ in killing of *L. sigmodontis* worms. The mechanism through which BMDMΦ exert their immunosuppressive functions remains elusive, though it is likely that expression of PD-L2 by monocytes is one potential mechanism. Given the association of F4/80hi MΦ with the resistant phenotype, I propose that encouraging successful integration of BMDMΦ into the resident niche in susceptible BALB/c mice may enhance their resistance. This could potentially be achieved through breeding BALB/c mice on a Vitamin A supplemented diet or through direct administration of retinoic acid, both of which should promote conversion of BMDMΦ into resMΦ through GATA6 induction. To surmise, I have uncovered a previously unappreciated difference in the dynamics of the MΦ compartment of C57BL/6 and BALB/c mice, which reflects their ability to mount a protective immune response against *L. sigmodontis*. I predict that further study of these diverse MΦ dynamics will reveal novel mechanisms of MΦ-mediated worm killing.

## 6.1 Future directions

The findings presented in this thesis have highlighted the distinct differences in the dynamics of pleural macrophages compartment between C57BL/6 and BALB/c mice both in the naïve situation and during *L. sigmodontis* infection. Furthermore, the results from chapter 3 have highlighted the potential impact of diverse Mϕ compartments upon worm killing. The experiments listed below would enable further elucidation of the role of Mϕ in resistance and susceptibility during *L. sigmodontis* infection.

**Hypothesis 1:** Recently recruited BMDMϕ are detrimental to worm killing in BALB/c mice through the induction of a hyporesponsive T cell phenotype. **Experiment 1**: Infection of WT and CCR2$^{-/-}$ BALB/c mice with *L. sigmodontis* and assessment of worm burden, Mϕ activation and T cell phenotype at day 35 and 50 pi.

**Hypothesis 2:** Expression of PD-L2 by recently recruited AABMDMϕ is responsible for the hyporesponsive T cell phenotype which underpins susceptibility in the BALB/c strain. **Experiment 2**: Generation of bone marrow chimeric mice, in

which CCR2$^{-/-}$ hosts would receive total irradiation, followed by engraftment with bone marrow from CCR2$^{-/-}$ and PDL-2$^{-/-}$ donors at a ratio of 80:20. The reconstituted hosts would then be infected with *L. sigmodontis* for 35 and 50 days at which time points worm burden, Mϕ activation and T cell phenotype would be assessed.

**Hypothesis 3:** Maintenance of a resMϕ population in the susceptible BALB/c strain would promote resistance. **Experiment 3**: Breed susceptible BALB/c mice on a high fat diet, which will provide an excess of retinoic acid, the driver of the tissue specific transcription factor GATA6.The mice on the high fat diet would then be infected with *L. sigmodontis* for 50 days, at which time point worm recovery, macrophage activation and T cell phenotype would be assessed.

**Hypothesis 4:** *L. sigmodontis* infection of resistance C57BL/6 mice deficient in resident macrophages and monocyte recruitment would result in enhanced susceptibility. **Experiment 4:** *L. sigmodontis* infection of GATA6$^{-/-}$CCR2$^{-/-}$ mice on the C57BL/6 background for 35 and 50 days, potentially also 55/60 days to determine if microfilariae ensues. At these endpoints, worm burden, macrophage activation and T cell phenotype would be characterised.

**Hypothesis 5**: Secretory IgM collaborates with resMϕ to trap and kill *L. sigmodontis* worms. **Experiment 5:** Infection of secIgM deficient mice with *L. sigmodontis* and analysis of worm burden at day 35 and 50 post infection. **Experiment 6** Detailed histological analysis of granulomas isolated from WT and SecIgM deficient mice on day 35/50 post infection.

# Chapter 7 Materials and methods

## 7.1 Mice

### 7.1.1 Source and housing

WT CD45.1$^{+/+}$ / CD45.2$^{+/+}$ C57BL/6 and BALB/c, C3$^{-/-}$ and PD-L2$^{-/-}$ mice were bred in house and maintained in specific pathogen free (SPF) facility at the University of Edinburgh. All animals were aged 6-8 weeks at the beginning of the experiment and due to sex differences in susceptibility to *L. sigmodontis* infection only female mice were used. Prof. Ludger Klein at the Ludwig-Maximiliansi-Universitat-Munchen kindly gifted us the CD45.1$^{+/+}$ BALB/c mice. The Ccr2$^{-/-}$ mice were kindly provided by Dr. Stephen Jenkins from the Queens Medical Research Institute at the University of Edinburgh and originally sourced from Jackson Laboratories (Ccr2$^{tm1Ifc}$). Complement component C3 deficient mice (C3$^{-/-}$) mice were kindly provided by Professor Marina Botto at Imperial College London. Mice deficient in PD-L2 were kindly gifted by Prof. Arlene Sharpe at Harvard University.

### 7.1.2 Genotyping of C3$^{-/-}$ mice

The C3$^{-/-}$ mice were generated from heterozygote C3$^{-/+}$ breeding pairs; this enabled the comparison of C3$^{-/-}$ mice with their WT control littermates. Ear snips were digested to isolate DNA using the SIGMA-ALDRICH RED Extract-N-Amp tissue PCR kit. A PCR reaction to amplify up the gene of interest was set up using the isolated DNA and the following primers:

| | |
|---|---|
| mC3/2371 | ACC CAG CTC TGT GGG AAG TG |
| mC3/2225- | CTT CAT AGA CTG CTG CAA CCA |
| C3/C4 NEO 1 | AAG GGA CTG GCT GCT ATT GG |

The PCR reaction was subsequently run on a 2 % agarose gel to identify homozygotes, heterozygotes or WT pups. The homozygote is identified by the presence of a single band of 1100 base pairs, the WT by a band at 920 base pairs and the heterozygote presents with a bands at 1100 and 920 base pairs.

### 7.1.3 Generation of partial bone marrow chimeric mice

40 female CD45.1$^{+/+}$ mice were anesthetised using Dormitor and Vetalar (80 µl/ 10 g body weight; 1ml Dormitor, 0.78 ml Vetalar in 8.24 ml $dH_2O$) intraperitoneally, in groups of 5. Once successfully anesthetised, the 5 mice were placed in bubble wrap (to maintain body temperature) on a Perspex tray over a 2 inch lead shield; the upper body was protected by the lead shield and the lower limbs exposed. The shelf holding the lead block, Perspex tray and mice was then placed into the irradiator. The irradiator has a cesium$^{137}$ source and the length of irradiation was calculated based on the rate of decay to ensure delivery of 9.5 Gy γ- irradiation. Once the period of irradiation was complete the mice were given an anti-anaesthetic (Antisedan 100 µl) into the scruff. The animals were kept in a heat box until they had fully recovered from the aesthetic and given an antibiotic for four weeks to avoid infection (Baytril in water). 24 hours post radiation host CD45.1$^{+/+}$ mice received 4.55 X $10^6$ CD45.2$^{+/+}$ bone marrow cells in 200 µl PBS i.v.

### 7.1.4 Isolation and preparation of donor bone marrow

14-16 CD45.2$^{+/+}$ female mice were sacrificed via $CO_2$ . The femurs and tibiae were removed. A 27G needle was used to flush the marrow from the bones and aggregates were broken up using a 23G needle. Centrifugation (1,200 rpm for 5 minutes) yielded a red pellet containing erythrocytes and pluripotent cells. This pellet was suspended in 5 ml of Red Blood Cell Lysis Buffer (R7757 SIGMA) solution for 2 minutes to lyse unwanted erythrocytes. The solution was brought up to 50 ml and passed through a 100 µm strainer before centrifugation of the filtrate. This yielded a white pellet, which was suspended in 10 ml Dulbecco's Phosphate Buffered Saline (PBS) (SIGMA: D8537) and counted using a Nexcelom Bioscience Auto T4 Cellometer cell counter. The cells were finally passed through a 40 µm strainer, centrifuged once more and resuspended in sterile PBS at 20 - 25 X $10^6$ cells/ ml to yield 4-5 X$10^6$ cells/ 200 µl.

## 7.2 Infections

### 7.2.1 *Litomosoides sigmodontis*

*L. sigmodontis* infective stage 3 larvae (L3) were isolated from the *ornithonyssus bacoti* mite vector. Subsequently, 30 L3s were counted and suspended in 200 µl

RPMI (5% horse serum). The mice were then injected subcutaneously into the scruff using a 23G needle to ensure larval transmission.

### 7.2.2 In vivo infection with *Salmonella Typhimurium SL3261*

Mice were injected with *S.* Typhimurium SL3261 GFP ($1X10^6$ CFU/200 ul PBS) or PBS i.p. At 1, 3, 6 and 24 hours post infection the animals were culled via schedule 1 ($CO_2$). The PEC was isolated through washing the cavity with 9 ml of RPMI supplemented with 0.2% mouse sera and the cells were subsequently stained for flow cytometric analysis.

## 7.3 Administration of anti-CCR2 Mab

The anti-CCR2 Mab (MC-21) and control Rat IgG (MC-69) were kindly provided by Prof. Matthias Mack at the Mannheim University of Applied Sciences. 20 μg of MC-21 / Rat IgG was administered on a daily basis from day 31-34 post infection; the animals were subsequently sacrificed on day 35 or 50- post infection. A Rat IgG2B antibody from BioXcell (Clone; LTF2) was also used as a control prior to provision of MC-69. All antibodies were prepared under sterile conditions and administered intraperitoneally in 200 μl of PBS.

## 7.4 Clodronate liposome administration

Clodronate containing liposomes were sourced from clodronateliposomes.Org. C57BL/6 mice infected with *L. sigmodontis* were rendered temporarily unconscious through exposure to the inhalable anaesthetic isofluorane. The chest area was then sprayed with 70 % ethanol and shaved using a scalpel. 200 μl of clodronate liposomes or PBS was subsequently injected into the pleural space. The injection was carried out with a 23G needle which had been bent ~0.5mm below the bevel to generate a needle containing a 90° angle. This angled needle enabled the exploration of the exposed chest area until the needle gently slipped between the ribs. The short bend prevented over insertion of the needle into the cavity. The mice quickly regained consciousness and were monitored while they recovered.

## 7.5 Tissue processing

### 7.5.1 Isolation of tissues

Isolation of the pleural exudate cells (PLEC) and worms residing in the pleural cavity was achieved through washing the pleural cavity with 10 ml (2ml and 8ml washes) complete Roswell Park Memorial Institute (RPMI) media containing 1 % penicillin-Streptomycin (ThermoFisher Cat#; 15140122) and 1 % L-Glutamine (ThermoFisher Cat #; 25030081). The parathymic lymph nodes were also isolated and placed in RMPI (1% PS, 1% LG). Under sterile conditions the lymph nodes were crushed between two pieces of gauze in a mini-petri dish and collected in 7 ml media. The lymph node suspension was centrifuged and suspended at 20 X $10^6$ cells/ ml.

### 7.5.2 Worm recovery

Worms were recovered through passing the 10 ml of PLEC wash through a 40 μm strainer placed in a 6 well plate, keeping the 2ml and 8ml washes separate. The worms and any granuloma material captured in the strainer were stored in RPMI and either analysed immediately or stored at 4°C for a maximum of 48 hours. The parasite counts and morphological analysis of *L. sigmodontis* worms, presented in this thesis, were carried out by Alison Fulton, the life cycle manager within our lab. Granuloma were identified as any solid tissue material isolated from the PLEC wash, either containing worm debris or not. Worms and granuloma isolated on day 12 p.i. were fixed in 4 % formalin, whereas those isolated on day 28, 35 and 50 p.i. were fixed in 70 % warm ethanol. The fixed worms and granuloma were counted using a Leica DM2000 microscope and Leica MZ9.5 software package. For measurement and sex identification, the worms were placed individually on a glass slide in a drop of 40 % glycerol. Worms isolated on day 11 and 28 post infection are photographed at X 20 magnification and a magnification of X 6.3 is used to photograph day 35 and day 50 worms. Furthermore, the presence of the buccal cavity was used to distinguish L4 from L3 larvae. Using the X 60 magnification lens, female worms are identified through the presence of vulva and male through the identification of the spematheaca. Mature male worms possess a characteristic coiled tail. The recovery rate was calculated as: (number of recovered worms/ number of larvae used for infection) X 100.

### 7.5.3 Isolation of the pleural exudate cells

Once filtered through a cell strainer to isolate the worms, the first 2 ml of PLEC wash was collected, centrifuged and the supernatant was retained for analysis by enzyme-linked immunosorbent assay (ELISA). The remaining 8 ml was filtered and the PLEC was combined with the pellet of the first 2 ml before an additional centrifugation step. The pellet was then lysed in 2 ml Red Blood Cell Lysis Buffer if necessary or suspended in 5 ml RPMI (1% PS, 1% LG) and counted using the Nexcelom cell counter. The pellet was suspended at 5 X $10^6$ cells/ ml and 200 µl was used for flow cytometric staining.

### 7.5.4 Restimulation of lymph node and pleural cells

Lymph node cells (1-2 X $10^6$/ 100ul) were placed in a round bottomed 96 well plate and stimulated with phorbol 12-myristate 13 acetate (PMA, Sigma-Aldrich; P8139, 0.5 µg/ml) and Ionomycin (Sigma-Aldrich, 1 µg/ml) for 2 hours and subsequently treated with a Brefeldin A (Sigma-Aldrich , 10 µg/ml) for an additional 2 hours. The plate was subsequently centrifuged, the supernatant discarded and the pellet stained for analysis via multiparameter flow cytometry.

### 7.5.5 Flow cytometry staining

Pleural cells (5 X $10^5$/ 1 X $10^6$/ 100/200 µl) were suspended in RPMI (1% PS, 1% LG) were placed in 96 well round bottomed plate and centrifuged. The pellet was re-suspended (briefly run plate over vortexor) and 180 µl of PBS was added to each well, the plate was then centrifuged again (this is a wash). The cells were washed once more in PBS. The cells were re-suspended in 10 µl Aqua/Blue Live Dead Stain (life technologies, stock resuspended in 12.5 µl DMSO, 1:500 dilution of stock in PBS for working concentration, Cat #L34957/L23105) for 10 minutes. Unspecific binding was prevented by the addition of a block solution (10 µl) containing anti CD16/32 (1:100) and purified mouse sera (1:100) in FACS buffer (PBS supplemented with 2mM EDTA and 0.5% BSA) for 30min on ice. A 30 µl mix (see table) of surface stain antibodies were added to the wells for 30 minutes on ice. The samples were washed twice in FACS buffer and re-suspended in 50 µl of detection antibody (Streptavidin/anti rabbit) for 30min on ice. For cells that were only stained

for surface antigens, the plate was washed twice more in FACS buffer and the pellet suspended in 300 µl before acquiring on the LSR II.

For cells which were stained for intracellular antigen the plate was washed twice in FACS buffer after surface staining, suspended in 150 µl/ well of BD permeablization buffer (1 part fixative: 3 part dilution buffer, eBioScience, Foxp3/Transcription Factor Staining Buffer Set, Cat #: 00552300) and stored at 4°C over night. The following morning the plates were centrifuged and washed once with 1 X permeablization buffer (1:10 in $dH_2O$, eBioScience, Foxp3/Transcription Factor Staining Buffer Set, Cat # : 00552300). The intracellular antibodies were then added to the wells (20 µl) for 30 minutes at room temperature (RT). This was followed by two washes with 1 X permeablization buffer. Secondary antibodies were subsequently added to the wells for 45 minutes on ice. The plates were washed twice more with 1 X permeablization buffer and then once in FACS buffer, before suspension in 300 µl and acquisition on the LSR II ( BD Biosciences, USA) or in 100 µl for acquisition on the Canto II (BD Biosciences, USA) using BD FACS Diva software. Data was analysed using FlowJo software.

# Table 3 Complete List of antibodies used

| Laser | Antigen | Source | Catalogue number | Isotype | Clone | Dilution in 30 µl surface stain | Dilution in 20 µl intracellular stain | Dilution in 50µl detection stain |
|---|---|---|---|---|---|---|---|---|
| FITC | Ki67 | Miltenyi | 130-100-340 | Recombinant human IgG1 | REA183 | | 5 µl/sample | |
| | CD45.1 | BD Pharm | 553775 | Ms IgG2a, κ | A20 | 200 | | |
| | Zenon Rabbit IgG | Molecular Probes | Z25302 | X | X | | | 300 |
| | Streptavidin | BioLegend | 405201 | X | X | | | 300 |
| | TNFα | BioLegend | 506313 | Rat IgG1, κ | MP6-XT22 | | 240 | |
| | Gata3 | Miltenyi | 130-100-689 | Recombinant human IgG | REA174 | | 8 | |
| PE | TIM4 | BioLegend | 130005 | Rat IgG2a | RMT4-54 | 600 | | |
| | PD-L2 | eBioscience | 12-5986 | Rat IgG2a | TY25 | 200 | | |
| | Zenon Rabbit IgG | Molecular Probes | Z25355 | X | X | | | 300 |
| | Siglec F | BD Pharm | 552126 | Rat IgG2a, κ | E50-2440 | 80 | | |
| | IL-4 | BioLegend | 504104 | Rat IgG1, κ | 11B11 | 100 | | |
| | PD-1 | eBioscience | 12-9985-81 | Armenian hamster IgG | J43 | 100 | | |
| PerCP | MHC II | BioLegend | 107624 | Rat IgG2b, κ | M5/115.15.2 | 240 | | |
| | CD45.2 | Biolegend | 109286 | Ms IgG2a | 104 | 60 | | |
| | Gr1 | Biolegend | 108426 | Rat IgG2b, κ | RB6-8C5 | 80 | | |
| | CD4 | Biolegend | 100432 | Rat IgG2b, κ | GK1.5 | 200 | | |
| Pe-Cy7 | F4/80 | eBioSciences | 25-4801-82 | Rat IgG2a, κ | BM8 | 180 | | |
| | CD8 | Biolegend | 100722 | Rat IgG2a, κ | 53-6.7 | 200 | | |
| | IFNγ | BioLegend | 505826 | Rat IgG1, κ | XMG1.2 | 100 | | |
| APC | CD115 | BioLegend | 135510 | Rat IgG2a, κ | AFS98 | 60 | | |
| | IL-5 | BioLegend | 504306 | Rat IgG1, κ | TRFK5 | | 100 | |
| AF700 | CD45.2 | BioLegend | 109822 | Ms (SJL) IgG2a, κ | 104 | 200 | | |
| | MHC II | BioLegend | 107622 | Rat IgG2b, κ | M5/115.15.2 | 600 | | |
| | CD4 | BioLedgend | 100536 | Rat IgG2a, κ | RM4-5 | 100 | | |
| AF780 | CD11b | eBioSciences | 47-0112-82 | Rat IgG2a, κ | M1/70 | 480 | | |
| | Streptavidin | eBioSciences | 47431782 | X | X | | | 400 |
| | TCRβ | BioLedgend | 109220 | Armenian hamster IgG | H57-597 | 200 | | |
| BV421 | CD19 | BioLegend | 115538 | Rat IgG2a, κ | 6D5 | 180 | | |
| | Ly6G | BioLegend | 127627 | Rat IgG2a, κ | 1A8 | 180 | | |
| | SigF | BD Pharm | 562681 | Rat IgG2a | E50-2440 | 180 | | |
| PacBlue | TCRβ | BioLegend | 109226 | Armenian hamster IgG | H57-597 | 180 | | |
| | CD45.2 | BioLegend | 109820 | Ms IgG2a, κ | 104 | 80 | | |
| | MHC II | eBiosciences | 47-5321-82 | Rat IgG2b, κ | M5/115.15.2 | 300 | | |
| | CD4 | BioLegend | 100534 | Rat IgG2a, κ | RM4-5 | 200 | | |
| BV570 | Ly6C | BioLegend | 128029 | Rat IgG2c, κ | HK1.4 | 100 | | |
| BV605 | CD11c | BioLegend | 117334 | Armenian hamster IgG | N418 | 120 | | |
| BV711 | CD11b | BioLegend | 101241 | Rat IgG2b, κ | M1/70 | 1000 | | |
| Purified | Realmα | Peprotech | 500-P214 | Rab IgG | X | | 100 | |
| | GATA6 | Cell signalling technologies | 5851s | Rabbit IgG | D61E4 | | 240 | |
| Biotinylated | CD102 | BioLegend | 105604 | Rat IgG2a, κ | 3C4 (MIC2/4) | 100 | | |
| | CD45.1 | eBioSciences | 13-0453-85 | Ms IgG2a, κ | A20 | 200 | | |
| | Ly6C | BioLedgend | 128004 | Rat IgG2c, κ | HK1.4 | 80 | | |

**Table 4 Staining panels used for *L. sigmodontis* infection time course experiments**

| LSR II | Stain I | Stain II | Stain III |
|---|---|---|---|
| **FITC** | Relmα (Pur) | Ki67 | CD102 (Biotin) |
| **PE** | TIM4 | GATA6 (Pur) | PD-L2 |
| **PerCP** | MHC II | | |
| **Pe-Cy7** | F4/80 | | |
| **APC** | CD115 | | |
| **AF700** | CD45.2 | | |
| **AF780** | CD11b | | |
| **PacBlue** | CD19,Ly6G,SigF, TCRβ | | |
| **BV570** | Ly6C | | |
| **BV605** | CD11c | | |
| **Amycan** | Live Dead | | |

The pleural exudate cells were stained for analysis via multi-parameter flow cytometry using the above staining panels. Stain I and II were stained for surface antigens, permeabilized overnight, stained for intracellular antigens and incubated with respective secondary antibodies. Stain III was stained for surface antigens and subsequently incubated with a FITC conjugated anti-streptavidin detection antibody.

**Table 5 Staining panel used for *L. sigmodontis* infected partial bone marrow chimeric mice.**

| Machine | LSR II | | | Canto II |
|---|---|---|---|---|
| | Stain I | Stain II | Stain III | Blood stain |
| FITC | Relmα | Ki67 | CD45.1 | CD45.1 |
| PE | TIM4 | GATA6 | PD-L2 | Siglec F |
| PerCP | CD45.2 | CD45.2 | MHC II | Gr1 |
| Pe-Cy7 | F4/80 | | | CD11b |
| APC | CD115 | | | CD115 |
| AF700 | MHC II | | CD45.2 | |
| AF780 | CD45.1 (Bio) | | CD102 (Bio) | Ly6C (Bio) |
| PacBlue | CD19,Ly6G,SigF, TCRβ | | | CD45.2 |
| BV570 | Ly6C | | | |
| BV605 | CD11c | | | |
| BV711 | CD11b | | | |
| UV | Live Dead | | | |
| AmCyan | | | | Live dead |

The pleural exudate cells were stained for analysis via multi-parameter flow cytometry using the above staining panels. Stain I and II were stained for surface antigens, incubated with AF780 conjugated anti-streptavidin secondary antibody, permeabilized overnight, stained for intracellular antigens and incubated with respective secondary antibodies (FITC/PE – Anti-rabbit IgG). Stain III and the blood strain were stained for surface antigens and subsequently incubated with an AF780 conjugated anti-steptavidin detection antibody.

**Table 6 Staining panel used for analysis of $T_H2$ immune response**

| | Stain I | Stain II |
|---|---|---|
| **FITC** | Gata3 | Gata3 |
| **PE** | PD-1 | IL-4 |
| **PerCP** | CD45.2 | |
| **Pe-Cy7** | | IFNγ |
| **APC** | | IL-5 |
| **AF700** | | CD4 |
| **PacBlue** | CD4 | |
| **Amycan** | Live Dead | Live Dead |

The parathymic lymph nodes and pleural exudate cells were stained by Dr. Johanna Knipper to investigate the strength of the $T_H2$ immune response as measured by production of cytokines by $GATA3^+$ T cells. Stain I, cells were incubated with surface antigen antibodies only. Stain II cells were incubated with surface antigens, permeabilized and the stained for intracellular antigens.

### 7.5.6 Generation of MoMΦ and resMΦ

Mice were injected with thioglycollate (4%, 400µl) i.p and subsequently culled via schedule 1 ($CO_2$) on day 3. The peritoneal cavity was washed with 9 ml ice cold complete Roswell Park Memorial Institute media, supplemented with 0.2% mouse sera, to isolate the peritoneal exudate cells (PEC). ResMΦ were isolated from the peritoneal cavity of naive mice PEC from multiple naïve mice (9/pool) were pooled to create technical replicates.

### 7.5.7 Salmonella Typhimurium culture

Bacteria from frozen stock (500 µl) was defrosted, a small volume (~1 µl) was dispensed into 20 ml of LB broth and incubated at 37°C for 18 hrs at which point the

bacteria is assumed to be at a concentration of $500X10^6$ bacteria/ml. This o/n culture was then diluted to an MOI 1 ($8X10^6$ bacteria/ml) and MOI 5 ($4 X 10^7$ bacteria/ml).

### 7.5.8 Salmonella Typhimurium SL3261 infection of PEC.

Thioglycollate elicited and tissue resident cells were cultured separately or together at a concentration of $4X10^5$cells/100 µl/well and let settle for 2 hours. For co-culture experiments, C57BL/6 *Cd45.1* mice were thioglycollate injected and naïve C57BL/6 *Cd45.2* mice were a source of tissue resident cells. The cells were infected with a multiplicity of infection (MOI, 50 µl) of 0, 1 or 5 for 1 hour at 37˚C in 5% $CO_2$. Subsequently the samples were stimulated with RPMI (50ul, 1% L-glutamine, 5% foetal calf serum and 200 µg/ml) for 1, 24 or 48 hours. After this incubation period the supernatant (150 µl) was removed and the cells were stained for flow cytometry. Serial dilutions of the MOI was plated on lysogeny broth (LB) agar plates and incubated at 37˚C in 5% $CO_2$ for 24 hours. The resultant colonies were counted to confirm the infectious dose.

### 7.5.9 Statistical analysis

For all experiments in this thesis comparing naïve and infected C57BL/6 and BALB/c mice statistical significance was determined using a two way-ANOVA analysis. A two way ANOVA compares the differences of the mean between two groups (C57BL/6 and BALB/c) which are divided on two independent variables (naïve and infected). The data generated from the experiments presented here was in line with all six assumptions necessary to enable a two way- ANOVA analysis. For experiments in which only two sample sets were being compared (e.g. WT infected vs $CCR2^{-/-}$ infected) statistical significance was determined through use of a student's T test. The students t test enables the comparison of the mean of two groups with unknown variance and group size need not be equal.

# Chapter 8 Appendices

## 8.1 Appendix 1: Worm recovery rate and health throughout other experiments.

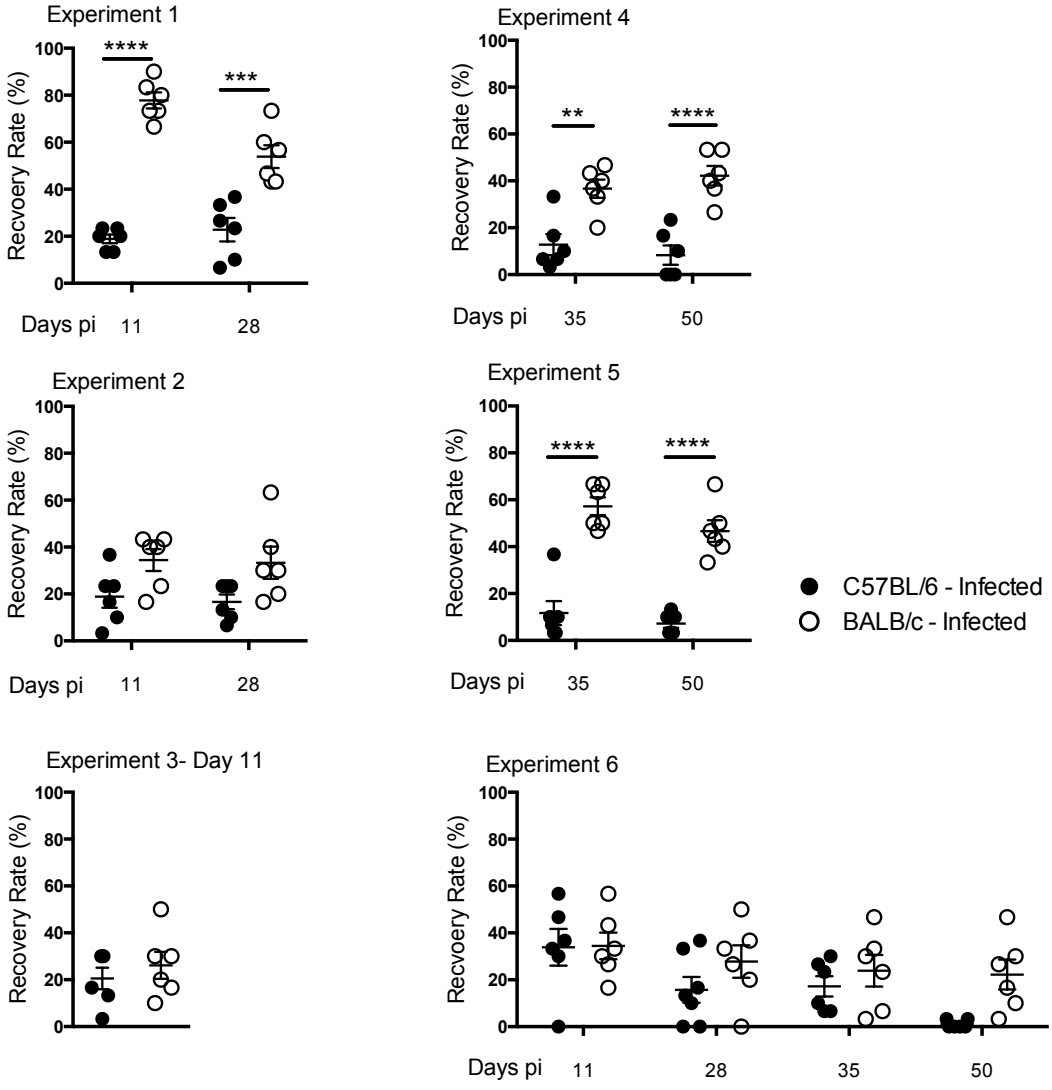


Experiments 2 and 5 were chosen as representative and combined for presentation in Chapter 2. Experiment 1 was excluded as the very high recovery rate was indicative of a higher infectious dose.

## 8.2 Appendix 2: Worm health at day 35 and 50 post infection - Experiment 4

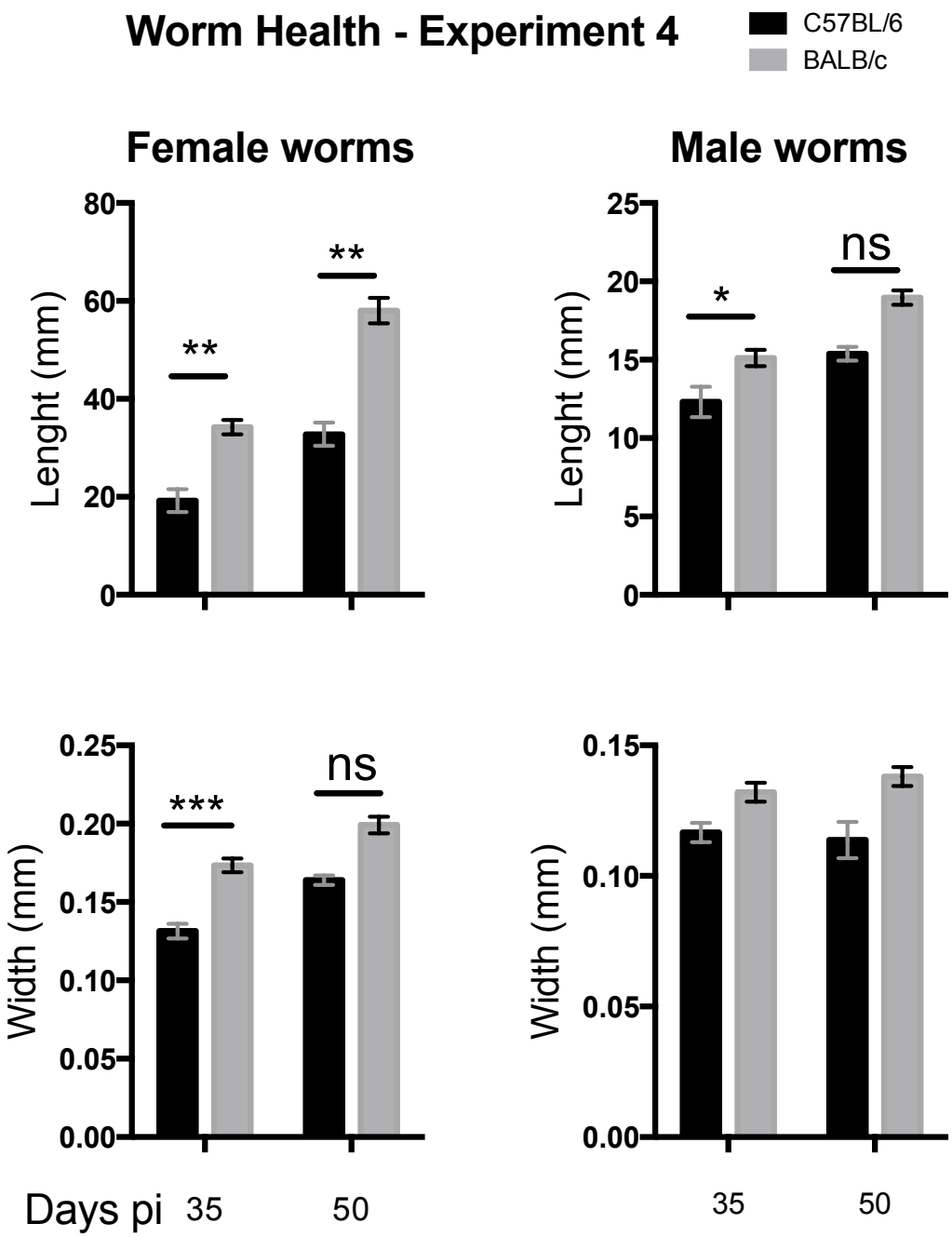

## 8.3 Appendix 3: Worm health at day 35 and 50 post infection – Experiment 6

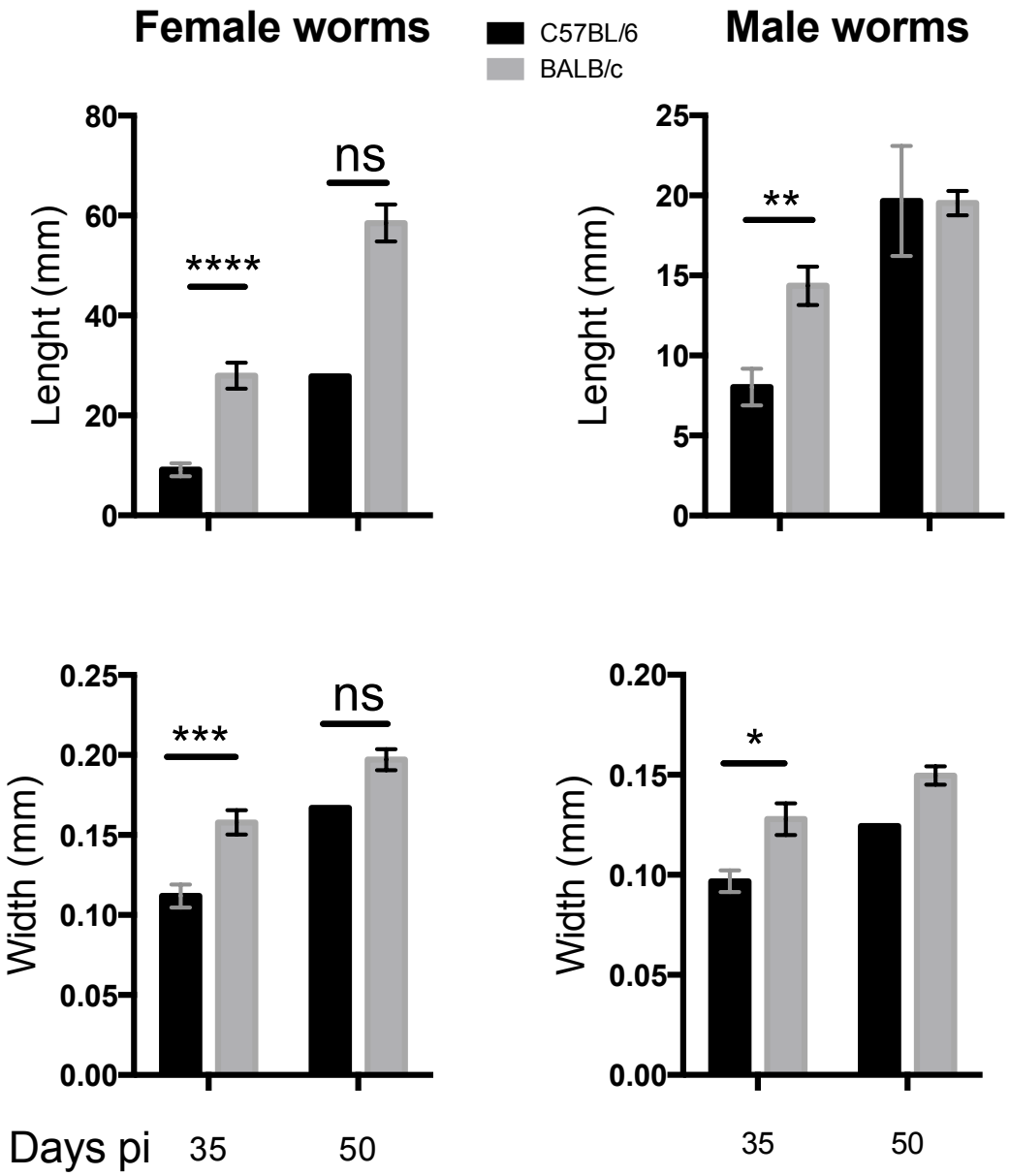

## 8.4 Appendix 4: Proliferation of F4/80$^{hi}$ MΦ throughout time course

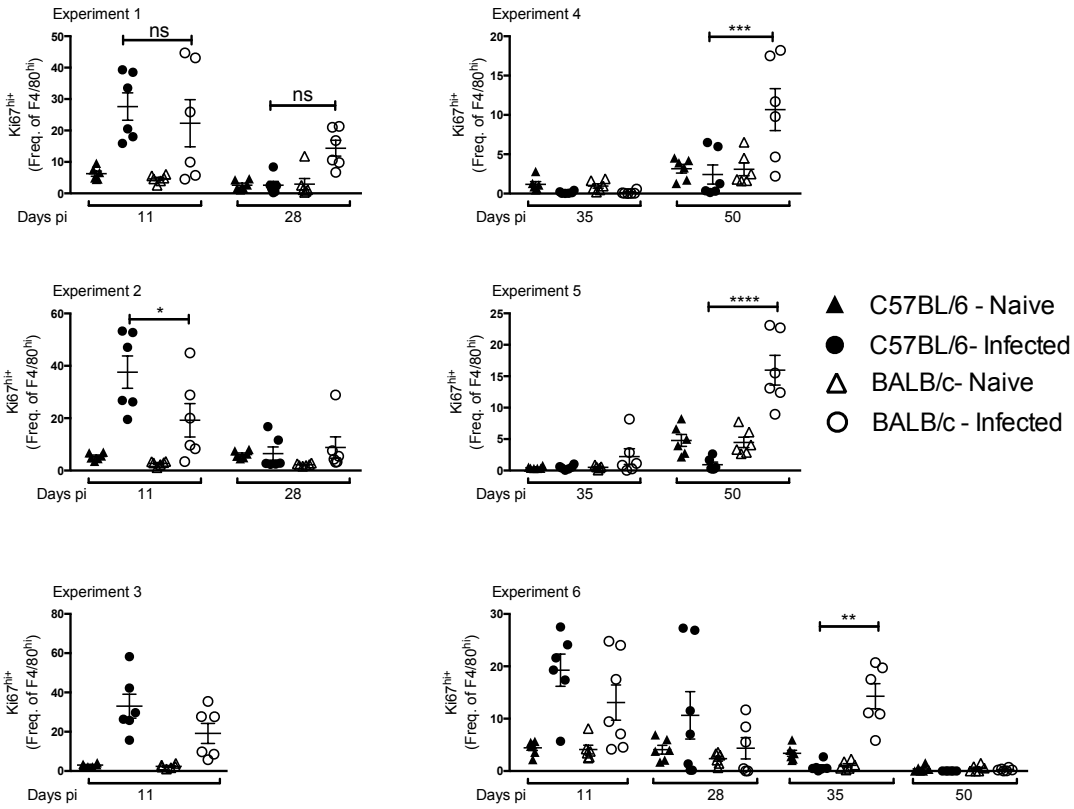


Combination of Ki67$^{hi}$ staining at day 11 pi from experiments 2, 3 and 6 are represented in Chapter 2. Experiment 1 was excluded due to an abnormal recovery rate. Of note is the increase in Ki67$^{hi}$ staining of the F4/80$^{hi}$ population in infected BALB/c mice at day 50 pi in experiment 4 and 5. This is reflective of the migration of bone marrow derived MoMΦ and monocytes into the F4/80$^{hi}$ gate rather than increased proliferation.

# Chapter 9 References

<AAMacs in intestinal helminth infection effects on concurrent bacterial colitis.pdf>.

local proliferation of macrophages in adipose tissue during obesity induced inflammation.


ABUTBUL, S., SHAPIRO, J., SZAINGURTEN-SOLODKIN, I., LEVY, N., CARMY, Y., BARON, R., JUNG, S. & MONSONEGO, A. 2012. TGF-beta signaling through SMAD2/3 induces the quiescent microglial phenotype within the CNS environment. *Glia,* 60**,** 1160-71.

AKIHO, H., BLENNERHASSETT, P., DENG, Y. & COLLINS, S. M. 2002. Role of IL-4, IL-13, and STAT6 in inflammation-induced hypercontractility of murine smooth muscle cells. *Am J Physiol Gastrointest Liver Physiol,* 282**,** G226-32.

AKIRA, S. 2011. Innate immunity and adjuvants. *Philos Trans R Soc Lond B Biol Sci,* 366**,** 2748-55.

AL-QAOUD, K. M., FLEISCHER, B. & HOERAUF, A. 1998. The Xid defect imparts susceptibility to experimental murine filariosis--association with a lack of antibody and IL-10 production by B cells in response to phosphorylcholine. *Int Immunol,* 10**,** 17-25.

AL-QAOUD, K. M., PEARLMAN, E., HARTUNG, T., KLUKOWSKI, J., FLEISCHER, B. & HOERAUF, A. 2000. A new mechanism for IL-5-dependent helminth control: neutrophil accumulation and neutrophil-mediated worm encapsulation in murine filariasis are abolished in the absence of IL-5. *Int Immunol,* 12**,** 899-908.

ALBINA, J. E., ABATE, J. A. & MASTROFRANCESCO, B. 1993. Role of ornithine as a proline precursor in healing wounds. *J Surg Res,* 55**,** 97-102.

ANGKASEKWINAI, P., PARK, H., WANG, Y. H., WANG, Y. H., CHANG, S. H., CORRY, D. B., LIU, Y. J., ZHU, Z. & DONG, C. 2007. Interleukin 25 promotes the initiation of proallergic type 2 responses. *J Exp Med,* 204**,** 1509-17.

ANTHONY, R. M., URBAN, J. F., JR., ALEM, F., HAMED, H. A., ROZO, C. T., BOUCHER, J. L., VAN ROOIJEN, N. & GAUSE, W. C. 2006. Memory T(H)2 cells induce alternatively activated macrophages to mediate protection against nematode parasites. *Nat Med,* 12**,** 955-60.

ARORA, M., CHEN, L., PAGLIA, M., GALLAGHER, I., ALLEN, J. E., VYAS, Y. M., RAY, A. & RAY, P. 2006. Simvastatin promotes Th2-type responses through the induction of the chitinase family member Ym1 in dendritic cells. *Proc Natl Acad Sci U S A,* 103**,** 7777-82.

ARTIS, D., WANG, M. L., KEILBAUGH, S. A., HE, W., BRENES, M., SWAIN, G. P., KNIGHT, P. A., DONALDSON, D. D., LAZAR, M. A., MILLER, H. R., SCHAD, G. A., SCOTT, P. & WU, G. D. 2004. RELMbeta/FIZZ2 is a goblet cell-specific immune-effector molecule in the gastrointestinal tract. *Proc Natl Acad Sci U S A,* 101**,** 13596-600.

ATTOUT, T., MARTIN, C., BABAYAN, S. A., KOZEK, W. J., BAZZOCCHI, C., OUDET, F., GALLAGHER, I. J., SPECHT, S. & BAIN, O. 2008. Pleural cellular reaction to the filarial infection Litomosoides sigmodontis is determined by the moulting process, the worm alteration, and the host strain. *Parasitol Int,* 57**,** 201-11.

AUFFRAY, C., FOGG, D., GARFA, M., ELAIN, G., JOIN-LAMBERT, O., KAYAL, S., SARNACKI, S., CUMANO, A., LAUVAU, G. & GEISSMANN, F. 2007. Monitoring of blood vessels and tissues by a population of monocytes with patrolling behavior. *Science,* 317**,** 666-70.

BABAYAN, S., UNGEHEUER, M. N., MARTIN, C., ATTOUT, T., BELNOUE, E., SNOUNOU, G., RENIA, L., KORENAGA, M. & BAIN, O. 2003. Resistance and susceptibility to filarial infection with Litomosoides sigmodontis are associated with early differences in parasite development and in localized immune reactions. *Infect Immun,* 71**,** 6820-9.

BAIN, C. C., BRAVO-BLAS, A., SCOTT, C. L., GOMEZ PERDIGUERO, E., GEISSMANN, F., HENRI, S., MALISSEN, B., OSBORNE, L. C., ARTIS, D. & MOWAT, A. M. 2014. Constant replenishment from circulating monocytes maintains the macrophage pool in the intestine of adult mice. *Nat Immunol,* 15**,** 929-37.

BAIN, C. C., HAWLEY, C. A., GARNER, H., SCOTT, C. L., SCHRIDDE, A., STEERS, N. J., MACK, M., JOSHI, A., GUILLIAMS, M., MOWAT, A. M., GEISSMANN, F. & JENKINS, S. J. 2016. Long-lived self-renewing bone marrow-derived macrophages displace embryo-derived cells to inhabit adult serous cavities. *Nat Commun,* 7**,** ncomms11852.

BAIN, C. C., SCOTT, C. L., URONEN-HANSSON, H., GUDJONSSON, S., JANSSON, O., GRIP, O., GUILLIAMS, M., MALISSEN, B., AGACE, W. W. & MOWAT, A. M. 2013. Resident and pro-inflammatory macrophages in the colon represent alternative context-dependent fates of the same Ly6Chi monocyte precursors. *Mucosal Immunol,* 6**,** 498-510.

BARTH, M. W., HENDRZAK, J. A., MELNICOFF, M. J. & MORAHAN, P. S. 1995. Review of the macrophage disappearance reaction. *J Leukoc Biol,* 57**,** 361-7.

BELTOWSKI, J. 2003. Adiponectin and resistin--new hormones of white adipose tissue. *Med Sci Monit,* 9**,** RA55-61.

BLAXTER, M. & KOUTSOVOULOS, G. 2015. The evolution of parasitism in Nematoda. *Parasitology,* 142 Suppl 1**,** S26-39.

BONNE-ANNEE, S., KEREPESI, L. A., HESS, J. A., O'CONNELL, A. E., LOK, J. B., NOLAN, T. J. & ABRAHAM, D. 2013. Human and mouse macrophages collaborate with neutrophils to kill larval Strongyloides stercoralis. *Infect Immun,* 81**,** 3346-55.

BRONTE, V. & ZANOVELLO, P. 2005. Regulation of immune responses by L-arginine metabolism. *Nat Rev Immunol,* 5**,** 641-54.

BROZ, P., OHLSON, M. B. & MONACK, D. M. 2012. Innate immune response to Salmonella typhimurium, a model enteric pathogen. *Gut Microbes,* 3**,** 62-70.

BUENO, S. M., WOZNIAK, A., LEIVA, E. D., RIQUELME, S. A., CARRENO, L. J., HARDT, W. D., RIEDEL, C. A. & KALERGIS, A. M. 2010. Salmonella pathogenicity island 1 differentially modulates bacterial entry to dendritic and non-phagocytic cells. *Immunology,* 130**,** 273-87.

BURTON, N. A., SCHURMANN, N., CASSE, O., STEEB, A. K., CLAUDI, B., ZANKL, J., SCHMIDT, A. & BUMANN, D. 2014. Disparate impact of oxidative host defenses determines the fate of Salmonella during systemic infection in mice. *Cell Host Microbe,* 15**,** 72-83.

BURYACHKOVSKAYA, L., SUMAROKOV, A. & LOMAKIN, N. 2013. Historical overview of studies on inflammation in Russia. *Inflamm Res,* 62**,** 441-50.

BUTOVSKY, O., JEDRYCHOWSKI, M. P., MOORE, C. S., CIALIC, R., LANSER, A. J., GABRIELY, G., KOEGLSPERGER, T., DAKE, B., WU, P. M., DOYKAN, C. E., FANEK, Z., LIU, L., CHEN, Z., ROTHSTEIN, J. D., RANSOHOFF, R. M., GYGI, S. P., ANTEL, J. P. & WEINER, H. L. 2014. Identification of a unique TGF-beta-dependent molecular and functional signature in microglia. *Nat Neurosci,* 17**,** 131-43.

CAI, Y., KUMAR, R. K., ZHOU, J., FOSTER, P. S. & WEBB, D. C. 2009. Ym1/2 promotes Th2 cytokine expression by inhibiting 12/15(S)-lipoxygenase: identification of a novel pathway for regulating allergic inflammation. *J Immunol,* 182**,** 5393-9.

CARLIN, L. M., STAMATIADES, E. G., AUFFRAY, C., HANNA, R. N., GLOVER, L., VIZCAY-BARRENA, G., HEDRICK, C. C., COOK, H. T., DIEBOLD, S. & GEISSMANN, F. 2013. Nr4a1-dependent Ly6C(low) monocytes monitor endothelial cells and orchestrate their disposal. *Cell,* 153**,** 362-75.

CARTER, T., SUMIYA, M., REILLY, K., AHMED, R., SOBIESZCZUK, P., SUMMERFIELD, J. A. & LAWRENCE, R. A. 2007. Mannose-binding lectin A-deficient mice have abrogated antigen-specific IgM responses and increased susceptibility to a nematode infection. *J Immunol,* 178**,** 5116-23.

CECCHINI, M. G., DOMINGUEZ, M. G., MOCCI, S., WETTERWALD, A., FELIX, R., FLEISCH, H., CHISHOLM, O., HOFSTETTER, W., POLLARD, J. W. & STANLEY, E. R. 1994. Role of colony stimulating factor-1 in the establishment and regulation of tissue macrophages during postnatal development of the mouse. *Development,* 120**,** 1357-72.

CHANG, N. C., HUNG, S. I., HWA, K. Y., KATO, I., CHEN, J. E., LIU, C. H. & CHANG, A. C. 2001. A macrophage protein, Ym1, transiently expressed during inflammation is a novel mammalian lectin. *J Biol Chem,* 276**,** 17497-506.

CLIFFE, L. J., HUMPHREYS, N. E., LANE, T. E., POTTEN, C. S., BOOTH, C. & GRENCIS, R. K. 2005. Accelerated intestinal epithelial cell turnover: a new mechanism of parasite expulsion. *Science,* 308**,** 1463-5.

COLLEY, D. G., SASSER, L. E. & REED, A. M. 2005. PD-L2+ dendritic cells and PD-1+ CD4+ T cells in schistosomiasis correlate with morbidity. *Parasite Immunol,* 27**,** 45-53.

COOK, P. C., JONES, L. H., JENKINS, S. J., WYNN, T. A., ALLEN, J. E. & MACDONALD, A. S. 2012. Alternatively activated dendritic cells regulate CD4+ T-cell polarization in vitro and in vivo. *Proc Natl Acad Sci U S A,* 109**,** 9977-82.

DAI, X. M., RYAN, G. R., HAPEL, A. J., DOMINGUEZ, M. G., RUSSELL, R. G., KAPP, S., SYLVESTRE, V. & STANLEY, E. R. 2002. Targeted disruption of the mouse colony-stimulating factor 1 receptor gene results in osteopetrosis, mononuclear phagocyte deficiency, increased primitive progenitor cell frequencies, and reproductive defects. *Blood,* 99**,** 111-20.

DAVIES, J. B. 1994. Sixty years of onchocerciasis vector control: a chronological summary with comments on eradication, reinvasion, and insecticide resistance. *Annu Rev Entomol,* 39**,** 23-45.

DAVIES, L. C., ROSAS, M., JENKINS, S. J., LIAO, C. T., SCURR, M. J., BROMBACHER, F., FRASER, D. J., ALLEN, J. E., JONES, S. A. & TAYLOR, P. R. 2013. Distinct bone marrow-derived and tissue-resident macrophage lineages proliferate at key stages during inflammation. *Nat Commun,* 4**,** 1886.

DAVIES, L. C., ROSAS, M., SMITH, P. J., FRASER, D. J., JONES, S. A. & TAYLOR, P. R. 2011. A quantifiable proliferative burst of tissue macrophages restores homeostatic macrophage populations after acute inflammation. *Eur J Immunol,* 41**,** 2155-64.

DE JONG, H. K., PARRY, C. M., VAN DER POLL, T. & WIERSINGA, W. J. 2012. Host-pathogen interaction in invasive Salmonellosis. *PLoS Pathog,* 8**,** e1002933.

DOYLE, A. G., HERBEIN, G., MONTANER, L. J., MINTY, A. J., CAPUT, D., FERRARA, P. & GORDON, S. 1994. Interleukin-13 alters the activation state of murine macrophages in vitro: comparison with interleukin-4 and interferon-gamma. *Eur J Immunol,* 24**,** 1441-5.

DRANOFF, G., CRAWFORD, A. D., SADELAIN, M., REAM, B., RASHID, A., BRONSON, R. T., DICKERSIN, G. R., BACHURSKI, C. J., MARK, E. L., WHITSETT, J. A. & ET AL. 1994. Involvement of granulocyte-macrophage colony-stimulating factor in pulmonary homeostasis. *Science,* 264**,** 713-6.

DRECKTRAH, D., KNODLER, L. A., IRELAND, R. & STEELE-MORTIMER, O. 2006. The mechanism of Salmonella entry determines the vacuolar environment and intracellular gene expression. *Traffic,* 7**,** 39-51.

EDWARDS, A. D., MANICKASINGHAM, S. P., SPORRI, R., DIEBOLD, S. S., SCHULZ, O., SHER, A., KAISHO, T., AKIRA, S. & REIS E SOUSA, C. 2002. Microbial recognition via Toll-like receptor-dependent and -independent pathways determines the cytokine response of murine dendritic cell subsets to CD40 triggering. *J Immunol,* 169**,** 3652-60.

ENSAN, S., LI, A., BESLA, R., DEGOUSEE, N., COSME, J., ROUFAIEL, M., SHIKATANI, E. A., EL-MAKLIZI, M., WILLIAMS, J. W., ROBINS, L., LI, C., LEWIS, B., YUN, T. J., LEE, J. S., WIEGHOFER, P., KHATTAR, R., FARROKHI, K., BYRNE, J., OUZOUNIAN, M., ZAVITZ, C. C., LEVY, G. A., BAUER, C. M., LIBBY, P., HUSAIN, M., SWIRSKI, F. K., CHEONG, C., PRINZ, M., HILGENDORF, I., RANDOLPH, G. J., EPELMAN, S., GRAMOLINI, A. O., CYBULSKY, M. I., RUBIN, B. B. & ROBBINS, C. S. 2016. Self-renewing resident arterial macrophages arise from embryonic CX3CR1(+) precursors and circulating monocytes immediately after birth. *Nat Immunol,* 17**,** 159-68.

EPELMAN, S., LAVINE, K. J., BEAUDIN, A. E., SOJKA, D. K., CARRERO, J. A., CALDERON, B., BRIJA, T., GAUTIER, E. L., IVANOV, S., SATPATHY, A. T., SCHILLING, J. D., SCHWENDENER, R., SERGIN, I., RAZANI, B., FORSBERG, E. C., YOKOYAMA, W. M., UNANUE, E. R., COLONNA, M., RANDOLPH, G. J. & MANN, D. L. 2014. Embryonic and adult-derived resident cardiac macrophages are maintained through distinct mechanisms at steady state and during inflammation. *Immunity,* 40**,** 91-104.

ERBLICH, B., ZHU, L., ETGEN, A. M., DOBRENIS, K. & POLLARD, J. W. 2011. Absence of colony stimulation factor-1 receptor results in loss of microglia, disrupted brain development and olfactory deficits. *PLoS One,* 6**,** e26317.

ESSER-VON BIEREN, J., MOSCONI, I., GUIET, R., PIERSGILLI, A., VOLPE, B., CHEN, F., GAUSE, W. C., SEITZ, A., VERBEEK, J. S. & HARRIS, N. L. 2013. Antibodies trap tissue migrating helminth larvae and prevent tissue damage by driving IL-4Ralpha-independent alternative differentiation of macrophages. *PLoS Pathog,* 9**,** e1003771.

EVANS, D. B., GELBAND, H. & VLASSOFF, C. 1993. Social and economic factors and the control of lymphatic filariasis: a review. *Acta Trop,* 53**,** 1-26.

FALLON, P. G., BALLANTYNE, S. J., MANGAN, N. E., BARLOW, J. L., DASVARMA, A., HEWETT, D. R., MCILGORM, A., JOLIN, H. E. & MCKENZIE, A. N. 2006. Identification of an interleukin (IL)-25-dependent cell population that provides IL-4, IL-5, and IL-13 at the onset of helminth expulsion. *J Exp Med,* 203**,** 1105-16.

FANG, F. C. 2004. Antimicrobial reactive oxygen and nitrogen species: concepts and controversies. *Nat Rev Microbiol,* 2**,** 820-32.

FEDORENKO, A., LISHKO, P. V. & KIRICHOK, Y. 2012. Mechanism of fatty-acid-dependent UCP1 uncoupling in brown fat mitochondria. *Cell,* 151**,** 400-13.

FLAHERTY, S. F., GOLENBOCK, D. T., MILHAM, F. H. & INGALLS, R. R. 1997. CD11/CD18 leukocyte integrins: new signaling receptors for bacterial endotoxin. *J Surg Res,* 73**,** 85-9.

FLORES-LANGARICA, A., MARSHALL, J. L., BOBAT, S., MOHR, E., HITCHCOCK, J., ROSS, E. A., COUGHLAN, R. E., KHAN, M., VAN ROOIJEN, N., HENDERSON, I. R., MACLENNAN, I. C. & CUNNINGHAM, A. F. 2011. T-zone localized monocyte-derived dendritic cells promote Th1 priming to Salmonella. *Eur J Immunol,* 41**,** 2654-65.

FOGG, D. K., SIBON, C., MILED, C., JUNG, S., AUCOUTURIER, P., LITTMAN, D. R., CUMANO, A. & GEISSMANN, F. 2006. A clonogenic bone marrow progenitor specific for macrophages and dendritic cells. *Science,* 311**,** 83-7.

GARNER, M. J., HAYWARD, R. D. & KORONAKIS, V. 2002. The Salmonella pathogenicity island 1 secretion system directs cellular cholesterol redistribution during mammalian cell entry and intracellular trafficking. *Cell Microbiol,* 4**,** 153-65.

GAUTIER, E. L., SHAY, T., MILLER, J., GRETER, M., JAKUBZICK, C., IVANOV, S., HELFT, J., CHOW, A., ELPEK, K. G., GORDONOV, S., MAZLOOM, A. R., MA'AYAN, A., CHUA, W. J., HANSEN, T. H., TURLEY, S. J., MERAD, M., RANDOLPH, G. J. & IMMUNOLOGICAL GENOME, C. 2012. Gene-expression profiles and transcriptional regulatory pathways that underlie the identity and diversity of mouse tissue macrophages. *Nat Immunol,* 13**,** 1118-28.

GHOSN, E. E., CASSADO, A. A., GOVONI, G. R., FUKUHARA, T., YANG, Y., MONACK, D. M., BORTOLUCI, K. R., ALMEIDA, S. R., HERZENBERG, L. A. & HERZENBERG, L. A. 2010. Two physically, functionally, and developmentally distinct peritoneal macrophage subsets. *Proc Natl Acad Sci U S A,* 107**,** 2568-73.

GIBBONS, M. A., MACKINNON, A. C., RAMACHANDRAN, P., DHALIWAL, K., DUFFIN, R., PHYTHIAN-ADAMS, A. T., VAN ROOIJEN, N., HASLETT, C., HOWIE, S. E., SIMPSON, A. J., HIRANI, N., GAULDIE, J., IREDALE, J. P., SETHI, T. & FORBES, S. J. 2011. Ly6Chi monocytes direct alternatively activated profibrotic macrophage regulation of lung fibrosis. *Am J Respir Crit Care Med,* 184**,** 569-81.

GINHOUX, F., GRETER, M., LEBOEUF, M., NANDI, S., SEE, P., GOKHAN, S., MEHLER, M. F., CONWAY, S. J., NG, L. G., STANLEY, E. R., SAMOKHVALOV, I. M. & MERAD, M. 2010. Fate mapping analysis reveals that adult microglia derive from primitive macrophages. *Science,* 330**,** 841-5.

GINHOUX, F. & GUILLIAMS, M. 2016. Tissue-Resident Macrophage Ontogeny and Homeostasis. *Immunity,* 44**,** 439-49.

GINHOUX, F. & JUNG, S. 2014. Monocytes and macrophages: developmental pathways and tissue homeostasis. *Nat Rev Immunol,* 14**,** 392-404.

GINHOUX, F., LIU, K., HELFT, J., BOGUNOVIC, M., GRETER, M., HASHIMOTO, D., PRICE, J., YIN, N., BROMBERG, J., LIRA, S. A., STANLEY, E. R., NUSSENZWEIG, M. & MERAD, M. 2009. The origin and development of nonlymphoid tissue CD103+ DCs. *J Exp Med,* 206**,** 3115-30.

GIRGIS, N. M., GUNDRA, U. M., WARD, L. N., CABRERA, M., FREVERT, U. & LOKE, P. 2014. Ly6C(high) monocytes become alternatively activated macrophages in schistosome granulomas with help from CD4+ cells. *PLoS Pathog,* 10**,** e1004080.

GOMEZ PERDIGUERO, E., KLAPPROTH, K., SCHULZ, C., BUSCH, K., AZZONI, E., CROZET, L., GARNER, H., TROUILLET, C., DE BRUIJN, M. F., GEISSMANN, F. & RODEWALD, H. R. 2015. Tissue-resident macrophages originate from yolk-sac-derived erythro-myeloid progenitors. *Nature,* 518**,** 547-51.

GRAHAM, A. L., TAYLOR, M. D., LE GOFF, L., LAMB, T. J., MAGENNIS, M. & ALLEN, J. E. 2005. Quantitative appraisal of murine filariasis confirms host strain differences but reveals that BALB/c females are more susceptible than males to Litomosoides sigmodontis. *Microbes Infect,* 7**,** 612-8.

GUNDRA, U. M., GIRGIS, N. M., RUCKERL, D., JENKINS, S., WARD, L. N., KURTZ, Z. D., WIENS, K. E., TANG, M. S., BASU-ROY, U., MANSUKHANI, A., ALLEN, J. E. & LOKE, P. 2014. Alternatively activated macrophages derived from monocytes and tissue macrophages are phenotypically and functionally distinct. *Blood*.

HAILMAN, E., LICHENSTEIN, H. S., WURFEL, M. M., MILLER, D. S., JOHNSON, D. A., KELLEY, M., BUSSE, L. A., ZUKOWSKI, M. M. & WRIGHT, S. D. 1994. Lipopolysaccharide (LPS)-binding protein accelerates the binding of LPS to CD14. *J Exp Med,* 179**,** 269-77.

HALDAR, M., KOHYAMA, M., SO, A. Y., KC, W., WU, X., BRISENO, C. G., SATPATHY, A. T., KRETZER, N. M., ARASE, H., RAJASEKARAN, N. S., WANG, L., EGAWA, T., IGARASHI, K., BALTIMORE, D., MURPHY, T. L. & MURPHY, K. M. 2014. Heme-mediated SPI-C induction promotes monocyte differentiation into iron-recycling macrophages. *Cell,* 156**,** 1223-34.

HASHIMOTO, D., CHOW, A., NOIZAT, C., TEO, P., BEASLEY, M. B., LEBOEUF, M., BECKER, C. D., SEE, P., PRICE, J., LUCAS, D., GRETER, M., MORTHA, A., BOYER, S. W., FORSBERG, E. C., TANAKA, M., VAN ROOIJEN, N., GARCÍA-SASTRE, A., STANLEY, E. R., GINHOUX, F., FRENETTE, P. S. & MERAD, M. 2013. Tissue-resident macrophages self-maintain locally throughout adult life with minimal contribution from circulating monocytes. *Immunity,* 38**,** 792-804.

HASHIMOTO, D., MILLER, J. & MERAD, M. 2011. Dendritic cell and macrophage heterogeneity in vivo. *Immunity,* 35**,** 323-35.

HASNAIN, S. Z., EVANS, C. M., ROY, M., GALLAGHER, A. L., KINDRACHUK, K. N., BARRON, L., DICKEY, B. F., WILSON, M. S., WYNN, T. A., GRENCIS, R. K. & THORNTON, D. J. 2011. Muc5ac: a critical component mediating the rejection of enteric nematodes. *J Exp Med,* 208**,** 893-900.

HERBERT, D. R., YANG, J. Q., HOGAN, S. P., GROSCHWITZ, K., KHODOUN, M., MUNITZ, A., OREKOV, T., PERKINS, C., WANG, Q., BROMBACHER, F., URBAN, J. F., JR., ROTHENBERG, M. E. & FINKELMAN, F. D. 2009. Intestinal epithelial cell secretion of RELM-beta protects against gastrointestinal worm infection. *J Exp Med,* 206**,** 2947-57.

HETTINGER, J., RICHARDS, D. M., HANSSON, J., BARRA, M. M., JOSCHKO, A. C., KRIJGSVELD, J. & FEUERER, M. 2013. Origin of monocytes and macrophages in a committed progenitor. *Nat Immunol,* 14**,** 821-30.

HOFFMANN, W., PETIT, G., SCHULZ-KEY, H., TAYLOR, D., BAIN, O. & LE GOFF, L. 2000. Litomosoides sigmodontis in mice: reappraisal of an old model for filarial research. *Parasitol Today,* 16**,** 387-9.

HOFFMANN, W. H., PFAFF, A. W., SCHULZ-KEY, H. & SOBOSLAY, P. T. 2001. Determinants for resistance and susceptibility to microfilaraemia in Litomosoides sigmodontis filariasis. *Parasitology,* 122**,** 641-9.

HOISETH, S. K. & STOCKER, B. A. 1981. Aromatic-dependent Salmonella typhimurium are non-virulent and effective as live vaccines. *Nature,* 291**,** 238-9.

HOLCOMB, I. N., KABAKOFF, R. C., CHAN, B., BAKER, T. W., GURNEY, A., HENZEL, W., NELSON, C., LOWMAN, H. B., WRIGHT, B. D., SKELTON, N. J., FRANTZ, G. D., TUMAS, D. B., PEALE, F. V., JR., SHELTON, D. L. & HEBERT, C. C. 2000. FIZZ1, a novel cysteine-rich secreted protein associated with pulmonary inflammation, defines a new gene family. *EMBO J,* 19**,** 4046-55.

HOLERS, V. M. 2014. Complement and its receptors: new insights into human disease. *Annu Rev Immunol,* 32**,** 433-59.

HUANG, S. C., EVERTS, B., IVANOVA, Y., O'SULLIVAN, D., NASCIMENTO, M., SMITH, A. M., BEATTY, W., LOVE-GREGORY, L., LAM, W. Y., O'NEILL, C. M., YAN, C., DU, H., ABUMRAD, N. A., URBAN, J. F., JR., ARTYOMOV, M. N., PEARCE, E. L. & PEARCE, E. J. 2014. Cell-intrinsic lysosomal lipolysis is essential for alternative activation of macrophages. *Nat Immunol,* 15**,** 846-55.

HUBER, S., HOFFMANN, R., MUSKENS, F. & VOEHRINGER, D. 2010. Alternatively activated macrophages inhibit T-cell proliferation by Stat6-dependent expression of PD-L2. *Blood,* 116**,** 3311-20.

HUGOT, J. P., CHAMAILLARD, M., ZOUALI, H., LESAGE, S., CEZARD, J. P., BELAICHE, J., ALMER, S., TYSK, C., O'MORAIN, C. A., GASSULL, M., BINDER, V., FINKEL, Y., CORTOT, A., MODIGLIANI, R., LAURENT-PUIG, P., GOWER-ROUSSEAU, C., MACRY, J., COLOMBEL, J. F., SAHBATOU, M. & THOMAS, G. 2001. Association of NOD2 leucine-rich repeat variants with susceptibility to Crohn's disease. *Nature,* 411**,** 599-603.

HUMPHREYS, N. E., XU, D., HEPWORTH, M. R., LIEW, F. Y. & GRENCIS, R. K. 2008. IL-33, a potent inducer of adaptive immunity to intestinal nematodes. *J Immunol,* 180**,** 2443-9.

IGARASHI, K. & KASHIWAGI, K. 2000. Polyamines: mysterious modulators of cellular functions. *Biochem Biophys Res Commun,* 271**,** 559-64.

INGALLS, R. R. & GOLENBOCK, D. T. 1995. CD11c/CD18, a transmembrane signaling receptor for lipopolysaccharide. *J Exp Med,* 181**,** 1473-9.

INOHARA, N., OGURA, Y., FONTALBA, A., GUTIERREZ, O., PONS, F., CRESPO, J., FUKASE, K., INAMURA, S., KUSUMOTO, S., HASHIMOTO, M., FOSTER, S. J., MORAN, A. P., FERNANDEZ-LUNA, J. L. & NUNEZ, G. 2003. Host recognition of bacterial muramyl dipeptide mediated through NOD2. Implications for Crohn's disease. *J Biol Chem,* 278**,** 5509-12.

ISCHIROPOULOS, H., ZHU, L. & BECKMAN, J. S. 1992. Peroxynitrite formation from macrophage-derived nitric oxide. *Arch Biochem Biophys,* 298**,** 446-51.

JACKSON-JONES, L. H., DUNCAN, S. M., MAGALHAES, M. S., CAMPBELL, S. M., MAIZELS, R. M., MCSORLEY, H. J., ALLEN, J. E. & BENEZECH, C. 2016. Fat-associated lymphoid clusters control local IgM secretion during pleural infection and lung inflammation. *Nat Commun,* 7**,** 12651.

JANEWAY, C. A., JR. 1989. Approaching the asymptote? Evolution and revolution in immunology. *Cold Spring Harb Symp Quant Biol,* 54 Pt 1**,** 1-13.

JENKINS, S. J. & ALLEN, J. E. 2010. Similarity and diversity in macrophage activation by nematodes, trematodes, and cestodes. *J Biomed Biotechnol,* 2010**,** 262609.

JENKINS, S. J., RUCKERL, D., COOK, P. C., JONES, L. H., FINKELMAN, F. D., VAN ROOIJEN, N., MACDONALD, A. S. & ALLEN, J. E. 2011. Local macrophage proliferation, rather than recruitment from the blood, is a signature of TH2 inflammation. *Science,* 332**,** 1284-8.

JENKINS, S. J., RUCKERL, D., THOMAS, G. D., HEWITSON, J. P., DUNCAN, S., BROMBACHER, F., MAIZELS, R. M., HUME, D. A. & ALLEN, J. E. 2013. IL-4 directly signals tissue-resident macrophages to proliferate beyond homeostatic levels controlled by CSF-1. *J Exp Med,* 210**,** 2477-91.

JUNG, S., ALIBERTI, J., GRAEMMEL, P., SUNSHINE, M. J., KREUTZBERG, G. W., SHER, A. & LITTMAN, D. R. 2000. Analysis of fractalkine receptor CX(3)CR1 function by targeted deletion and green fluorescent protein reporter gene insertion. *Mol Cell Biol,* 20**,** 4106-14.

KERSCHER, B., WILLMENT, J. A. & BROWN, G. D. 2013. The Dectin-2 family of C-type lectin-like receptors: an update. *Int Immunol,* 25**,** 271-7.

KNIPPER, J. A., WILLENBORG, S., BRINCKMANN, J., BLOCH, W., MAASS, T., WAGENER, R., KRIEG, T., SUTHERLAND, T., MUNITZ, A., ROTHENBERG, M. E., NIEHOFF, A., RICHARDSON, R., HAMMERSCHMIDT, M., ALLEN, J. E. & EMING, S. A. 2015. Interleukin-

4 Receptor alpha Signaling in Myeloid Cells Controls Collagen Fibril Assembly in Skin Repair. *Immunity,* 43**,** 803-16.

KOHYAMA, M., ISE, W., EDELSON, B. T., WILKER, P. R., HILDNER, K., MEJIA, C., FRAZIER, W. A., MURPHY, T. L. & MURPHY, K. M. 2009. Role for Spi-C in the development of red pulp macrophages and splenic iron homeostasis. *Nature,* 457**,** 318-21.

LAVIN, Y., WINTER, D., BLECHER-GONEN, R., DAVID, E., KEREN-SHAUL, H., MERAD, M., JUNG, S. & AMIT, I. 2014. Tissue-resident macrophage enhancer landscapes are shaped by the local microenvironment. *Cell,* 159**,** 1312-26.

LAWRENCE, R. A., ALLEN, J. E., OSBORNE, J. & MAIZELS, R. M. 1994. Adult and microfilarial stages of the filarial parasite Brugia malayi stimulate contrasting cytokine and Ig isotype responses in BALB/c mice. *J Immunol,* 153**,** 1216-24.

LE GOFF, L., LAMB, T. J., GRAHAM, A. L., HARCUS, Y. & ALLEN, J. E. 2002. IL-4 is required to prevent filarial nematode development in resistant but not susceptible strains of mice. *Int J Parasitol,* 32**,** 1277-84.

LE GOFF, L., LOKE, P., ALI, H. F., TAYLOR, D. W. & ALLEN, J. E. 2000. Interleukin-5 is essential for vaccine-mediated immunity but not innate resistance to a filarial parasite. *Infect Immun,* 68**,** 2513-7.

LIANG, L. & SHA, W. C. 2002. The right place at the right time: novel B7 family members regulate effector T cell responses. *Curr Opin Immunol,* 14**,** 384-90.

LICHANSKA, A. M. & HUME, D. A. 2000. Origins and functions of phagocytes in the embryo. *Exp Hematol,* 28**,** 601-11.

LIEN, E., MEANS, T. K., HEINE, H., YOSHIMURA, A., KUSUMOTO, S., FUKASE, K., FENTON, M. J., OIKAWA, M., QURESHI, N., MONKS, B., FINBERG, R. W., INGALLS, R. R. & GOLENBOCK, D. T. 2000. Toll-like receptor 4 imparts ligand-specific recognition of bacterial lipopolysaccharide. *J Clin Invest,* 105**,** 497-504.

LIU, K., VICTORA, G. D., SCHWICKERT, T. A., GUERMONPREZ, P., MEREDITH, M. M., YAO, K., CHU, F. F., RANDOLPH, G. J., RUDENSKY, A. Y. & NUSSENZWEIG, M. 2009. In vivo analysis of dendritic cell development and homeostasis. *Science,* 324**,** 392-7.

LIU, T., JIN, H., ULLENBRUCH, M., HU, B., HASHIMOTO, N., MOORE, B., MCKENZIE, A., LUKACS, N. W. & PHAN, S. H. 2004. Regulation of found in inflammatory zone 1 expression in bleomycin-induced lung fibrosis: role of IL-4/IL-13 and mediation via STAT-6. *J Immunol,* 173**,** 3425-31.

LOKE, P. & ALLISON, J. P. 2003. PD-L1 and PD-L2 are differentially regulated by Th1 and Th2 cells. *Proc Natl Acad Sci U S A,* 100**,** 5336-41.

LOKE, P., MACDONALD, A. S., ROBB, A., MAIZELS, R. M. & ALLEN, J. E. 2000. Alternatively activated macrophages induced by nematode infection inhibit proliferation via cell-to-cell contact. *Eur J Immunol,* 30**,** 2669-78.

LOKE, P., NAIR, M. G., PARKINSON, J., GUILIANO, D., BLAXTER, M. & ALLEN, J. E. 2002. IL-4 dependent alternatively-activated macrophages have a distinctive in vivo gene expression phenotype. *BMC Immunol,* 3**,** 7.

LOWELL, B. B. & SPIEGELMAN, B. M. 2000. Towards a molecular understanding of adaptive thermogenesis. *Nature,* 404**,** 652-60.

LUMENG, C. N., BODZIN, J. L. & SALTIEL, A. R. 2007. Obesity induces a phenotypic switch in adipose tissue macrophage polarization. *J Clin Invest,* 117**,** 175-84.

MACKANESS, G. B. 2014. Pillars article: cellular resistance to infection. J. Exp. Med. 1962. 116: 381-406. *J Immunol,* 193**,** 3185-221.

MARKS, S. C., JR. & LANE, P. W. 1976. Osteopetrosis, a new recessive skeletal mutation on chromosome 12 of the mouse. *J Hered,* 67**,** 11-18.

MARTIN, C., AL-QAOUD, K. M., UNGEHEUER, M. N., PAEHLE, K., VUONG, P. N., BAIN, O., FLEISCHER, B. & HOERAUF, A. 2000. IL-5 is essential for vaccine-induced protection and for resolution of primary infection in murine filariasis. *Med Microbiol Immunol,* 189**,** 67-74.

MARTIN, C., SAEFTEL, M., VUONG, P. N., BABAYAN, S., FISCHER, K., BAIN, O. & HOERAUF, A. 2001. B-cell deficiency suppresses vaccine-induced protection against murine filariasis but does not increase the recovery rate for primary infection. *Infect Immun,* 69**,** 7067-73.

MCDERMOTT, J. R., BARTRAM, R. E., KNIGHT, P. A., MILLER, H. R., GARROD, D. R. & GRENCIS, R. K. 2003. Mast cells disrupt epithelial barrier function during enteric nematode infection. *Proc Natl Acad Sci U S A,* 100**,** 7761-6.

MELNICOFF, M. J., HORAN, P. K., BRESLIN, E. W. & MORAHAN, P. S. 1988. Maintenance of peritoneal macrophages in the steady state. *J Leukoc Biol,* 44**,** 367-75.

MENDOZA, N., LI, A., GILL, A. & TYRING, S. 2009. Filariasis: diagnosis and treatment. *Dermatol Ther,* 22**,** 475-90.

MERAD, M., GINHOUX, F. & COLLIN, M. 2008. Origin, homeostasis and function of Langerhans cells and other langerin-expressing dendritic cells. *Nat Rev Immunol,* 8**,** 935-47.

MILLER, R. A. & BRITIGAN, B. E. 1997. Role of oxidants in microbial pathophysiology. *Clin Microbiol Rev,* 10**,** 1-18.

MIYANISHI, M., TADA, K., KOIKE, M., UCHIYAMA, Y., KITAMURA, T. & NAGATA, S. 2007. Identification of Tim4 as a phosphatidylserine receptor. *Nature,* 450**,** 435-9.

MOLAWI, K., WOLF, Y., KANDALLA, P. K., FAVRET, J., HAGEMEYER, N., FRENZEL, K., PINTO, A. R., KLAPPROTH, K., HENRI, S., MALISSEN, B., RODEWALD, H. R., ROSENTHAL, N. A., BAJENOFF, M., PRINZ, M., JUNG, S. & SIEWEKE, M. H. 2014. Progressive replacement of embryo-derived cardiac macrophages with age. *J Exp Med,* 211**,** 2151-8.

MORO, K., YAMADA, T., TANABE, M., TAKEUCHI, T., IKAWA, T., KAWAMOTO, H., FURUSAWA, J., OHTANI, M., FUJII, H. & KOYASU, S. 2010. Innate production of T(H)2 cytokines by adipose tissue-associated c-Kit(+)Sca-1(+) lymphoid cells. *Nature,* 463**,** 540-4.

MUNDER, M., EICHMANN, K. & MODOLELL, M. 1998. Alternative metabolic states in murine macrophages reflected by the nitric oxide synthase/arginase balance: competitive regulation by CD4+ T cells correlates with Th1/Th2 phenotype. *J Immunol,* 160**,** 5347-54.

MUNITZ, A., SEIDU, L., COLE, E. T., AHRENS, R., HOGAN, S. P. & ROTHENBERG, M. E. 2009. Resistin-like molecule alpha decreases glucose tolerance during intestinal inflammation. *J Immunol,* 182**,** 2357-63.

MURRAY, P. J., ALLEN, J. E., BISWAS, S. K., FISHER, E. A., GILROY, D. W., GOERDT, S., GORDON, S., HAMILTON, J. A., IVASHKIV, L. B., LAWRENCE, T., LOCATI, M., MANTOVANI, A., MARTINEZ, F. O., MEGE, J. L., MOSSER, D. M., NATOLI, G., SAEIJ, J. P., SCHULTZE, J. L., SHIREY, K. A., SICA, A., SUTTLES, J., UDALOVA, I., VAN GINDERACHTER, J. A., VOGEL, S. N. & WYNN, T. A. 2014. Macrophage activation and polarization: nomenclature and experimental guidelines. *Immunity,* 41**,** 14-20.

N, A. G., GUILLEN, J. A., GALLARDO, G., DIAZ, M., DE LA ROSA, J. V., HERNANDEZ, I. H., CASANOVA-ACEBES, M., LOPEZ, F., TABRAUE, C., BECEIRO, S., HONG, C., LARA, P. C., ANDUJAR, M., ARAI, S., MIYAZAKI, T., LI, S., CORBI, A. L., TONTONOZ, P., HIDALGO, A. & CASTRILLO, A. 2013. The nuclear receptor LXRalpha controls the functional specialization of splenic macrophages. *Nat Immunol,* 14**,** 831-9.

NAIK, S. H., SATHE, P., PARK, H. Y., METCALF, D., PROIETTO, A. I., DAKIC, A., CAROTTA, S., O'KEEFFE, M., BAHLO, M., PAPENFUSS, A., KWAK, J. Y., WU, L. & SHORTMAN, K. 2007. Development of plasmacytoid and conventional dendritic cell subtypes from single precursor cells derived in vitro and in vivo. *Nat Immunol,* 8**,** 1217-26.

NAIR, M. G., COCHRANE, D. W. & ALLEN, J. E. 2003. Macrophages in chronic type 2 inflammation have a novel phenotype characterized by the abundant expression of Ym1 and Fizz1 that can be partly replicated in vitro. *Immunol Lett,* 85**,** 173-80.

NAIR, M. G., DU, Y., PERRIGOUE, J. G., ZAPH, C., TAYLOR, J. J., GOLDSCHMIDT, M., SWAIN, G. P., YANCOPOULOS, G. D., VALENZUELA, D. M., MURPHY, A., KAROW, M., STEVENS, S., PEARCE, E. J. & ARTIS, D. 2009. Alternatively activated macrophage-derived RELM-{alpha} is a negative regulator of type 2 inflammation in the lung. *J Exp Med,* 206**,** 937-52.

NAITO, M., UMEDA, S., YAMAMOTO, T., MORIYAMA, H., UMEZU, H., HASEGAWA, G., USUDA, H., SHULTZ, L. D. & TAKAHASHI, K. 1996. Development, differentiation, and phenotypic heterogeneity of murine tissue macrophages. *J Leukoc Biol,* 59**,** 133-8.

NANCE, J. P., VANNELLA, K. M., WORTH, D., DAVID, C., CARTER, D., NOOR, S., HUBEAU, C., FITZ, L., LANE, T. E., WYNN, T. A. & WILSON, E. H. 2012. Chitinase dependent control of protozoan cyst burden in the brain. *PLoS Pathog,* 8**,** e1002990.

NASCIMENTO, M., HUANG, S. C., SMITH, A., EVERTS, B., LAM, W., BASSITY, E., GAUTIER, E. L., RANDOLPH, G. J. & PEARCE, E. J. 2014. Ly6Chi monocyte recruitment is responsible for Th2 associated host-protective macrophage accumulation in liver inflammation due to schistosomiasis. *PLoS Pathog,* 10**,** e1004282.

NEDERGAARD, J. & CANNON, B. 2013. UCP1 mRNA does not produce heat. *Biochim Biophys Acta,* 1831**,** 943-9.

NEILL, D. R., WONG, S. H., BELLOSI, A., FLYNN, R. J., DALY, M., LANGFORD, T. K., BUCKS, C., KANE, C. M., FALLON, P. G., PANNELL, R., JOLIN, H. E. & MCKENZIE, A. N. 2010. Nuocytes

represent a new innate effector leukocyte that mediates type-2 immunity. *Nature,* 464**,** 1367-70.

NGUYEN, K. D., QIU, Y., CUI, X., GOH, Y. P., MWANGI, J., DAVID, T., MUKUNDAN, L., BROMBACHER, F., LOCKSLEY, R. M. & CHAWLA, A. 2011. Alternatively activated macrophages produce catecholamines to sustain adaptive thermogenesis. *Nature,* 480**,** 104-8.

ODEGAARD, J. I., RICARDO-GONZALEZ, R. R., GOFORTH, M. H., MOREL, C. R., SUBRAMANIAN, V., MUKUNDAN, L., RED EAGLE, A., VATS, D., BROMBACHER, F., FERRANTE, A. W. & CHAWLA, A. 2007. Macrophage-specific PPARgamma controls alternative activation and improves insulin resistance. *Nature,* 447**,** 1116-20.

OKABE, Y. & MEDZHITOV, R. 2014. Tissue-Specific Signals Control Reversible Program of Localization and Functional Polarization of Macrophages. *Cell*.

ONAI, N., OBATA-ONAI, A., SCHMID, M. A., OHTEKI, T., JARROSSAY, D. & MANZ, M. G. 2007. Identification of clonogenic common Flt3+M-CSFR+ plasmacytoid and conventional dendritic cell progenitors in mouse bone marrow. *Nat Immunol,* 8**,** 1207-16.

ORKIN, S. H. & ZON, L. I. 2008. Hematopoiesis: an evolving paradigm for stem cell biology. *Cell,* 132**,** 631-44.

OSBORNE, L. C., JOYCE, K. L., ALENGHAT, T., SONNENBERG, G. F., GIACOMIN, P. R., DU, Y., BERGSTROM, K. S., VALLANCE, B. A. & NAIR, M. G. 2013. Resistin-like molecule alpha promotes pathogenic Th17 cell responses and bacterial-induced intestinal inflammation. *J Immunol,* 190**,** 2292-300.

PAOLICELLI, R. C., BOLASCO, G., PAGANI, F., MAGGI, L., SCIANNI, M., PANZANELLI, P., GIUSTETTO, M., FERREIRA, T. A., GUIDUCCI, E., DUMAS, L., RAGOZZINO, D. & GROSS, C. T. 2011. Synaptic pruning by microglia is necessary for normal brain development. *Science,* 333**,** 1456-8.

PARKHURST, C. N., YANG, G., NINAN, I., SAVAS, J. N., YATES, J. R., 3RD, LAFAILLE, J. J., HEMPSTEAD, B. L., LITTMAN, D. R. & GAN, W. B. 2013. Microglia promote learning-dependent synapse formation through brain-derived neurotrophic factor. *Cell,* 155**,** 1596-609.

PAULEAU, A. L. & MURRAY, P. J. 2003. Role of nod2 in the response of macrophages to toll-like receptor agonists. *Mol Cell Biol,* 23**,** 7531-9.

PEARCE, E. J. & MACDONALD, A. S. 2002. The immunobiology of schistosomiasis. *Nat Rev Immunol,* 2**,** 499-511.

PERRIGOUE, J. G., SAENZ, S. A., SIRACUSA, M. C., ALLENSPACH, E. J., TAYLOR, B. C., GIACOMIN, P. R., NAIR, M. G., DU, Y., ZAPH, C., VAN ROOIJEN, N., COMEAU, M. R., PEARCE, E. J., LAUFER, T. M. & ARTIS, D. 2009. MHC class II-dependent basophil-CD4+ T cell interactions promote T(H)2 cytokine-dependent immunity. *Nat Immunol,* 10**,** 697-705.

PESCE, J. T., RAMALINGAM, T. R., MENTINK-KANE, M. M., WILSON, M. S., EL KASMI, K. C., SMITH, A. M., THOMPSON, R. W., CHEEVER, A. W., MURRAY, P. J. & WYNN, T. A. 2009a. Arginase-1-expressing macrophages suppress Th2 cytokine-driven inflammation and fibrosis. *PLoS Pathog,* 5**,** e1000371.

PESCE, J. T., RAMALINGAM, T. R., WILSON, M. S., MENTINK-KANE, M. M., THOMPSON, R. W., CHEEVER, A. W., URBAN, J. F., JR. & WYNN, T.

A. 2009b. Retnla (relmalpha/fizz1) suppresses helminth-induced Th2-type immunity. *PLoS Pathog,* 5**,** e1000393.

PETIT, G., DIAGNE, M., MARECHAL, P., OWEN, D., TAYLOR, D. & BAIN, O. 1992. Maturation of the filaria Litomosoides sigmodontis in BALB/c mice; comparative susceptibility of nine other inbred strains. *Ann Parasitol Hum Comp,* 67**,** 144-50.

PHYTHIAN-ADAMS, A. T., COOK, P. C., LUNDIE, R. J., JONES, L. H., SMITH, K. A., BARR, T. A., HOCHWELLER, K., ANDERTON, S. M., HAMMERLING, G. J., MAIZELS, R. M. & MACDONALD, A. S. 2010. CD11c depletion severely disrupts Th2 induction and development in vivo. *J Exp Med,* 207**,** 2089-96.

POLLARD, J. W. 2009. Trophic macrophages in development and disease. *Nat Rev Immunol,* 9**,** 259-70.

POLTORAK, A., HE, X., SMIRNOVA, I., LIU, M. Y., VAN HUFFEL, C., DU, X., BIRDWELL, D., ALEJOS, E., SILVA, M., GALANOS, C., FREUDENBERG, M., RICCIARDI-CASTAGNOLI, P., LAYTON, B. & BEUTLER, B. 1998. Defective LPS signaling in C3H/HeJ and C57BL/10ScCr mice: mutations in Tlr4 gene. *Science,* 282**,** 2085-8.

PRICE, A. E., LIANG, H. E., SULLIVAN, B. M., REINHARDT, R. L., EISLEY, C. J., ERLE, D. J. & LOCKSLEY, R. M. 2010. Systemically dispersed innate IL-13-expressing cells in type 2 immunity. *Proc Natl Acad Sci U S A,* 107**,** 11489-94.

RAES, G., DE BAETSELIER, P., NOEL, W., BESCHIN, A., BROMBACHER, F. & HASSANZADEH GH, G. 2002. Differential expression of FIZZ1 and Ym1 in alternatively versus classically activated macrophages. *J Leukoc Biol,* 71**,** 597-602.

RAJAN, B., RAMALINGAM, T. & RAJAN, T. V. 2005. Critical role for IgM in host protection in experimental filarial infection. *J Immunol,* 175**,** 1827-33.

RAJAN, T. V., GANLEY, L., PACIORKOWSKI, N., SPENCER, L., KLEI, T. R. & SHULTZ, L. D. 2002. Brugian infections in the peritoneal cavities of laboratory mice: kinetics of infection and cellular responses. *Exp Parasitol,* 100**,** 235-47.

RAO, S., LOBOV, I. B., VALLANCE, J. E., TSUJIKAWA, K., SHIOJIMA, I., AKUNURU, S., WALSH, K., BENJAMIN, L. E. & LANG, R. A. 2007. Obligatory participation of macrophages in an angiopoietin 2-mediated cell death switch. *Development,* 134**,** 4449-58.

RIMOLDI, M., CHIEPPA, M., SALUCCI, V., AVOGADRI, F., SONZOGNI, A., SAMPIETRO, G. M., NESPOLI, A., VIALE, G., ALLAVENA, P. & RESCIGNO, M. 2005. Intestinal immune homeostasis is regulated by the crosstalk between epithelial cells and dendritic cells. *Nat Immunol,* 6**,** 507-14.

RODRIGUEZ, P. C., QUICENO, D. G. & OCHOA, A. C. 2007. L-arginine availability regulates T-lymphocyte cell-cycle progression. *Blood,* 109**,** 1568-73.

ROSAS, M., DAVIES, L. C., GILES, P. J., LIAO, C. T., KHARFAN, B., STONE, T. C., O'DONNELL, V. B., FRASER, D. J., JONES, S. A. & TAYLOR, P. R. 2014. The transcription factor gata6 links tissue macrophage phenotype and proliferative renewal. *Science,* 344**,** 645-8.

RUCKERL, D. & ALLEN, J. E. 2014. Macrophage proliferation, provenance, and plasticity in macroparasite infection. *Immunol Rev,* 262**,** 113-33.

RYAN, G. B. & SPECTOR, W. G. 1970. Macrophage turnover in inflamed connective tissue. *Proc R Soc Lond B Biol Sci,* 174**,** 269-92.

SAEFTEL, M., ARNDT, M., SPECHT, S., VOLKMANN, L. & HOERAUF, A. 2003. Synergism of gamma interferon and interleukin-5 in the control of murine filariasis. *Infect Immun,* 71**,** 6978-85.

SAEFTEL, M., VOLKMANN, L., KORTEN, S., BRATTIG, N., AL-QAOUD, K., FLEISCHER, B. & HOERAUF, A. 2001. Lack of interferon-gamma confers impaired neutrophil granulocyte function and imparts prolonged survival of adult filarial worms in murine filariasis. *Microbes Infect,* 3**,** 203-13.

SAMUEL D.WRIGHT, S. M. L., MICHELLE T.C.JONG, ZAVE CHAD,* AND LYNDA G .KABBASHI 1989. CR3 (CD11b:CD18) expresses one binding site for Arg-Gly-Asp-containing peptides and a second site forbacterial lipopolysaccaride. *J. Exp. Med,* Vol. 169.

SANTOS, A. J., MEINECKE, M., FESSLER, M. B., HOLDEN, D. W. & BOUCROT, E. 2013. Preferential invasion of mitotic cells by Salmonella reveals that cell surface cholesterol is maximal during metaphase. *J Cell Sci,* 126**,** 2990-6.

SCHRAML, B. U. & REIS E SOUSA, C. 2015. Defining dendritic cells. *Curr Opin Immunol,* 32**,** 13-20.

SCHRAMM, G., FALCONE, F. H., GRONOW, A., HAISCH, K., MAMAT, U., DOENHOFF, M. J., OLIVEIRA, G., GALLE, J., DAHINDEN, C. A. & HAAS, H. 2003. Molecular characterization of an interleukin-4-inducing factor from Schistosoma mansoni eggs. *J Biol Chem,* 278**,** 18384-92.

SCHULZ, C., GOMEZ PERDIGUERO, E., CHORRO, L., SZABO-ROGERS, H., CAGNARD, N., KIERDORF, K., PRINZ, M., WU, B., JACOBSEN, S. E., POLLARD, J. W., FRAMPTON, J., LIU, K. J. & GEISSMANN, F. 2012. A lineage of myeloid cells independent of Myb and hematopoietic stem cells. *Science,* 336**,** 86-90.

SCOTT, C. L., ZHENG, F., DE BAETSELIER, P., MARTENS, L., SAEYS, Y., DE PRIJCK, S., LIPPENS, S., ABELS, C., SCHOONOOGHE, S., RAES, G., DEVOOGDT, N., LAMBRECHT, B. N., BESCHIN, A. & GUILLIAMS, M. 2016. Bone marrow-derived monocytes give rise to self-renewing and fully differentiated Kupffer cells. *Nat Commun,* 7**,** 10321.

SHENG, J., RUEDL, C. & KARJALAINEN, K. 2015. Most Tissue-Resident Macrophages Except Microglia Are Derived from Fetal Hematopoietic Stem Cells. *Immunity,* 43**,** 382-93.

SHIMAZU, R., AKASHI, S., OGATA, H., NAGAI, Y., FUKUDOME, K., MIYAKE, K. & KIMOTO, M. 1999. MD-2, a molecule that confers lipopolysaccharide responsiveness on Toll-like receptor 4. *J Exp Med,* 189**,** 1777-82.

SOLOVJOV, D. A., PLUSKOTA, E. & PLOW, E. F. 2005. Distinct roles for the alpha and beta subunits in the functions of integrin alphaMbeta2. *J Biol Chem,* 280**,** 1336-45.

SPECHT, S., TAYLOR, M. D., HOEVE, M. A., ALLEN, J. E., LANG, R. & HOERAUF, A. 2012. Over expression of IL-10 by macrophages overcomes resistance to murine filariasis. *Exp Parasitol,* 132**,** 90-6.

STEFATER, J. A., 3RD, LEWKOWICH, I., RAO, S., MARIGGI, G., CARPENTER, A. C., BURR, A. R., FAN, J., AJIMA, R., MOLKENTIN, J. D., WILLIAMS, B. O., WILLS-KARP, M., POLLARD, J. W., YAMAGUCHI, T., FERRARA, N., GERHARDT, H. & LANG, R. A. 2011. Regulation of angiogenesis by a non-canonical Wnt-Flt1 pathway in myeloid cells. *Nature,* 474**,** 511-5.

STEIN, M., KESHAV, S., HARRIS, N. & GORDON, S. 1992. Interleukin 4 potently enhances murine macrophage mannose receptor activity: a marker of alternative immunologic macrophage activation. *J Exp Med,* 176**,** 287-92.

SUN, C. M., HALL, J. A., BLANK, R. B., BOULADOUX, N., OUKKA, M., MORA, J. R. & BELKAID, Y. 2007. Small intestine lamina propria dendritic cells promote de novo generation of Foxp3 T reg cells via retinoic acid. *J Exp Med,* 204**,** 1775-85.

SUTHERLAND, T. E., ANDERSEN, O. A., BETOU, M., EGGLESTON, I. M., MAIZELS, R. M., VAN AALTEN, D. & ALLEN, J. E. 2011. Analyzing airway inflammation with chemical biology: dissection of acidic mammalian chitinase function with a selective drug-like inhibitor. *Chem Biol,* 18**,** 569-79.

SUTHERLAND, T. E., LOGAN, N., RUCKERL, D., HUMBLES, A. A., ALLAN, S. M., PAPAYANNOPOULOS, V., STOCKINGER, B., MAIZELS, R. M. & ALLEN, J. E. 2014. Chitinase-like proteins promote IL-17-mediated neutrophilia in a tradeoff between nematode killing and host damage. *Nat Immunol,* 15**,** 1116-25.

TAMOUTOUNOUR, S., GUILLIAMS, M., MONTANANA SANCHIS, F., LIU, H., TERHORST, D., MALOSSE, C., POLLET, E., ARDOUIN, L., LUCHE, H., SANCHEZ, C., DALOD, M., MALISSEN, B. & HENRI, S. 2013. Origins and functional specialization of macrophages and of conventional and monocyte-derived dendritic cells in mouse skin. *Immunity,* 39**,** 925-38.

TAYLOR, B. C., ZAPH, C., TROY, A. E., DU, Y., GUILD, K. J., COMEAU, M. R. & ARTIS, D. 2009. TSLP regulates intestinal immunity and inflammation in mouse models of helminth infection and colitis. *J Exp Med,* 206**,** 655-67.

TAYLOR, M. D., HARRIS, A., BABAYAN, S. A., BAIN, O., CULSHAW, A., ALLEN, J. E. & MAIZELS, R. M. 2007. CTLA-4 and CD4+ CD25+ regulatory T cells inhibit protective immunity to filarial parasites in vivo. *J Immunol,* 179**,** 4626-34.

TAYLOR, M. D., HARRIS, A., NAIR, M. G., MAIZELS, R. M. & ALLEN, J. E. 2006. F4/80+ Alternatively Activated Macrophages Control CD4+ T Cell Hyporesponsiveness at Sites Peripheral to Filarial Infection. *The Journal of Immunology,* 176**,** 6918-6927.

TERRAZAS, L. I., MONTERO, D., TERRAZAS, C. A., REYES, J. L. & RODRIGUEZ-SOSA, M. 2005. Role of the programmed Death-1 pathway in the suppressive activity of alternatively activated macrophages in experimental cysticercosis. *Int J Parasitol,* 35**,** 1349-58.

THEURL, I., HILGENDORF, I., NAIRZ, M., TYMOSZUK, P., HASCHKA, D., ASSHOFF, M., HE, S., GERHARDT, L. M., HOLDERRIED, T. A., SEIFERT, M., SOPPER, S., FENN, A. M., ANZAI, A., RATTIK, S., MCALPINE, C., THEURL, M., WIEGHOFER, P., IWAMOTO, Y., WEBER, G. F., HARDER, N. K., CHOUSTERMAN, B. G., ARVEDSON, T. L., MCKEE, M., WANG, F., LUTZ, O. M., REZOAGLI, E., BABITT, J.

L., BERRA, L., PRINZ, M., NAHRENDORF, M., WEISS, G., WEISSLEDER, R., LIN, H. Y. & SWIRSKI, F. K. 2016. On-demand erythrocyte disposal and iron recycling requires transient macrophages in the liver. *Nat Med,* 22**,** 945-51.

THOMAS, G. D., RUCKERL, D., MASKREY, B. H., WHITFIELD, P. D., BLAXTER, M. L. & ALLEN, J. E. 2012. The biology of nematode- and IL4Ralpha-dependent murine macrophage polarization in vivo as defined by RNA-Seq and targeted lipidomics. *Blood,* 120**,** e93-e104.

TSOU, C. L., PETERS, W., SI, Y., SLAYMAKER, S., ASLANIAN, A. M., WEISBERG, S. P., MACK, M. & CHARO, I. F. 2007. Critical roles for CCR2 and MCP-3 in monocyte mobilization from bone marrow and recruitment to inflammatory sites. *J Clin Invest,* 117**,** 902-9.

UDERHARDT, S., HERRMANN, M., OSKOLKOVA, O. V., ASCHERMANN, S., BICKER, W., IPSEIZ, N., SARTER, K., FREY, B., ROTHE, T., VOLL, R., NIMMERJAHN, F., BOCHKOV, V. N., SCHETT, G. & KRONKE, G. 2012. 12/15-lipoxygenase orchestrates the clearance of apoptotic cells and maintains immunologic tolerance. *Immunity,* 36**,** 834-46.

VAN BRUGGEN, R., ZWEERS, D., VAN DIEPEN, A., VAN DISSEL, J. T., ROOS, D., VERHOEVEN, A. J. & KUIJPERS, T. W. 2007. Complement receptor 3 and Toll-like receptor 4 act sequentially in uptake and intracellular killing of unopsonized Salmonella enterica serovar Typhimurium by human neutrophils. *Infect Immun,* 75**,** 2655-60.

VAN DE LAAR, L., SAELENS, W., DE PRIJCK, S., MARTENS, L., SCOTT, C. L., VAN ISTERDAEL, G., HOFFMANN, E., BEYAERT, R., SAEYS, Y., LAMBRECHT, B. N. & GUILLIAMS, M. 2016. Yolk Sac Macrophages, Fetal Liver, and Adult Monocytes Can Colonize an Empty Niche and Develop into Functional Tissue-Resident Macrophages. *Immunity,* 44**,** 755-68.

VAN DER WERF, N., REDPATH, S. A., AZUMA, M., YAGITA, H. & TAYLOR, M. D. 2013. Th2 cell-intrinsic hypo-responsiveness determines susceptibility to helminth infection. *PLoS Pathog,* 9**,** e1003215.

VAN FURTH, R. & COHN, Z. A. 1968. The origin and kinetics of mononuclear phagocytes. *J Exp Med,* 128**,** 415-35.

VAN LIEMPT, E., VAN VLIET, S. J., ENGERING, A., GARCIA VALLEJO, J. J., BANK, C. M., SANCHEZ-HERNANDEZ, M., VAN KOOYK, Y. & VAN DIE, I. 2007. Schistosoma mansoni soluble egg antigens are internalized by human dendritic cells through multiple C-type lectins and suppress TLR-induced dendritic cell activation. *Mol Immunol,* 44**,** 2605-15.

VAN ROOIJEN, N., SANDERS, A. & VAN DEN BERG, T. K. 1996. Apoptosis of macrophages induced by liposome-mediated intracellular delivery of clodronate and propamidine. *J Immunol Methods,* 193**,** 93-9.

VAZQUEZ-TORRES, A. & FANG, F. C. 2000. Cellular routes of invasion by enteropathogens. *Curr Opin Microbiol,* 3**,** 54-9.

VAZQUEZ-TORRES, A., JONES-CARSON, J., BAUMLER, A. J., FALKOW, S., VALDIVIA, R., BROWN, W., LE, M., BERGGREN, R., PARKS, W. T. & FANG, F. C. 1999. Extraintestinal dissemination of Salmonella by CD18-expressing phagocytes. *Nature,* 401**,** 804-8.

VAZQUEZ-TORRES, A., XU, Y., JONES-CARSON, J., HOLDEN, D. W., LUCIA, S. M., DINAUER, M. C., MASTROENI, P. & FANG, F. C. 2000. Salmonella pathogenicity island 2-dependent evasion of the phagocyte NADPH oxidase. *Science,* 287**,** 1655-8.

VOLKMAN, A. 1970. The origin and fate of the monocyte. *Ser Haematol,* 3**,** 62-92.

VOLKMANN, L., SAEFTEL, M., BAIN, O., FISCHER, K., FLEISCHER, B. & HOERAUF, A. 2001. Interleukin-4 is essential for the control of microfilariae in murine infection with the filaria Litomosoides sigmodontis. *Infect Immun,* 69**,** 2950-6.

WANG, J. & KUBES, P. 2016. A Reservoir of Mature Cavity Macrophages that Can Rapidly Invade Visceral Organs to Affect Tissue Repair. *Cell,* 165**,** 668-78.

WEBB, D. C., MCKENZIE, A. N. & FOSTER, P. S. 2001. Expression of the Ym2 lectin-binding protein is dependent on interleukin (IL)-4 and IL-13 signal transduction: identification of a novel allergy-associated protein. *J Biol Chem,* 276**,** 41969-76.

WEISBERG, S. P., MCCANN, D., DESAI, M., ROSENBAUM, M., LEIBEL, R. L. & FERRANTE, A. W., JR. 2003. Obesity is associated with macrophage accumulation in adipose tissue. *J Clin Invest,* 112**,** 1796-808.

WELCH, J. S., ESCOUBET-LOZACH, L., SYKES, D. B., LIDDIARD, K., GREAVES, D. R. & GLASS, C. K. 2002. TH2 cytokines and allergic challenge induce Ym1 expression in macrophages by a STAT6-dependent mechanism. *J Biol Chem,* 277**,** 42821-9.

WIJNANDS, K. A., HOEKSEMA, M. A., MEESTERS, D. M., VAN DEN AKKER, N. M., MOLIN, D. G., BRIEDE, J. J., GHOSH, M., KOHLER, S. E., VAN ZANDVOORT, M. A., DE WINTHER, M. P., BUURMAN, W. A., LAMERS, W. H. & POEZE, M. 2014. Arginase-1 deficiency regulates arginine concentrations and NOS2-mediated NO production during endotoxemia. *PLoS One,* 9**,** e86135.

WRIGHT, S. D., RAMOS, R. A., TOBIAS, P. S., ULEVITCH, R. J. & MATHISON, J. C. 1990. CD14, a receptor for complexes of lipopolysaccharide (LPS) and LPS binding protein. *Science,* 249**,** 1431-3.

WU, D., MOLOFSKY, A. B., LIANG, H. E., RICARDO-GONZALEZ, R. R., JOUIHAN, H. A., BANDO, J. K., CHAWLA, A. & LOCKSLEY, R. M. 2011. Eosinophils sustain adipose alternatively activated macrophages associated with glucose homeostasis. *Science,* 332**,** 243-7.

WU, H., GOWER, R. M., WANG, H., PERRARD, X. Y., MA, R., BULLARD, D. C., BURNS, A. R., PAUL, A., SMITH, C. W., SIMON, S. I. & BALLANTYNE, C. M. 2009. Functional role of CD11c+ monocytes in atherogenesis associated with hypercholesterolemia. *Circulation,* 119**,** 2708-17.

WYNN, T. A. & BARRON, L. 2010. Macrophages: master regulators of inflammation and fibrosis. *Semin Liver Dis,* 30**,** 245-57.

XIE, H., BAIN, O. & WILLIAMS, S. A. 1994. Molecular phylogenetic studies on filarial parasites based on 5S ribosomal spacer sequences. *Parasite,* 1**,** 141-51.

YAMAJI-KEGAN, K., SU, Q., ANGELINI, D. J., MYERS, A. C., CHEADLE, C. & JOHNS, R. A. 2010. Hypoxia-induced mitogenic factor (HIMF/FIZZ1/RELMalpha) increases lung inflammation and activates

pulmonary microvascular endothelial cells via an IL-4-dependent mechanism. *J Immunol,* 185**,** 5539-48.

YANG, C. Y., CHEN, J. B., TSAI, T. F., TSAI, Y. C., TSAI, C. Y., LIANG, P. H., HSU, T. L., WU, C. Y., NETEA, M. G., WONG, C. H. & HSIEH, S. L. 2013. CLEC4F is an inducible C-type lectin in F4/80-positive cells and is involved in alpha-galactosylceramide presentation in liver. *PLoS One,* 8**,** e65070.

YERAMIAN, A., MARTIN, L., SERRAT, N., ARPA, L., SOLER, C., BERTRAN, J., MCLEOD, C., PALACIN, M., MODOLELL, M., LLOBERAS, J. & CELADA, A. 2006. Arginine transport via cationic amino acid transporter 2 plays a critical regulatory role in classical or alternative activation of macrophages. *J Immunol,* 176**,** 5918-24.

YONA, S. & GORDON, S. 2015. From the Reticuloendothelial to Mononuclear Phagocyte System - The Unaccounted Years. *Front Immunol,* 6**,** 328.

YONA, S., KIM, K. W., WOLF, Y., MILDNER, A., VAROL, D., BREKER, M., STRAUSS-AYALI, D., VIUKOV, S., GUILLIAMS, M., MISHARIN, A., HUME, D. A., PERLMAN, H., MALISSEN, B., ZELZER, E. & JUNG, S. 2013. Fate mapping reveals origins and dynamics of monocytes and tissue macrophages under homeostasis. *Immunity,* 38**,** 79-91.

ZEUTHEN, L. H., FINK, L. N. & FROKIAER, H. 2008. Epithelial cells prime the immune response to an array of gut-derived commensals towards a tolerogenic phenotype through distinct actions of thymic stromal lymphopoietin and transforming growth factor-beta. *Immunology,* 123**,** 197-208.

ZHAO, A., URBAN, J. F., JR., ANTHONY, R. M., SUN, R., STILTZ, J., VAN ROOIJEN, N., WYNN, T. A., GAUSE, W. C. & SHEA-DONOHUE, T. 2008. Th2 cytokine-induced alterations in intestinal smooth muscle function depend on alternatively activated macrophages. *Gastroenterology,* 135**,** 217-225 e1.

ZIEGLER-HEITBROCK, L. & HOFER, T. P. 2013. Toward a refined definition of monocyte subsets. *Front Immunol,* 4**,** 23.

ZURAWSKI, S. M., VEGA, F., JR., HUYGHE, B. & ZURAWSKI, G. 1993. Receptors for interleukin-13 and interleukin-4 are complex and share a novel component that functions in signal transduction. *EMBO J,* 12**,** 2663-70.